高能对撞机上的高精度理论预言

Zhao Li
IHEP-CAS

2022-Nov-12

量子场论的成功

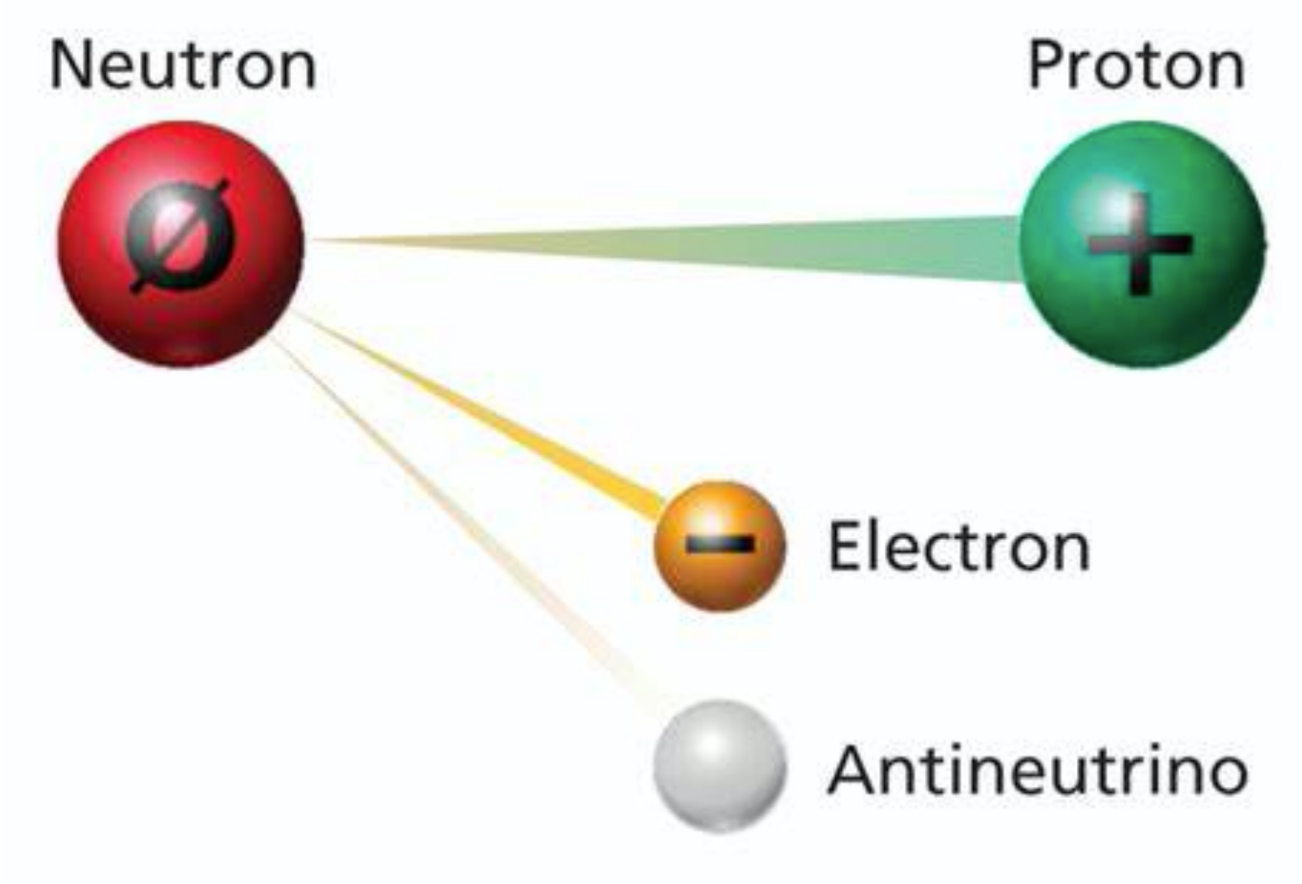

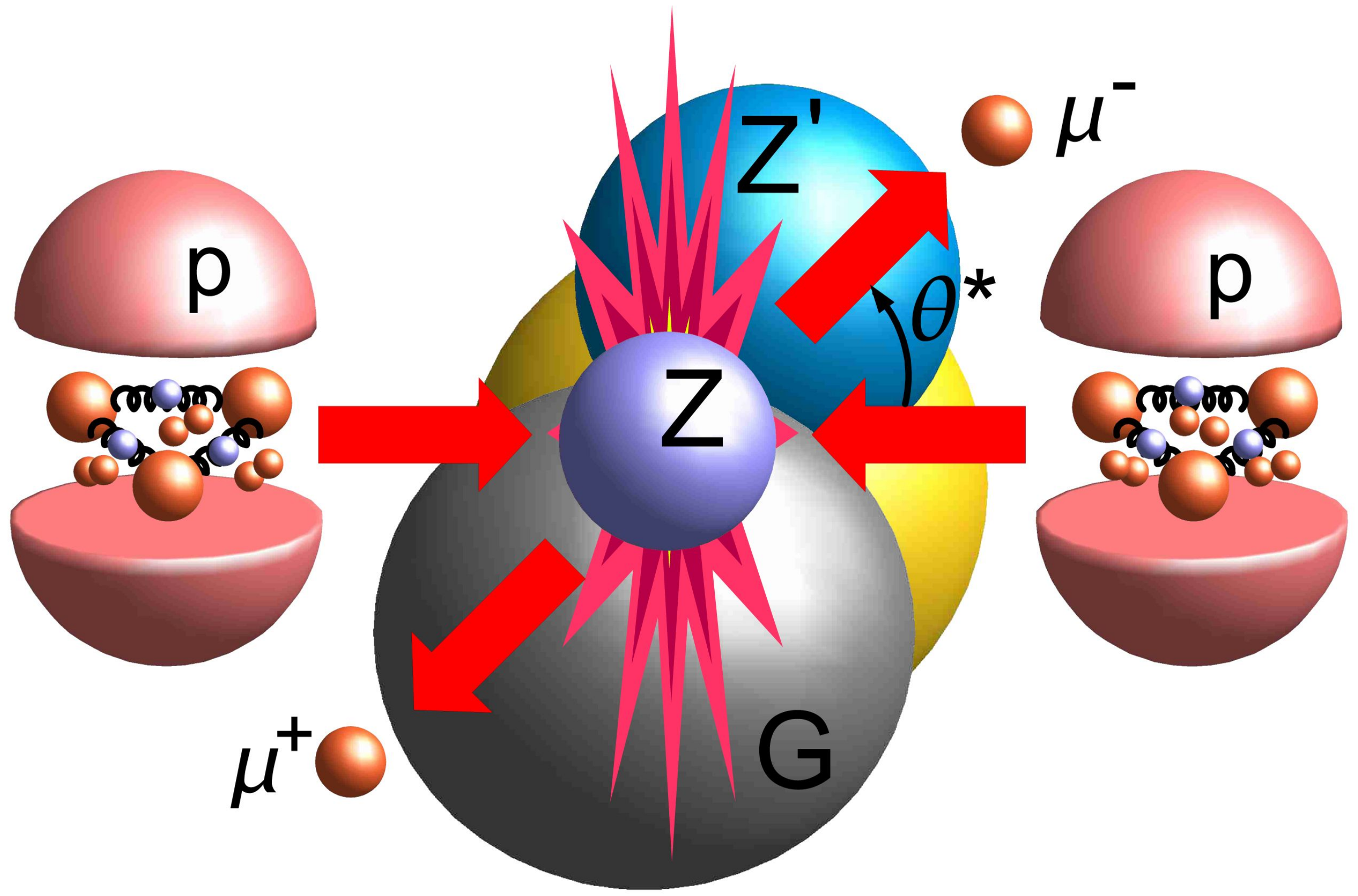

- 粒子的衰变和散射过程告诉我们粒子数并不一定守恒。
- 这类问题无法用非相对论量子力学处理。
- 人们换了另一种思路：从场出发。
- 万物皆场，粒子态是场在真空上的激发

量子场论的成功

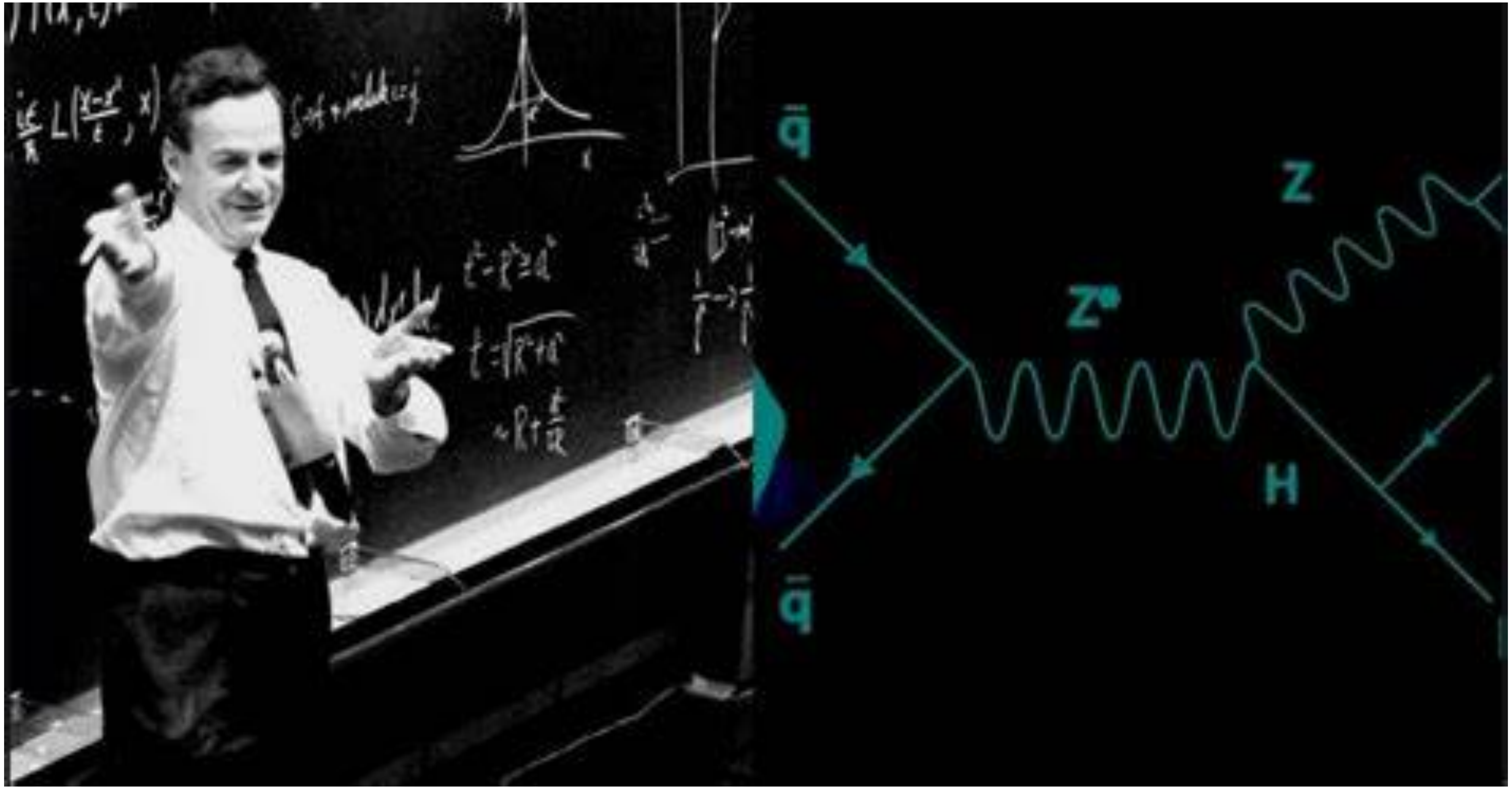

量子电动力学
(Quantum ElectroDynamics, QED)

$$\mathcal{L} = \underbrace{i\overline{\psi}\gamma^\mu\partial_\mu\psi - m\overline{\psi}\psi}_{\text{费米子动能项}} \underbrace{- \frac{1}{4}F_{\mu\nu}F^{\mu\nu}}_{\text{光子动能项}} \underbrace{- e\overline{\psi}\gamma_\mu A^\mu\psi}_{\text{相互作用项}}$$

$$\boxed{\text{U(1)规范对称性} \Rightarrow \text{电荷守恒}}$$

目前最为成功的物理量：电子反常磁矩

$$a_{\text{exp}} = 1159.65218091 \times 10^{-6}$$

$$a_{\text{th}} = 1159.652216 \times 10^{-6}$$

1965 Nobel Prize in Physics

SIN-ITIRO TOMONAGA
朝永振一郎

Richard Feynman

Julian Schwinger

for their fundamental work in quantum electrodynamics, with deep-ploughing consequences for the physics of elementary particles

标准模型很成功!

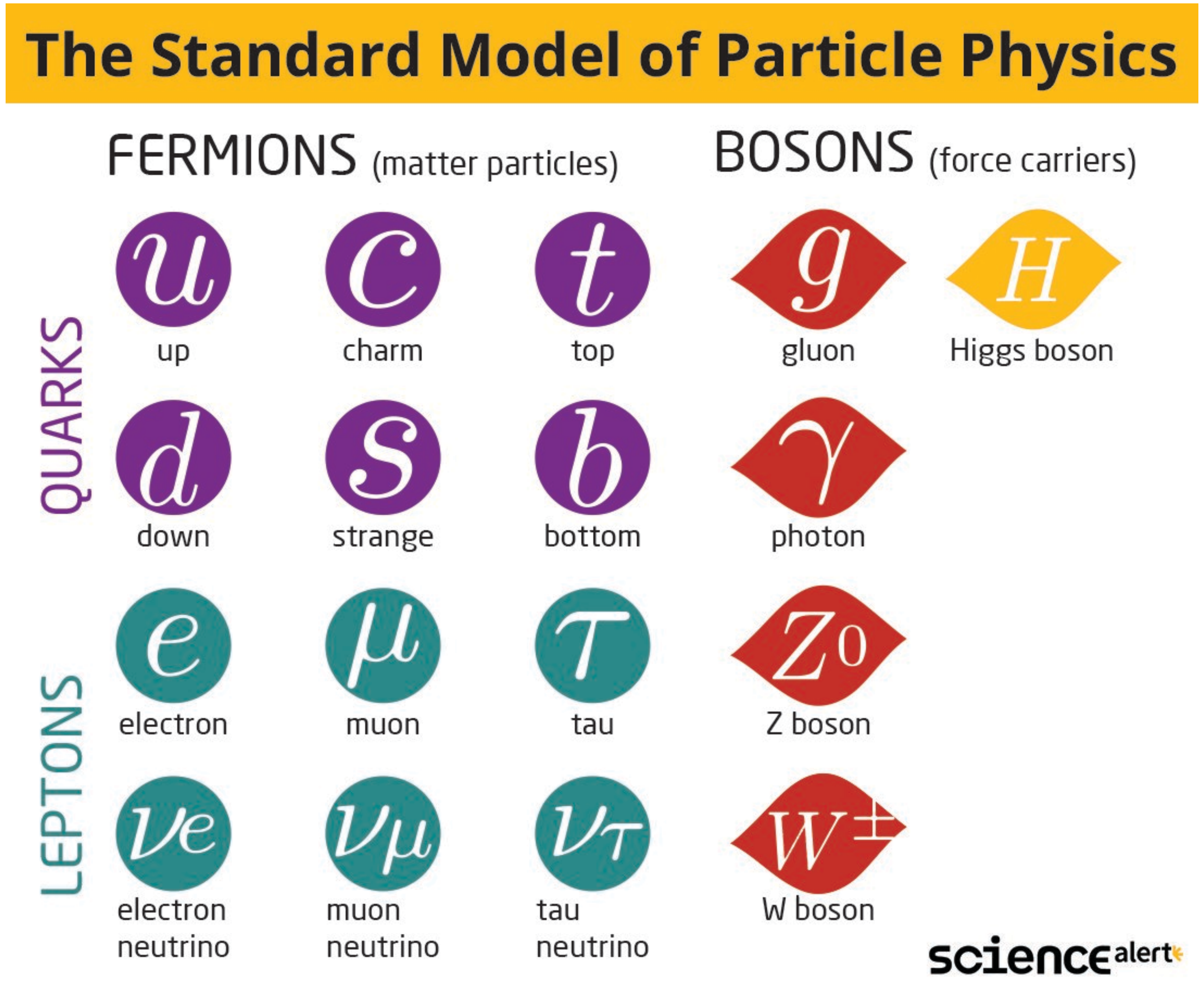
The Standard Model of Particle Physics
FERMIONS (matter particles)
BOSONS (force carriers)
QUARKS
LEPTONS
up
charm
top
gluon
Higgs boson
down
strange
bottom
photon
electron
muon
tau
Z boson
electron neutrino
muon neutrino
tau neutrino
W boson
sciencealert

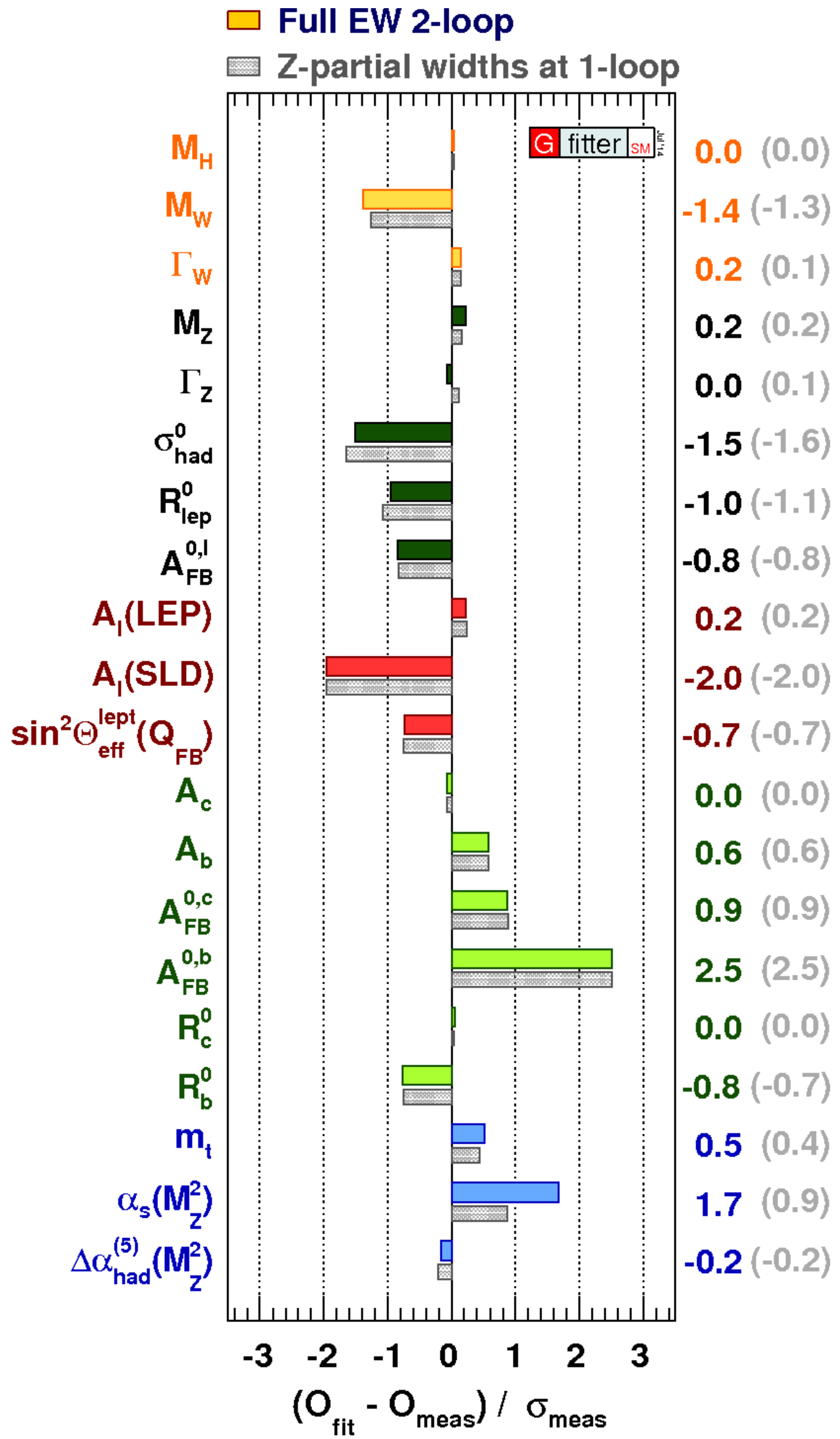
Full EW 2-loop
Z-partial widths at 1-loop
Gfitter SM
M_H 0.0 (0.0)
M_W -1.4 (-1.3)
Γ_W 0.2 (0.1)
M_Z 0.2 (0.2)
Γ_Z 0.0 (0.1)
σ^0_{had} -1.5 (-1.6)
R^0_{lep} -1.0 (-1.1)
$A^{0,l}_{FB}$ -0.8 (-0.8)
$A_l(LEP)$ 0.2 (0.2)
$A_l(SLD)$ -2.0 (-2.0)
$\sin^2\Theta^{lept}_{eff}(Q_{FB})$ -0.7 (-0.7)
A_c 0.0 (0.0)
A_b 0.6 (0.6)
$A^{0,c}_{FB}$ 0.9 (0.9)
$A^{0,b}_{FB}$ 2.5 (2.5)
R^0_c 0.0 (0.0)
R^0_b -0.8 (-0.7)
m_t 0.5 (0.4)
$\alpha_s(M_Z^2)$ 1.7 (0.9)
$\Delta\alpha^{(5)}_{had}(M_Z^2)$ -0.2 (-0.2)
-3 -2 -1 0 1 2 3
$(O_{fit} - O_{meas}) / \sigma_{meas}$

Some Numbers @ LHC

对撞能量：14TeV=2.2×10^{-6}J, v=0.999999991c

造价: 4332 兆瑞士法郎　　月球潮汐力影响：1毫米

周长：27km

平均深度：地下100米

高真空：10^{-13}标准大气压

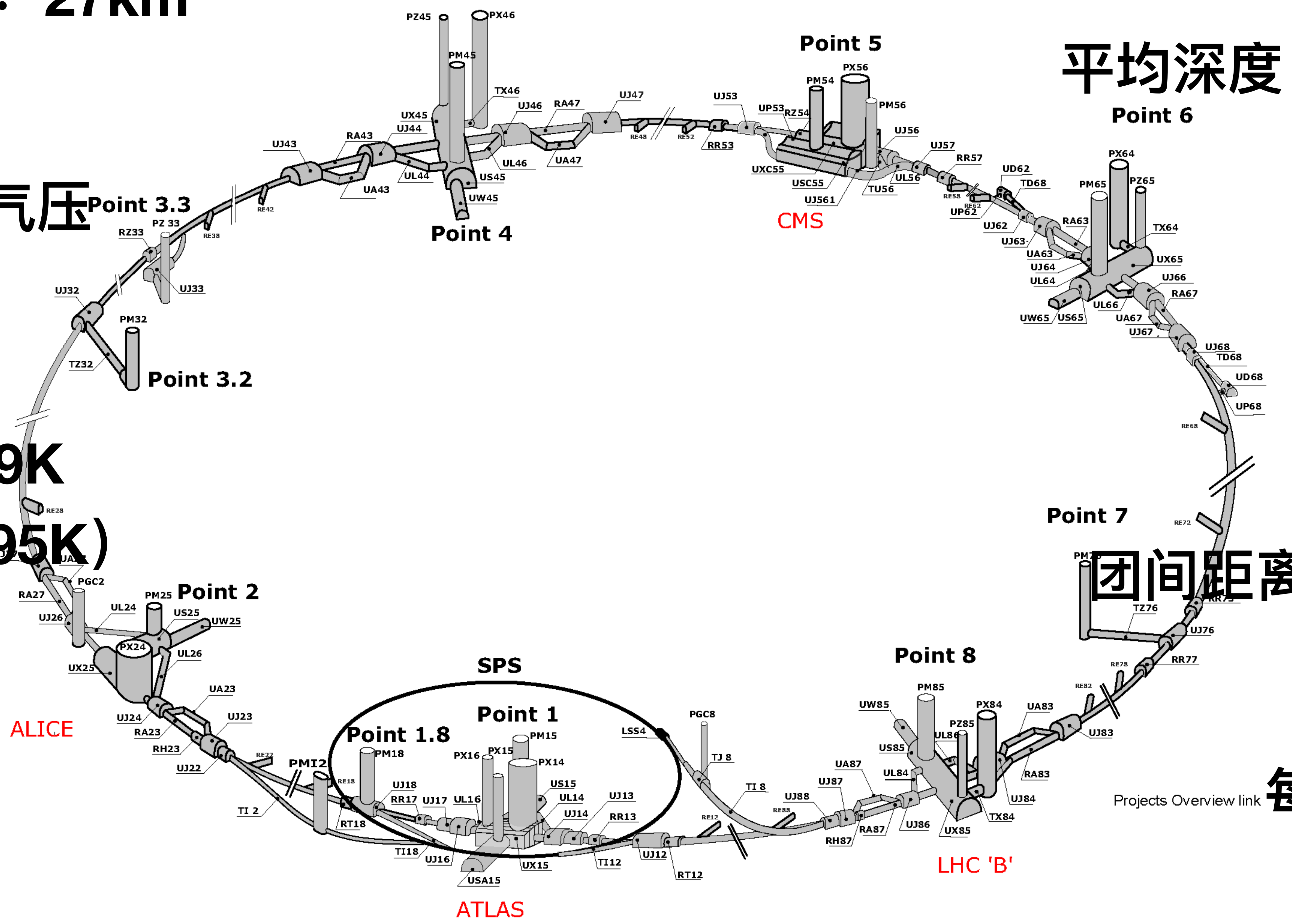

超低温：超导磁铁1.9K

（CMB 2.71K, CNB 1.95K）

每束团数：2808

团间距离：7.5米（25纳秒）

9593块各型磁铁

每团质子数：1.2×10^{11}

偶极磁铁1232块：15米长，35吨，超导线圈

（1.9K，电流强度11850安培），8.33特斯拉

每秒10亿次粒子对撞

The Detectors

记录数据量~50PB=5千万GB每年！

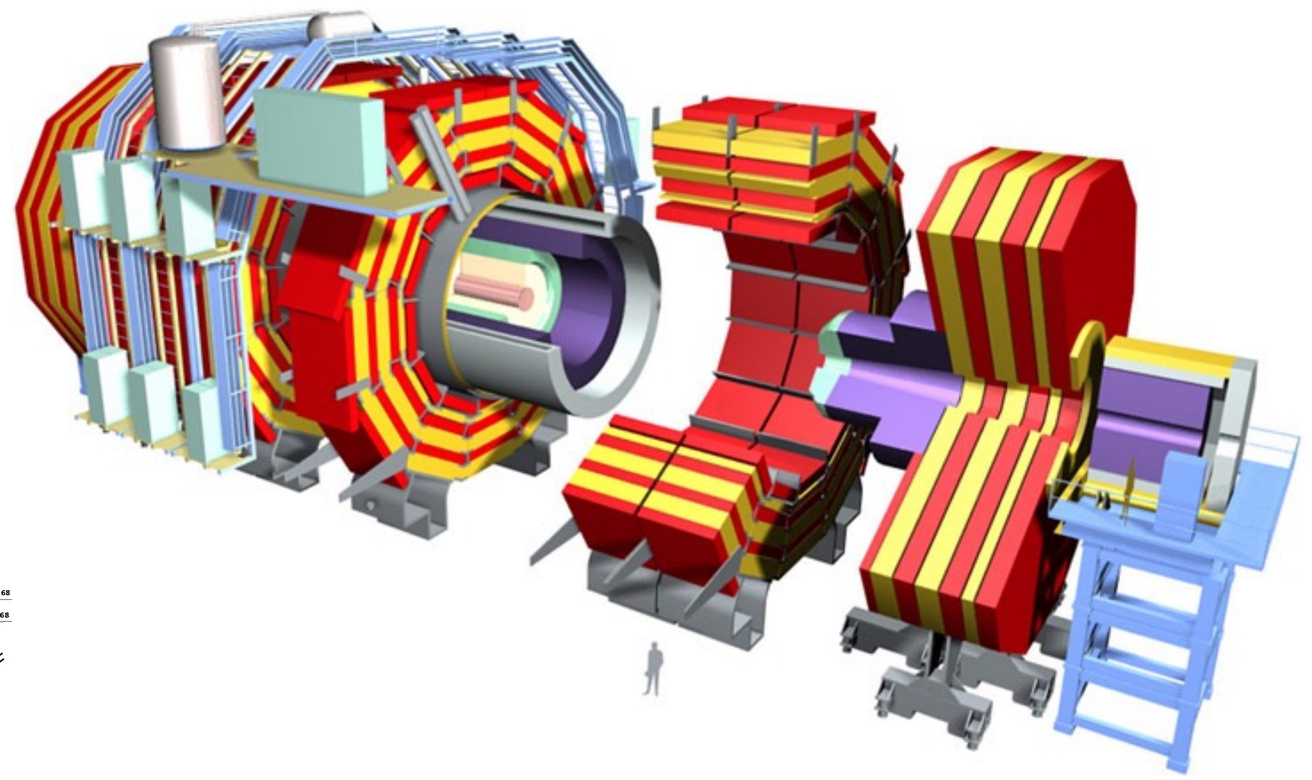

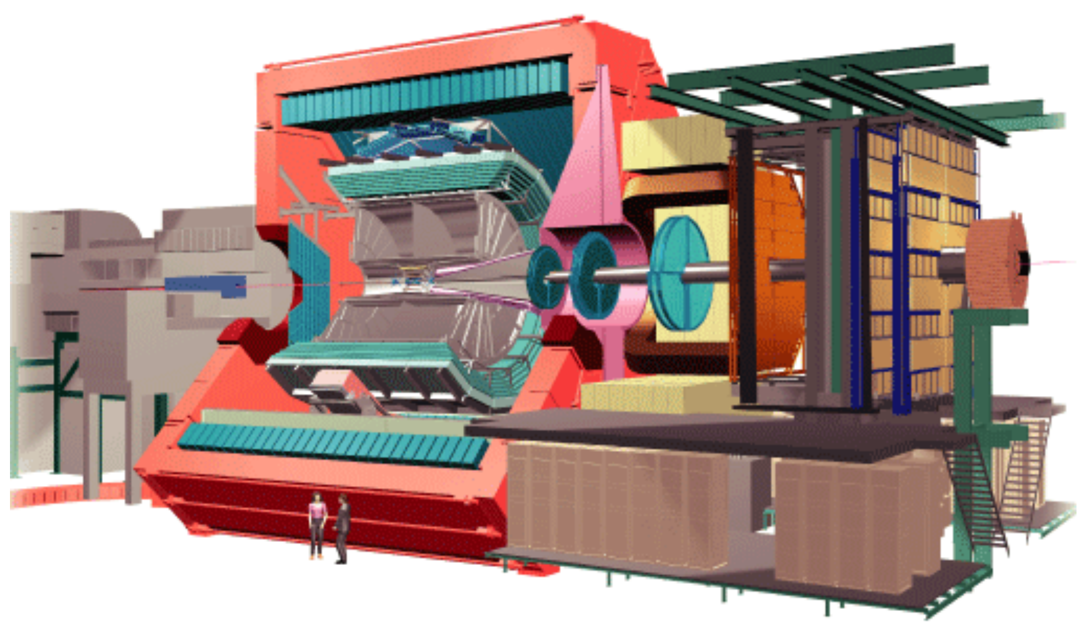

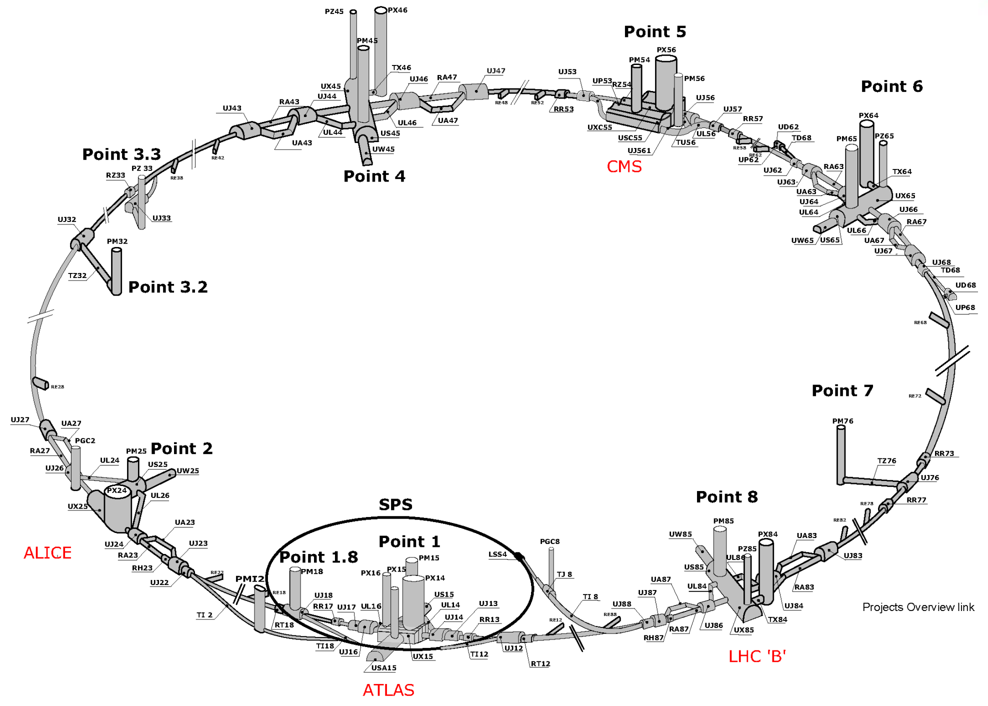

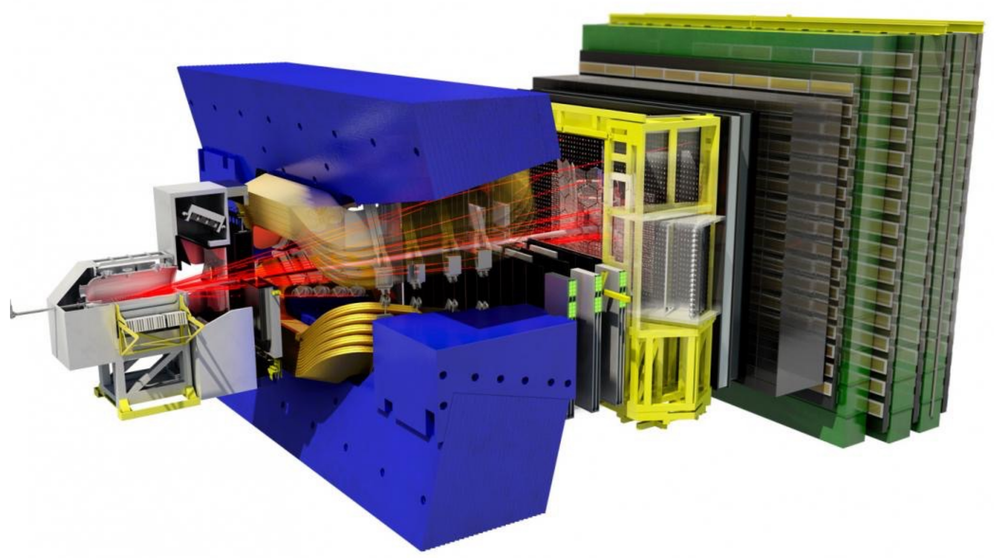

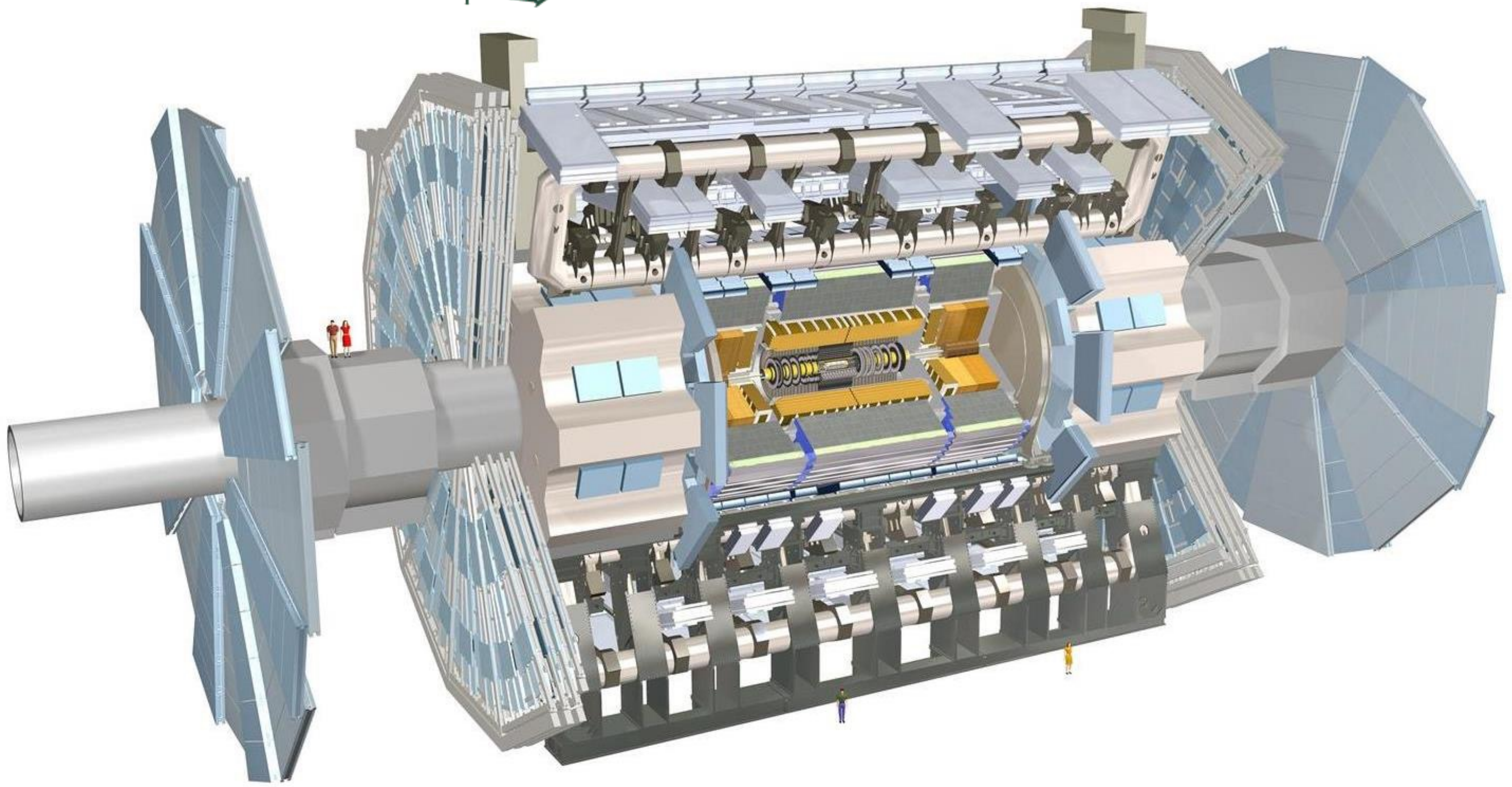

ATLAS produces about 1 GB/s

CMS produces about 1 GB/s

LHCb produces about 0.6 GB/s

ALICE produces several GB/s during heavy-ion running

Why need precise calculation?

Solution to SM QFT Lagrangian

Perturbative Algo

Fixed order, Resummation …

Non-Perturbative Algo

Lattice QCD, PDF, FF…

scattering cross sections
decay width

Drell-Yan过程中QCD效应

Catani, Ferrera, Grazzini, JHEP 1005 (2010) 006

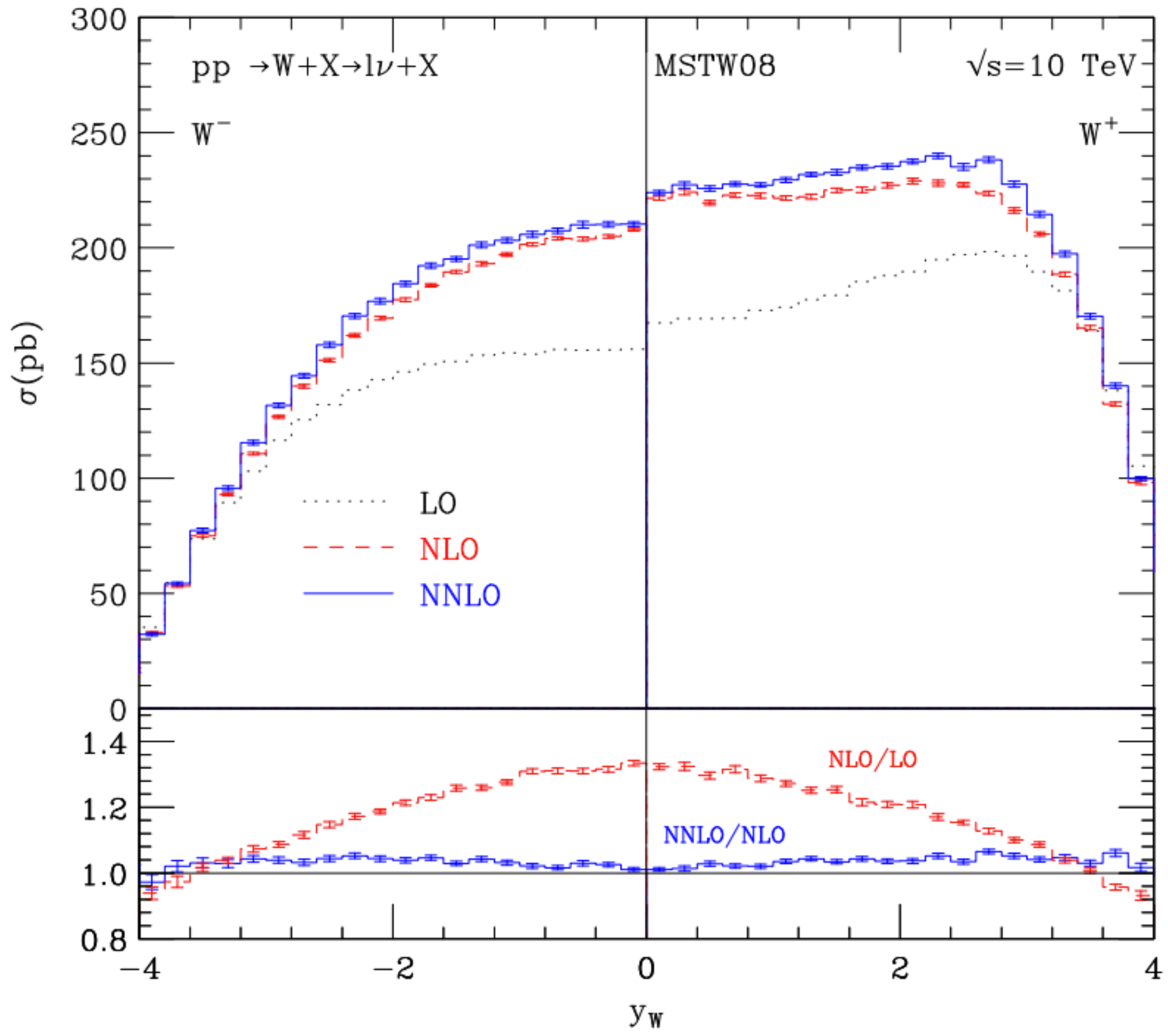

Z+photon产生

Grazzini et al, Phys.Lett. B731 (2014) 204-207

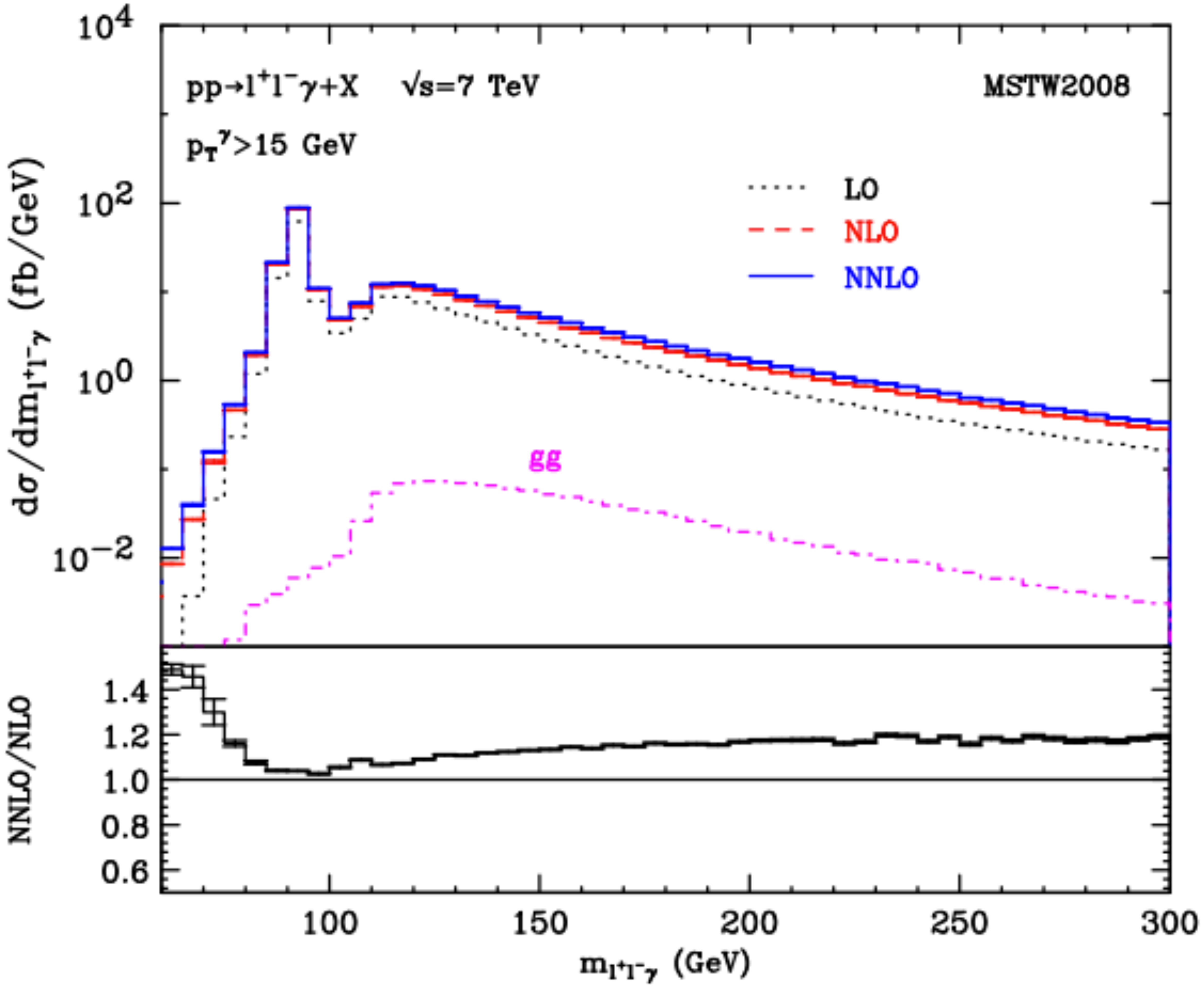

双光子产生

Catani et al, Phys.Rev.Lett. 108 (2012) 072001

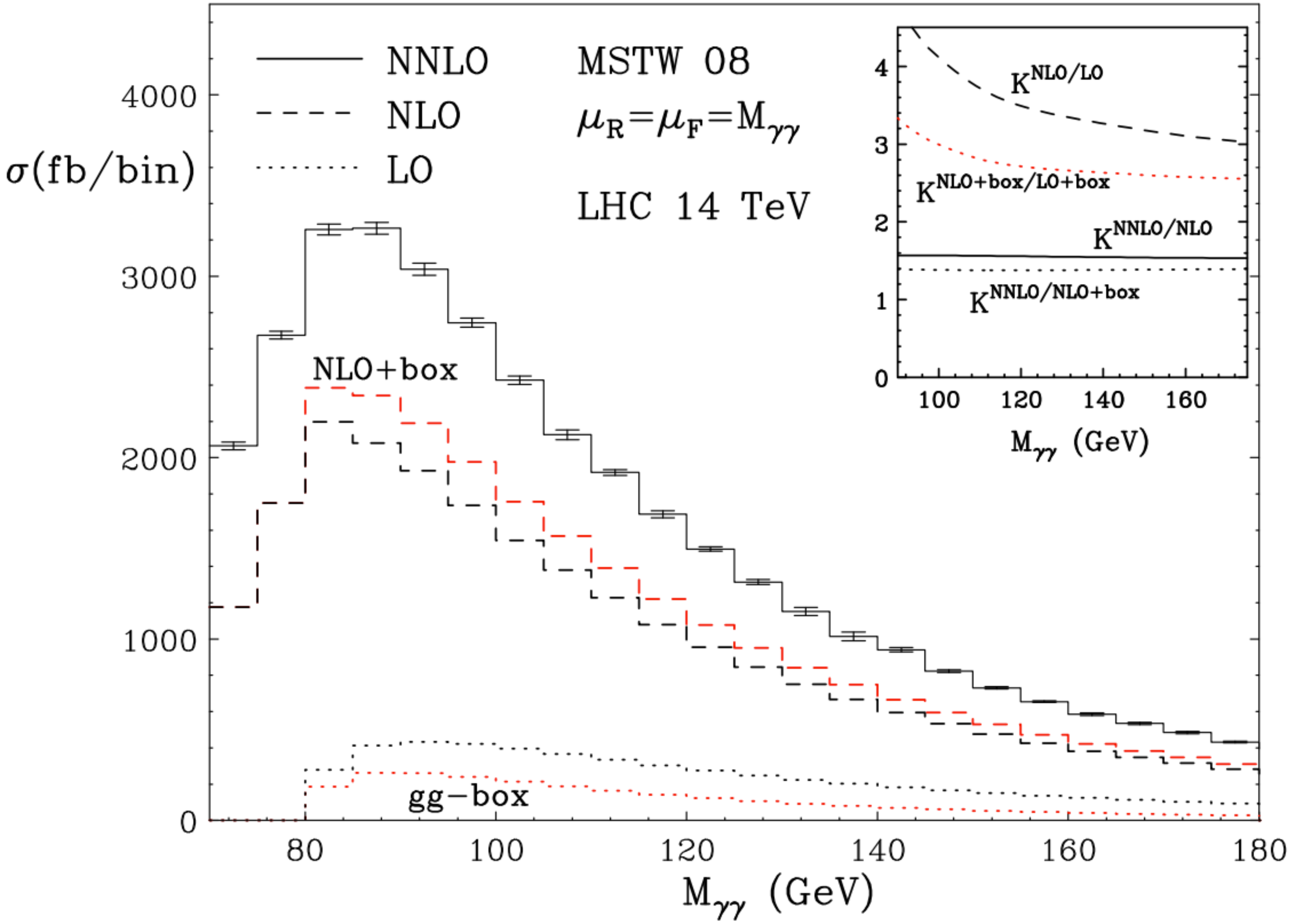

Higgs玻色子直接产生中QCD效应

Bonvini, et al, JHEP 1608 (2016) 105

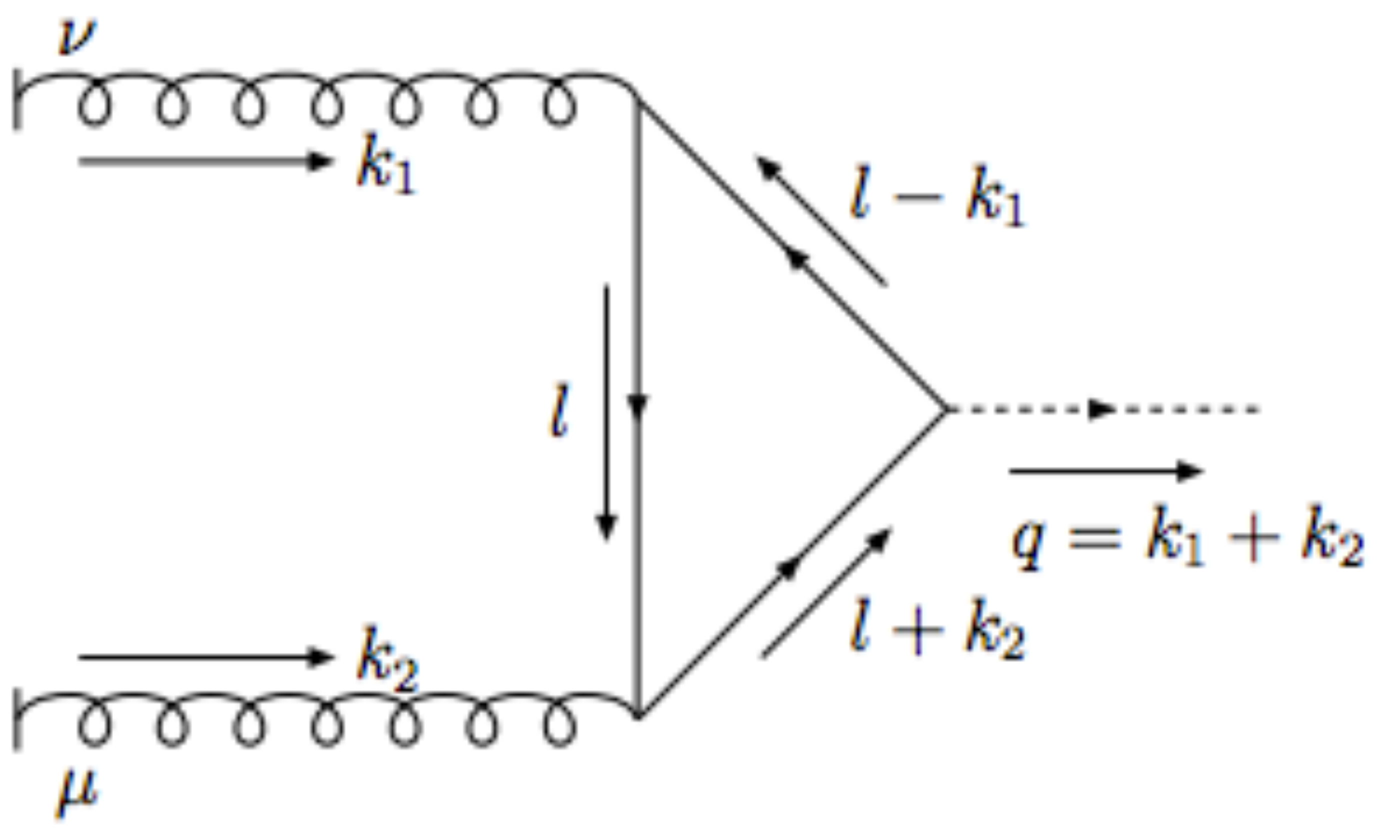

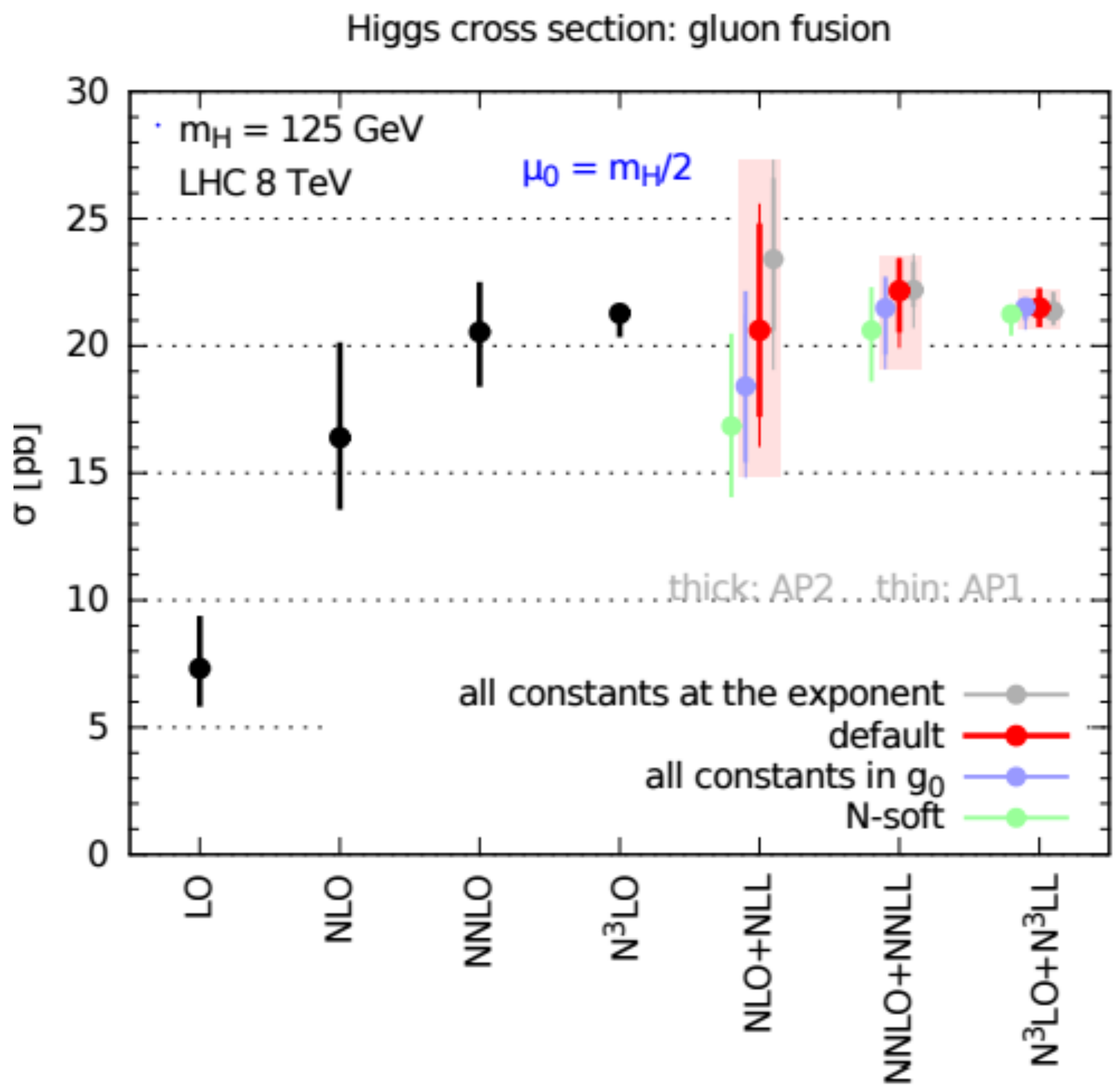

Higgs Pair

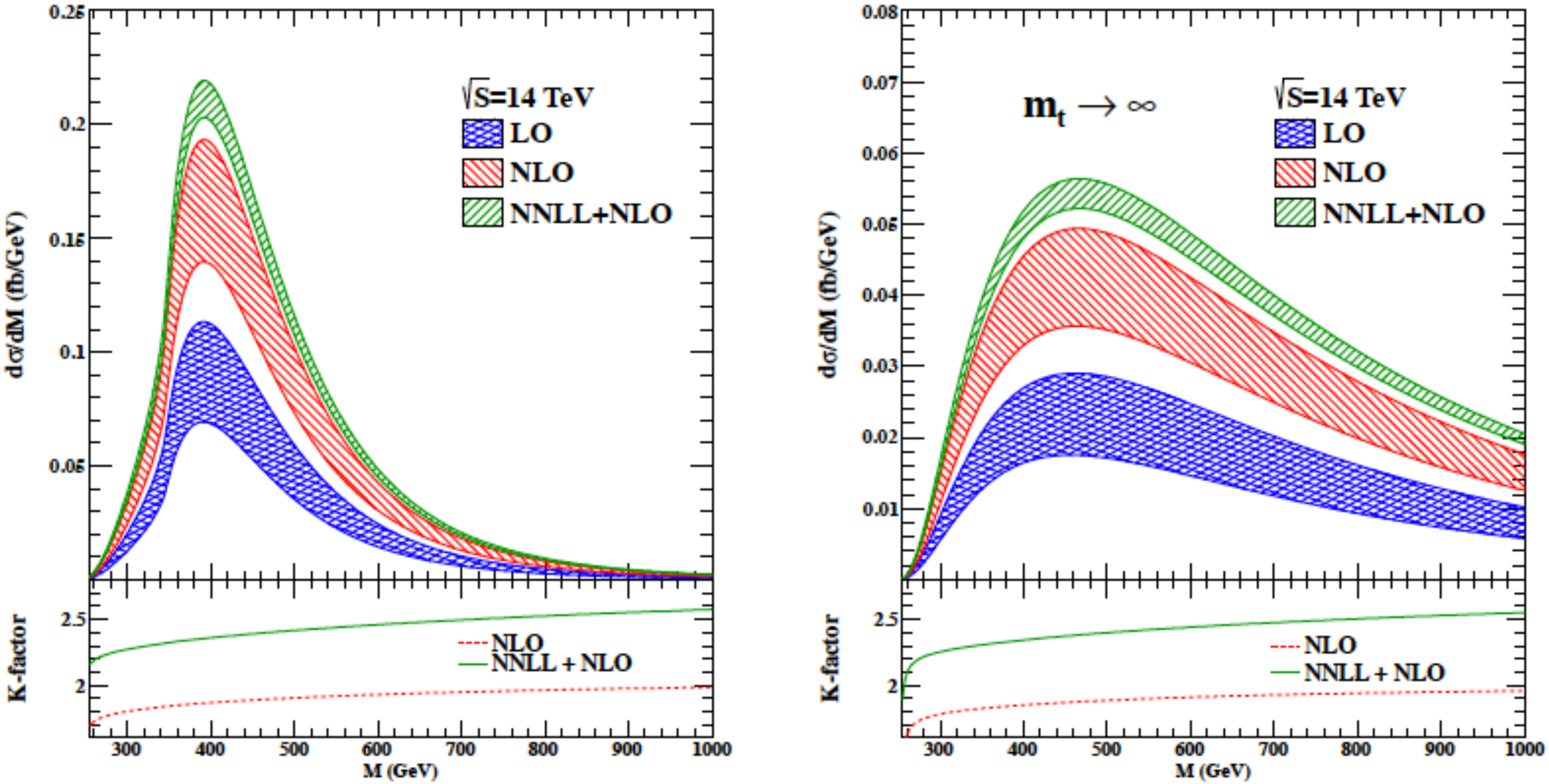

√S=14 TeV
LO
NLO
NNLL+NLO
dσ/dM (fb/GeV)
K-factor
NLO
NNLL + NLO
M (GeV)
0.25
0.2
0.15
0.1
0.05
2.5
2
300
400
500
600
700
800
900
1000
$m_t \to \infty$
√S=14 TeV
LO
NLO
NNLL+NLO
dσ/dM (fb/GeV)
K-factor
NLO
NNLL + NLO
M (GeV)
0.08
0.07
0.06
0.05
0.04
0.03
0.02
0.01
2.5
2

The wishlist(s)

Process	known	desired	motivation
H	d\sigma @ NNLO QCD d\sigma @ NLO EW finite quark mass effects @ NLO	d\sigma @ NNNLO QCD + NLO EW MC@NNLO finite quark mass effects @ NNLO	H branching ratios and couplings
H+j	d\sigma @ NNLO QCD (g only) d\sigma @ NLO EW	d\sigma @ NNLO QCD + NLO EW finite quark mass effects @ NLO	H p_T
H+2j	\sigma_tot(VBF) @ NNLO(DIS) QCD d\sigma(gg) @ NLO QCD d\sigma(VBF) @ NLO EW	d\sigma @ NNLO QCD + NLO EW	H couplings
H+V	d\sigma(V decays) @ NNLO QCD d\sigma @ NLO EW	with H→bb @ same accuracy	H couplings
t\bar tH	d\sigma(stable tops) @ NLO QCD	d\sigma(NWA top decays) @ NLO QCD + NLO EW	top Yukawa coupling
HH	d\sigma @ LO QCD finite quark mass effects d\sigma @ NLO QCD large m_t limit	d\sigma @ NLO QCD finite quark mass effects d\sigma @ NNLO QCD	Higgs self coupling

Process	known	desired	motivation
t\bar t	\sigma_tot @ NNLO QCD d\sigma(top decays) @ NLO QCD d\sigma(stable tops) @ NLO EW	d\sigma(top decays) @ NNLO QCD + NLO EW	precision top/QCD, gluon PDF effect of extra radiation at high rapidity top asymmetries
t\bar t+j	d\sigma(NWA top decays) @ NLO QCD	d\sigma(NWA top decays) @ NLO QCD + NLO EW	precision top/QCD, top asymmetries
single-top	d\sigma(NWA top decays) @ NLO QCD	d\sigma(NWA top decays) @ NNLO QCD (t channel)	precision top/QCD, V_tb
dijet	d\sigma @ NNLO QCD (g only) d\sigma @ NLO weak	d\sigma @ NNLO QCD + NLO EW	Obs.: incl. jets, dijet mass –> PDF fits (gluon at high x) –> alpha_s CMS x sections: http://arxiv.org/abs/1212.6660
3j	d\sigma @ NLO QCD	d\sigma @ NNLO QCD + NLO EW	Obs.: R3/2 or similar –> alpha_s at high pT dom. uncertainty: scales see http://arxiv.org/abs/1304.7498 (CMS)
\gamma+j	d\sigma @ NLO QCD d\sigma @ NLO EW	d\sigma @ NNLO QCD + NLO EW	gluon PDF, \gamma+b for bottom PDF

Precise Theory on Signals (Backgrounds?) now and future?

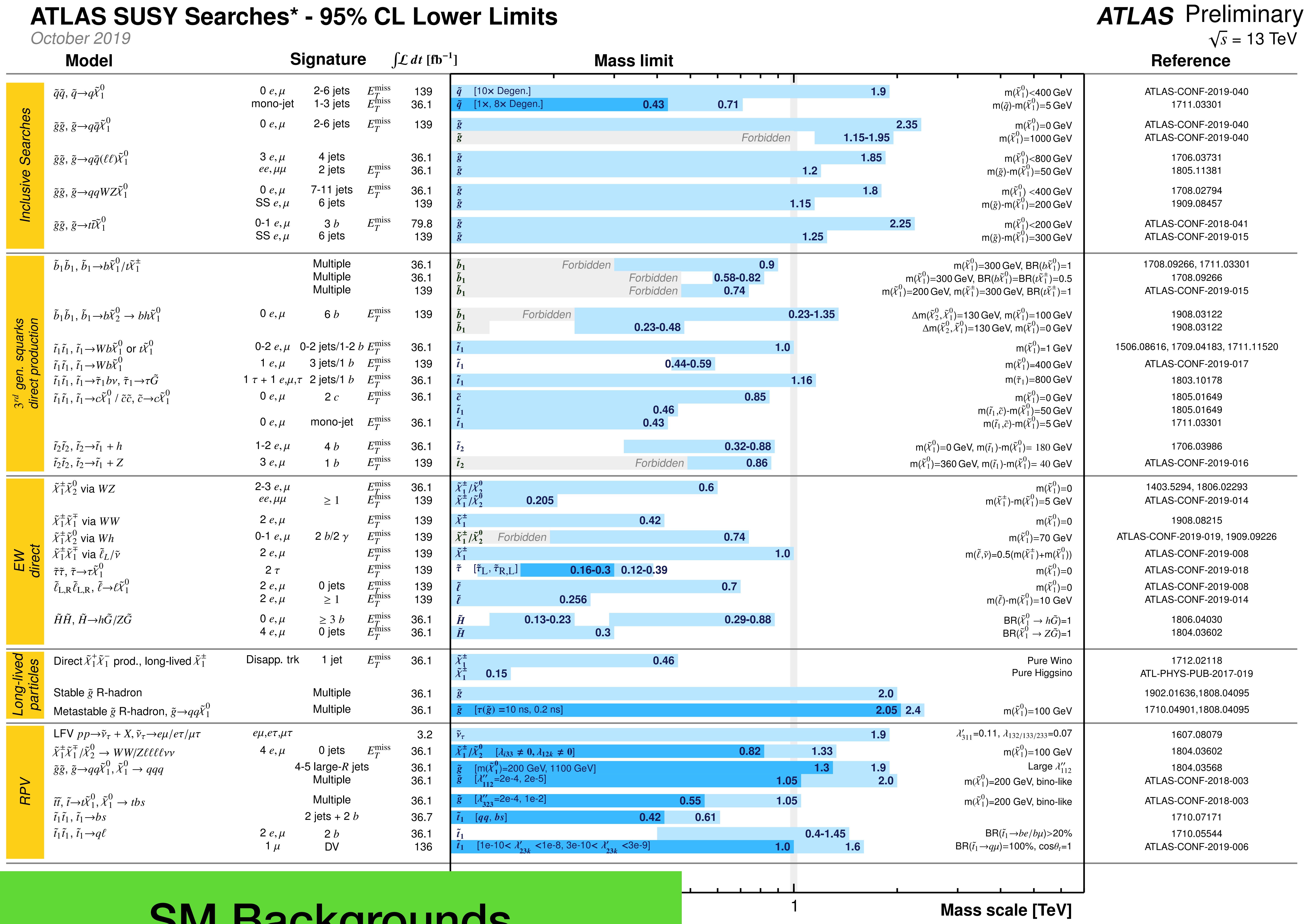

SM Backgrounds


LHCb
ATLAS
CERN
ALICE
CMS

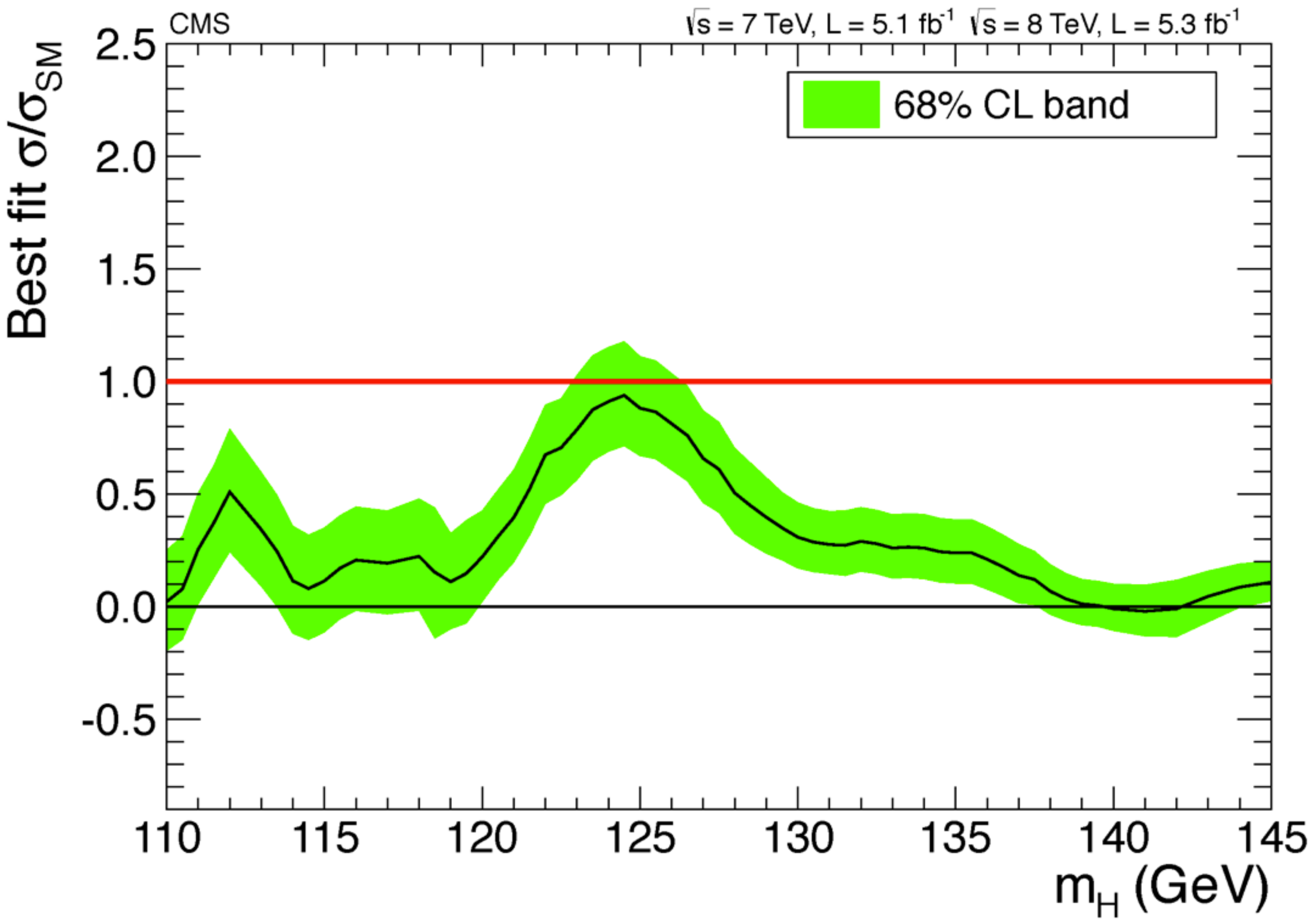
CMS
$\sqrt{s}$ = 7 TeV, L = 5.1 fb^{-1} $\sqrt{s}$ = 8 TeV, L = 5.3 fb^{-1}
68% CL band
Best fit σ/σ_{SM}
2.5
2.0
1.5
1.0
0.5
0.0
-0.5
110
115
120
125
130
135
140
145
m_H (GeV)

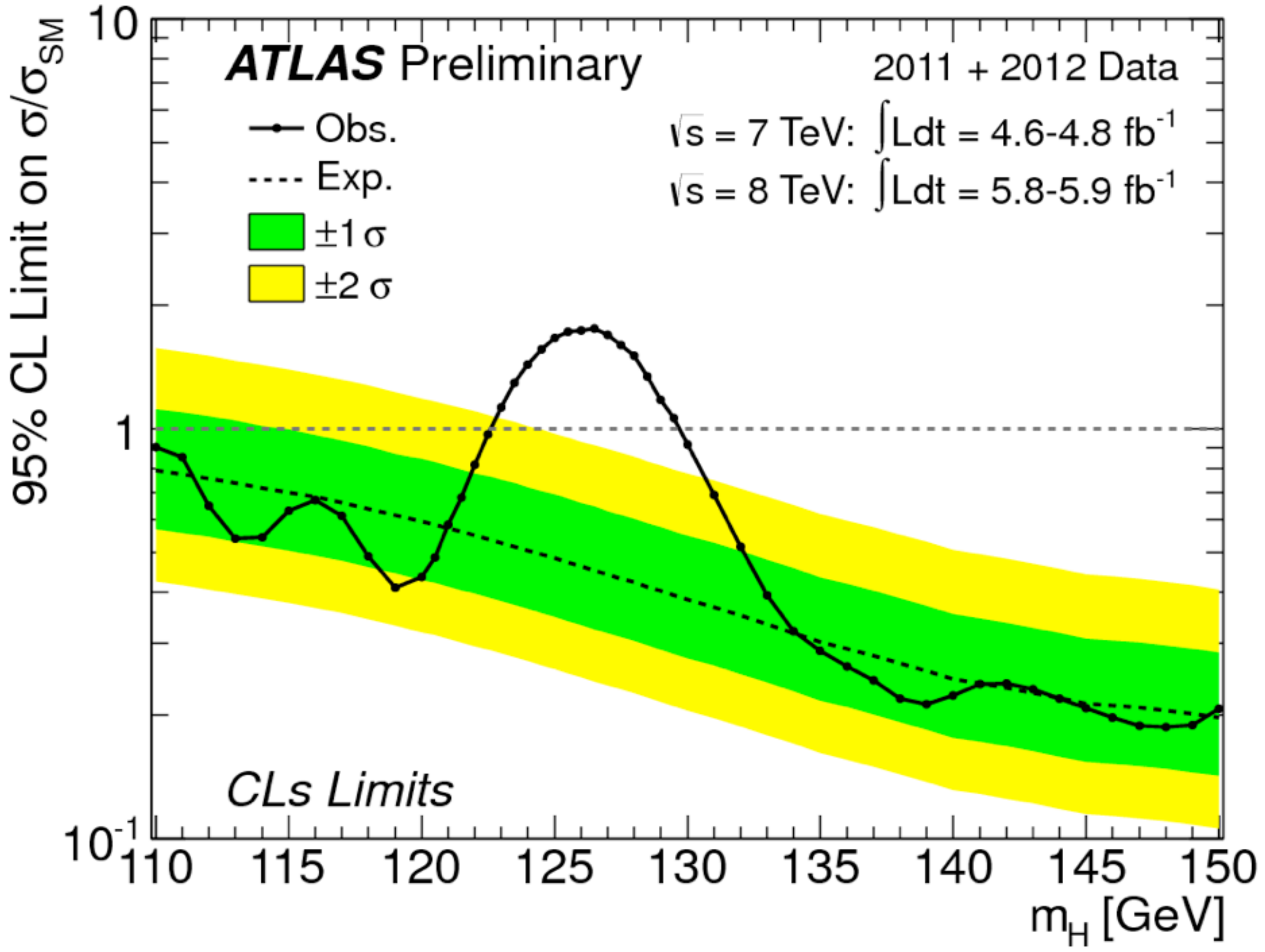
ATLAS Preliminary
2011 + 2012 Data
$\sqrt{s}$ = 7 TeV: $\int$Ldt = 4.6-4.8 fb^{-1}
$\sqrt{s}$ = 8 TeV: $\int$Ldt = 5.8-5.9 fb^{-1}
Obs.
Exp.
±1 σ
±2 σ
CLs Limits
95% CL Limit on σ/σ_{SM}
10
1
10^{-1}
110
115
120
125
130
135
140
145
150
m_H [GeV]

Higgs的质量

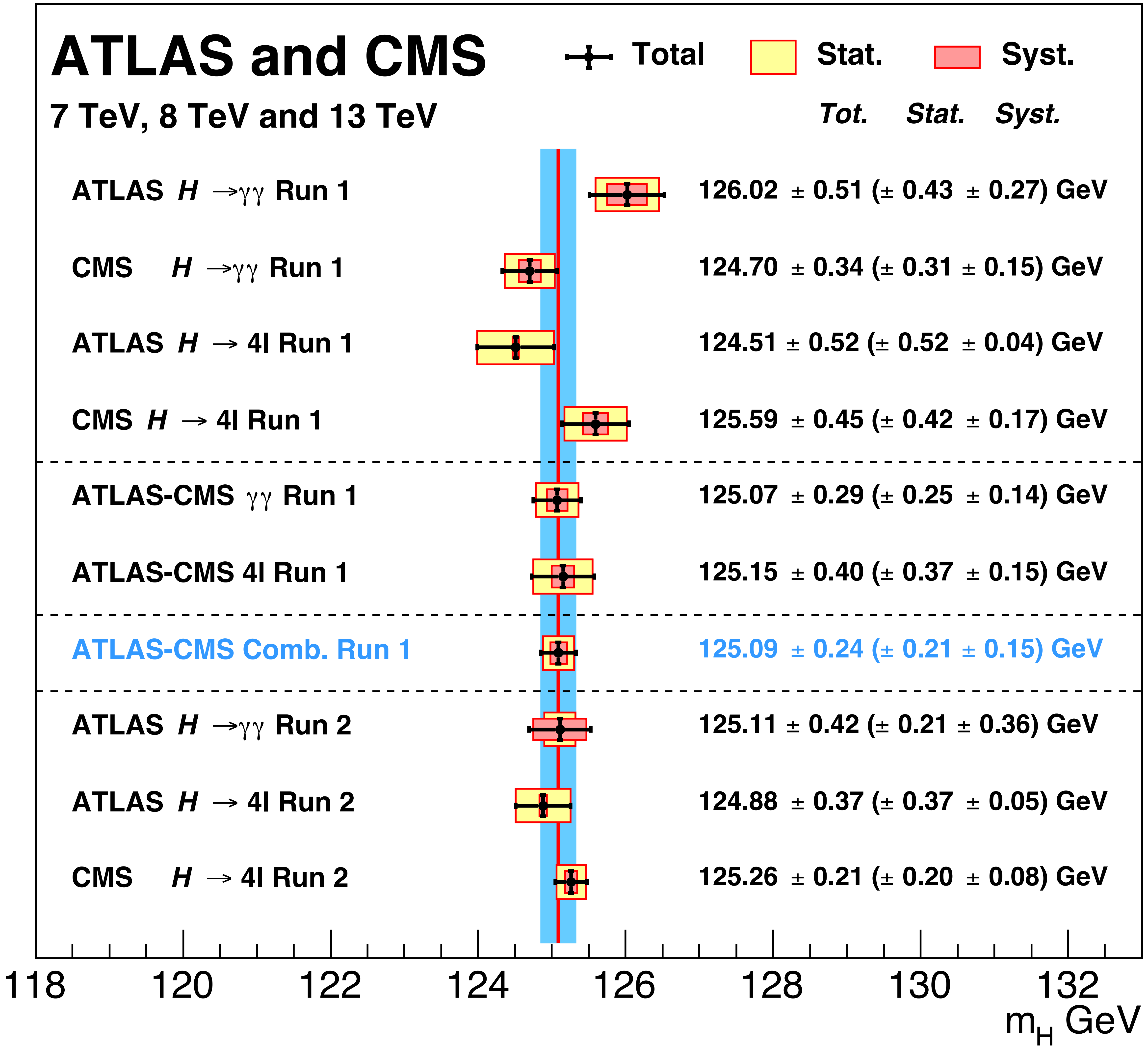
ATLAS and CMS
7 TeV, 8 TeV and 13 TeV
Total
Stat.
Syst.
Tot. Stat. Syst.
ATLAS H →γγ Run 1
126.02 ± 0.51 (± 0.43 ± 0.27) GeV
CMS H →γγ Run 1
124.70 ± 0.34 (± 0.31 ± 0.15) GeV
ATLAS H → 4l Run 1
124.51 ± 0.52 (± 0.52 ± 0.04) GeV
CMS H → 4l Run 1
125.59 ± 0.45 (± 0.42 ± 0.17) GeV
ATLAS-CMS γγ Run 1
125.07 ± 0.29 (± 0.25 ± 0.14) GeV
ATLAS-CMS 4l Run 1
125.15 ± 0.40 (± 0.37 ± 0.15) GeV
ATLAS-CMS Comb. Run 1
125.09 ± 0.24 (± 0.21 ± 0.15) GeV
ATLAS H →γγ Run 2
125.11 ± 0.42 (± 0.21 ± 0.36) GeV
ATLAS H → 4l Run 2
124.88 ± 0.37 (± 0.37 ± 0.05) GeV
CMS H → 4l Run 2
125.26 ± 0.21 (± 0.20 ± 0.08) GeV
118
120
122
124
126
128
130
132
m_H GeV

Higgs的直接耦合

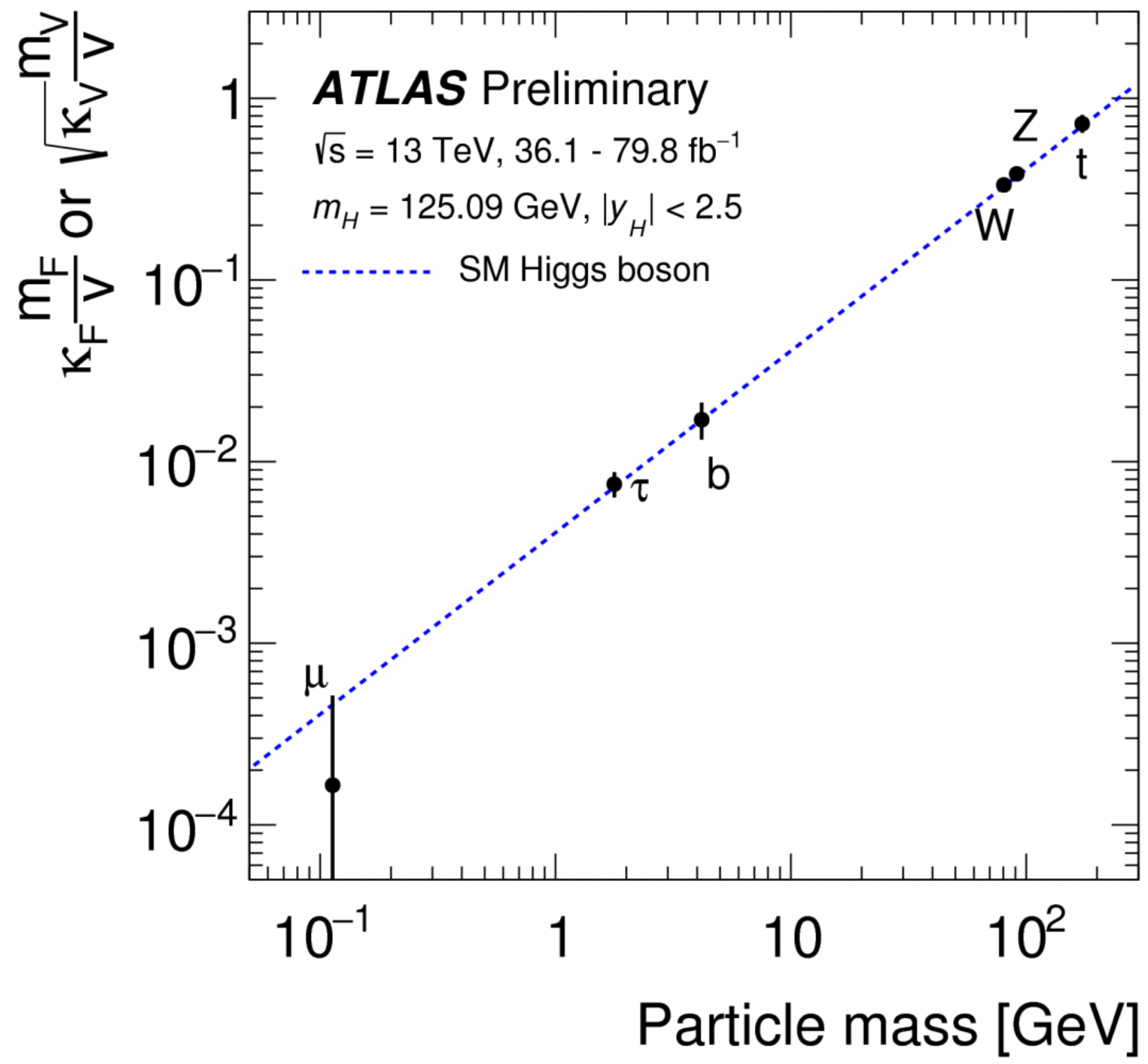

Higgs与费米子和有质量规范玻色子有树图水平的直接耦合，且正比于质量。

为什么需要CEPC

高能环形正负电子对撞机方案

- 建设一个100 公里周长的 环形正负电子对撞机(CEPC)， 高精度研究Higgs （Z）粒子，并寻找新物理
- CEPC的升级可能：在同一隧道中建设 pp/AA对撞机，也可以建设ep/eA 对撞机，或其它可能性

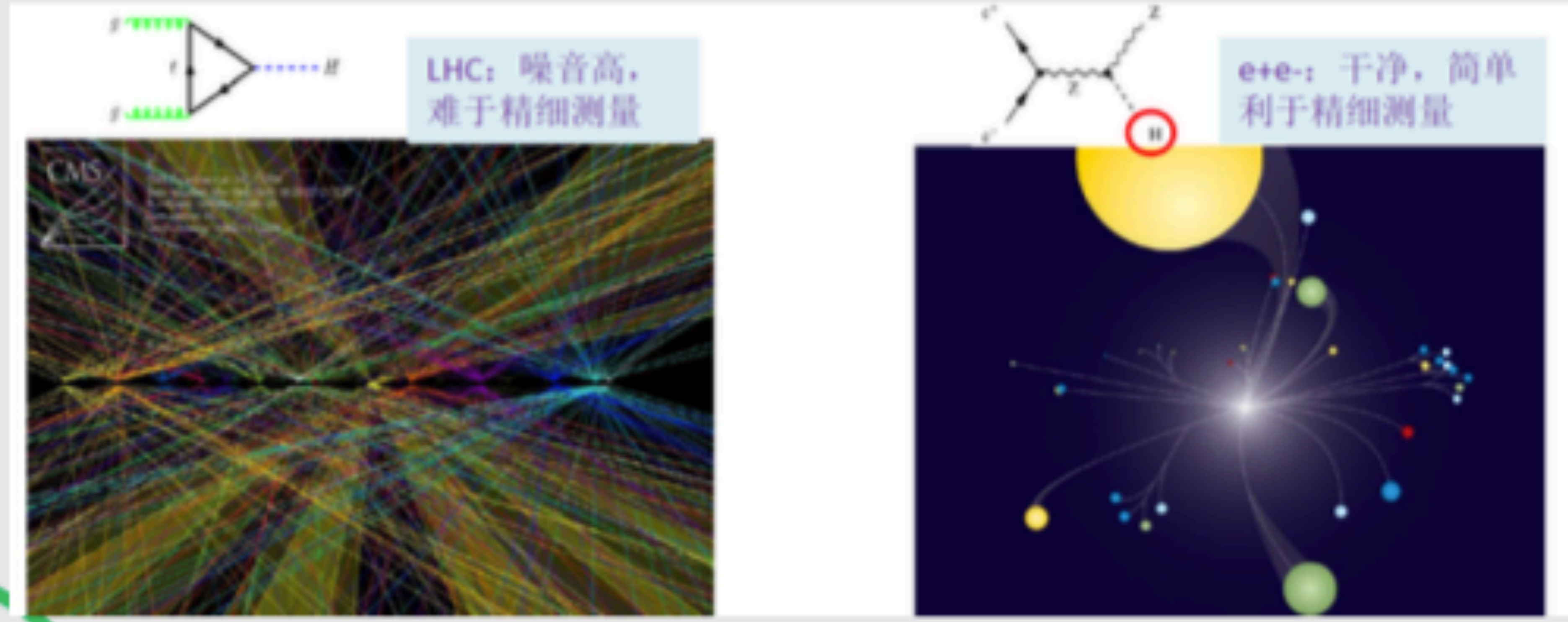

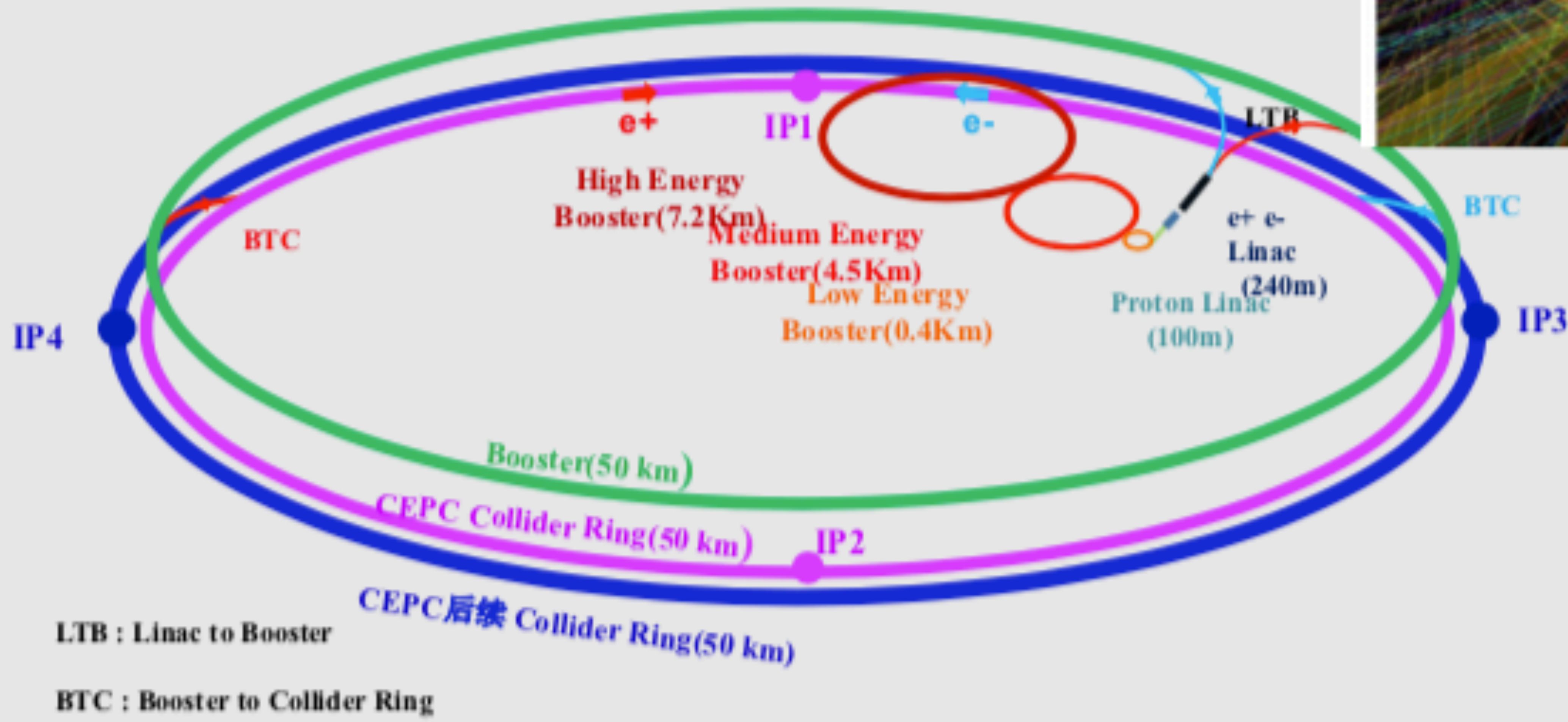

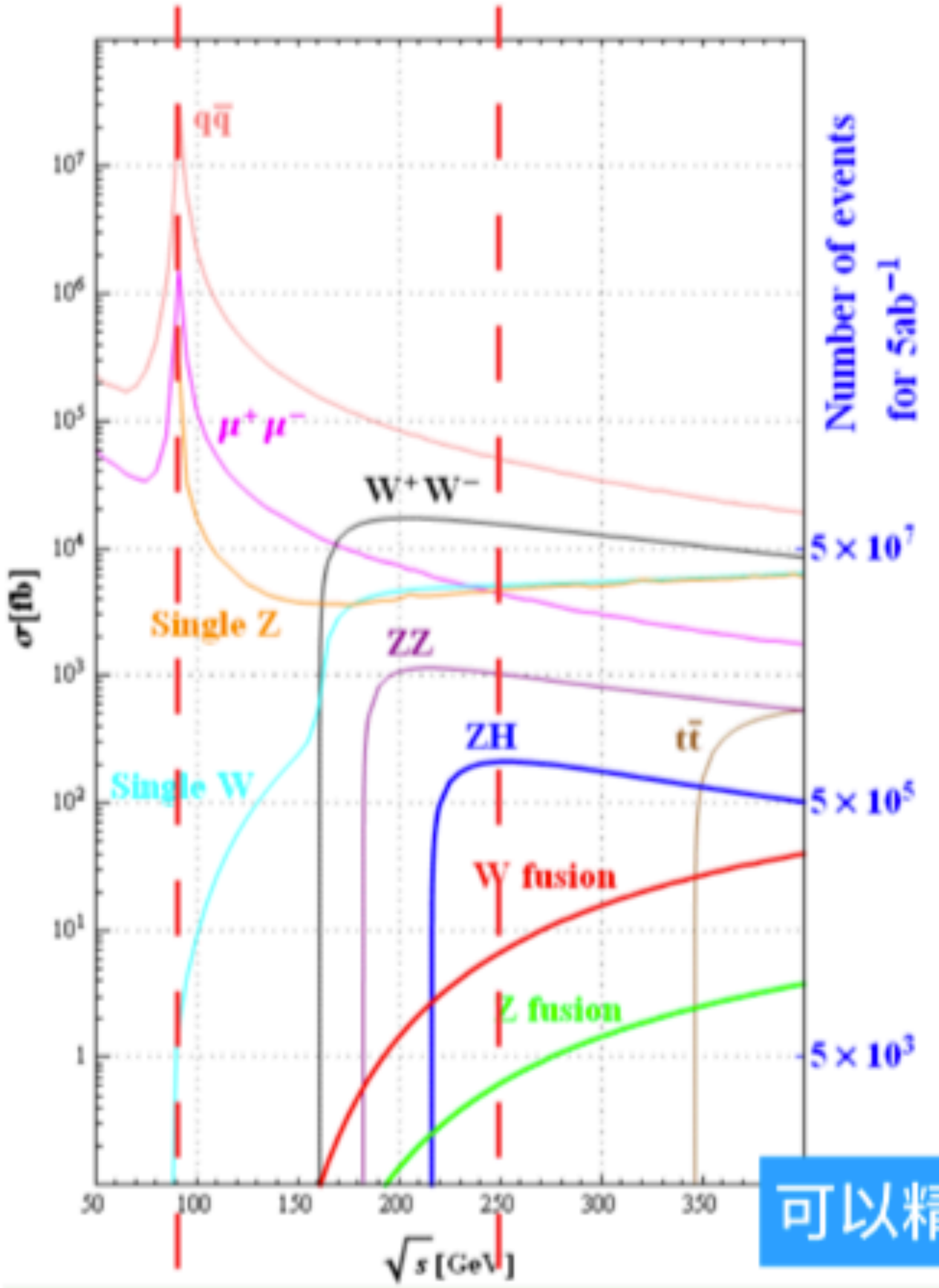

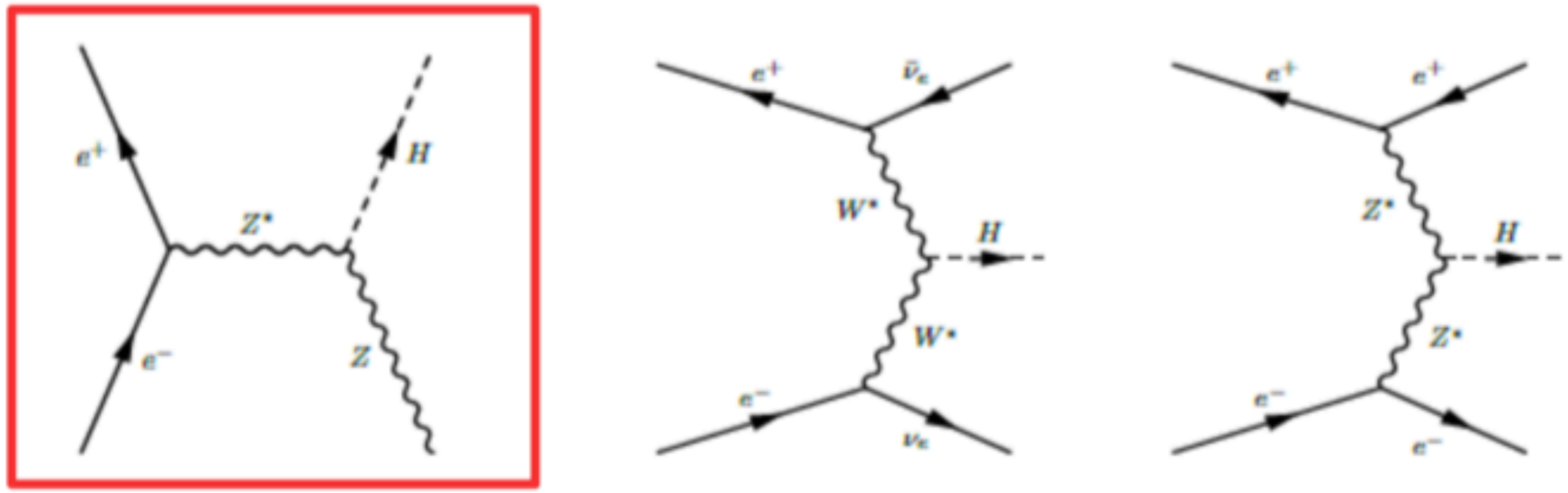

Process	Cross section	Events in 5 ab^{-1}
Higgs boson production, cross section in fb		
$e^+e^- \to ZH$	212	1.06×10^6
$e^+e^- \to \nu\bar{\nu}H$	6.72	3.36×10^4
$e^+e^- \to e^+e^-H$	0.63	3.15×10^3

可以精确测量除了 Higgs 自耦合以外的所有性质，精度比 LHC 高一个量级

CEPC: 1M Higgs events、10B+ Z boson

精确测量几乎所有 Higgs 性质，精度提高一个量级

标准模型关键参数的测量精度有望超过一个量级

Flavor physics at Z pole + 双光子对撞

How to do precise calculation?

pp Collision

- The proton-proton collision.

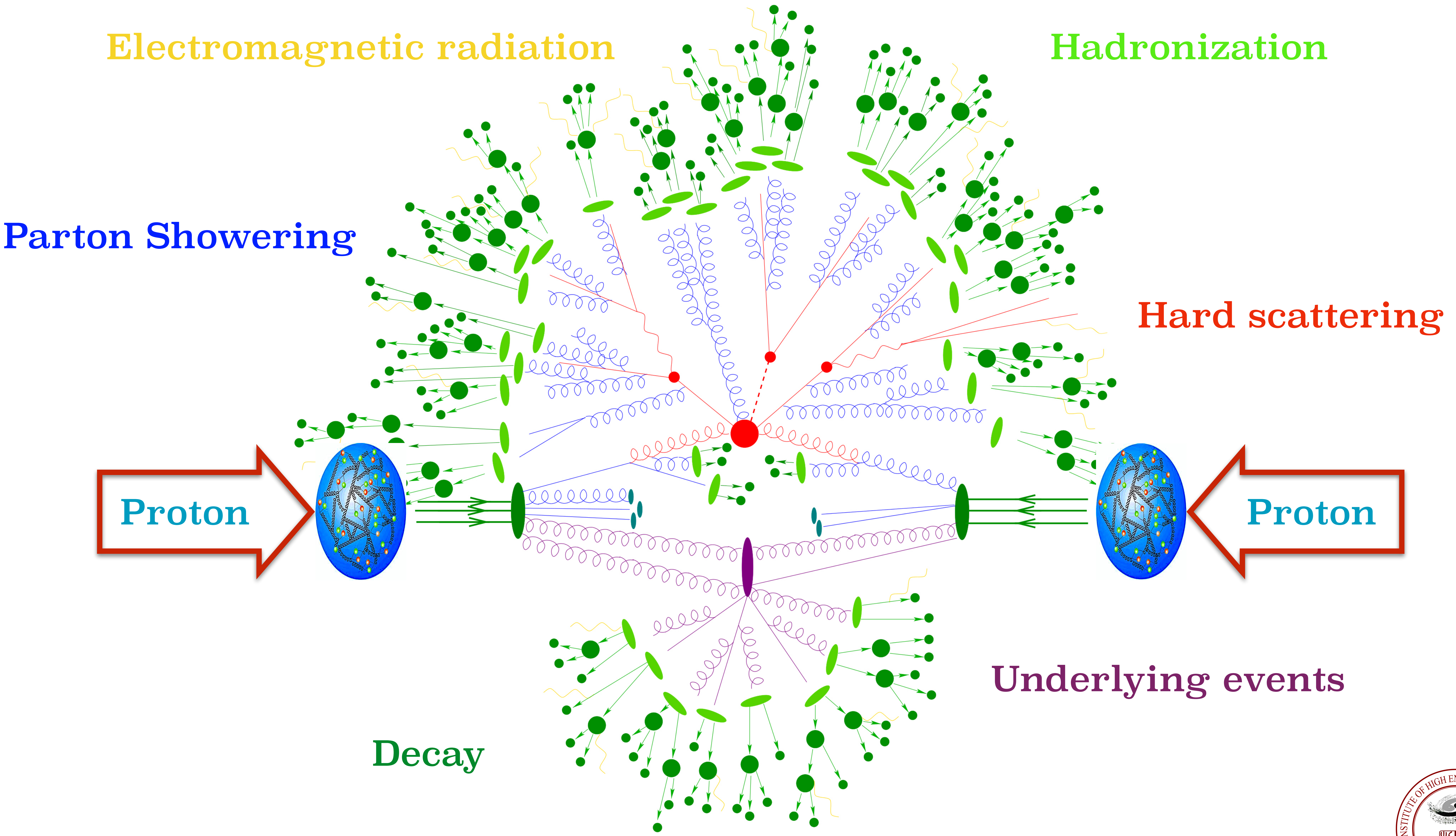

（强子）散射过程的因子化

- 部分子分布函数
- 部分子硬散射截面/振幅
- 喷柱函数（碎裂函数）

部分子分布函数（Parton Distribution Function）

部分子分布函数（Parton Distribution Function）

强子散射 ⟷ PDF ⟷ 部分子散射

$$f_{i/H}(x, \mu_F)$$

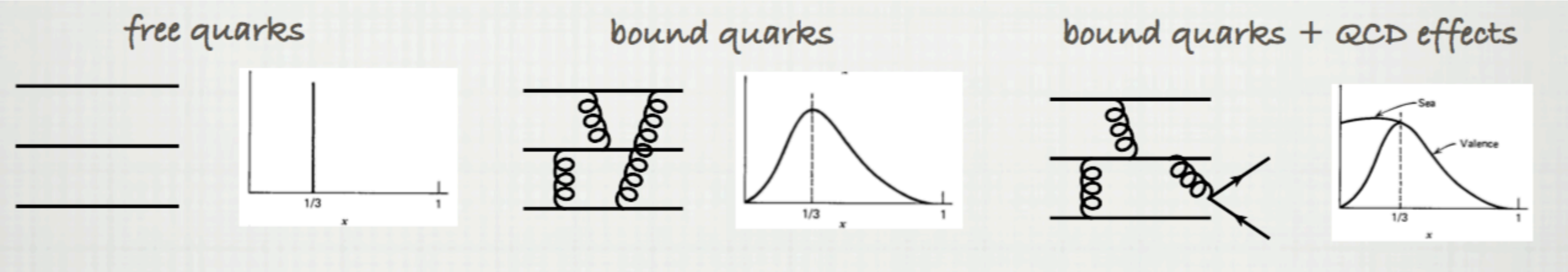

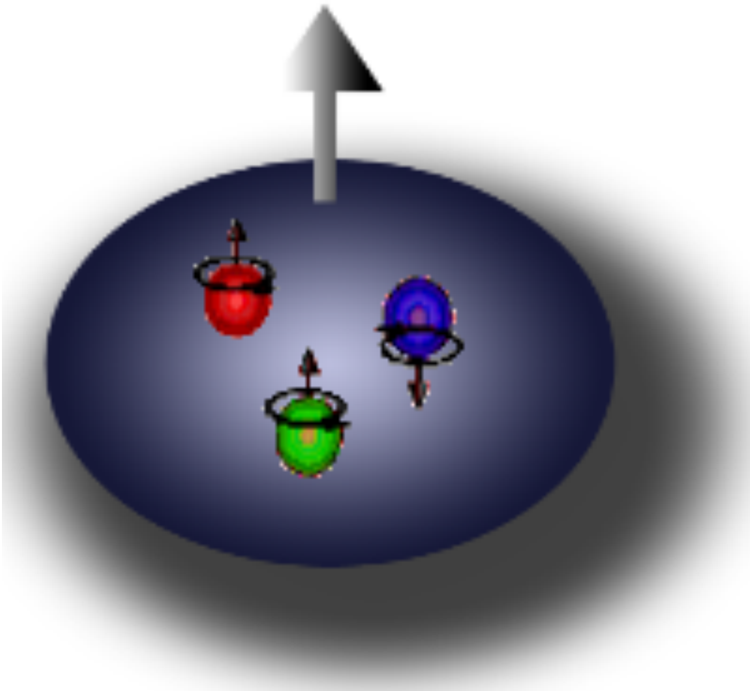

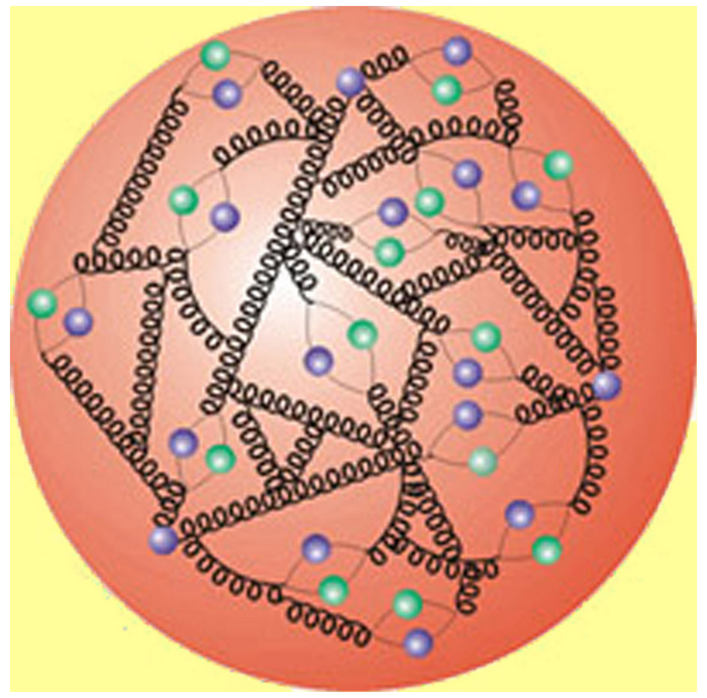

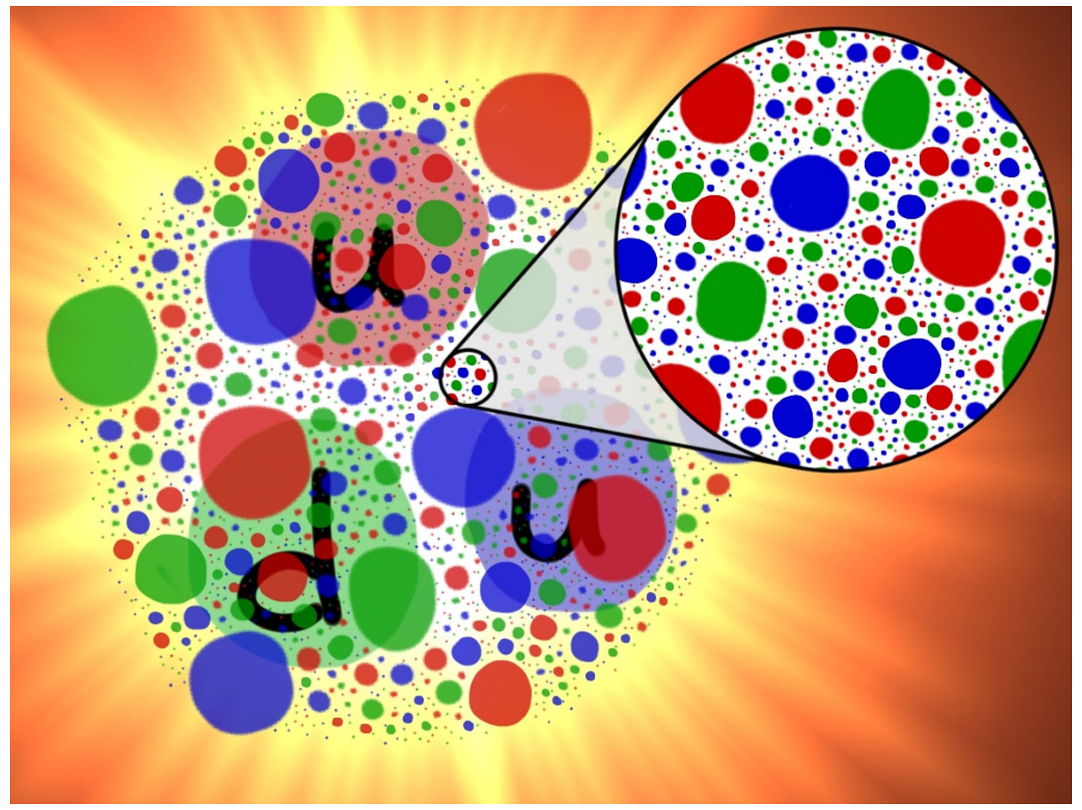

LHAPDF is hosted by Hepforge, IPPP Durham

LHAPDF 6.2.1

LHAPDF Documentation

Introduction

LHAPDF is a general purpose C++ interpolator, used for evaluating PDFs from discretised data files. Previous versions of **LHAPDF** were written in Fortran 77/90 and are documented at http://lhapdf.hepforge.org/lhapdf5/.

LHAPDF6 vastly reduces the memory overhead of the Fortran **LHAPDF** (from gigabytes to megabytes!), entirely removes restrictions on numbers of concurrent PDFs, allows access to single PDF members without needing to load whole sets, and separates a new standardised PDF data format from the code library so that new PDF sets may be created and released easier and faster. The C++ LHAPDF6 also permits arbitrary parton contents via the standard PDG ID code scheme, is computationally more efficient (particularly if only one or two flavours are required at each phase space point, as in PDF reweighting), and uses a flexible metadata system which fixes many fundamental metadata and concurrency bugs in LHAPDF5.

Compatibility routines are provided as standard for existing C++ and Fortran codes using the LHAPDF5 and PDFLIB legacy interfaces, so you can keep using your existing codes. But the new interface is much more powerful and pleasant to work with, so we think you'll want to switch once you've used it!

LHAPDF6 is documented in more detail in http://arxiv.org/abs/1412.7420

Table of Contents

LHC: CTEQ, MSTW/MMHT, NNPDF

PDF from Lattice

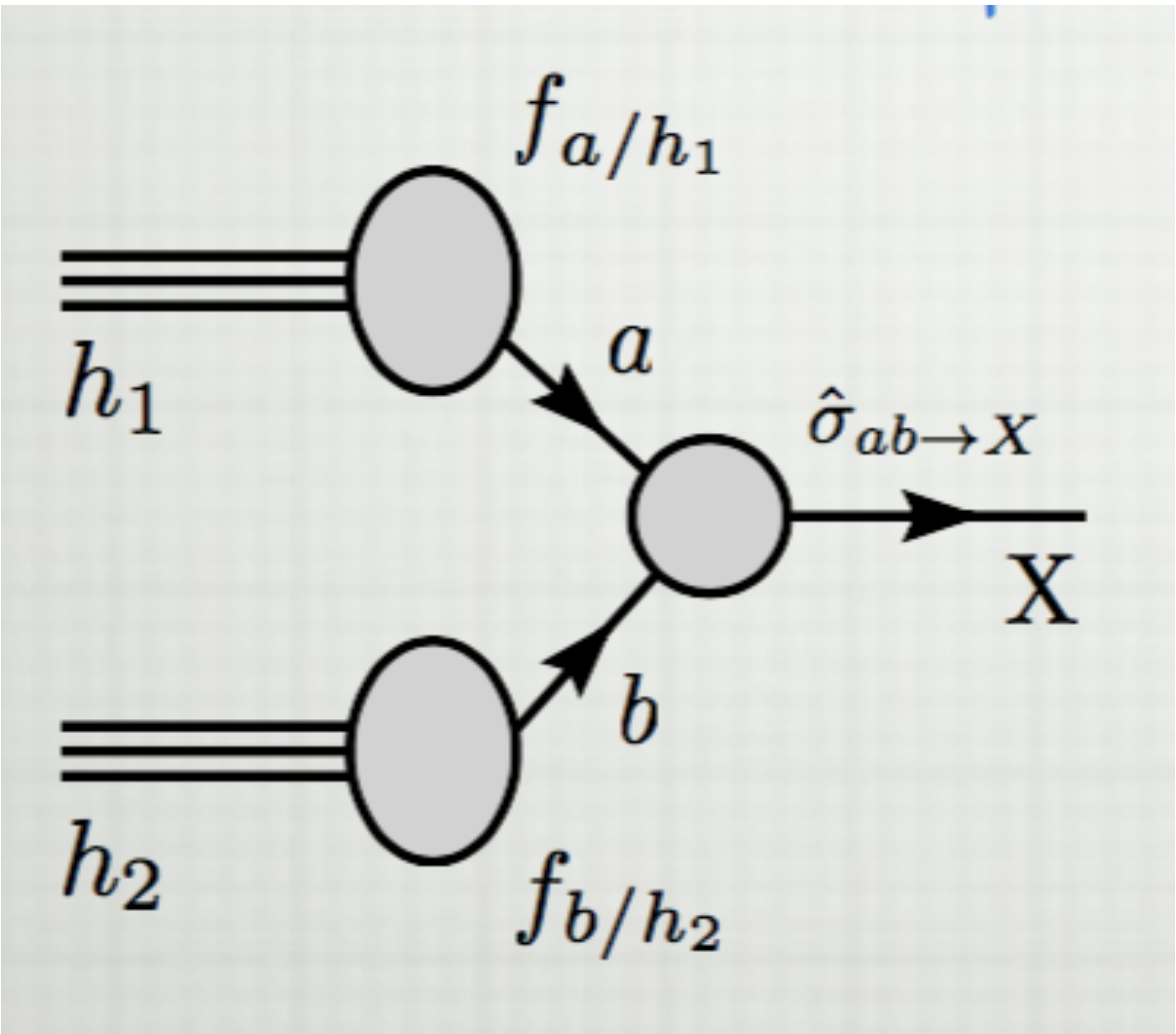

$$\sigma = \sum_{a,b} \int \mathrm{d}x_1 \mathrm{d}x_2 f_{a/h_1}(x_1) f_{b/h_2}(x_2) \hat{\sigma}_{ab\to X}(x_1, x_2).$$

实验

Universal
通过global fitting反解

微扰论计算

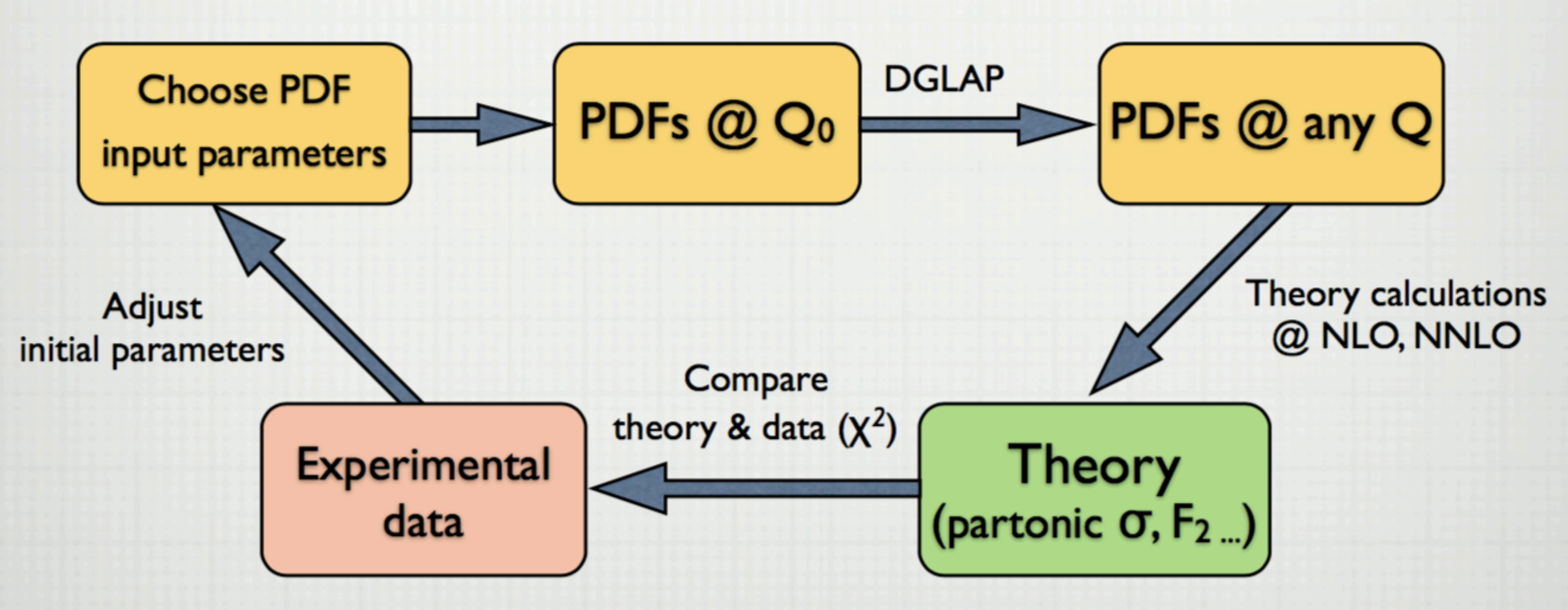

$$\sigma = \sum_{a,b} \int \mathrm{d}x_1 \mathrm{d}x_2 f_{a/h_1}(x_1) f_{b/h_2}(x_2) \hat{\sigma}_{ab\to X}(x_1, x_2).$$

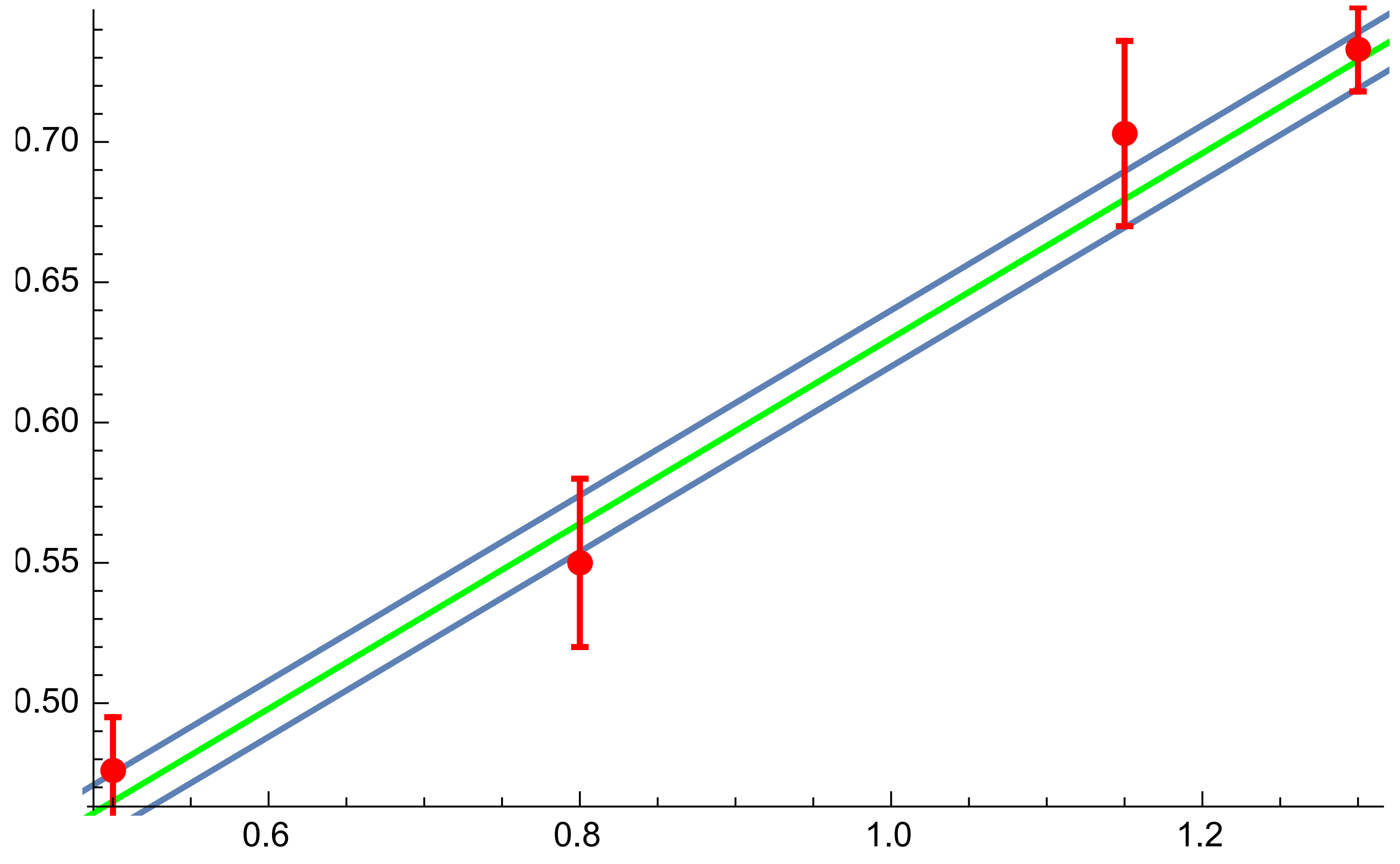

PDF 不确定度

LHAPDF ID	Set name	Number of set members
13100	CT14nlo	57
25300	MMHT2014nnlo68cl	51
260000	NNPDF30_nlo_as_0118	101

$$(\Delta\sigma)^2 \approx \frac{1}{4}\sum_{i}^{N_p}\left(\sigma(X_i^+) - \sigma(X_i^-)\right)^2$$

有效x的估计

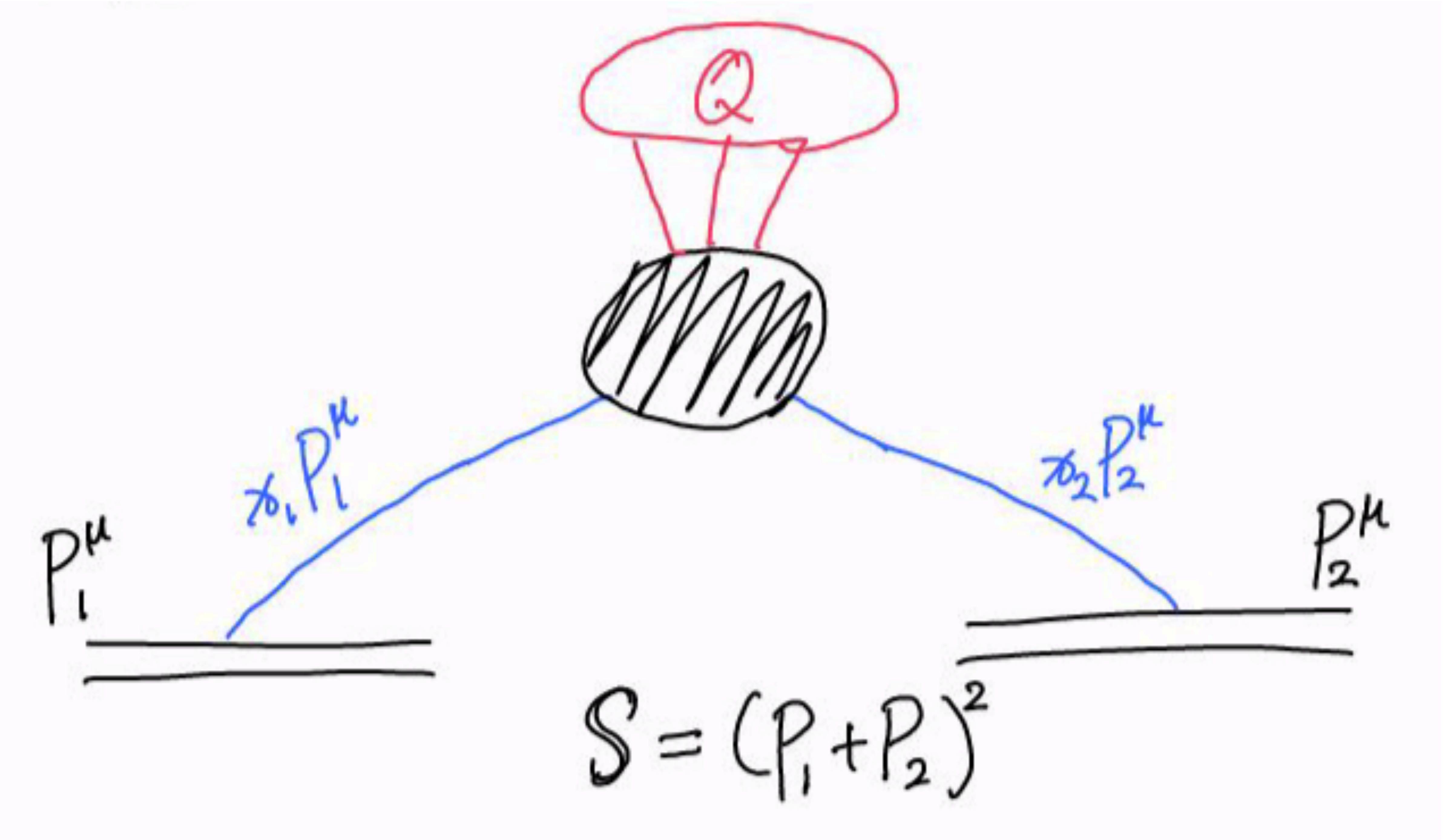

$$
\begin{aligned}
Q^2 &= (p_1 + p_2)^2 = 2p_1 \cdot p_2 \\
&= 2x_1 x_2 \mathbf{P}_1 \cdot \mathbf{P}_2 = x_1 x_2 \left(\mathbf{P}_1 + \mathbf{P}_2\right)^2 \\
&= x_1 x_2 \mathbf{S}
\end{aligned}
$$

$$x_1 \approx x_2$$

$$\hat{s} = x^2 \mathbf{S}$$

$$x \approx \frac{\sqrt{\hat{s}}}{\sqrt{\mathbf{S}}} \approx \frac{\sum_i m_i}{\sqrt{\mathbf{S}}}$$

- ***Parton Distribution Functions in Higgs production***
  - Higgs is pre-dominantly produced through gluon fusion -
    gluon PDFs at $x = M_H/\sqrt{s} \sim 0.02$ are crucial
  - sub-leading Higgs production via VBF is sensitive to quark & anti-quark PDFs

GLUON FUSION

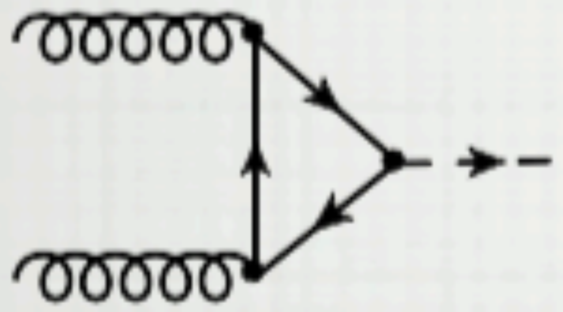

ASSOCIATED PRODUCTION

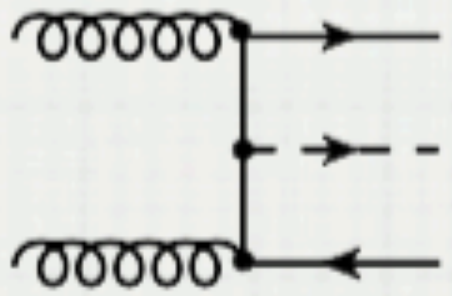

VECTOR-BOSON FUSION

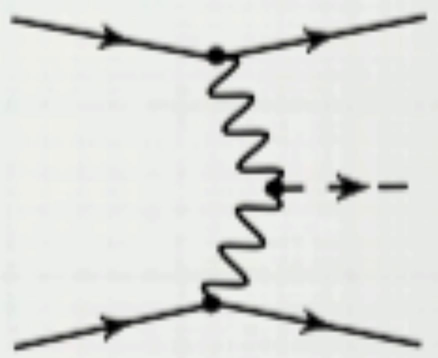

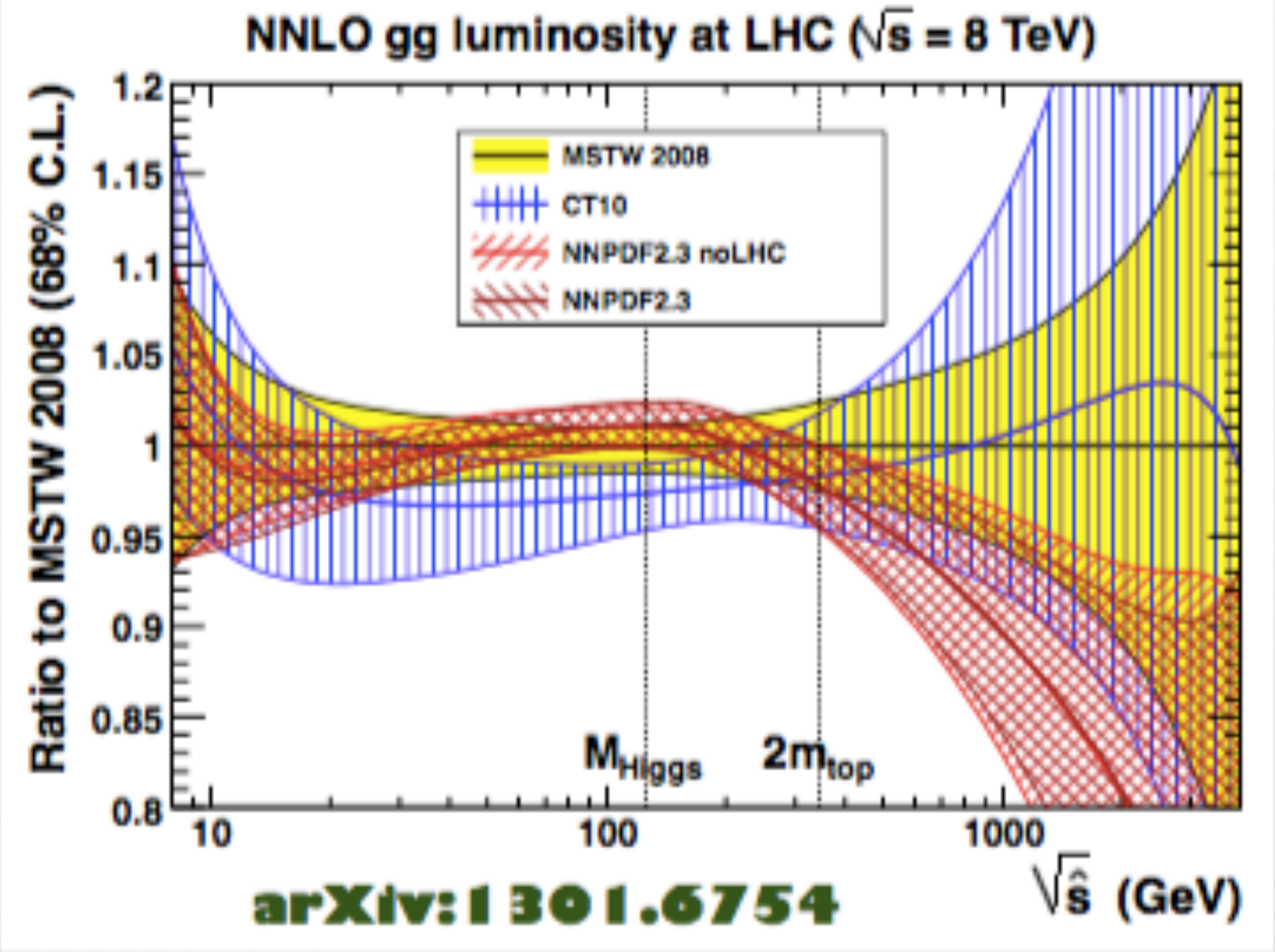

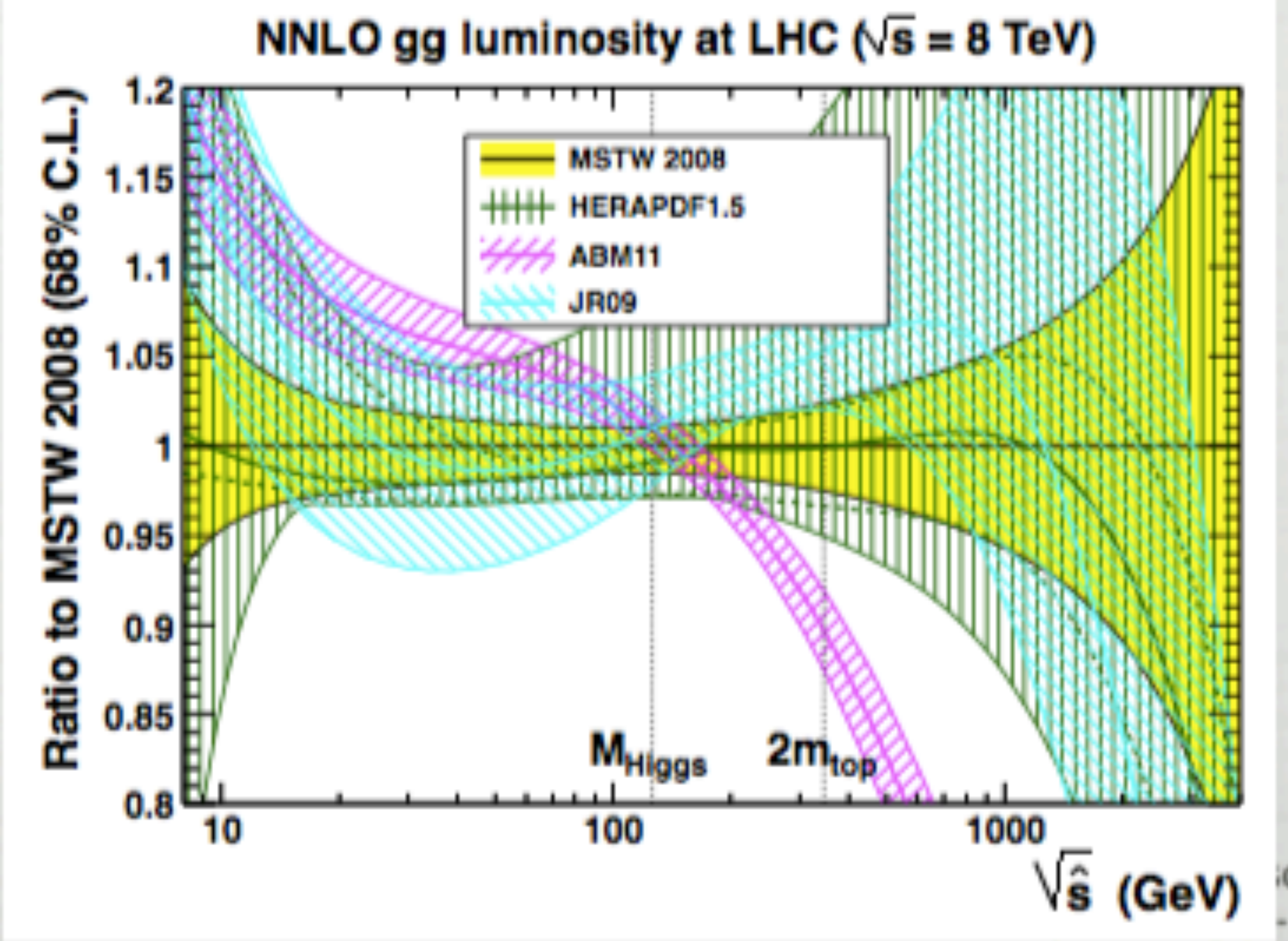

- ***Parton Distribution Functions in top quark pair production***
  - Top quark pair production is dominated by s-channel diagrams where valence quarks & gluons are important at $\mathbf{x=2m_t/\sqrt{s} \sim 0.05}$

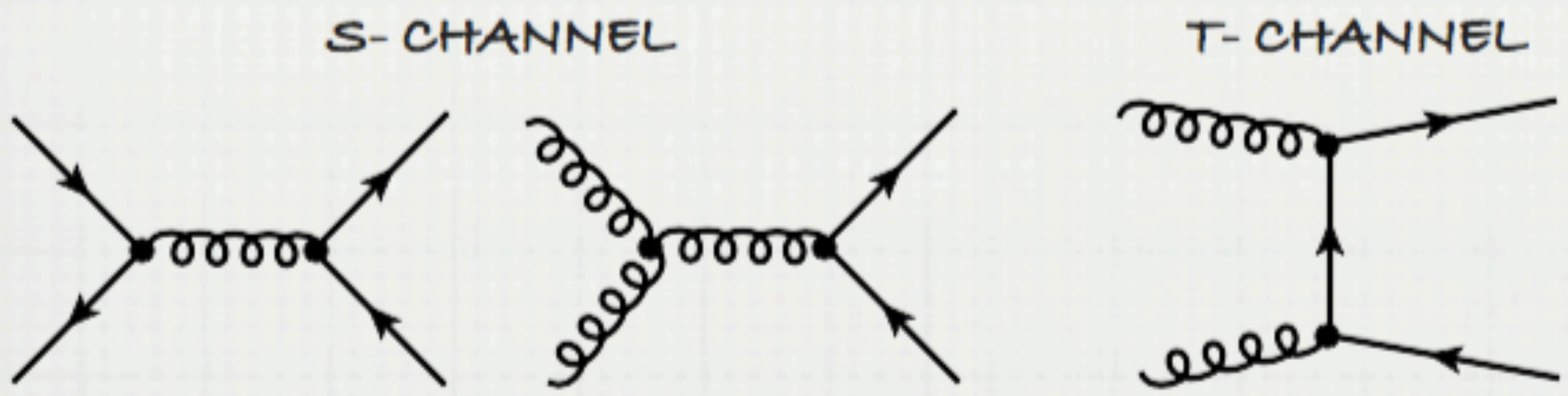

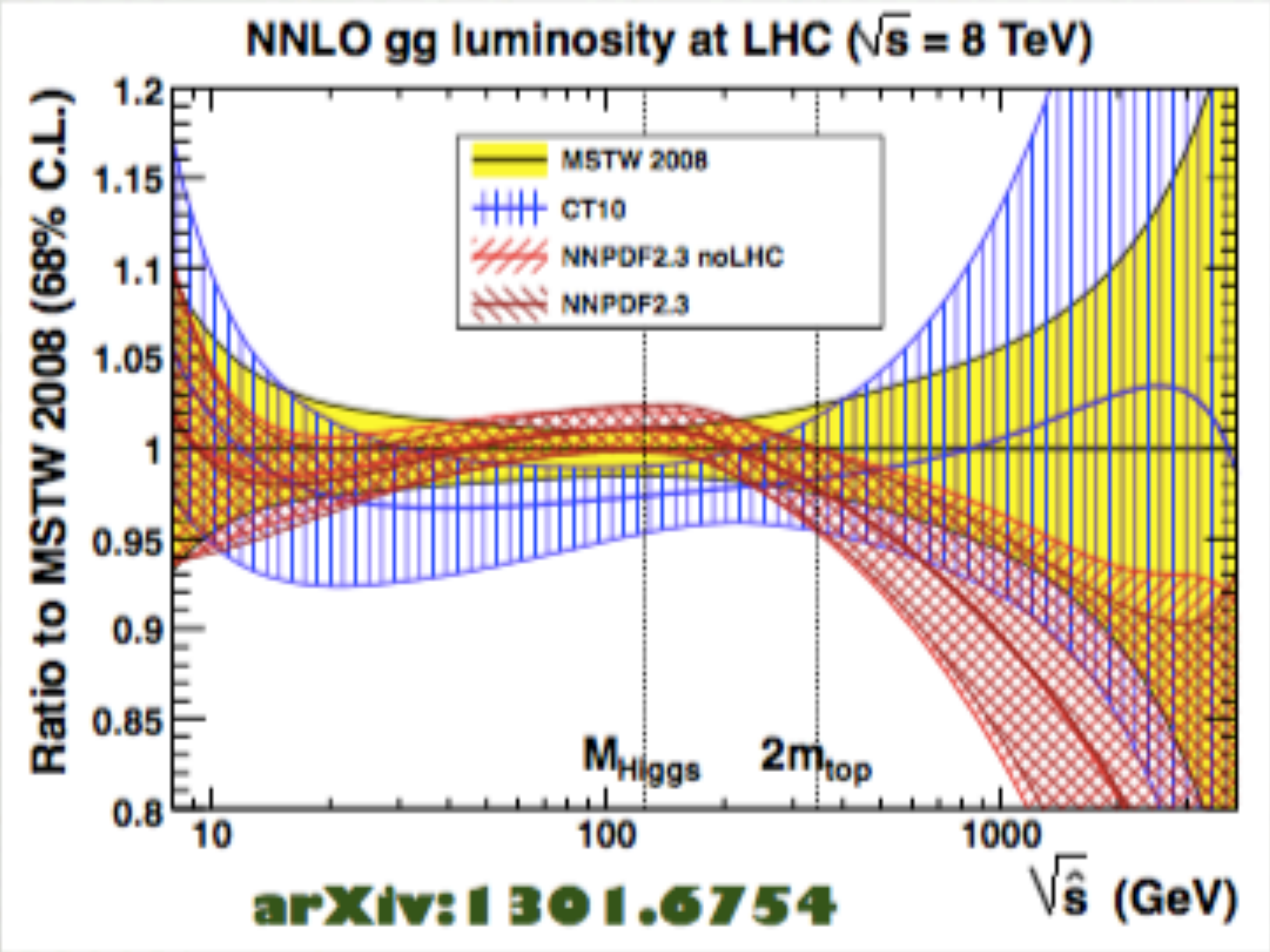

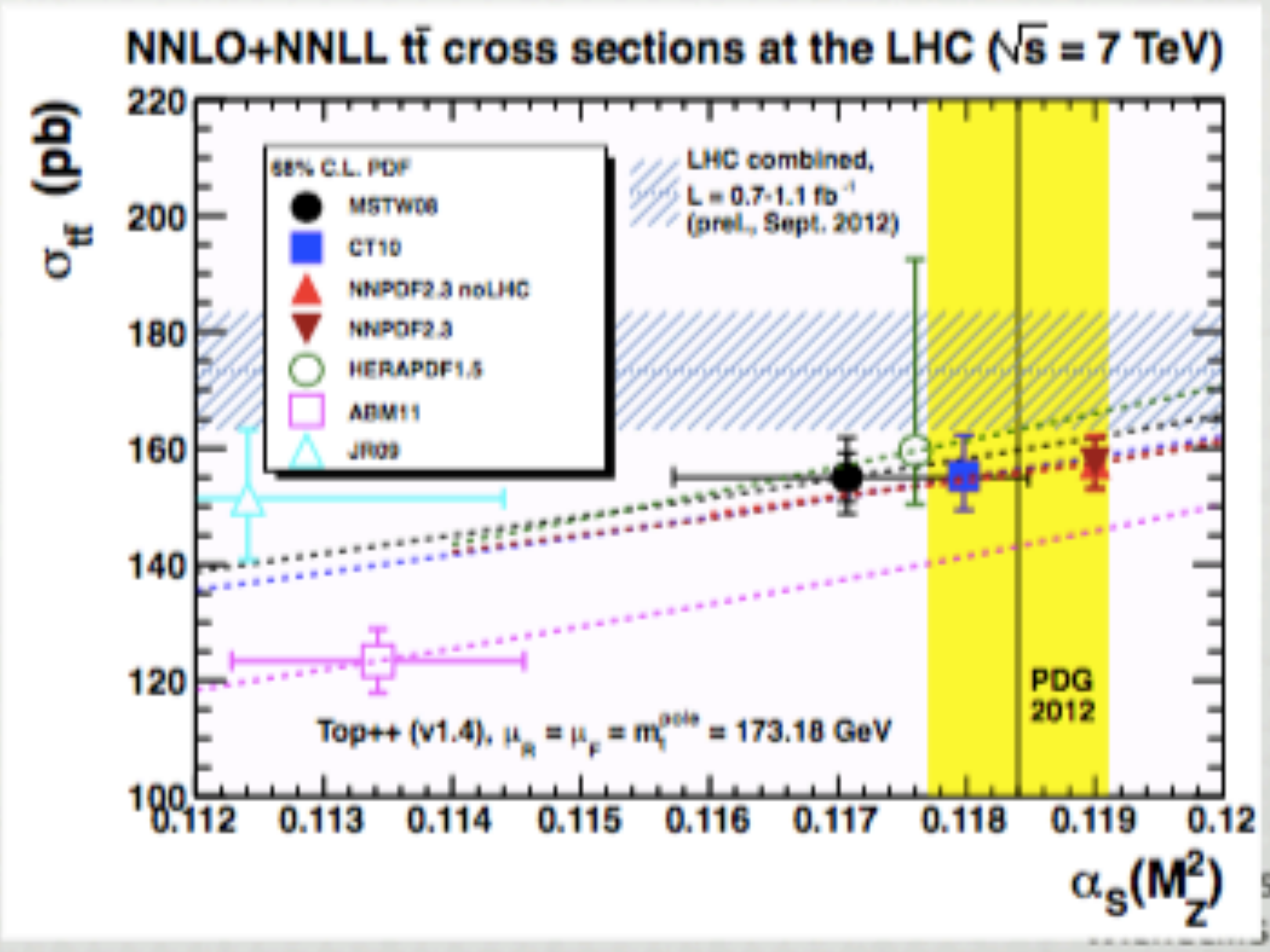

Parton Distribution Functions in SUSY production

- production of SUSY coloured particles (squarks & gluinos) very sensitive to gluon PDF at very high $x=2m_X/\sqrt{s}$ ~ 0.2-0.7

very problematic

SQUARK PRODUCTION

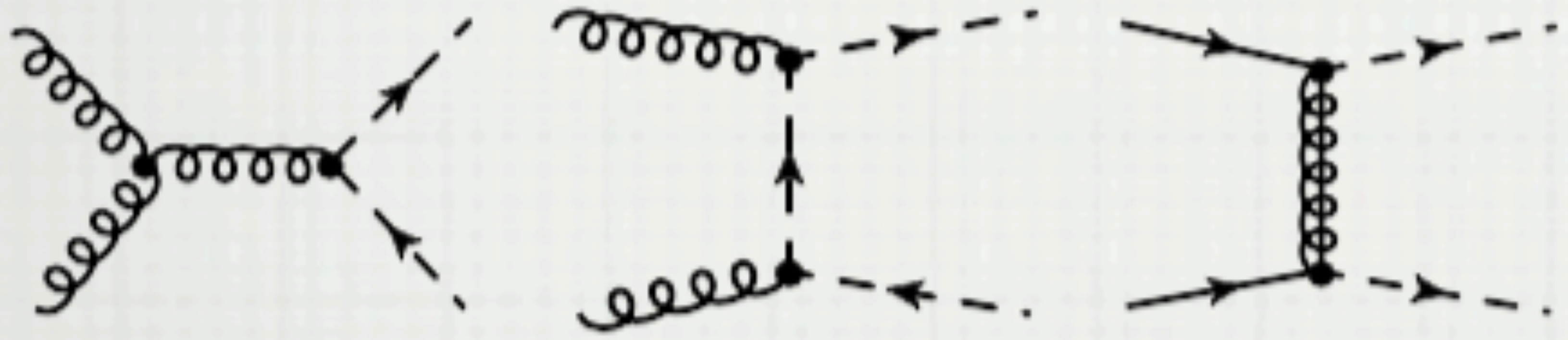

GLUINO PRODUCTION

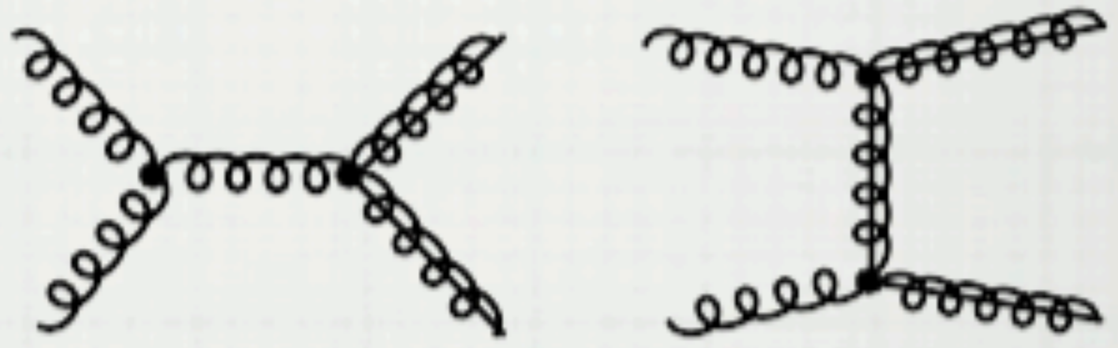

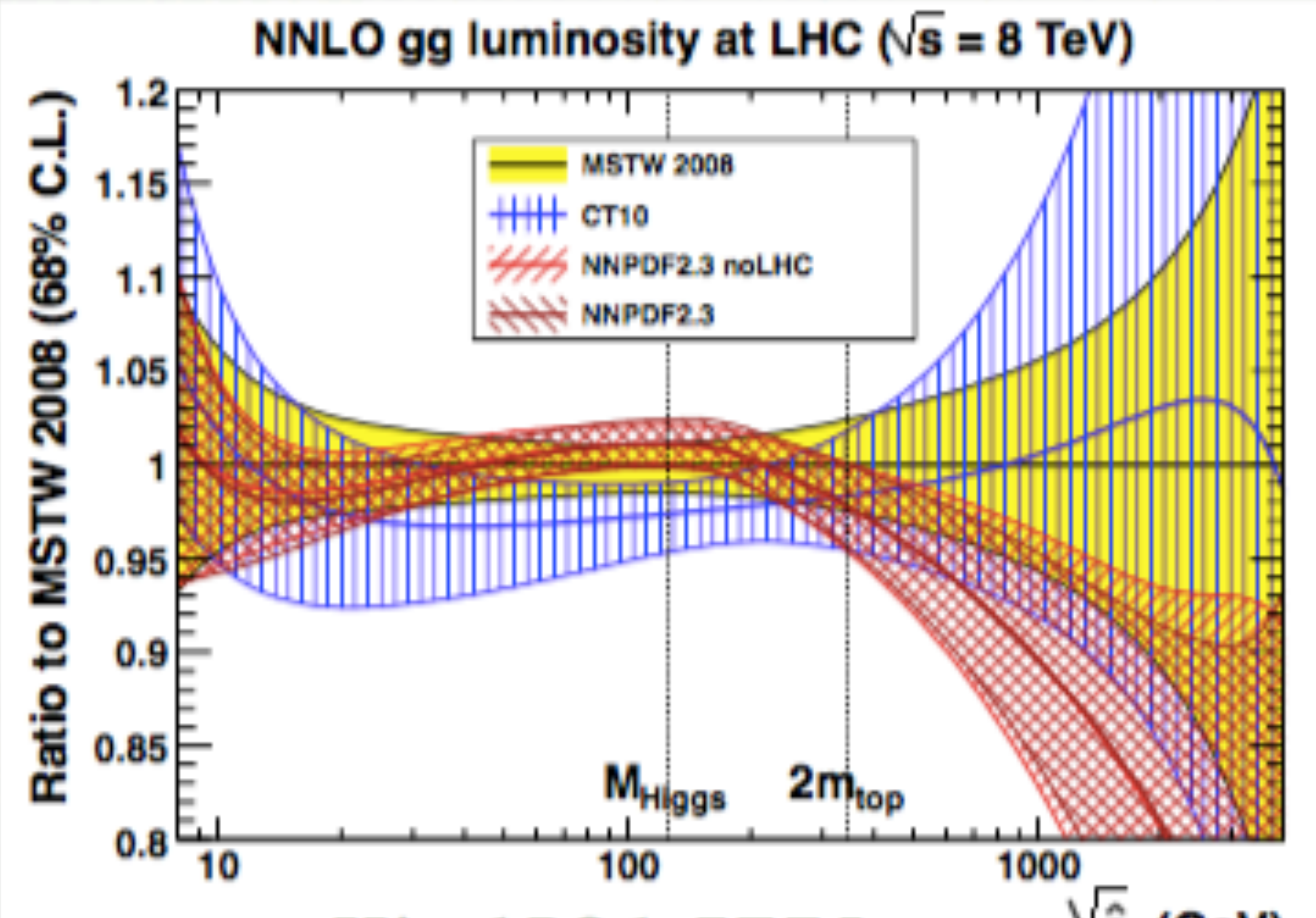

arXiv:1301.6754

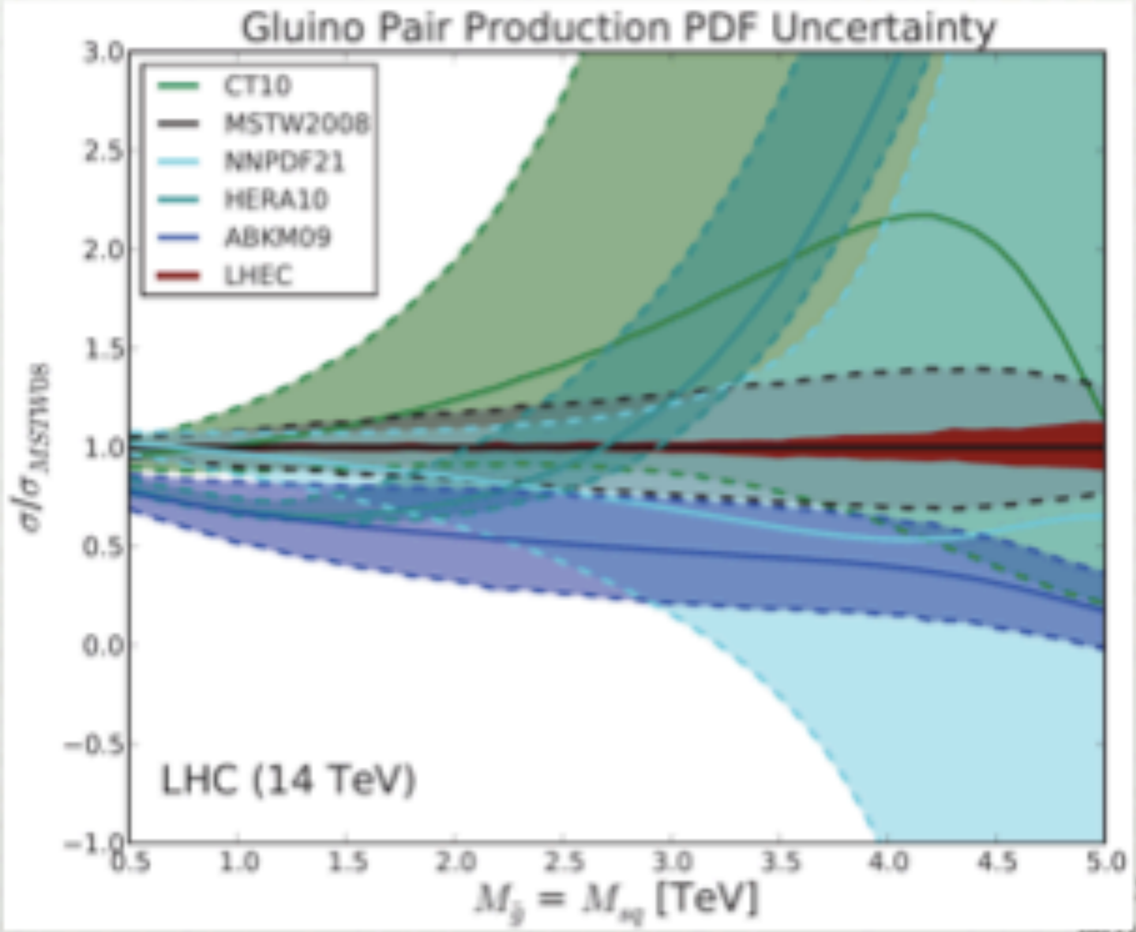

arXiv:1206.2913

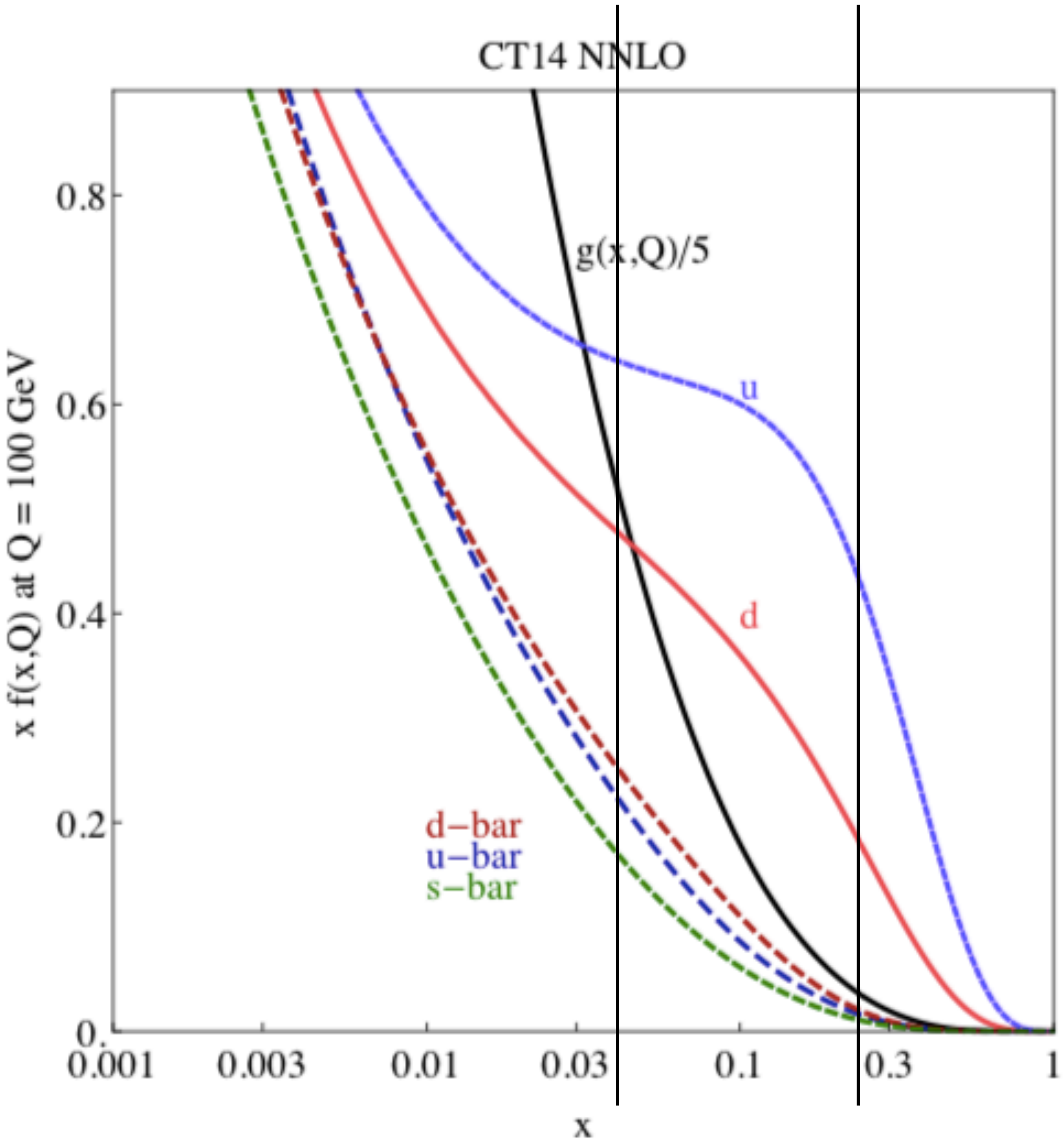

top pair @ Tevatron 1.96TeV

$$x \approx 0.2$$

$$q\bar{q} : f_{q/p} f_{\bar{q}/\bar{p}} = f_{q/p} f_{q/p}$$ **Dominant!**

$$gg : f_{g/p} f_{g/\bar{p}} = f_{g/p} f_{g/p}$$

top pair @ LHC 8 TeV

$$x \approx 0.04$$

$$q\bar{q} : f_{q/p} f_{\bar{q}/p}$$

$$gg : f_{g/p} f_{g/p}$$ **Dominant!**

散射截面的PDF不确定度

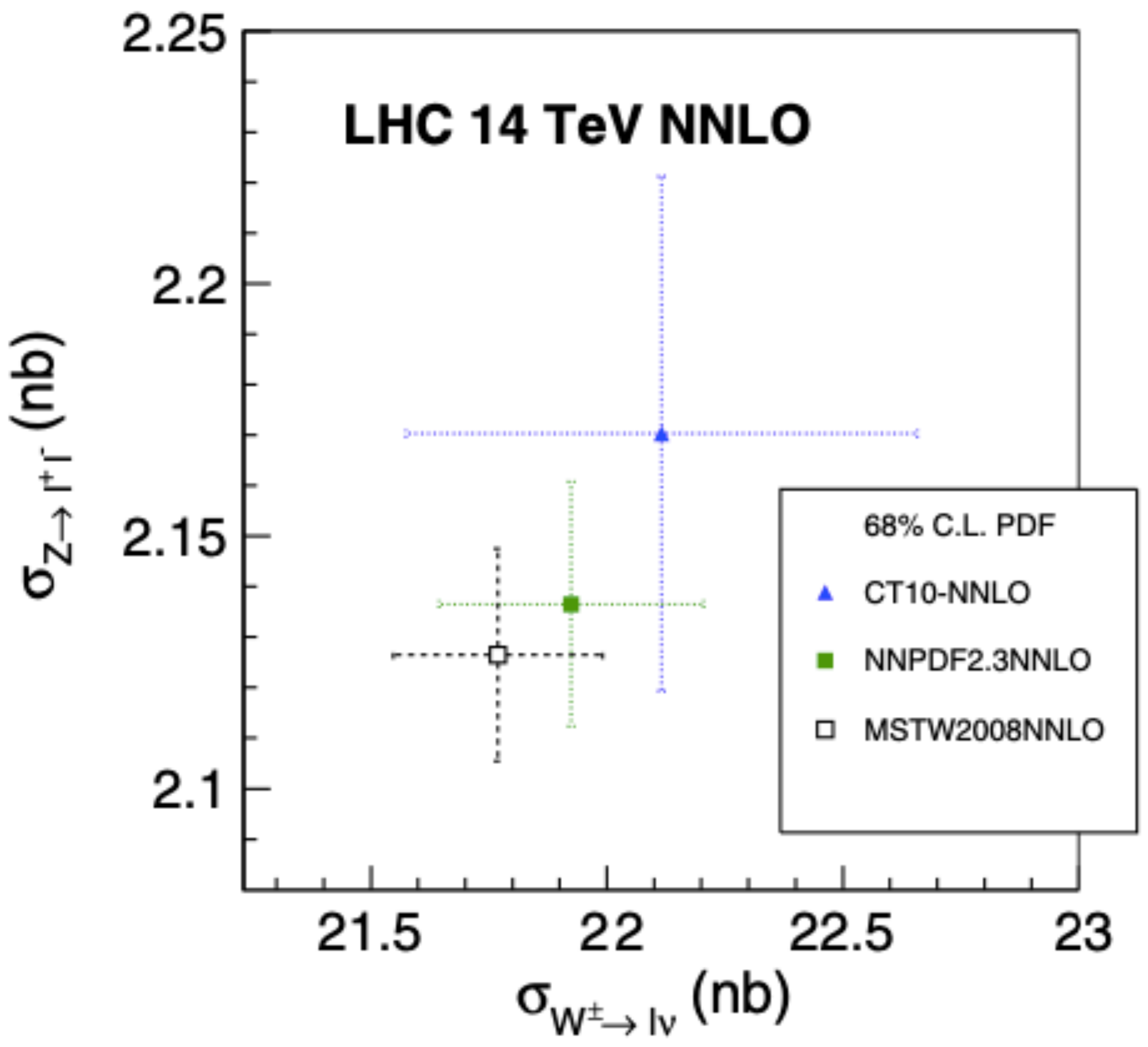

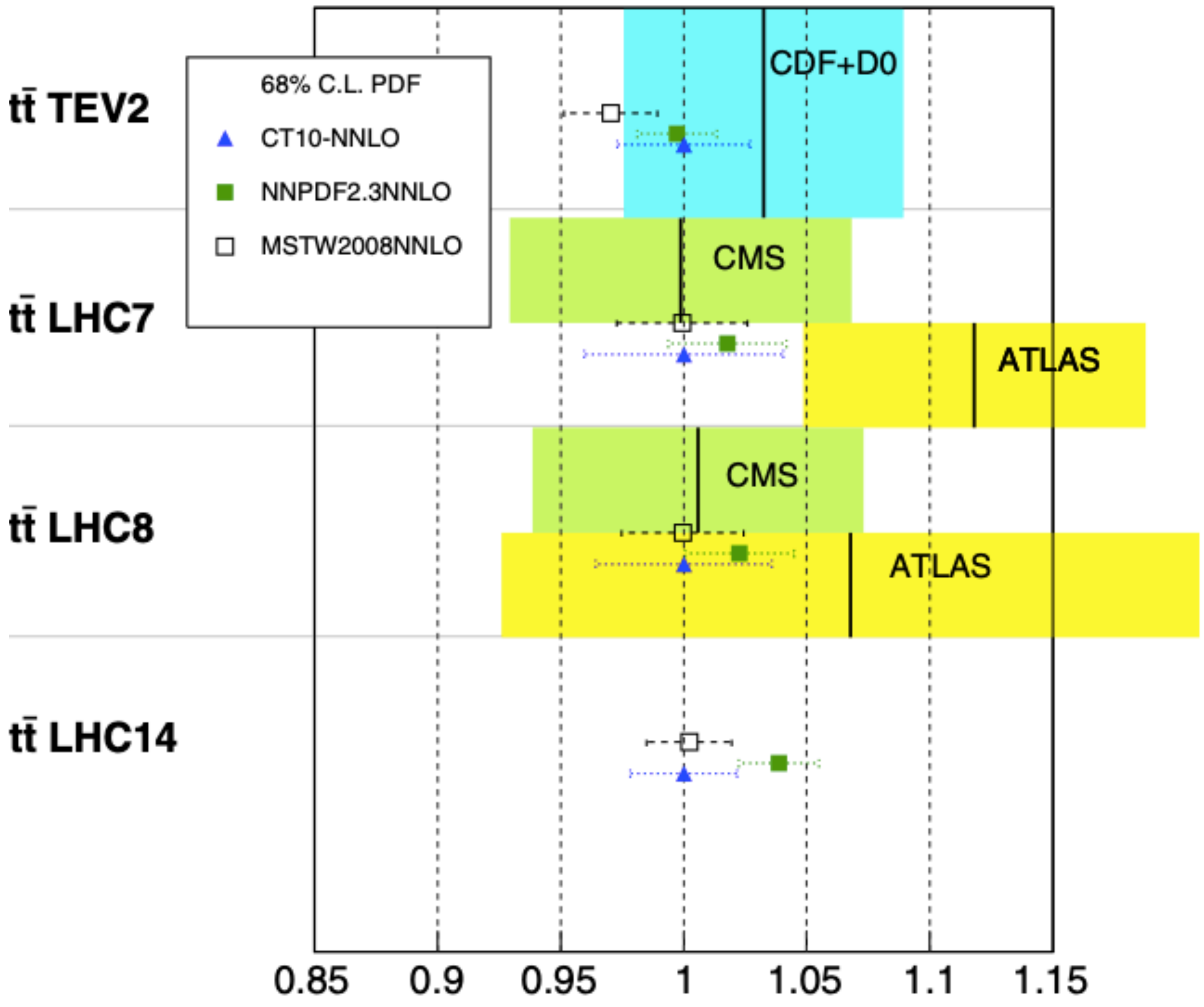

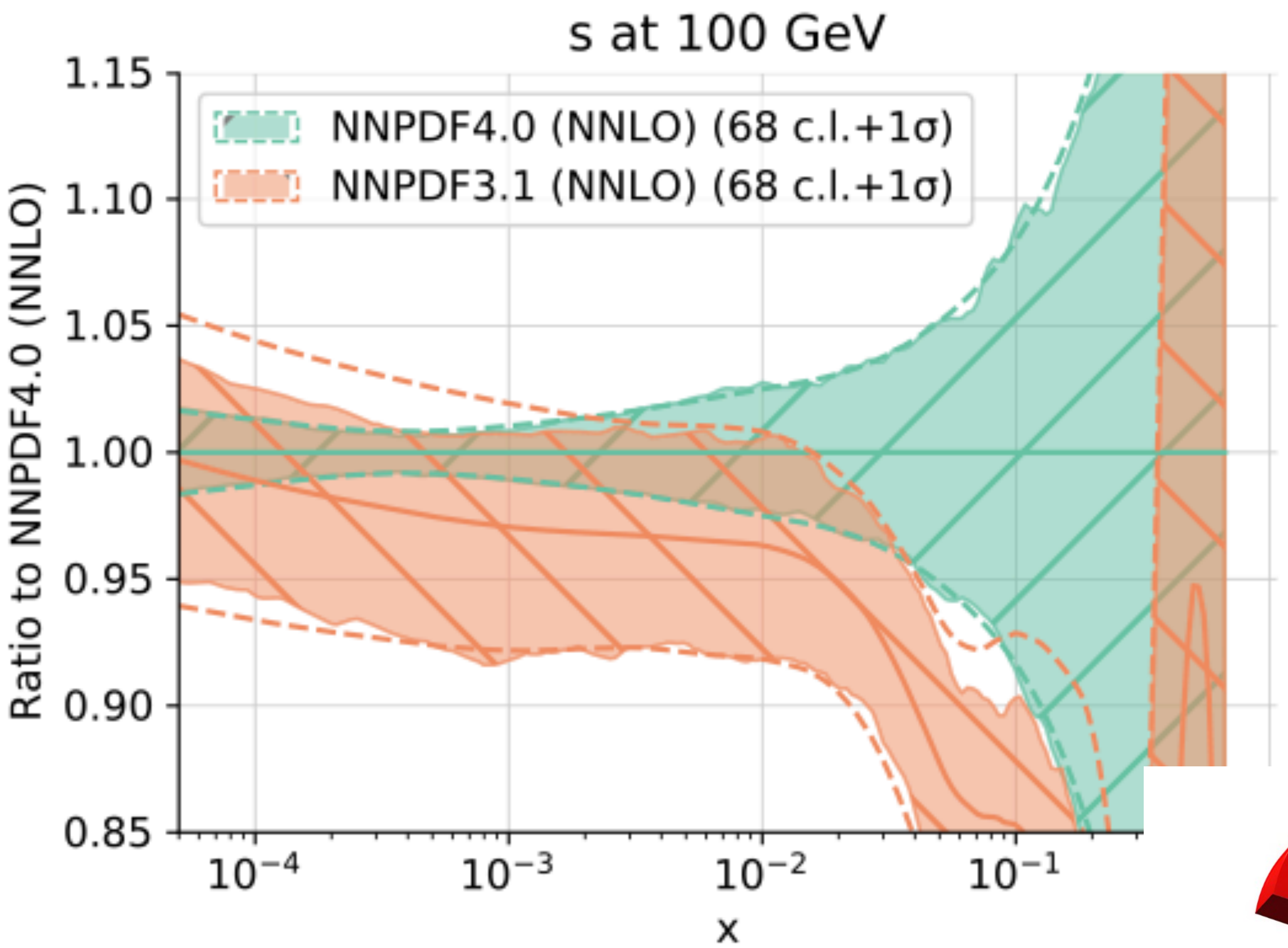

NNPDF Collaboration, R. D. Ball et al., Eur. Phys. J. C 82 no. 5, (2022) 428

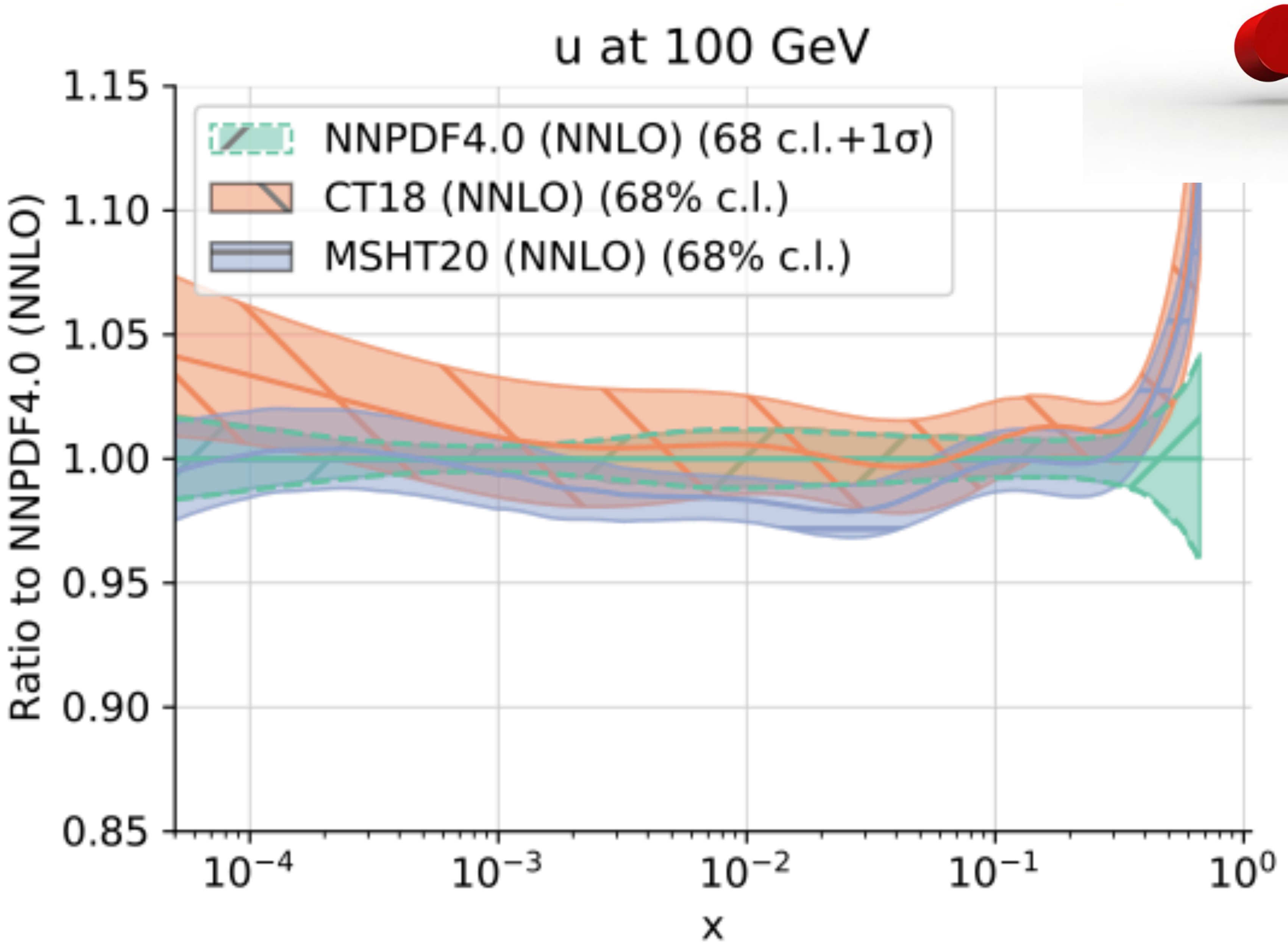

Possible Reason from a toy model

arXiv:2211.xxxxx, Mengshi Yan*, Tie-Jiun Hou, Zhao Li, Kritimaan Mohan, and C.–P. Yuan

$$g(x) = a_0\ x^{a_1}(1-x)^{a_2} e^{x a_3}(1+x e^{a_4})^{a_5}$$

$$\Delta g(x) = \frac{\alpha}{\sqrt{g(x)}}.$$

	$N_{\rm pt}$	a_0	a_1	a_2	a_3	a_4	a_5
pseudo-data #1	50	30	0.5	2.4	4.3	2.4	-3.0
pseudo-data #2	50	30	0.5	2.4	4.3	2.6	-2.8

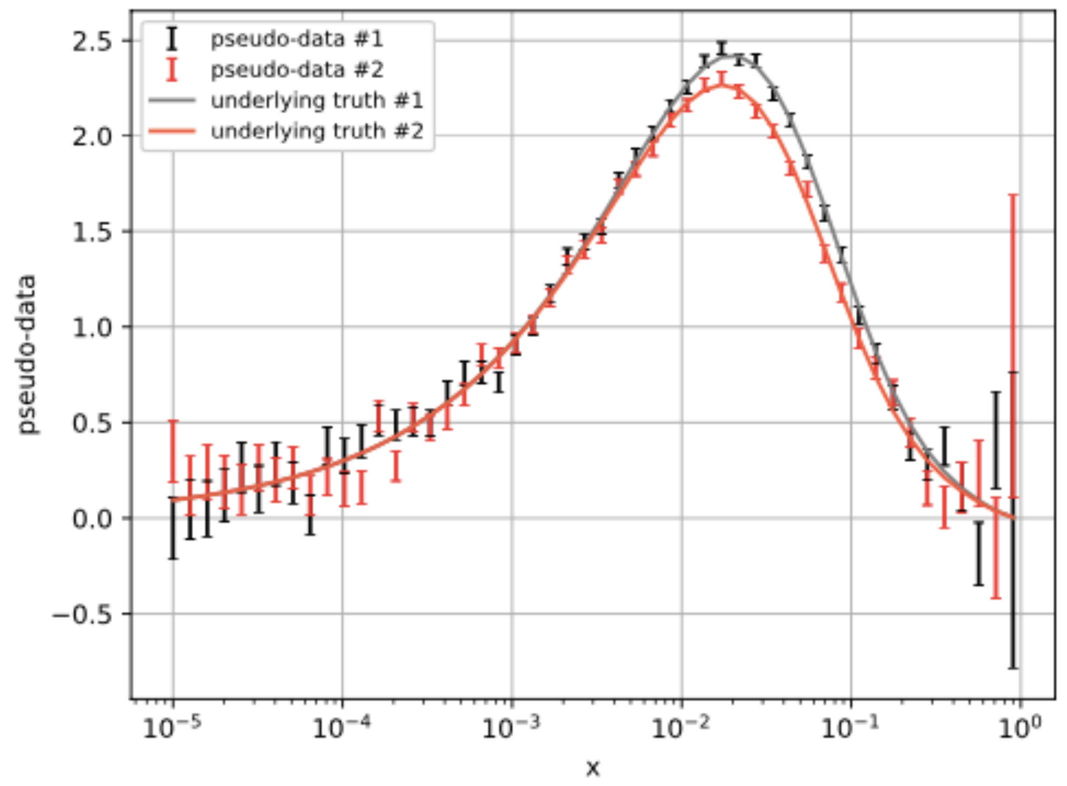

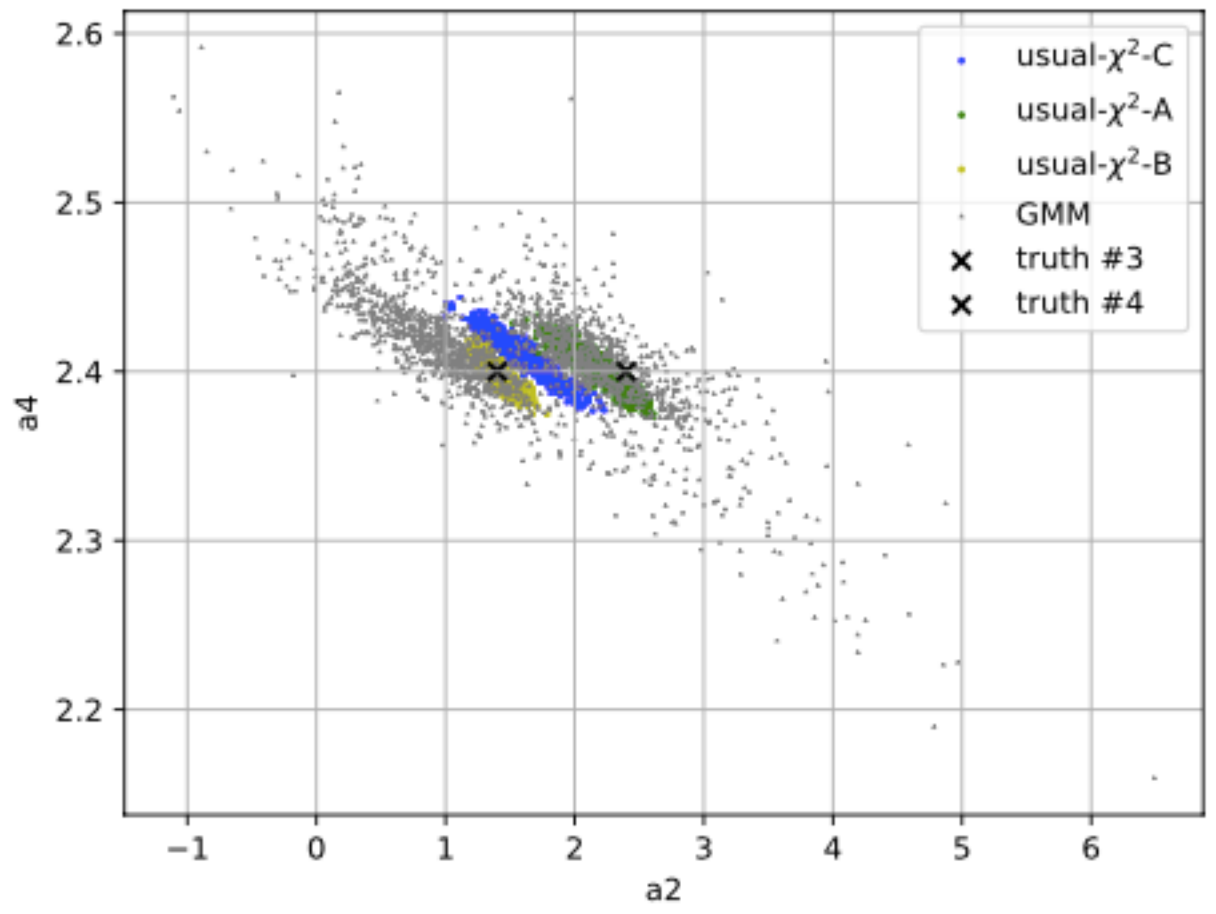

喷柱 Jet

喷柱 Jet

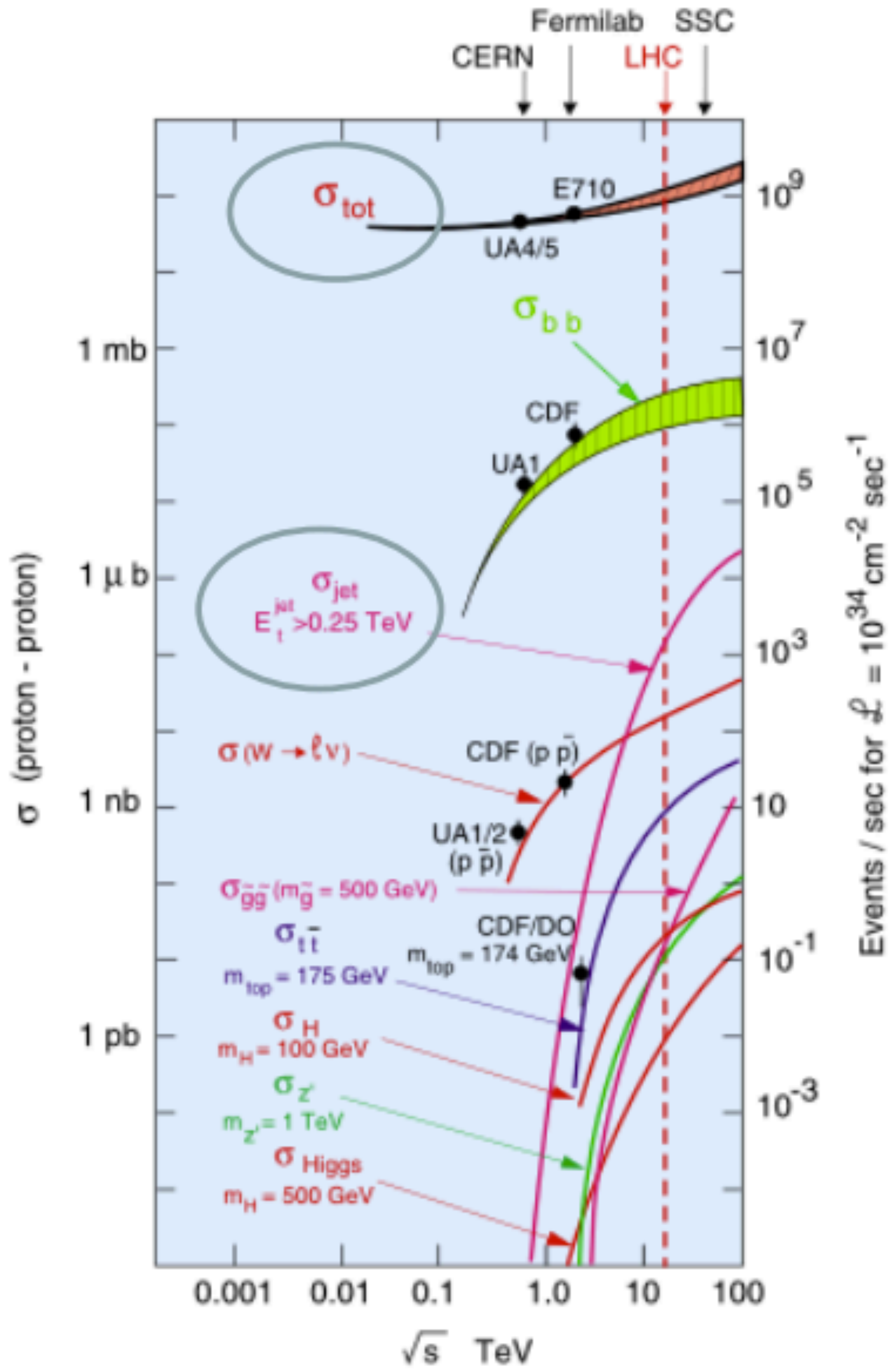

Fermilab
SSC
CERN
LHC
σ tot
E710
UA4/5
σ b b
CDF
UA1
1 mb
1 μ b
1 nb
1 pb
σ jet
E_t^jet >0.25 TeV
σ (W → ℓν)
CDF (p p̄)
UA1/2 (p p̄)
σ g̃g̃ (m g̃ = 500 GeV)
σ tt̄
m top = 175 GeV
CDF/DO
m top = 174 GeV
σ H
m H = 100 GeV
σ Z'
m Z' = 1 TeV
σ Higgs
m H = 500 GeV
σ (proton - proton)
Events / sec for ℒ = 10^34 cm^-2 sec^-1
10^9
10^7
10^5
10^3
10
10^-1
10^-3
0.001
0.01
0.1
1.0
10
100
√s TeV

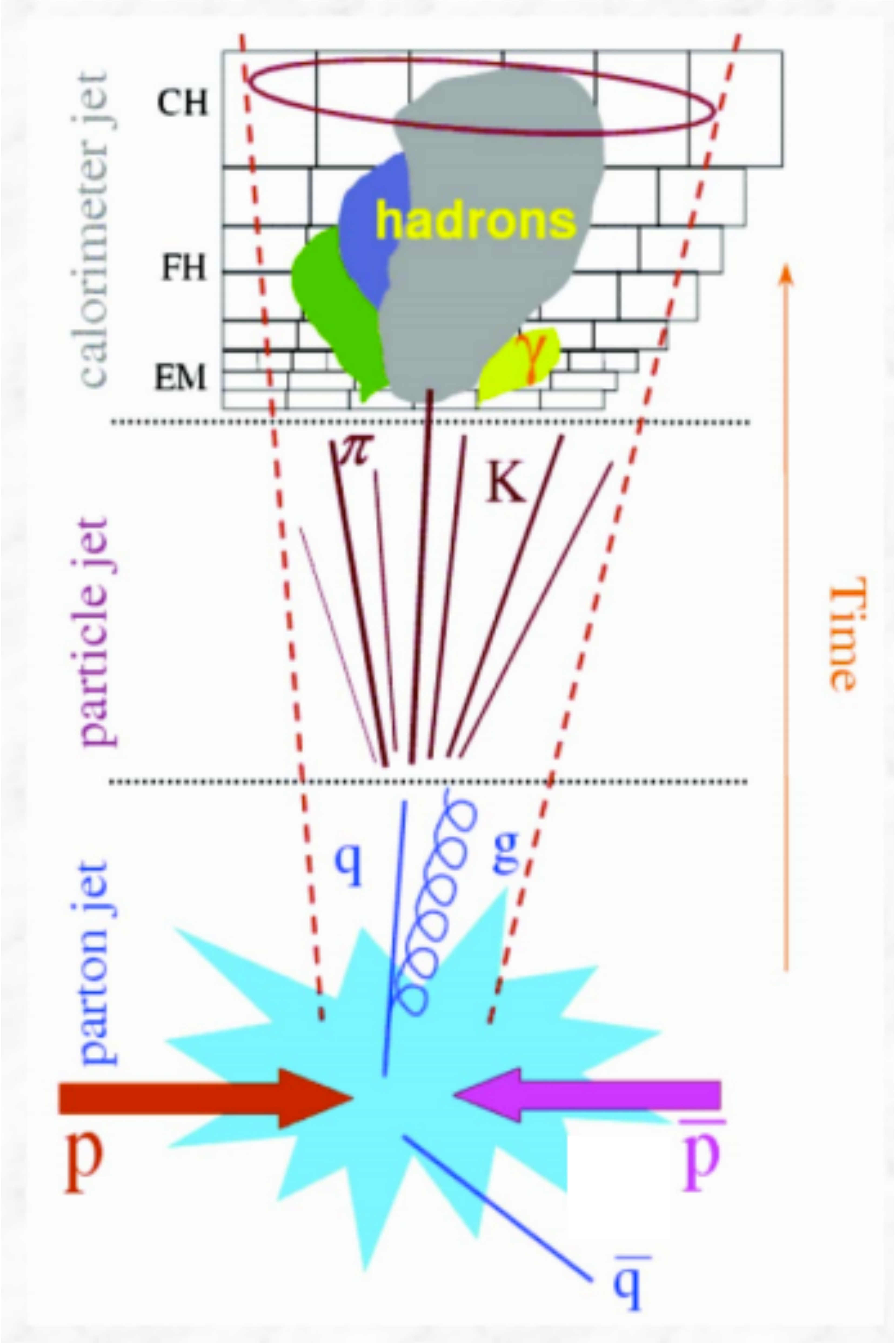

CH
FH
EM
hadrons
γ
calorimeter jet
π
K
particle jet
q
g
parton jet
Time
p
p̄
q̄

喷柱形成的动力学：QCD 辐射

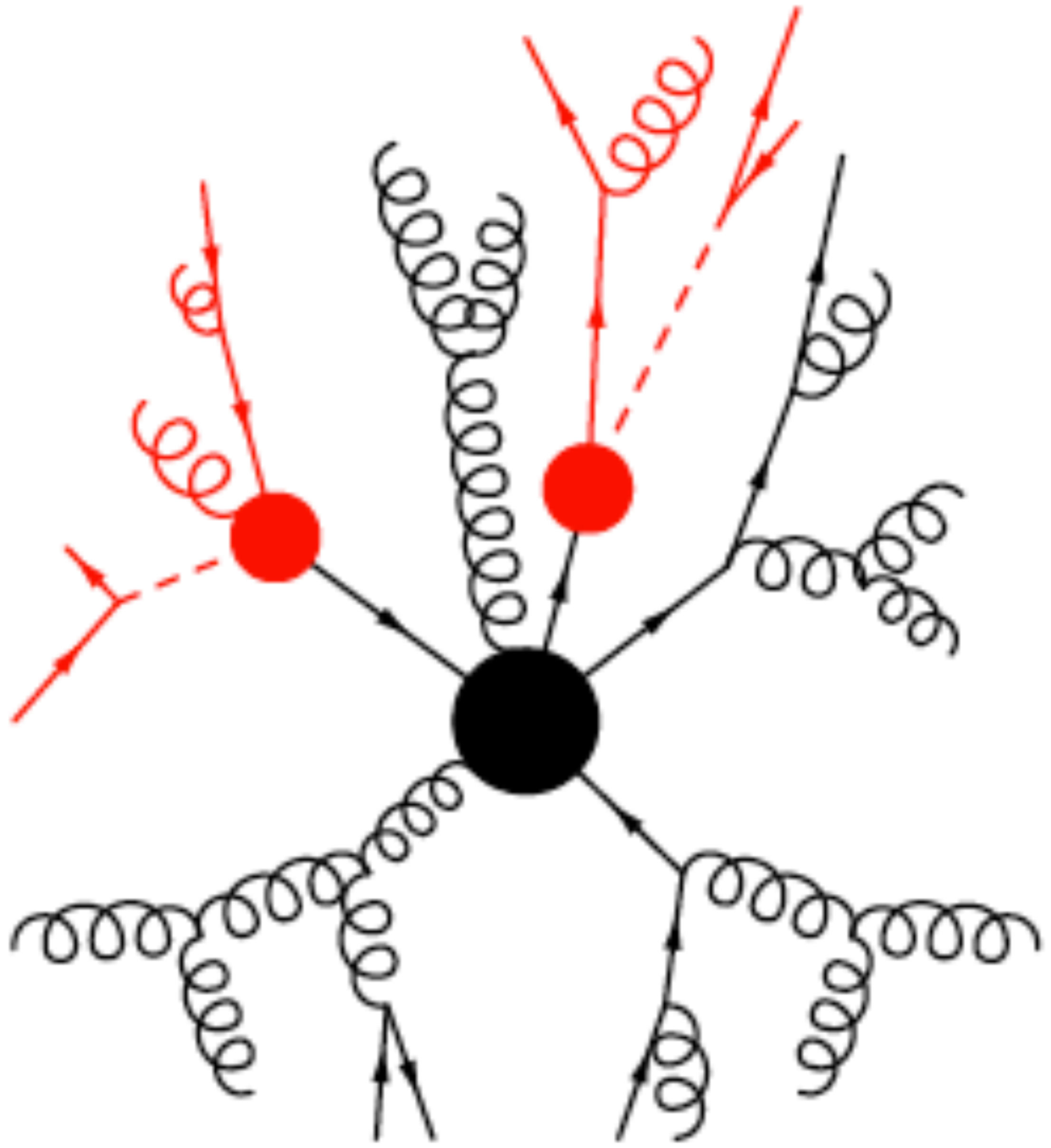

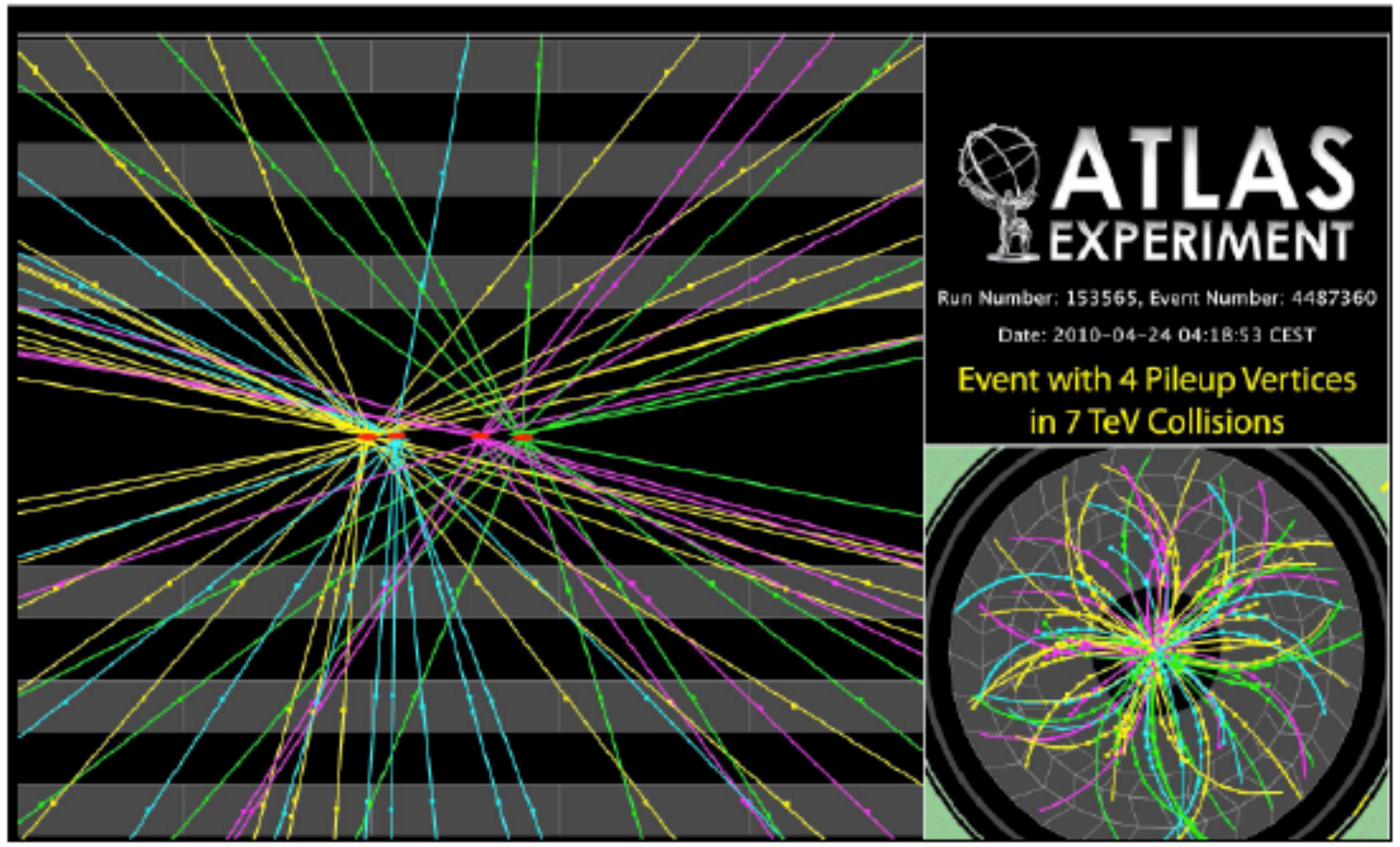

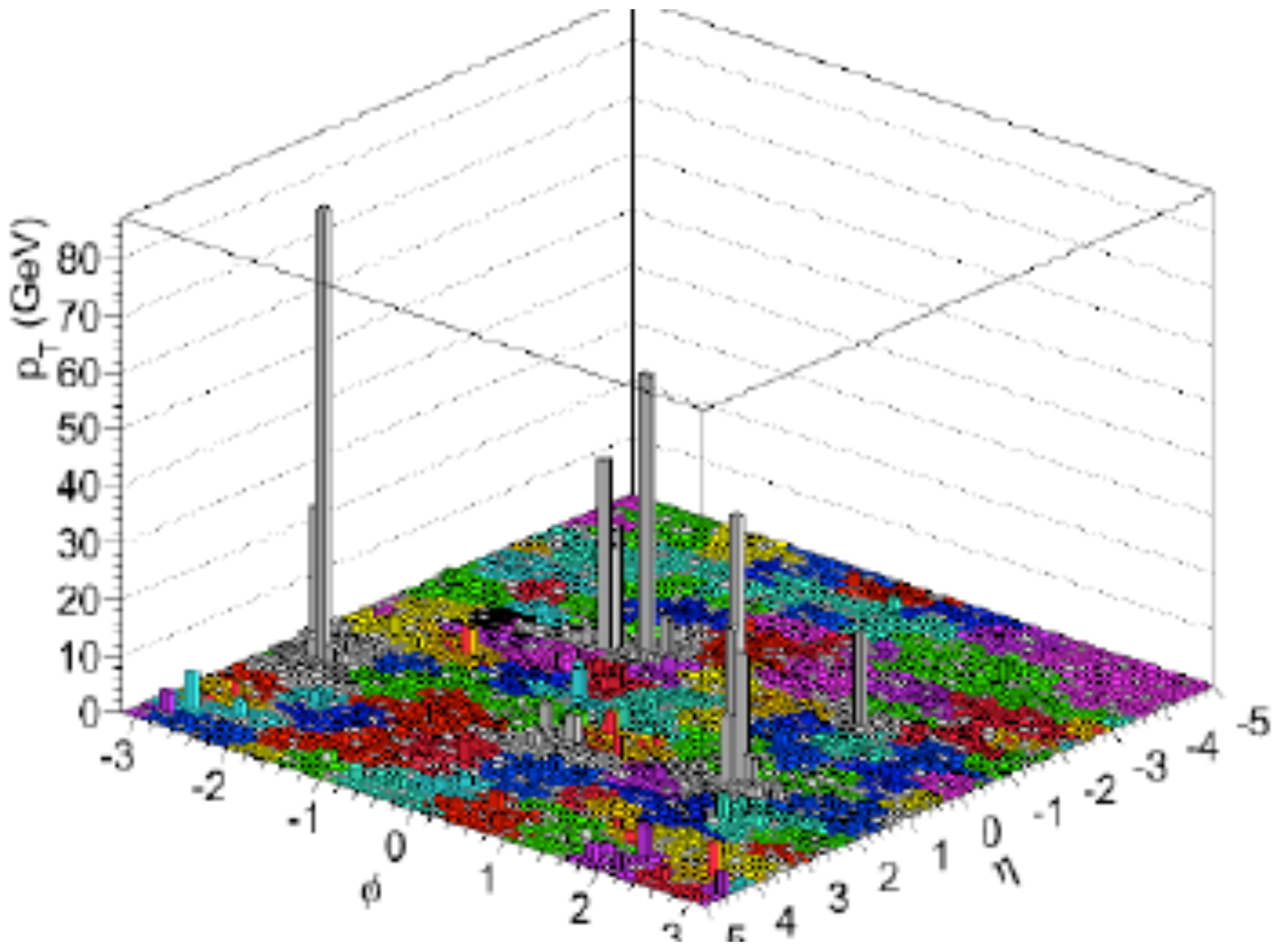

喷柱形成的动力学：强子化

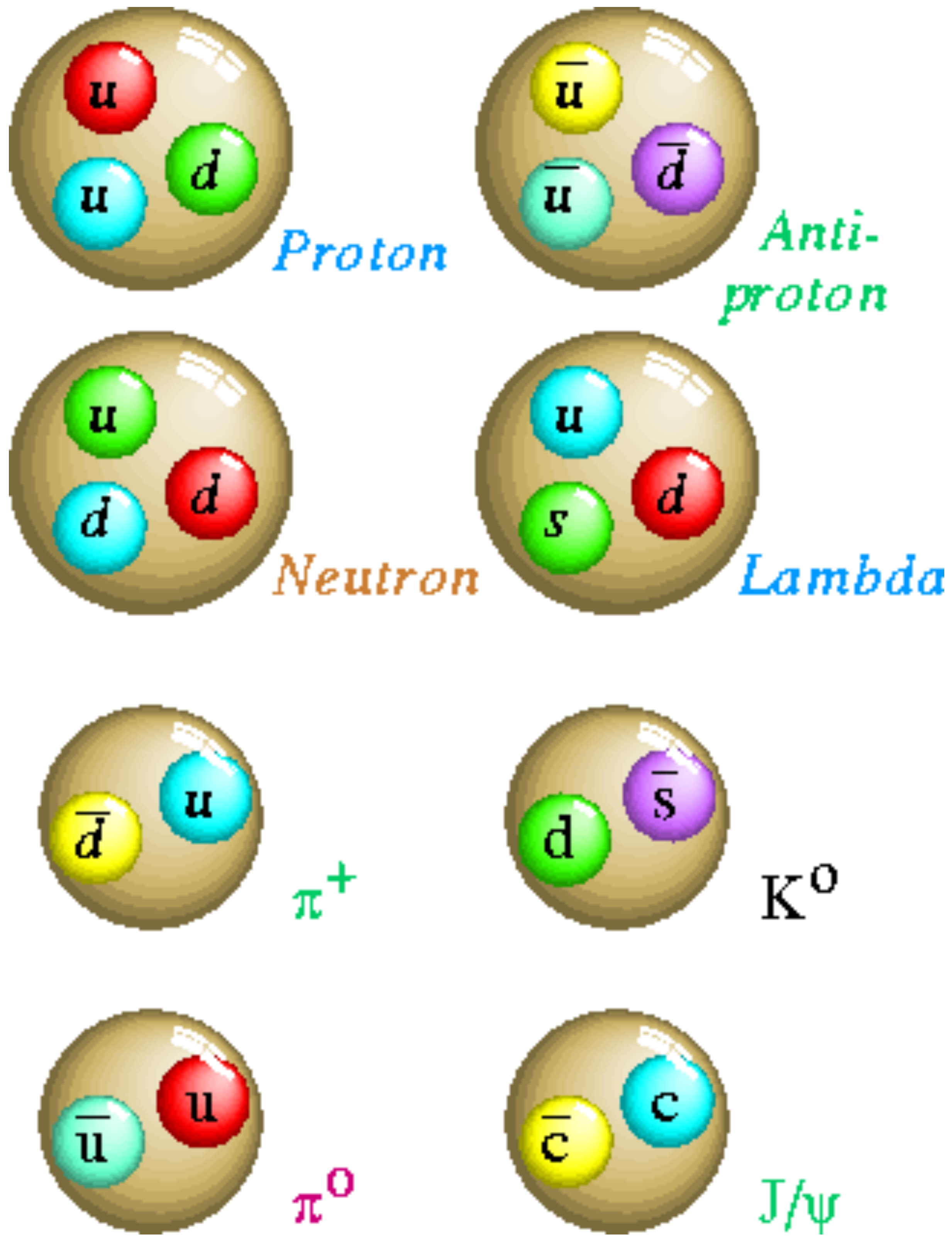

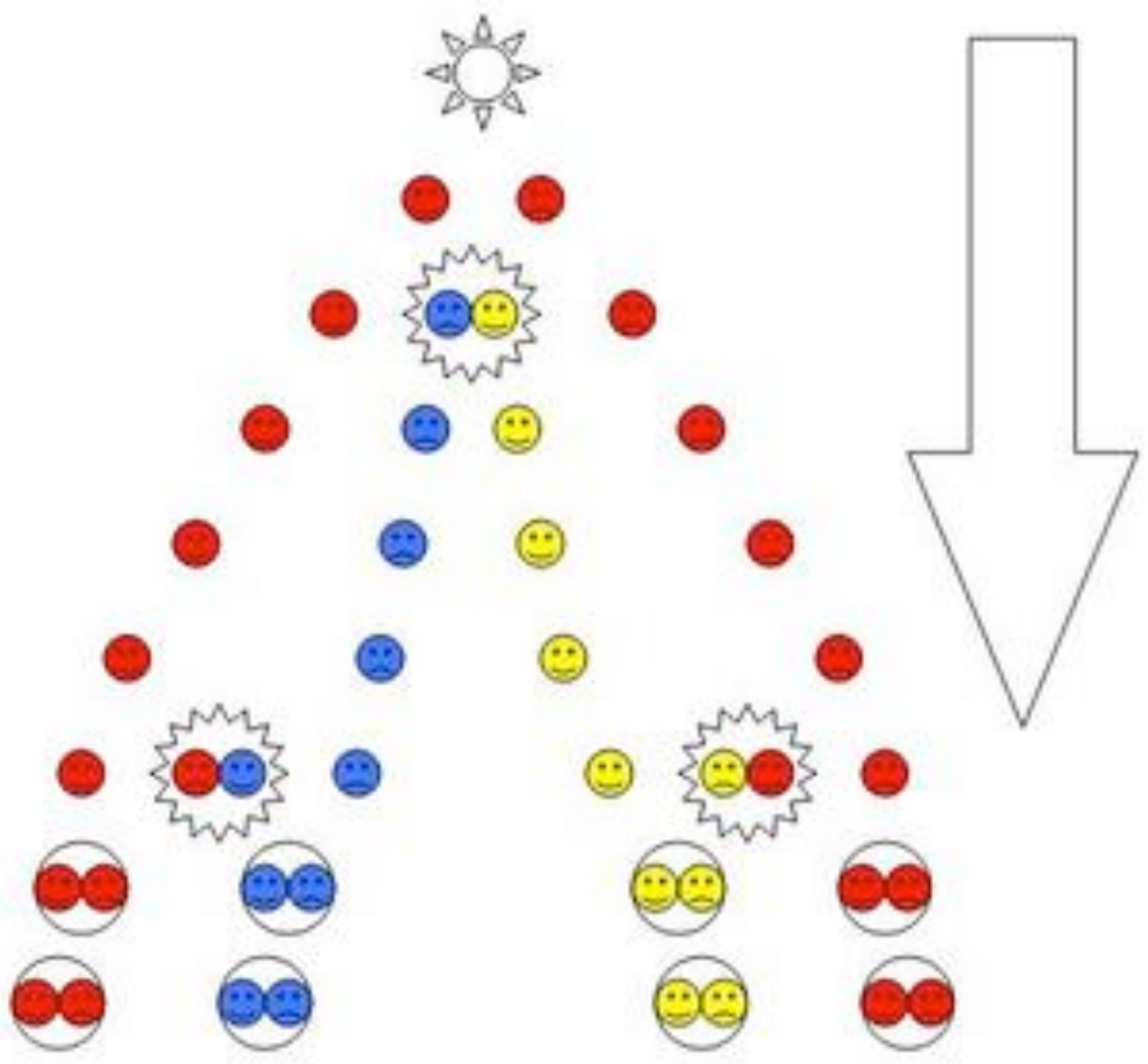

喷柱形成的动力学：underlying events

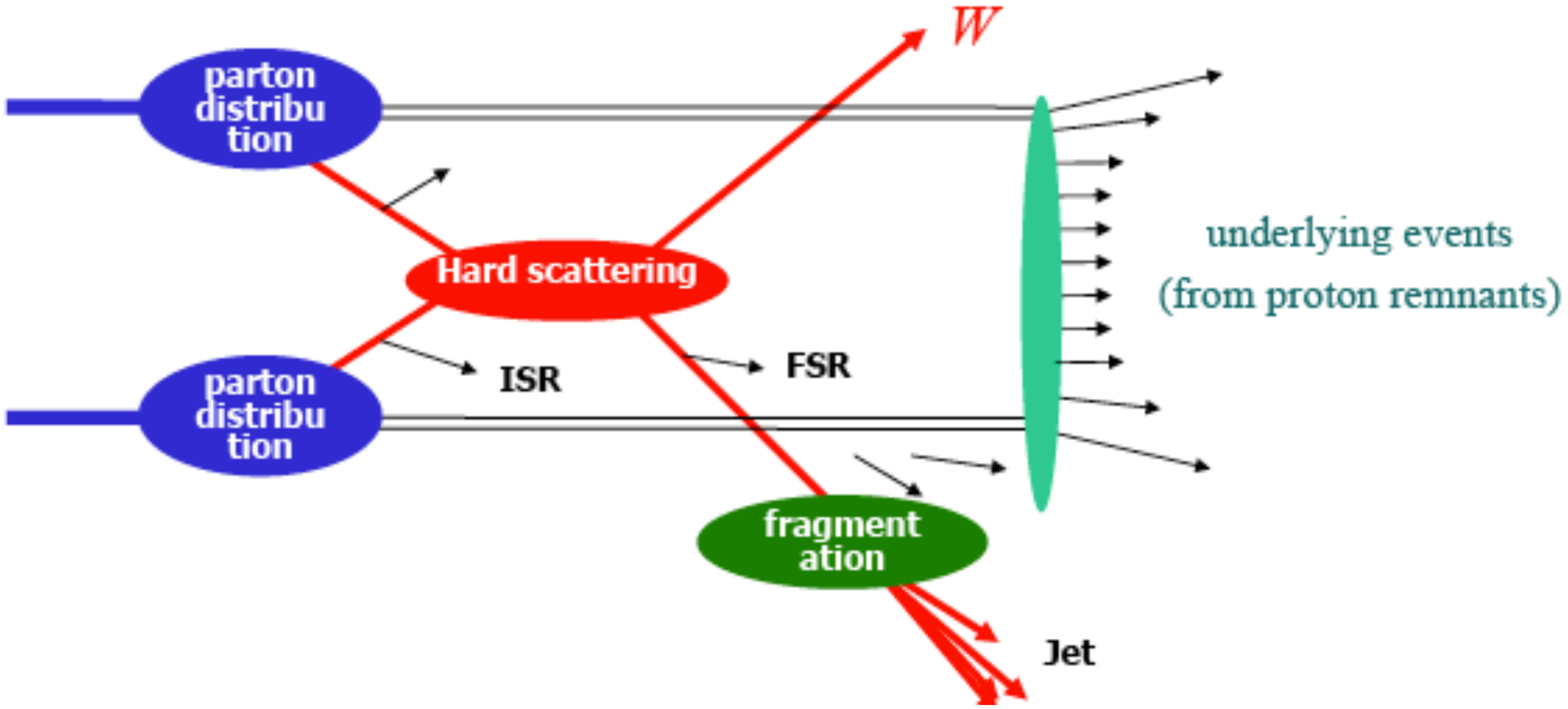

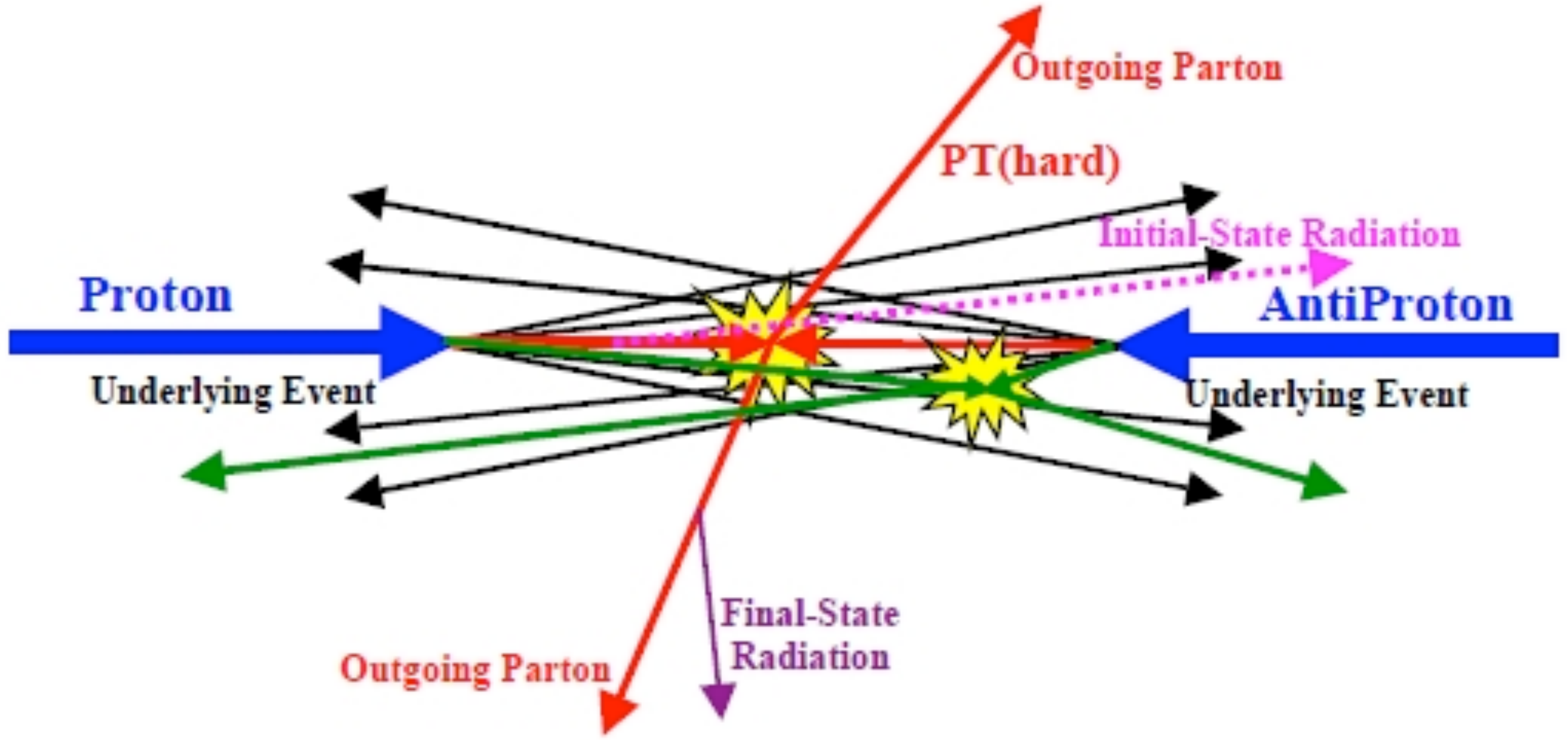

Pile-Up

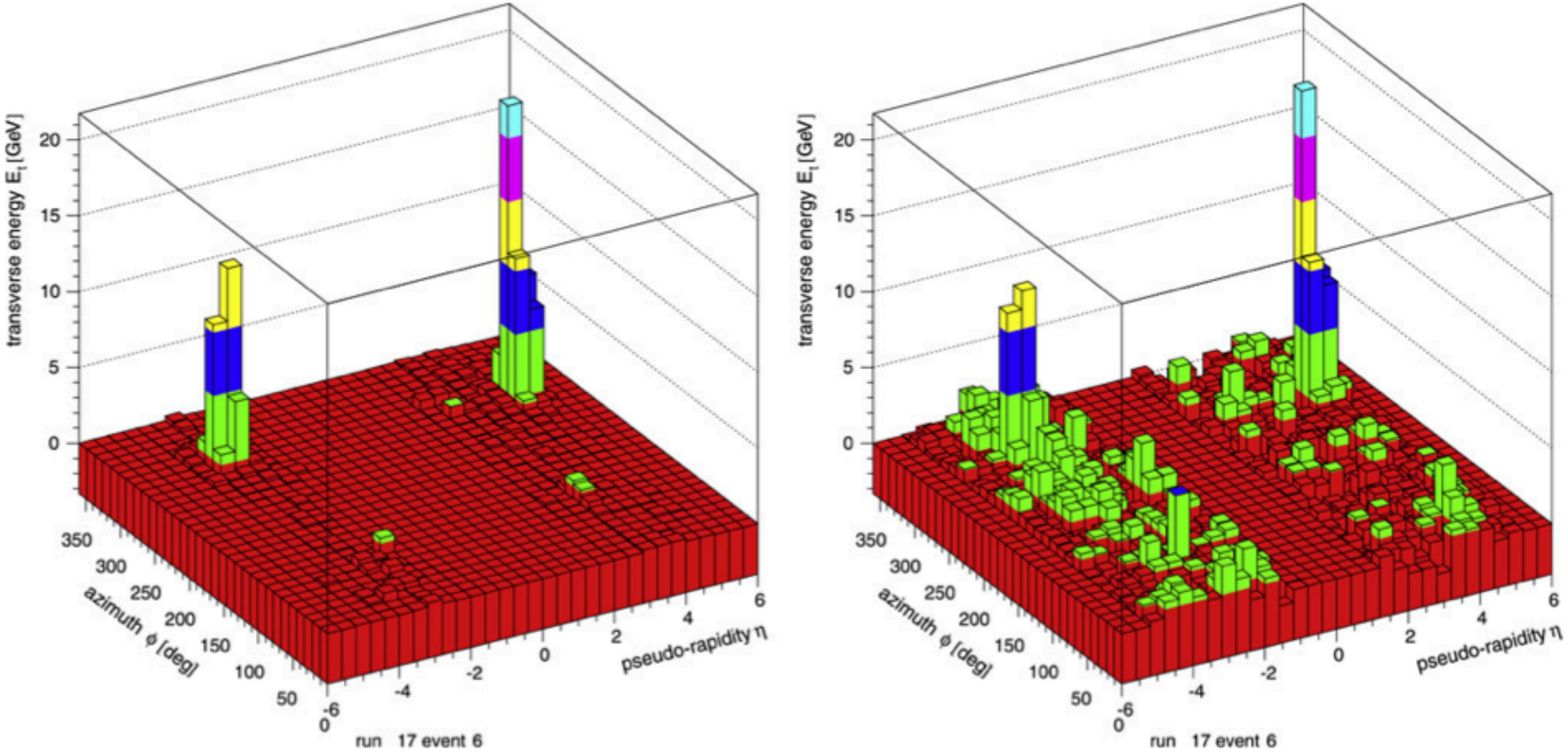
transverse energy E_t [GeV]
20
15
10
5
0
350
300
250
200
150
100
50
0
azimuth ϕ [deg]
-6
-4
-2
0
2
4
6
pseudo-rapidity η
run 17 event 6
transverse energy E_t [GeV]
20
15
10
5
0
350
300
250
200
150
100
50
0
azimuth ϕ [deg]
-6
-4
-2
0
2
4
6
pseudo-rapidity η
run 17 event 6

为什么软（soft）和共线（collinear）主导?

- 其中的quark传播子的分母部分：
$$\frac{1}{(q+k)^2} = \frac{1}{2q\cdot k} = \frac{1}{2q^0k^0(1-\cos\theta)}$$
- 两种发散：

1. 软发散 $k^0 \to 0$
2. 共线发散 $\theta \to 0$

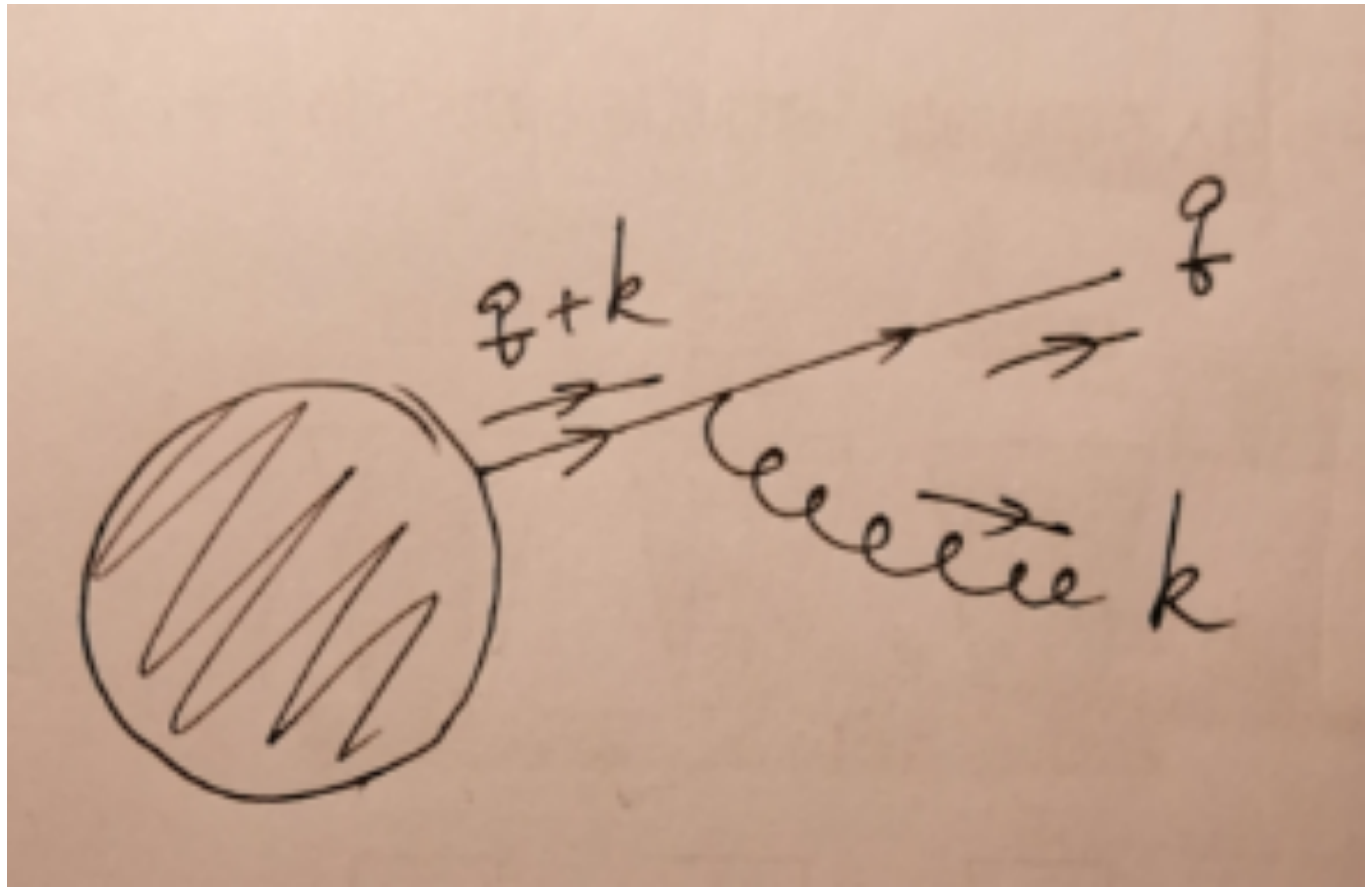

Jet algorithm 需要避免的

1. 红外安全：软胶子不应当改变喷柱构建的结果。

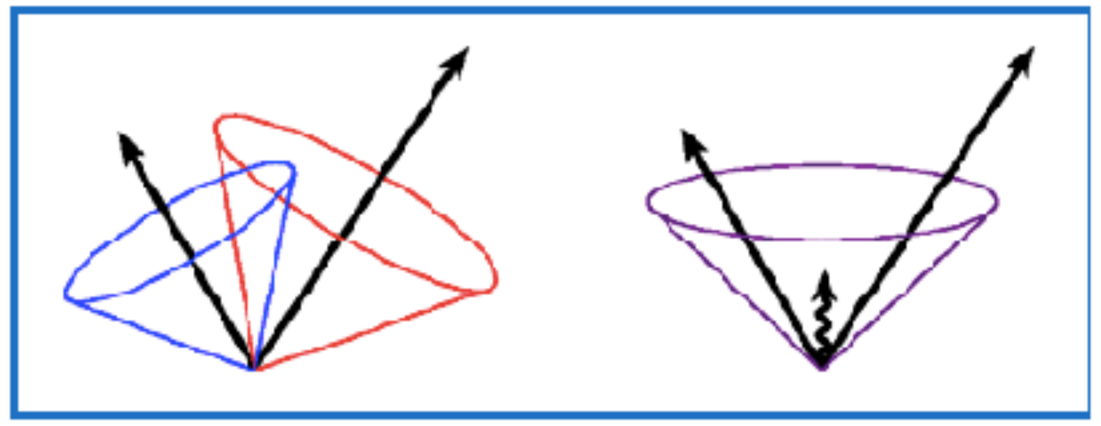

2. 共线安全：劈裂过程不应当改变喷柱构建的结果。

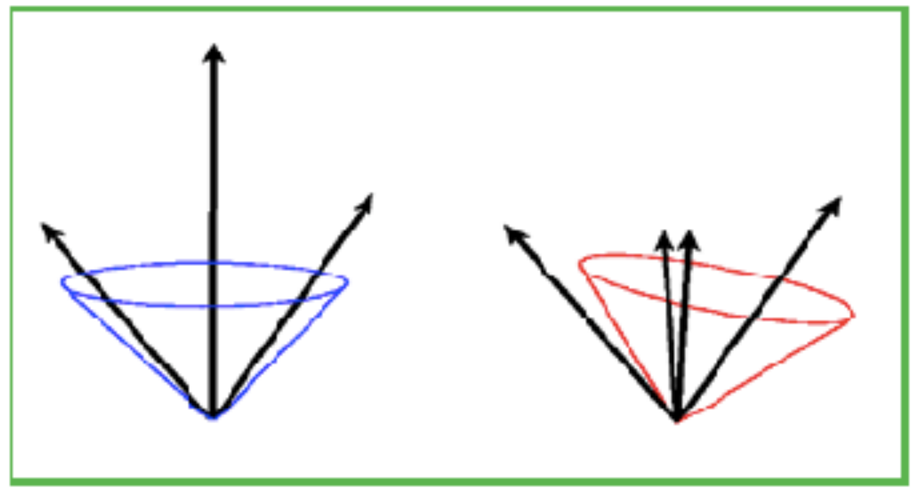

理想的Jet algorithm

喷柱构建方法在不同层面上应有相同的结果/行为。

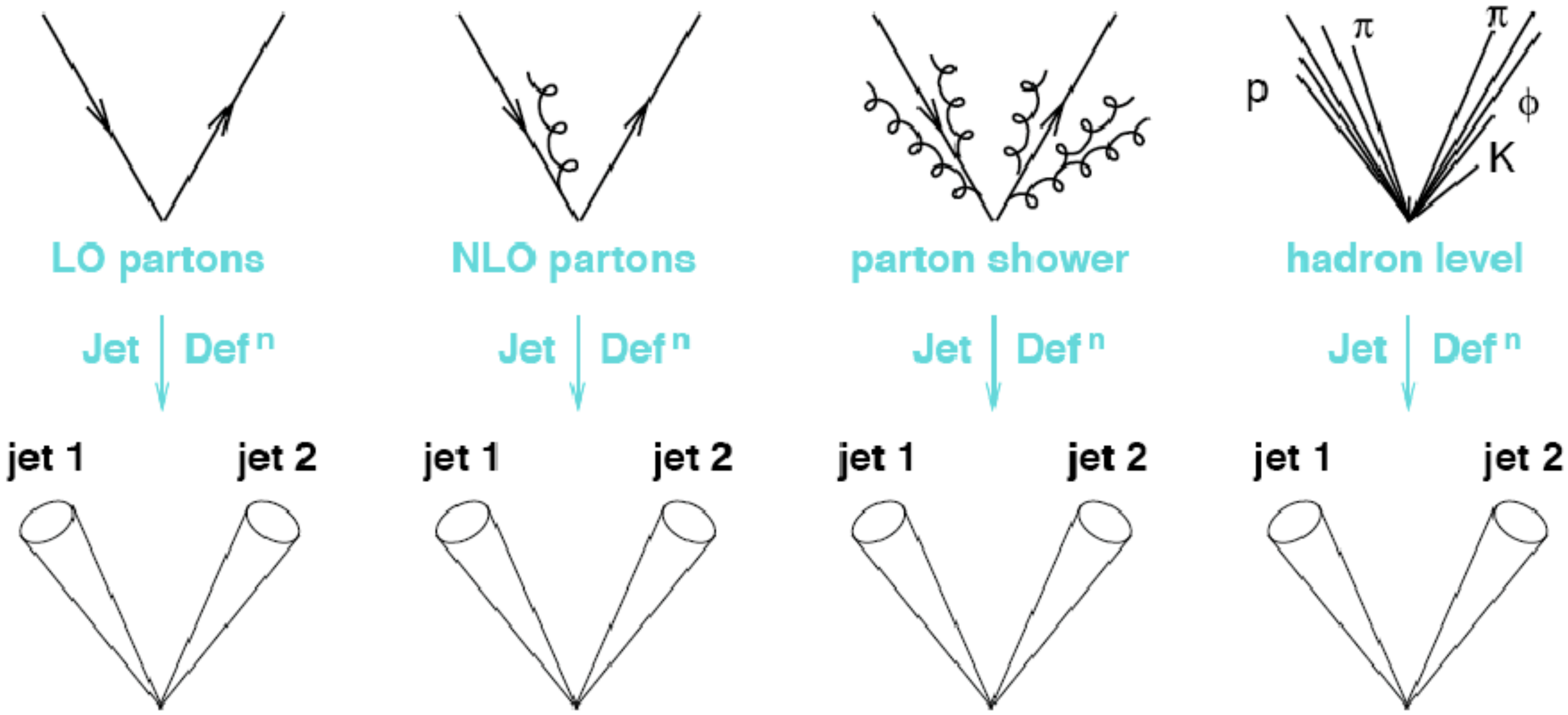

两类主流algorithm

- Cone-Type Algorithms
  ★ Midpoint Cone (Tev), Iterative Cone (CMS), SISCone (LHC)
  ★ Typically not Infrared- & Collinear-Safe (exception: SISCone)
  ★ Typically complex, involving several (non-phyiscal) parameters
  ★ Favored at hadron colliders (computational performance)
  ★ Strongly disfavored by theorists

- Sequential Clustering Algorithms
  ★ kT, Cambridge/Aachen, Anti-kT
  ★ Infrared- & Collinear-Safe by construction
  ★ Clean & Simple Algorithms
  ★ Strongly favored by theorists
  ★ Now widely used at the LHC

Iterative cone algorithm

$$k \subset C \quad \text{iff} \quad \sqrt{(y_k - y_C)^2 + (\phi_k - \phi_C)^2} \leq R_{\text{cone}},$$

$$\overline{y}_C \equiv \frac{\sum_{k \subset C} y_k \cdot p_{T,k}}{\sum_{l \subset C} p_{T,l}}, \qquad \overline{\phi}_C \equiv \frac{\sum_{k \subset C} \phi_k \cdot p_{T,k}}{\sum_{l \subset C} p_{T,l}}.$$

$$(\overline{y}_C, \overline{\phi}_C) \neq (y_C, \phi_C), \qquad (\overline{y}_C, \overline{\phi}_C) = (y_C, \phi_C),$$

Cone algorithm is IR unsafe

SISCone Algorithm

- “Seedless Infrared-Safe Cone” Algorithm
- Exact seedless cone algorithm which provably finds all stable cones
- Collinear- and Infrafred-Safe
- Acceptable computational performance ($\sim N^2 \ln N$)
  - ★ existing approach: $\sim N2^N$ -> 10^{17} years (!!) for N=100
- Currently: standard cone-type algorithm at CMS

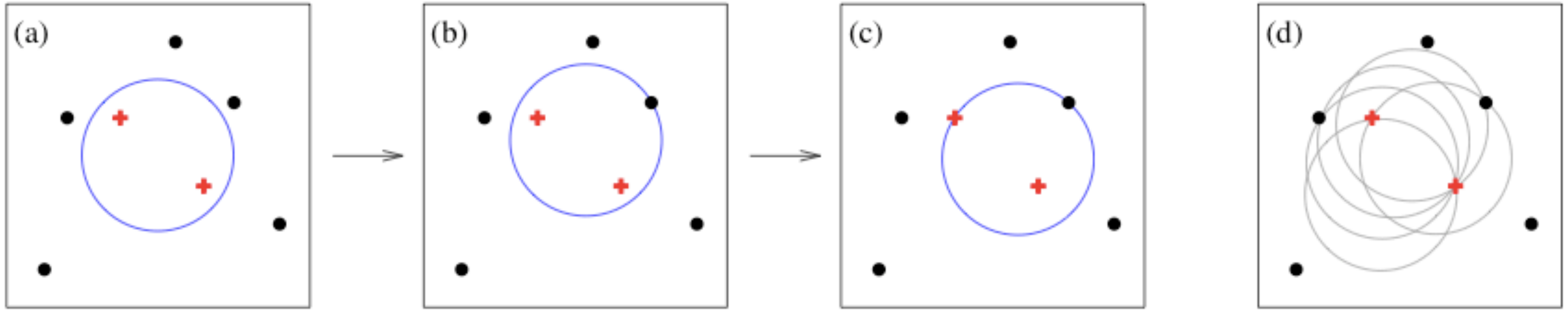

2D Simplification: Moving (a) initial circular enclosure in a random direction until it some **particle** (b) touches the circle, then pivot the circle around that edge point until (c) a second point touches the edge. (d) all circles defined by pairs of edge points are all stable cones

Sequential Clustering Algs

- Based on the following **distance measures**:
  - ★ distance $\mathbf{d_{ij}}$ between two particles i and j:

$$\boxed{d_{ij} = \min\left(k_{\mathrm{T}i}^{2p}, k_{\mathrm{T}j}^{2p}\right)\frac{\Delta_{ij}}{D}} \qquad \Delta_{ij}^2 = (y_i - y_j)^2 + (\phi_i - \phi_j)^2$$

  - ★ distance between any particle i and the beam (B) $\mathbf{d_{iB}}$:

$$\boxed{d_{iB} = k_{\mathrm{T}i}^{2p}}$$

- Compute all distances d_{ij} and d_{iB}, find the **smallest**
  - ★ if smallest is a dij, **combine** (sum four momenta) the two particles i and j, update distances, proceed findint next smallest
  - ★ if smallest is a diB, **remove** particle i, call it a **jet**

- Repeat until all particles are clustered into jet

- Parameter **D**: Scales the dij w.r.t. the diB such that any pair of final jets a and b are at least separated by $\Delta_{ab}^2 = D^2$

- Parameter **p**: governs the relative power of of energy vs geometrical scales to distinguish the three algorithms: **2**=kT, **0**=C/A, **-2**=Anti-kT

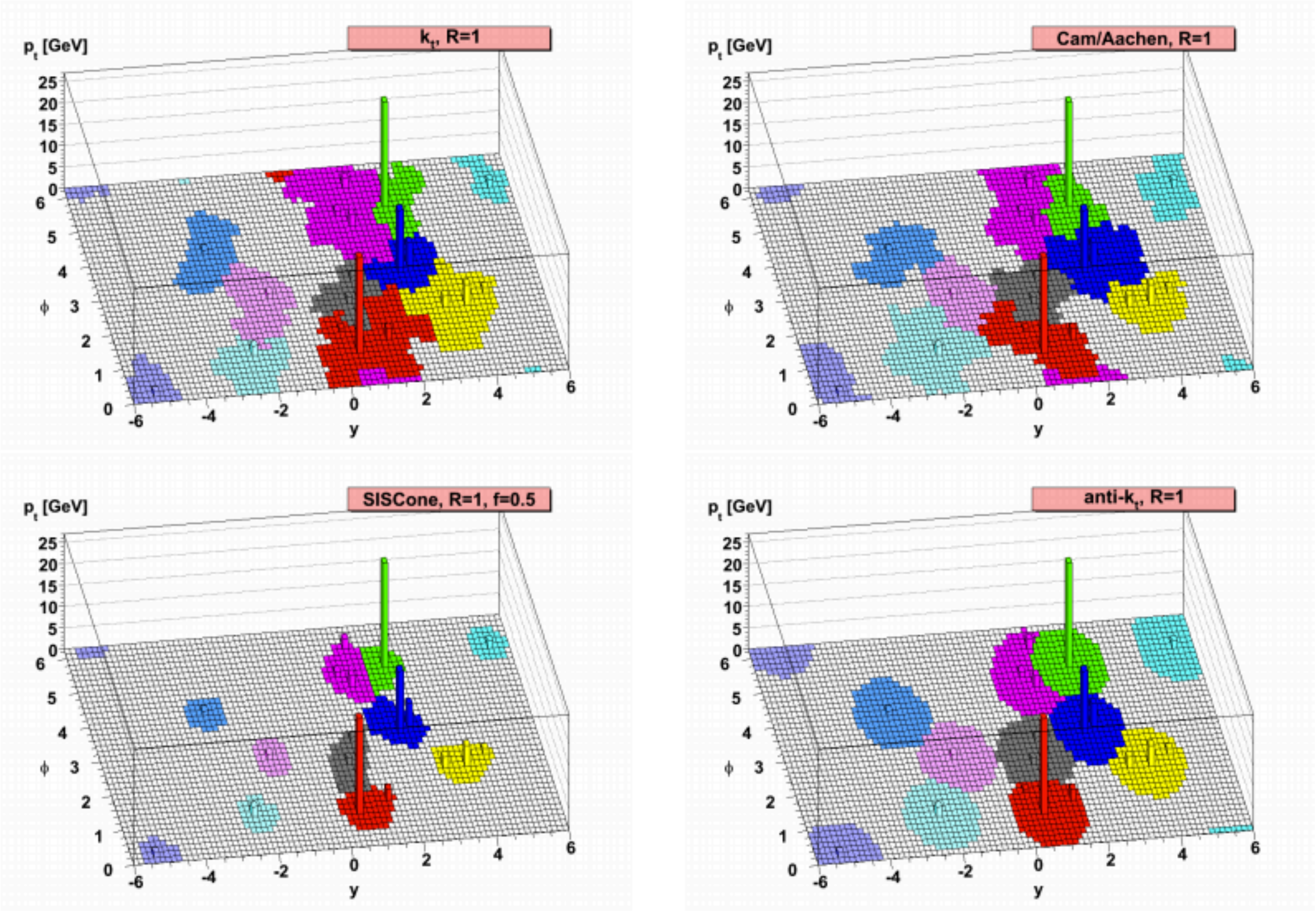

k_t, R=1
Cam/Aachen, R=1
SISCone, R=1, f=0.5
anti-k_t, R=1
p_t [GeV]
φ
y

Jet Energy Profile

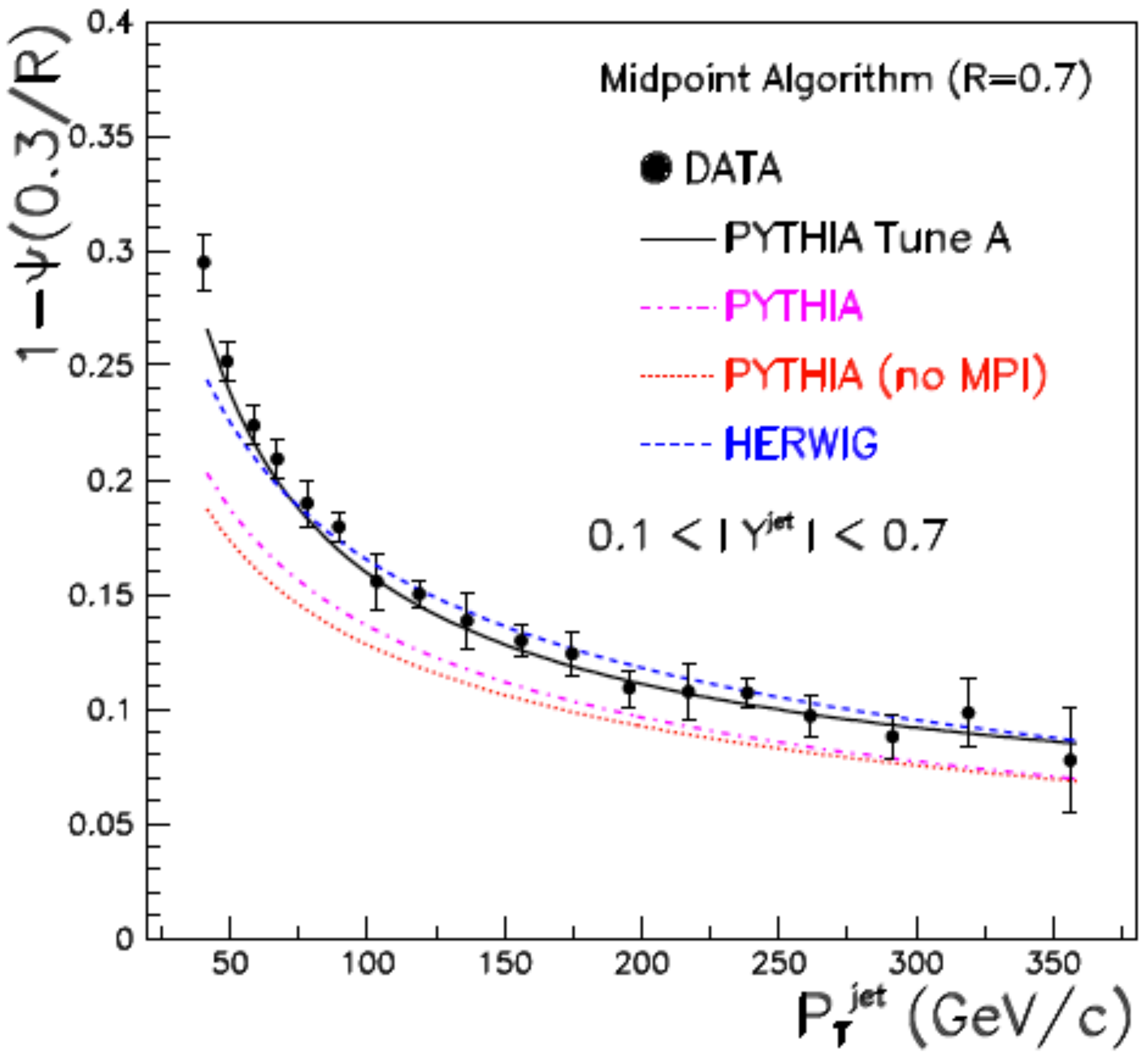

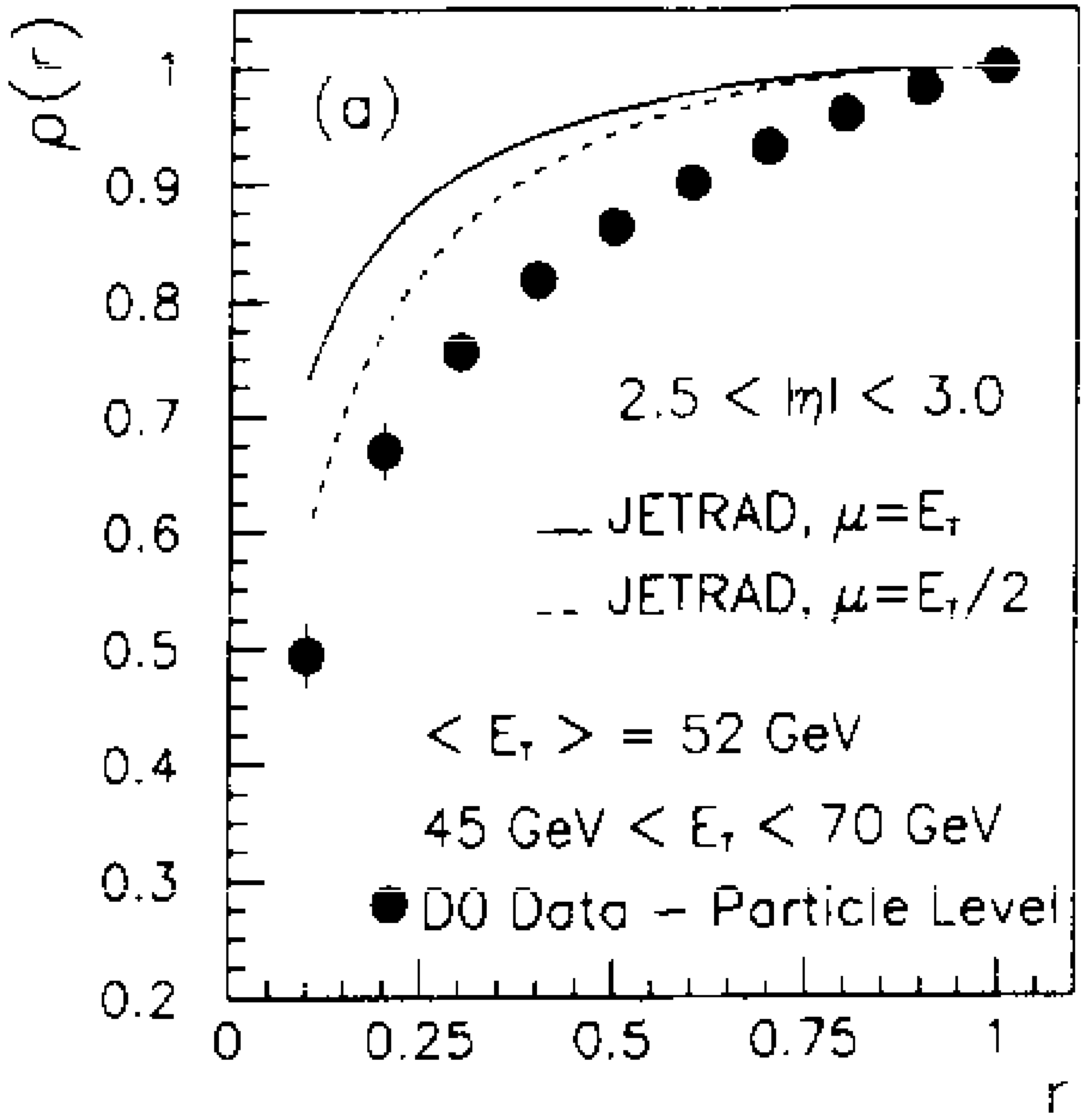

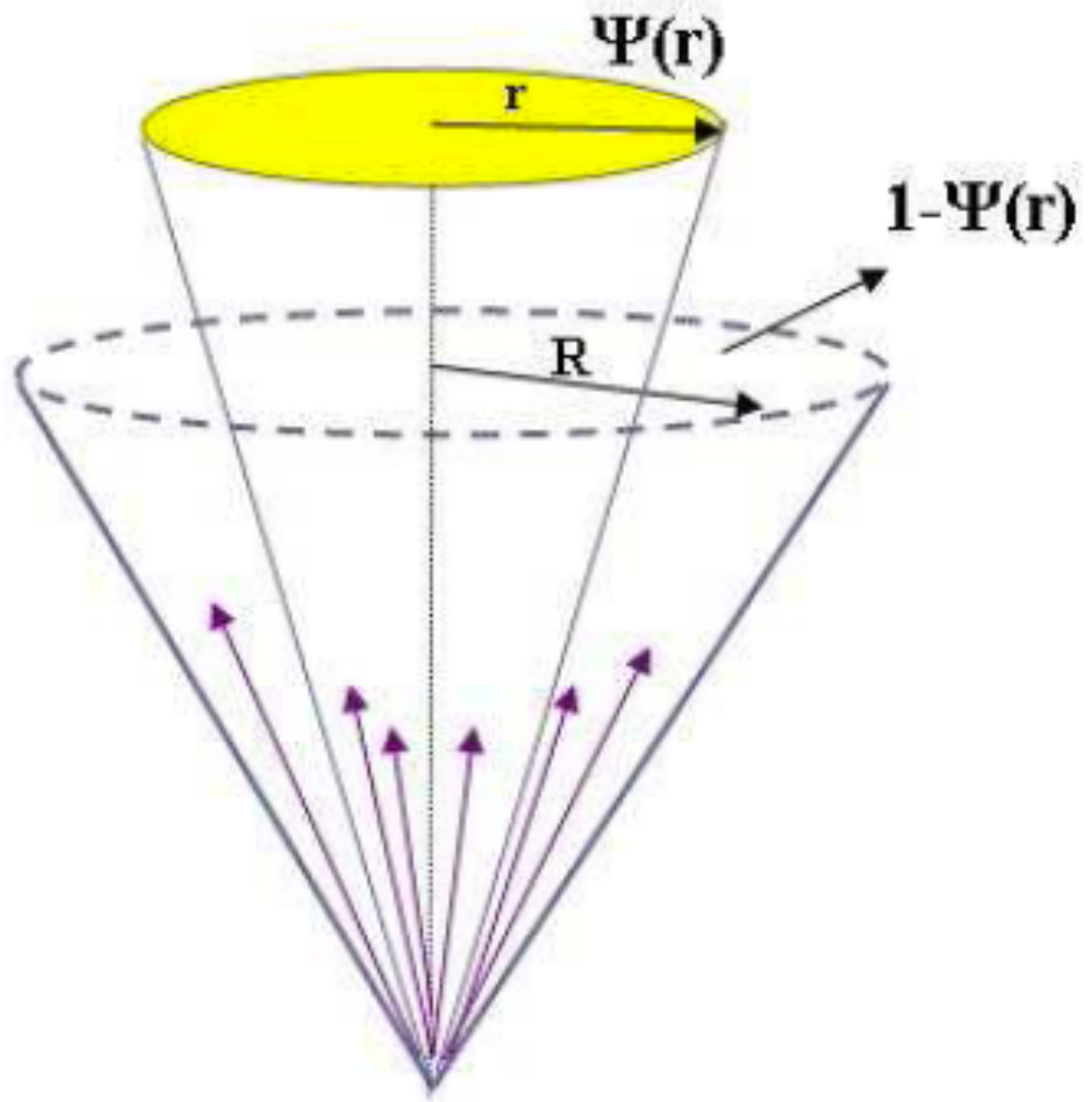

D0 Collaboration/Physics Letters B 357(1995) 500-508

$$\Psi(r) = \frac{1}{\mathrm{N_{jet}}} \sum_{\mathrm{jets}} \frac{P_T(0,r)}{P_T(0,R)}, \qquad 0 \le r \le R$$

典型的夸克喷柱与胶子喷柱的差异

- Quarks and gluons radiate proportional to their color factors

$$r \equiv \frac{\langle n_g \rangle}{\langle n_q \rangle} \equiv \frac{\langle \text{gluon jet multiplicity} \rangle}{\langle \text{quark jet multiplicity} \rangle}$$

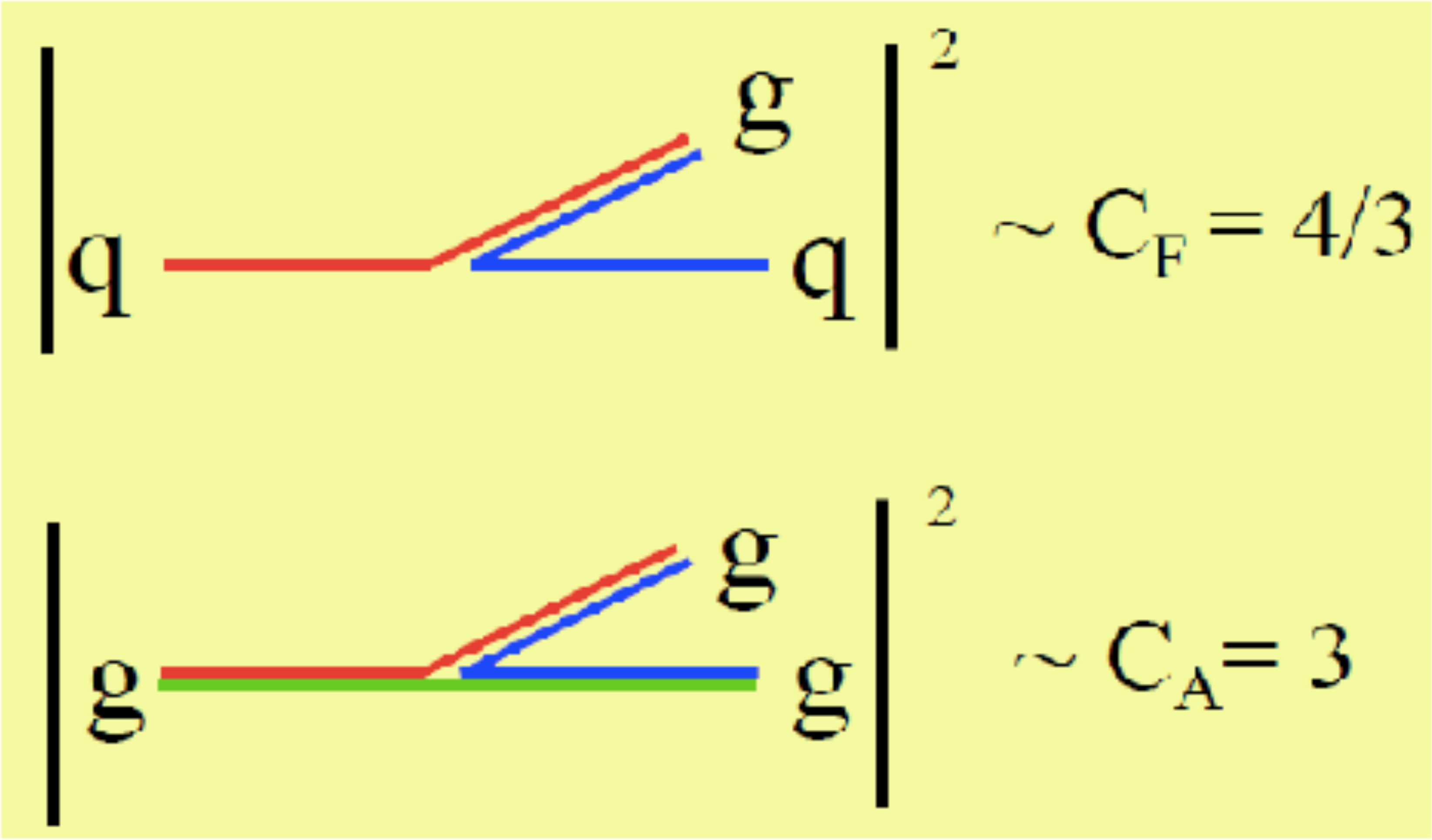

- At leading order

$$r = \frac{\langle C_A \rangle}{\langle C_F \rangle} = \frac{9}{4} = 2.25$$

- With higher order corrections, r~1.5

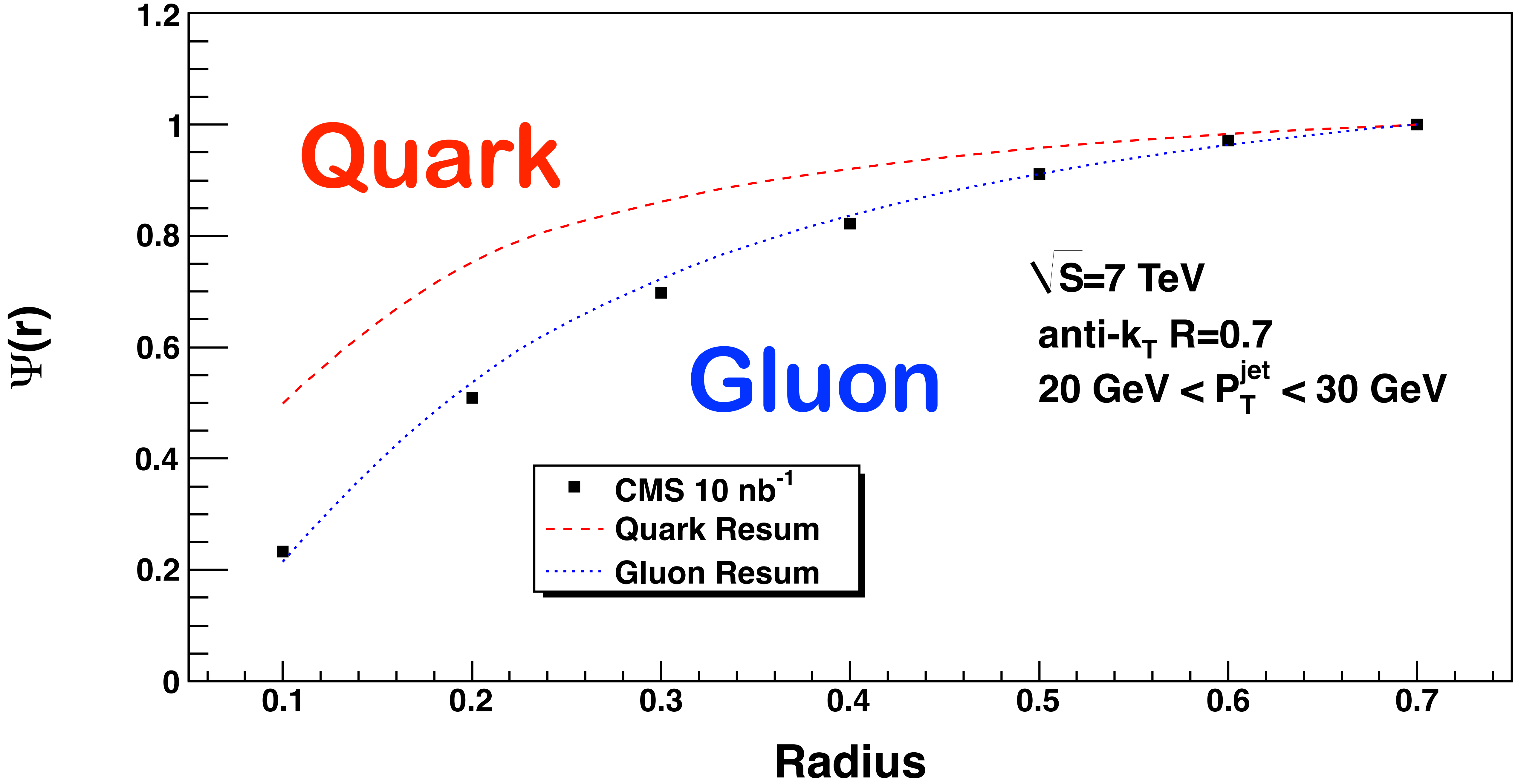

Jet energy profile $\mathbf{J^E}$ can be obtained by inserting the step function in the jet function:

$$J_q^{E(1)}(m_J^2, P_T, \nu^2, R, \mu^2) \ =$$

$$\frac{(2\pi)^3}{2\sqrt{2}(P_J^0)^2 N_c} \sum_{\sigma,\lambda} \int \frac{d^3p}{(2\pi)^3 2\omega_p} \frac{d^3k}{(2\pi)^3 2\omega_k} [p^0\Theta(R-\theta_p) + k^0\Theta(R-\theta_k)]$$

$$\times \mathrm{Tr}\left\{ \not{\xi} \langle 0|q(0)W_\xi^{(\bar{q})\dagger}(\infty,0)|p,\sigma;k,\lambda\rangle\langle k,\lambda;p,\sigma|W_\xi^{(\bar{q})}(\infty,0)\bar{q}(0)|0\rangle \right\}$$

$$\times\delta(m_J^2-(p+k)^2)\delta(\hat{n}-\hat{n}_{\vec{p}+\vec{k}})\delta(P_J^0-p^0-k^0),$$

At NLO, $\bar{J}_E^q \approx \dfrac{\alpha_s C_F}{P_J^0 \pi}\left[-\dfrac{1}{4}\ln^2\dfrac{R^2}{r^2} - \dfrac{3}{4}\ln\dfrac{R^2}{r^2}\right].$

which is an integrable singularity.

$$-\frac{n^2}{v\cdot n}v_\alpha\frac{d}{dn_\alpha}\frac{n_\mu}{n\cdot l}=\frac{n^2}{v\cdot n}\left(\frac{v\cdot l}{n\cdot l}n_\mu-v_\mu\right)\frac{1}{n\cdot l}\equiv\frac{\hat{n}_\mu}{n\cdot l},$$

LO soft kernel $K_v^{(1)}$

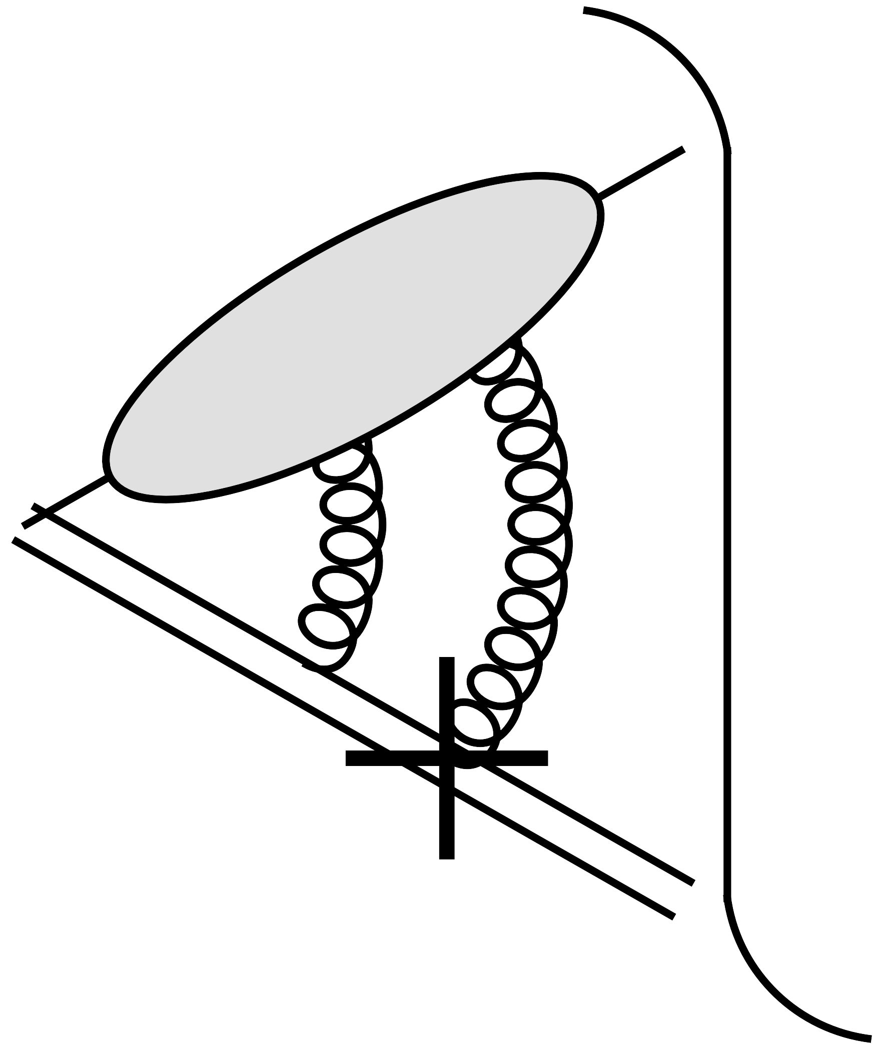 ~ 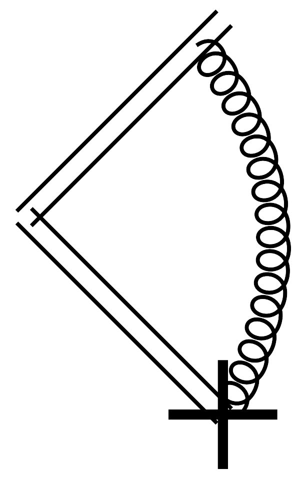 $\otimes$ 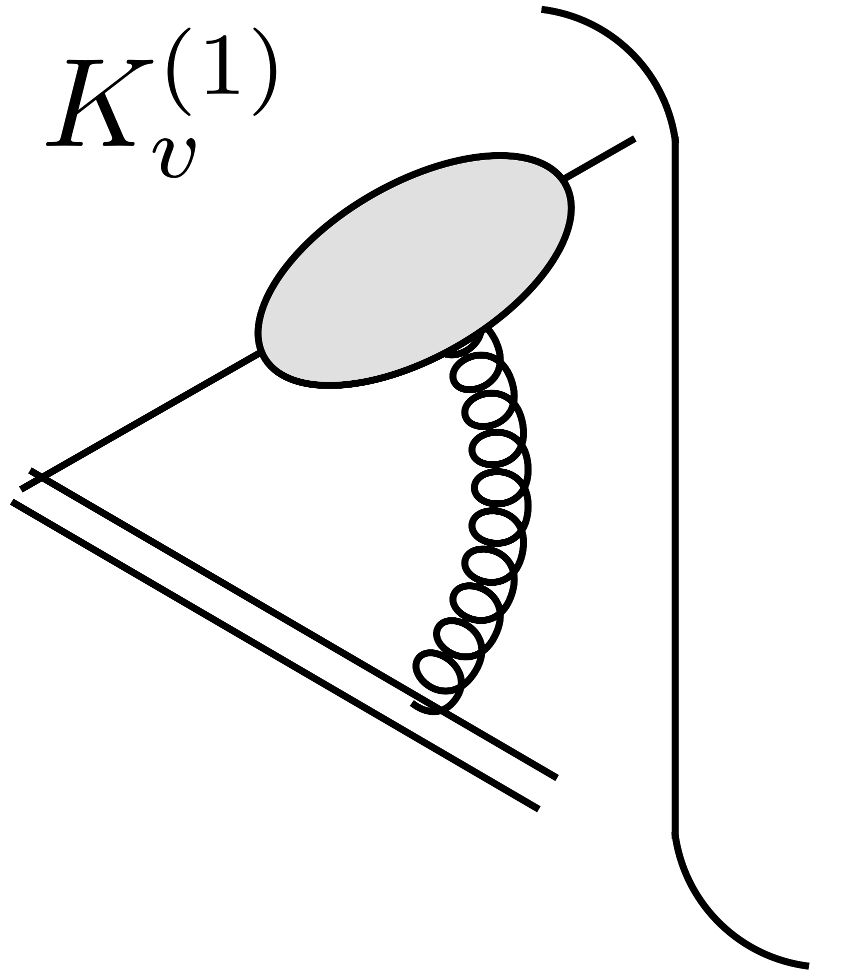

LO soft kernel $K_r^{(1)}$

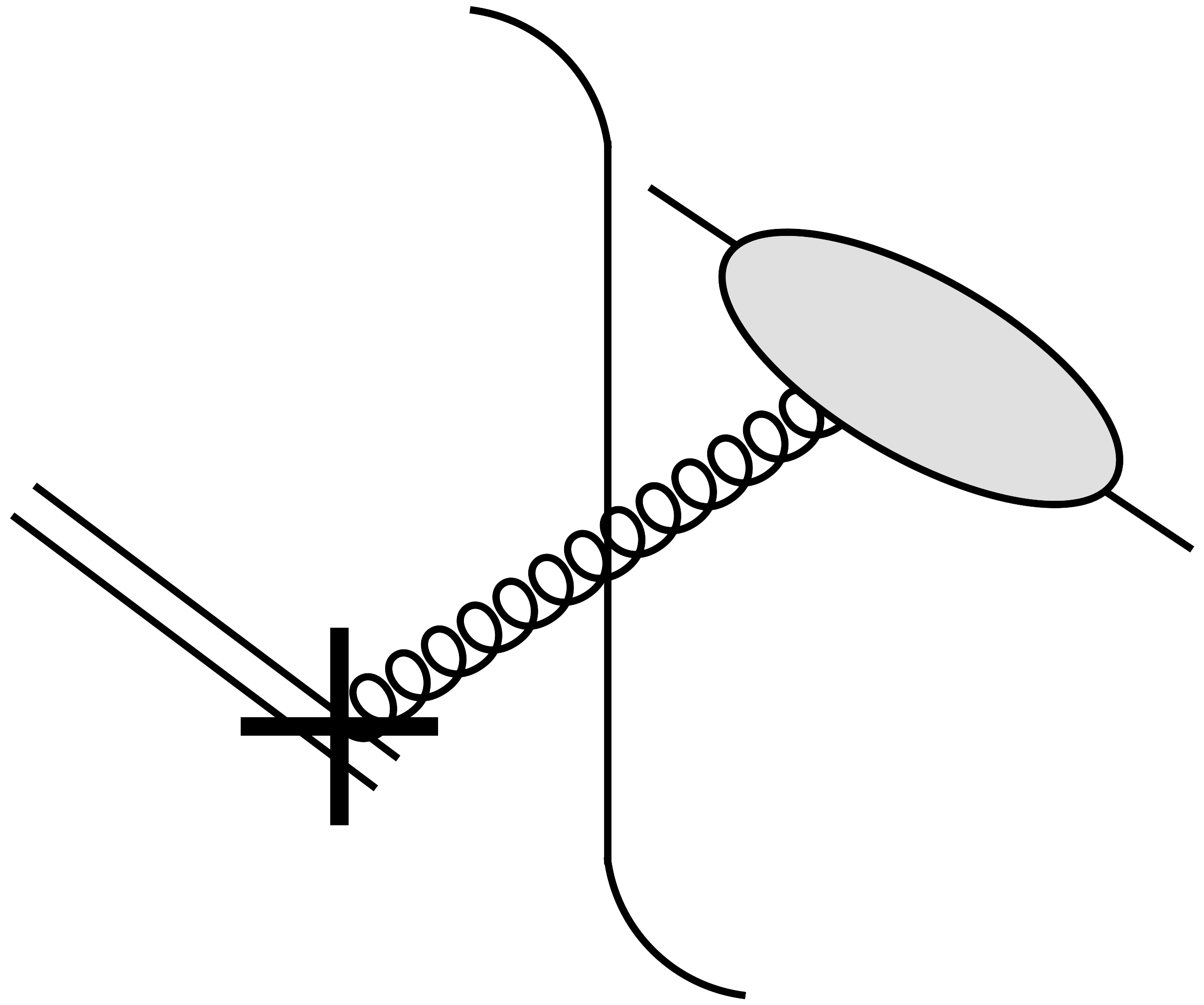 ~ 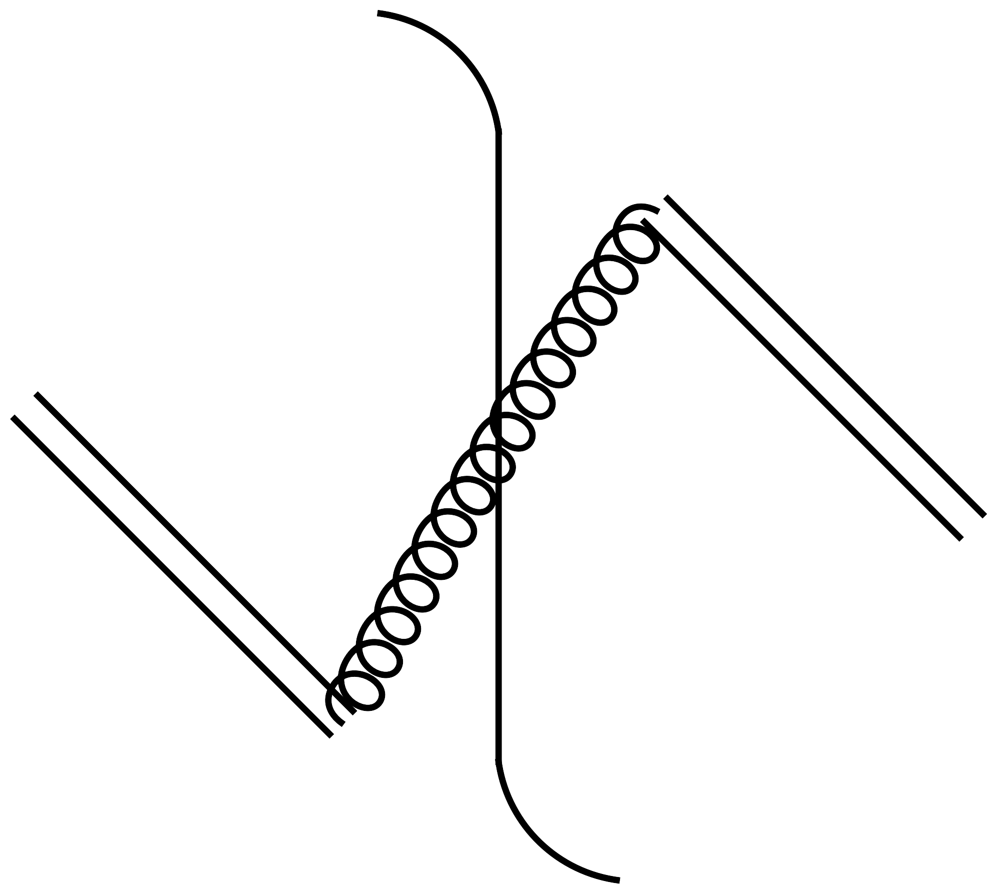 $\otimes$ 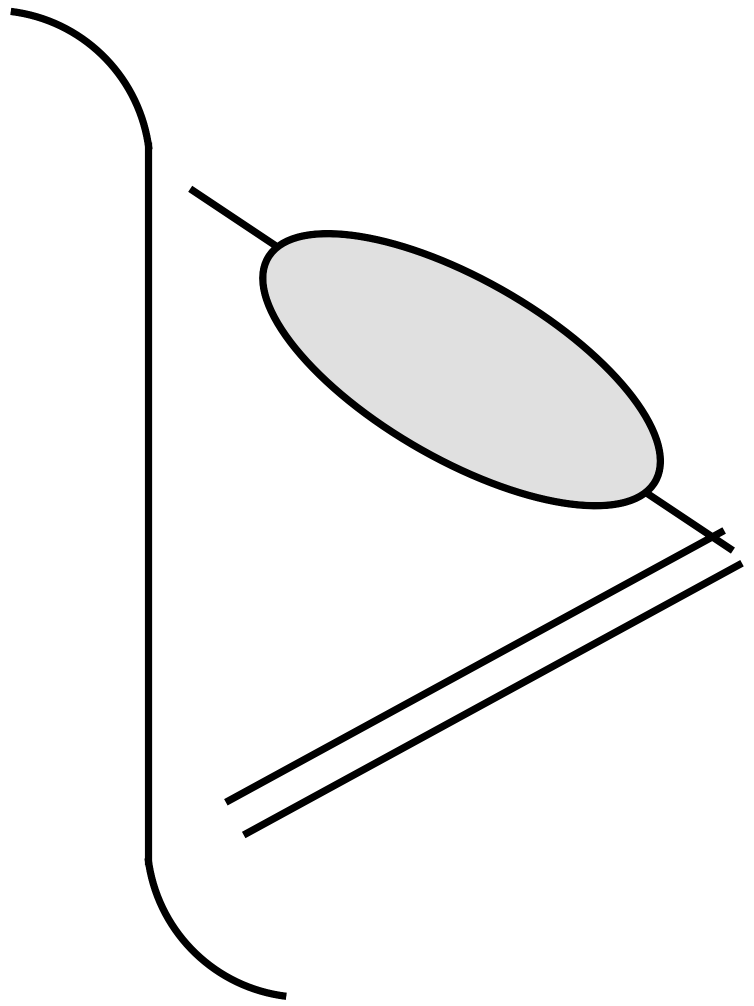

LO hard kernel $G^{(1)}$

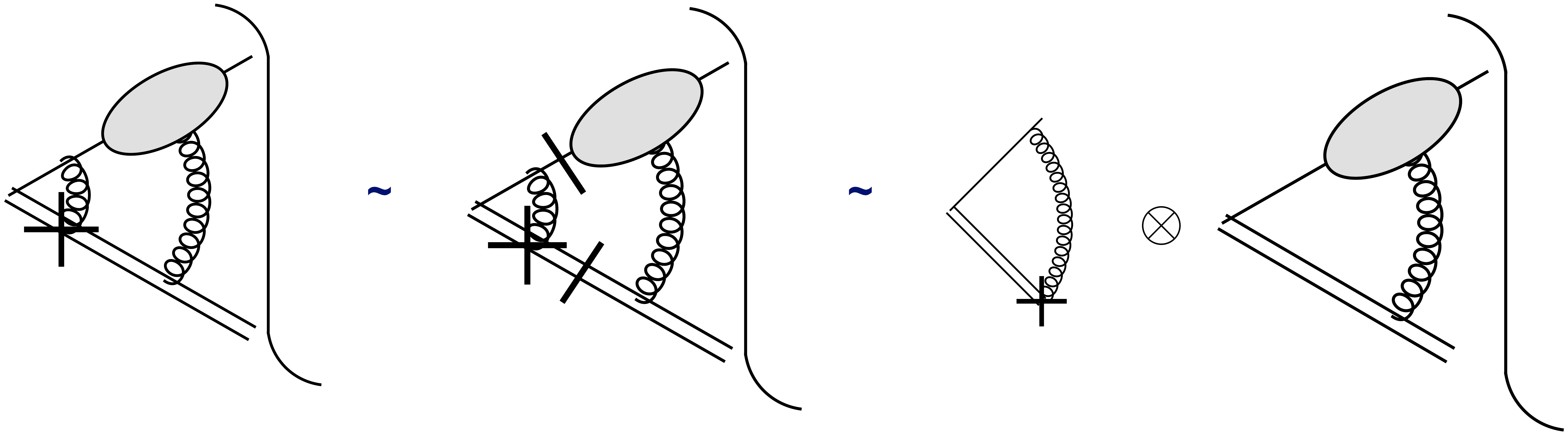

$$-\frac{n^2}{v\cdot n}v_\alpha\frac{d}{dn_\alpha}\bar{J}_q^E(1,P_T,\nu^2,R,r) = 2\nu^2\frac{d}{d\nu^2}\bar{J}_q^E(1,P_T,\nu^2,R,r)$$
$$= 2[G^{(1)}+K^{(1)}(1)]\bar{J}_q^E(1,P_T,\nu^2,R,r).$$

$$\bar{J}_q^E(1,P_T,\nu_{\rm fi}^2,R,r) = \bar{J}_q^E(1,P_T,\nu_{\rm in}^2,R,r)\exp\left\{-\int_{Cr^2}^{CR^2}\frac{dy}{y}\left[\frac{1}{2}\int_{yr^2}^{y^2}\frac{d\omega}{\omega}\lambda_K(\alpha_s(\omega P_T^2))-\frac{\alpha_s(y^2P_T^2)}{2\pi}C_F\right]\right\},$$

Resummed results become consistent

Phys.Rev.Lett. 107 (2011) 152001

$$\Psi_q(r) \equiv \frac{\bar{J}_q^E(1, P_T, \nu_{\rm fi}^2, R, r)}{\bar{J}_q^E(1, P_T, \nu_{\rm in}^2, R, R)},$$

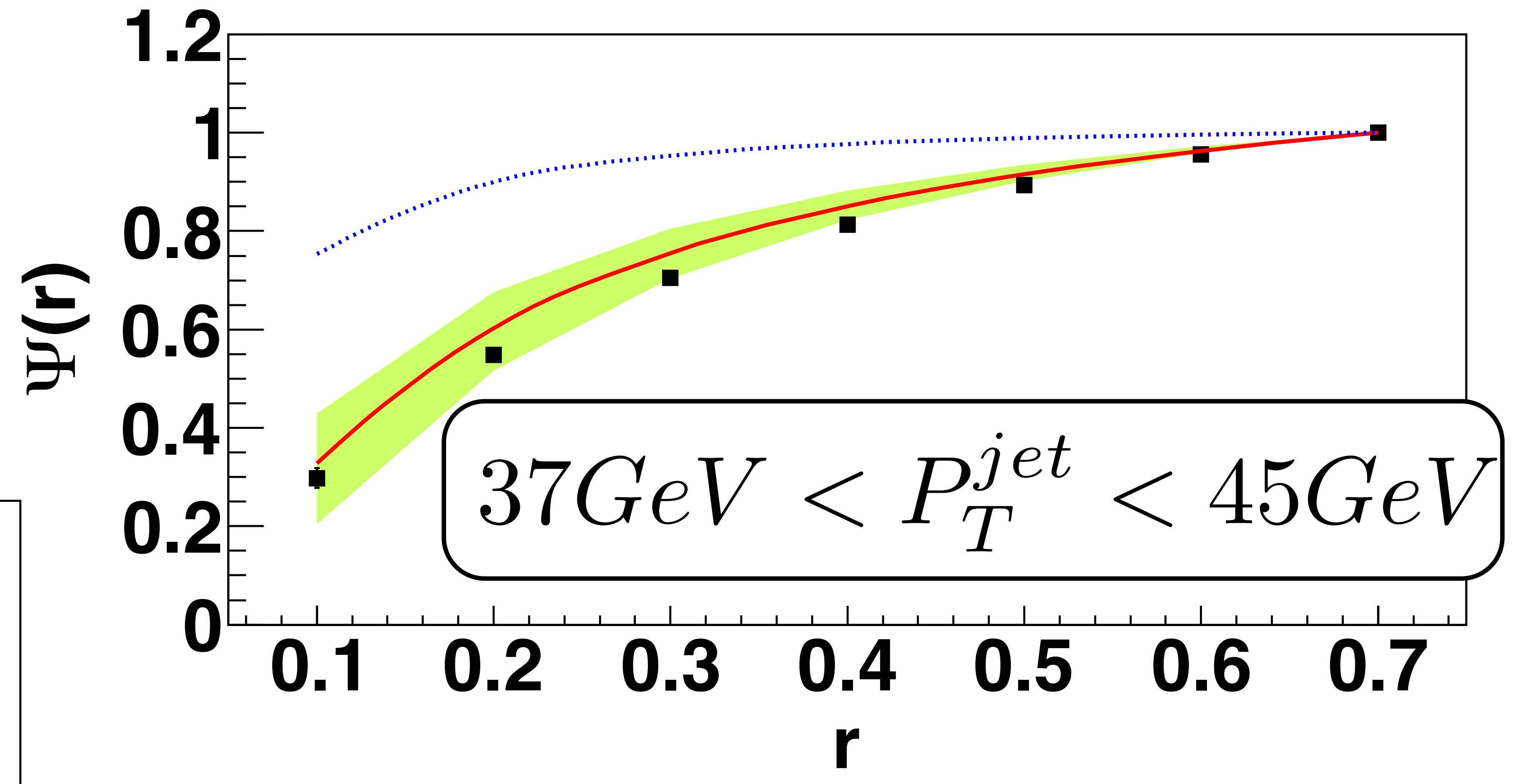

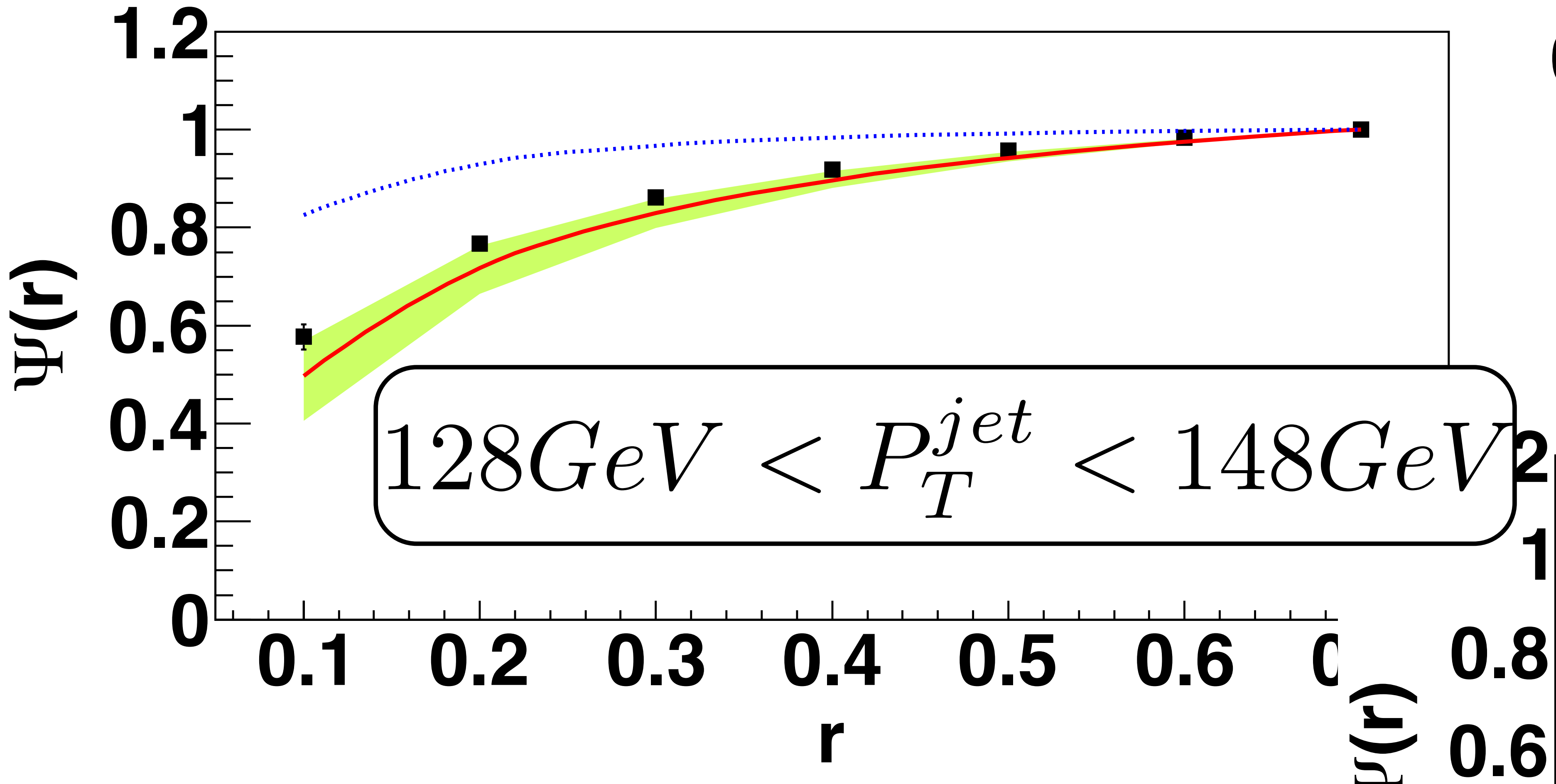

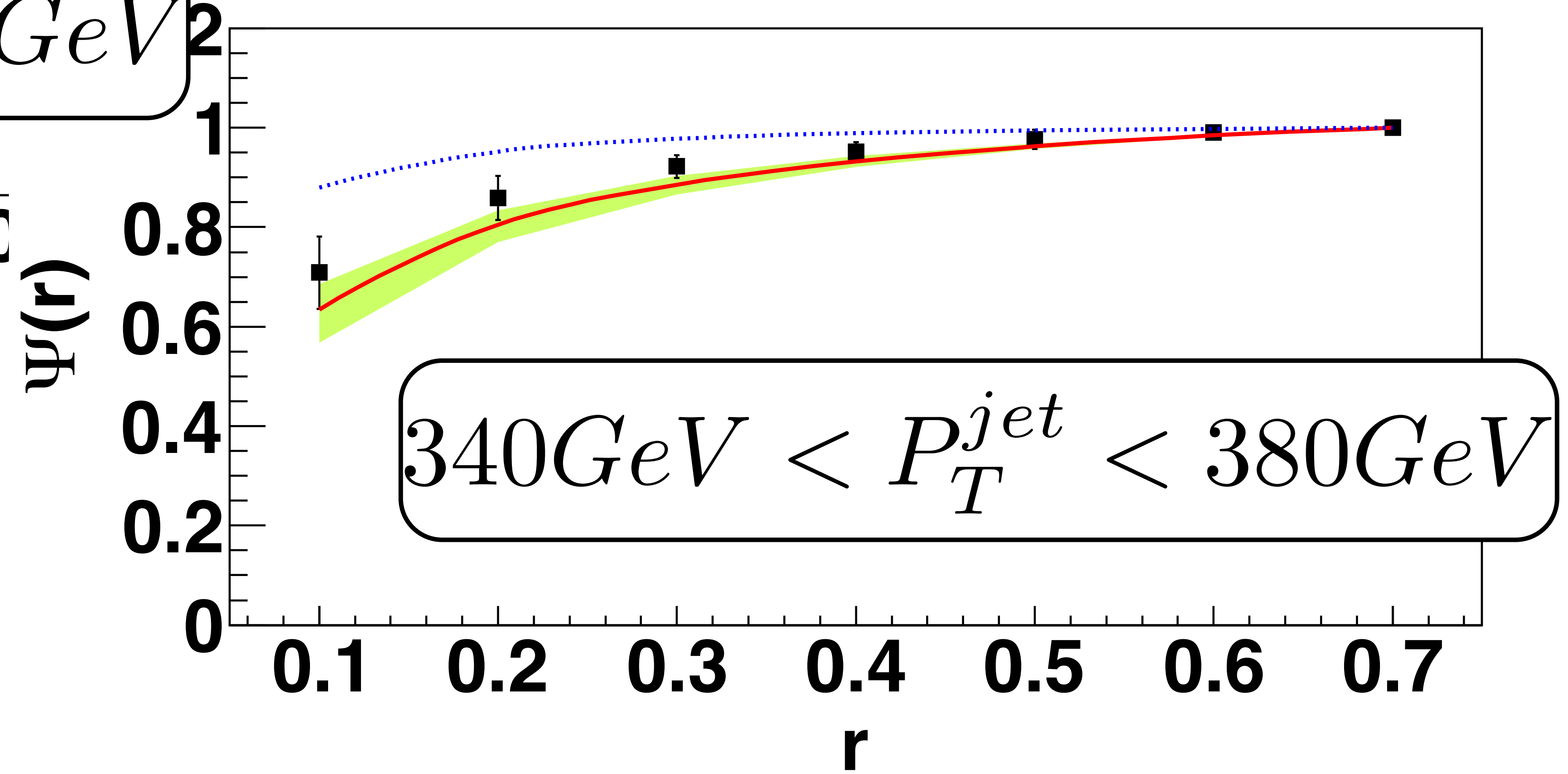

CDF data
PRD71(2005)112002

α_s from Jet Energy Profile

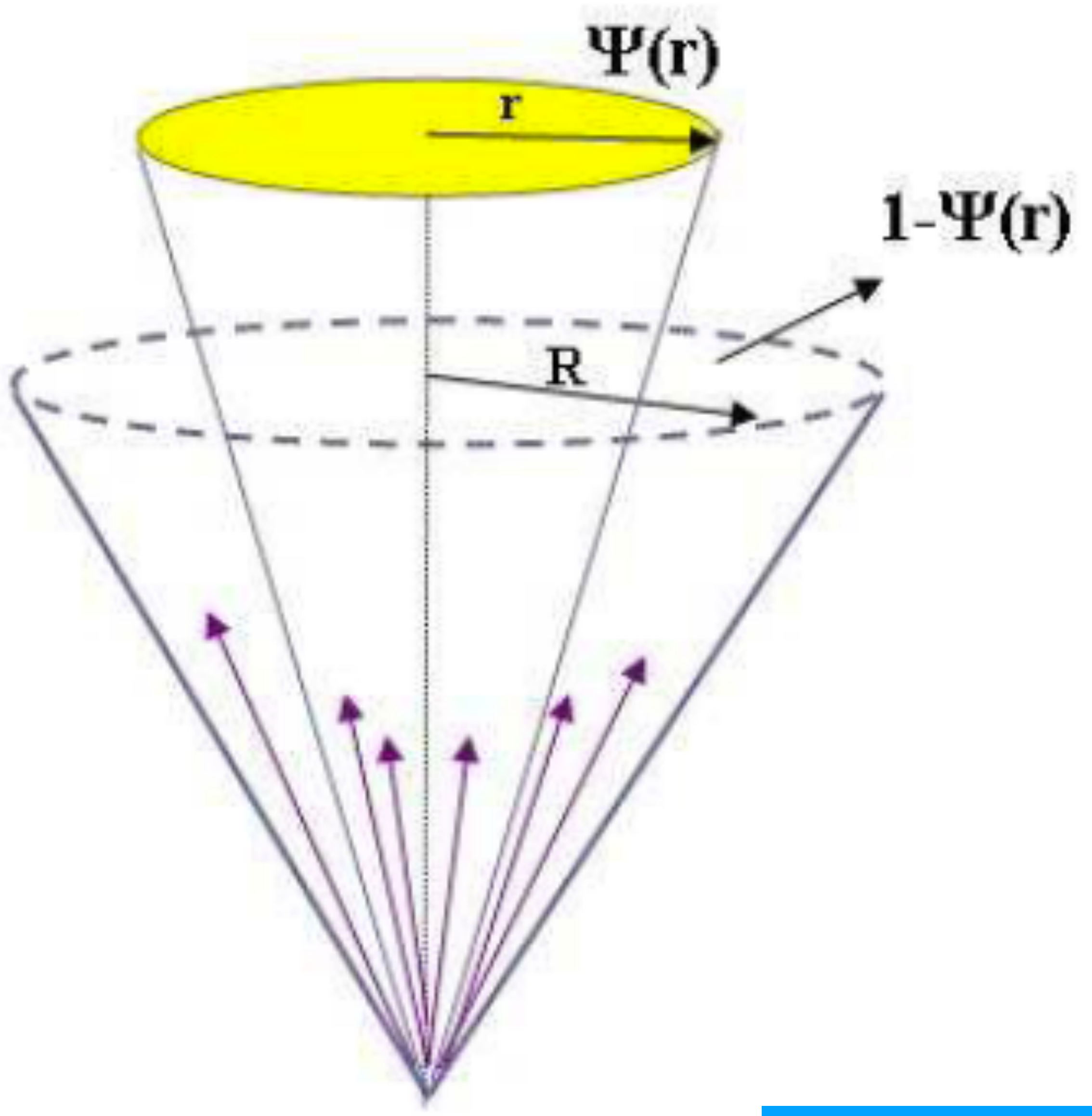

$$\Psi(r) = \frac{1}{N_{jet}} \sum_{jets} \frac{P_T(0,r)}{P_T(0,R)}, \qquad 0 \leq r \leq R$$

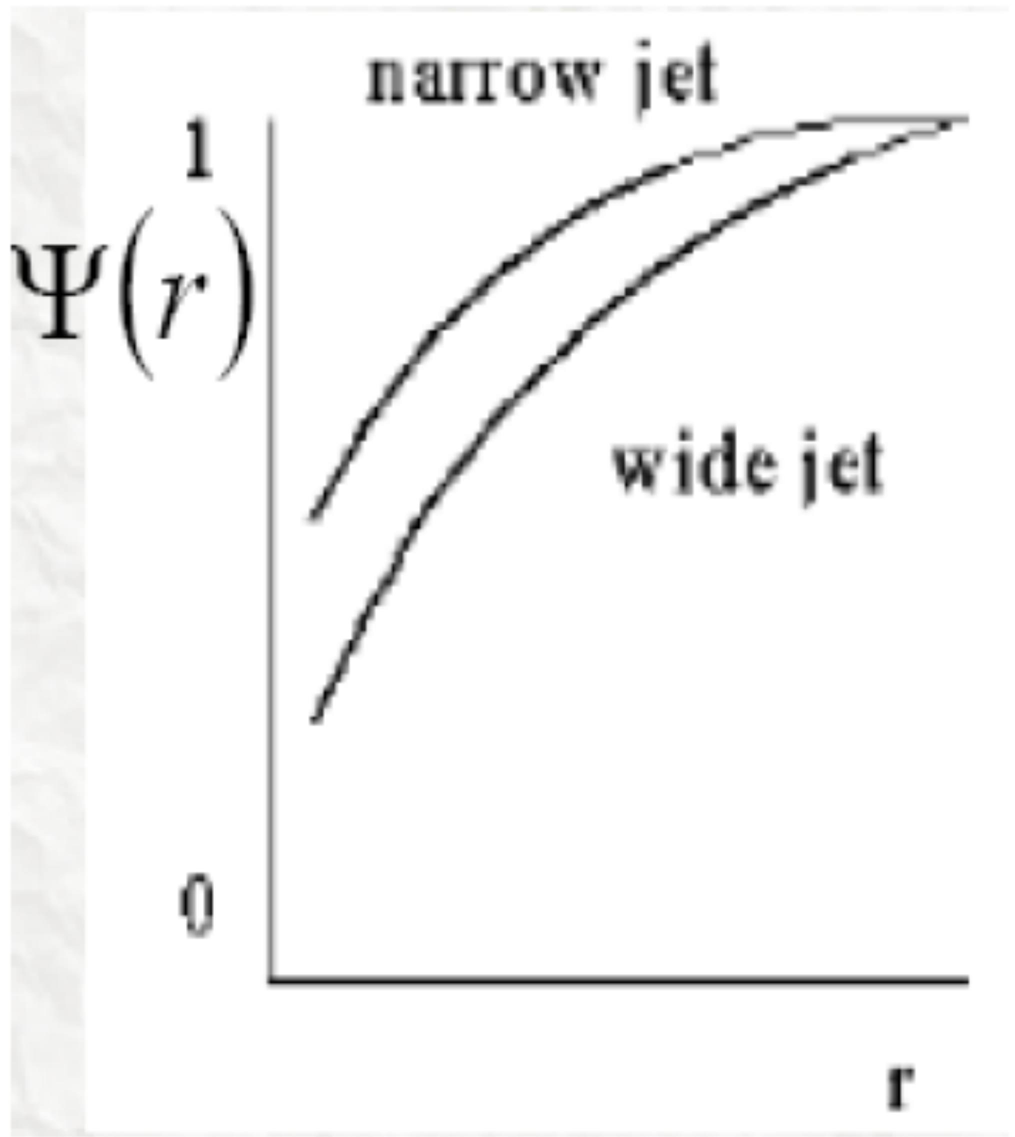

$$\Psi \propto \alpha_s P_T R$$

理论计算 $\Psi(r,\alpha_s)$

实验测量 $\Psi(r)$

抽取 α_s

α_s from Jet Energy Profile

- 未来Tera Z factory 可以提供约 10^{12} 个 Z 玻色子，通过 $Z \to q\bar{q} \to jj$ 可以将JEP的统计误差控制在 10^{-6}，系统误差拒信可以控制在 10^{-3} 以下。
- 这意味着 α_s 的测量精度可以提高至少一个量级。
- 但是大部分喷柱相关的观测量中，理论误差仍然 >1%，其中主要来源于非微扰部分的误差。

α_s from Jet Energy Profile

- 我们曾经的 JEP 理论预言中（NLO-NLL），非微扰部分的贡献极小，理论误差主要来源于微扰部分的标度依赖性 ~5%。
- 标度依赖性可以通过更高阶效应的修正降低。——有望将 α_s 精度降低到 10^{-3}
- 需要大量人力物力

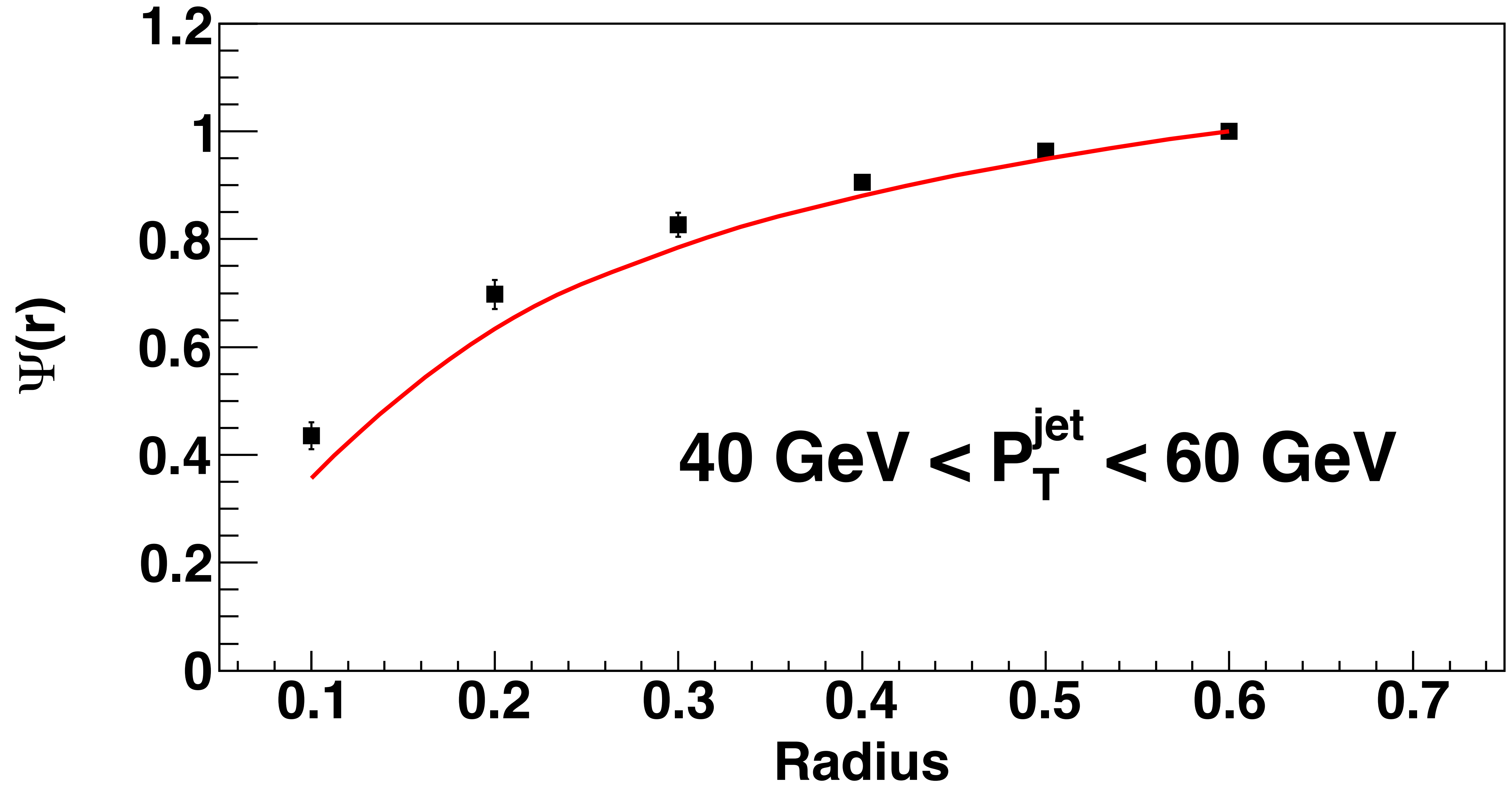

Boosted heavy particles

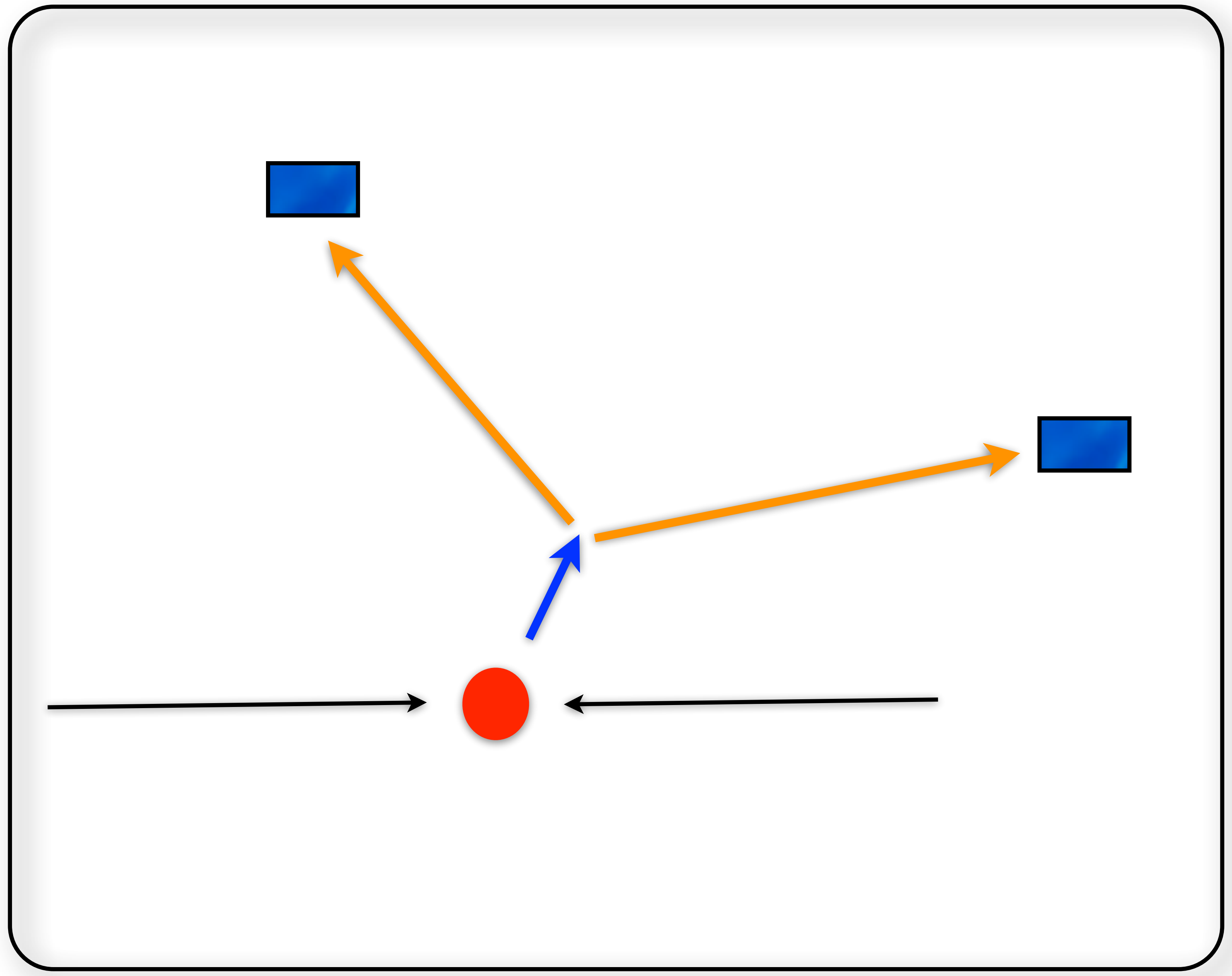

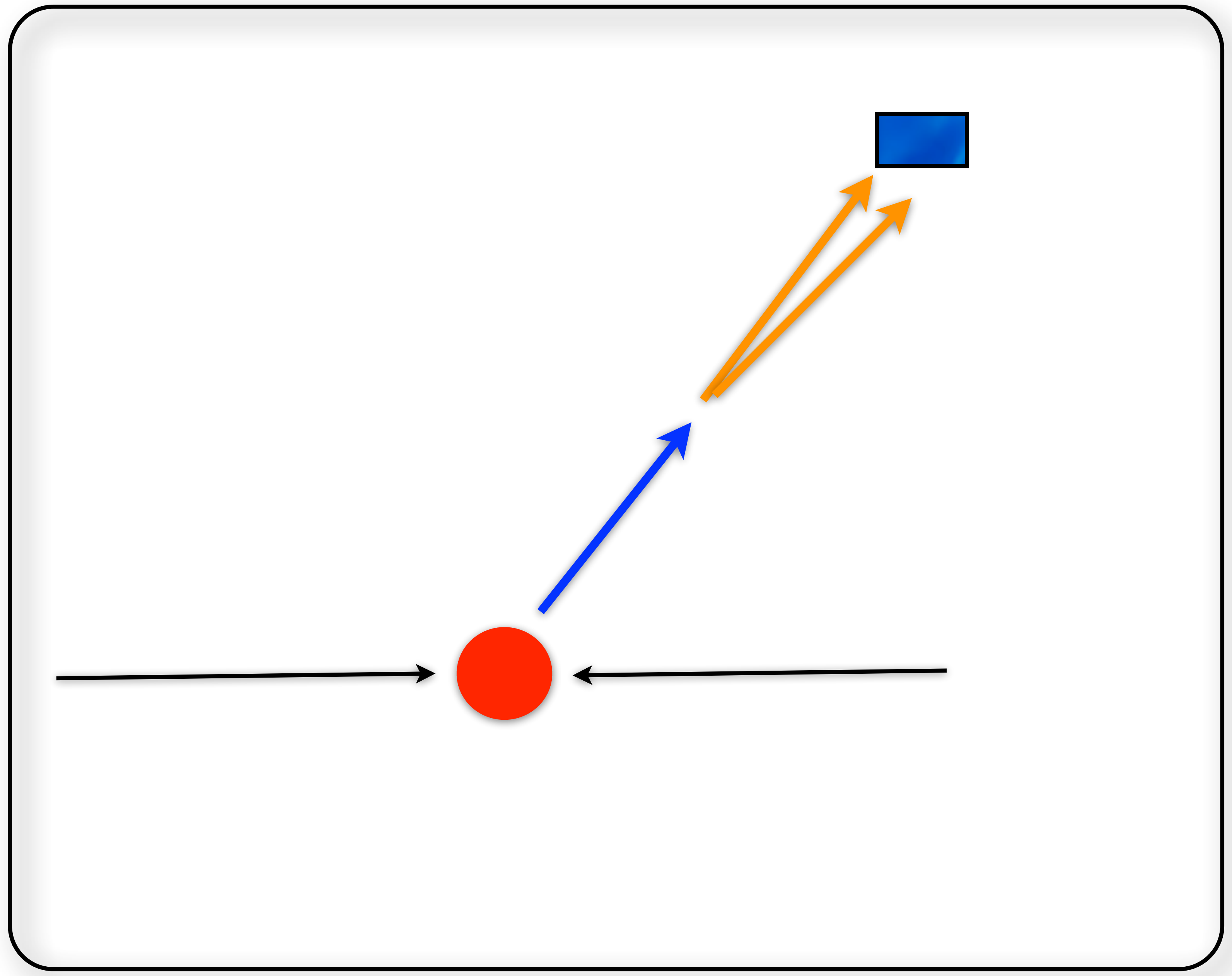

gluino

gaugino

squark

KK

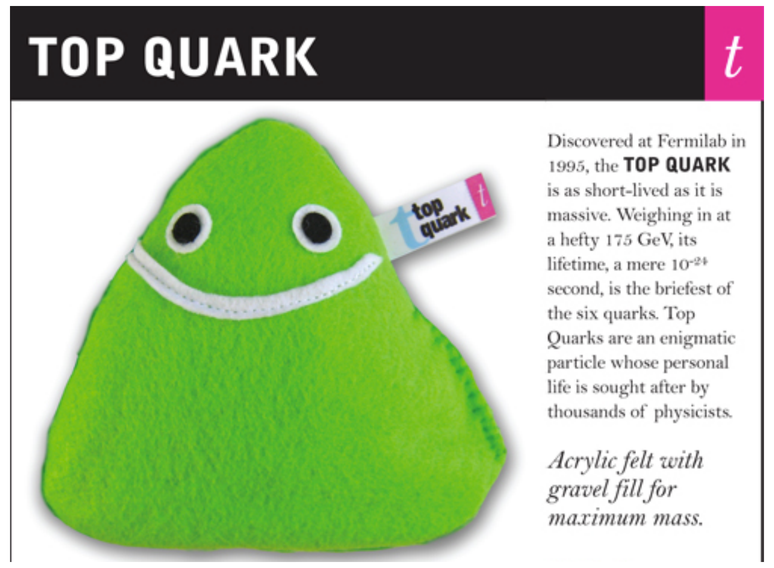

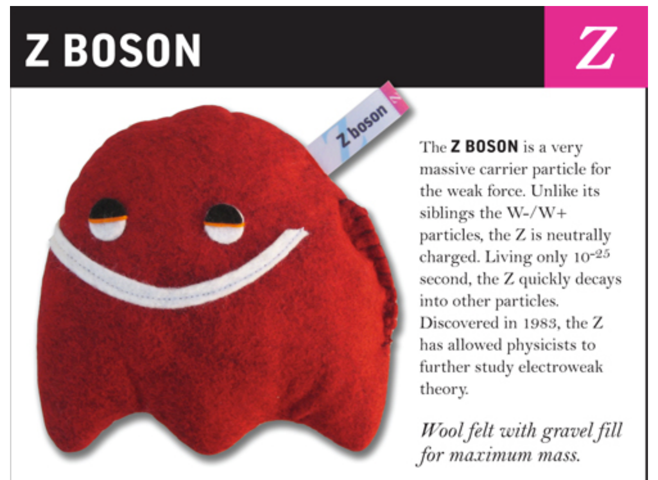

喷柱内部结构非常重要

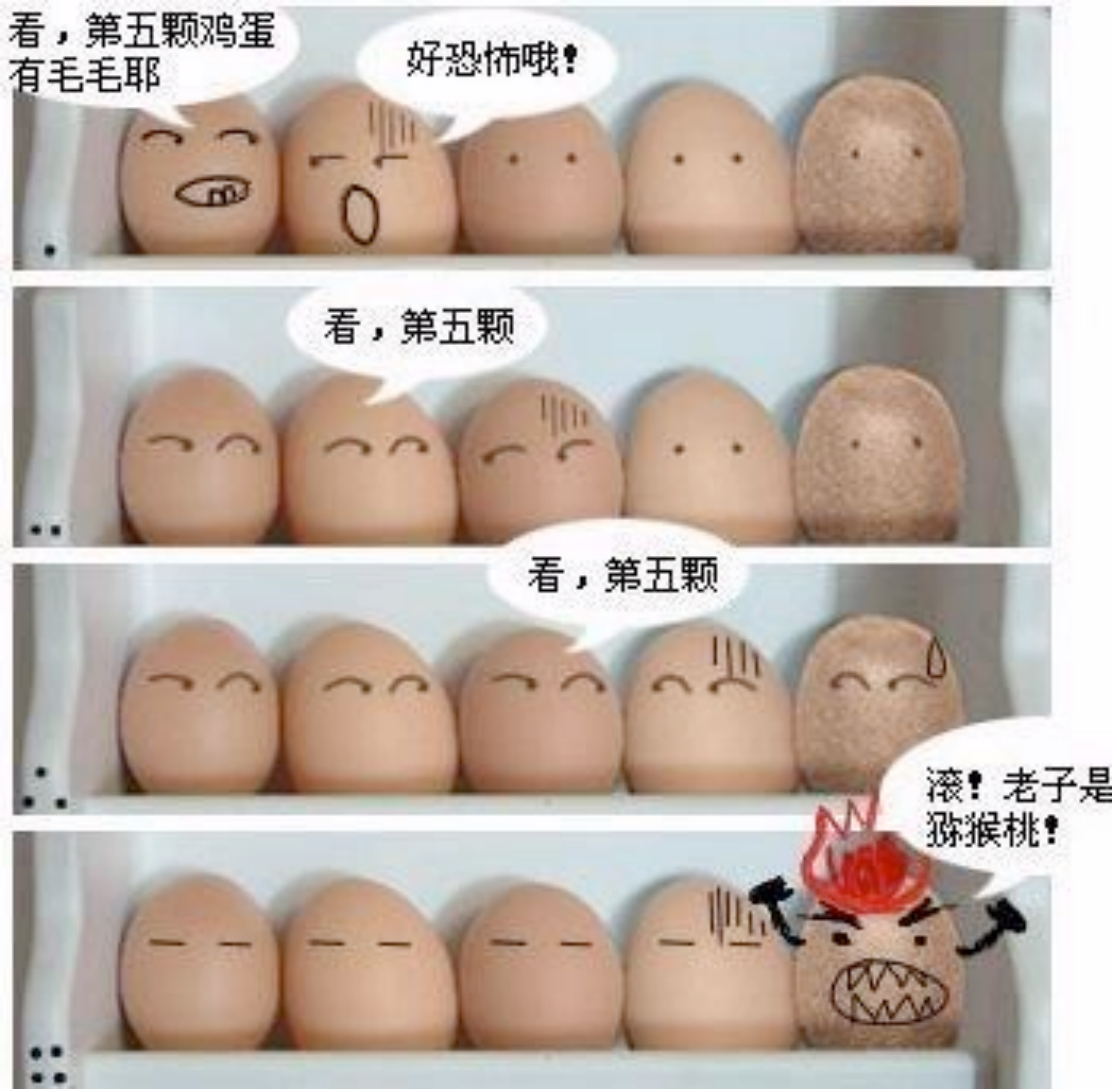

Girth

J. Gallicchio, M.D. Schwartz, PRL 107 (2011) 172001

$$g_J = \sum_{i \in J} \frac{p_{T,i} r_i}{p_{T,J}}.$$

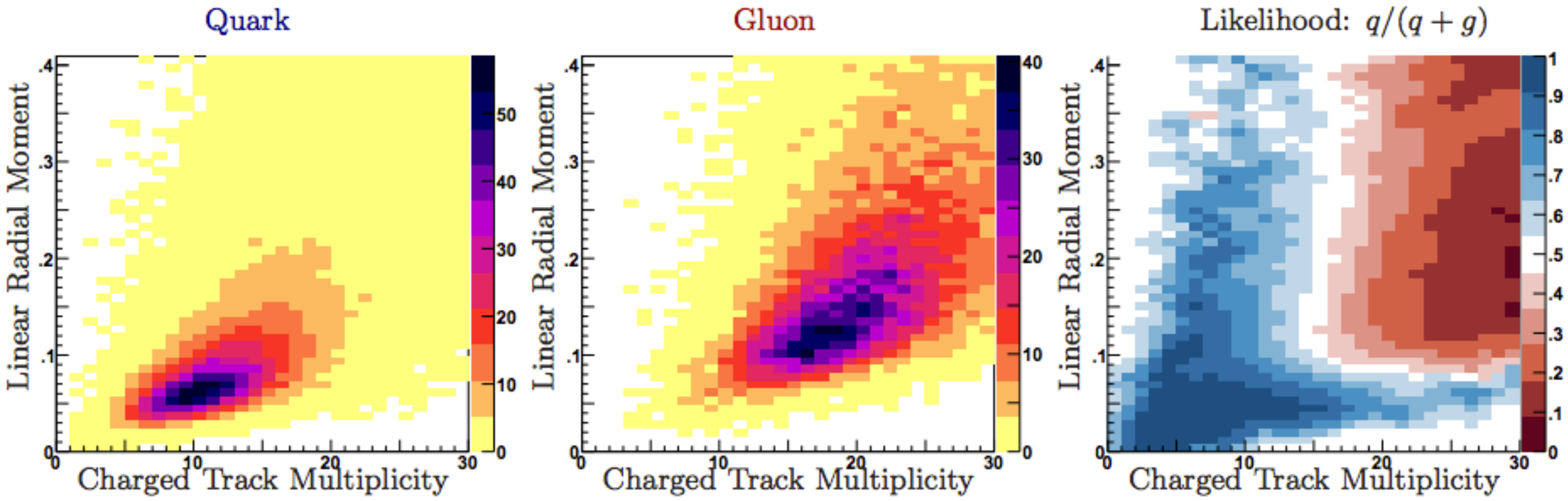

Planar Flow

L. G. Almeida, S. J. Lee, G. Perez, G. Sterman, I. Sung, J. Virzi, PRD79 (2009) 074017

$$I_\omega^{kl} = \frac{1}{m_J}\sum_i \omega_i \frac{p_{i,k}}{\omega_i}\frac{p_{i,l}}{\omega_i}, \qquad Pf = \frac{4\,\det(I_\omega)}{\mathrm{tr}(I_\omega)^2} = \frac{4\lambda_1\lambda_2}{(\lambda_1+\lambda_2)^2},$$

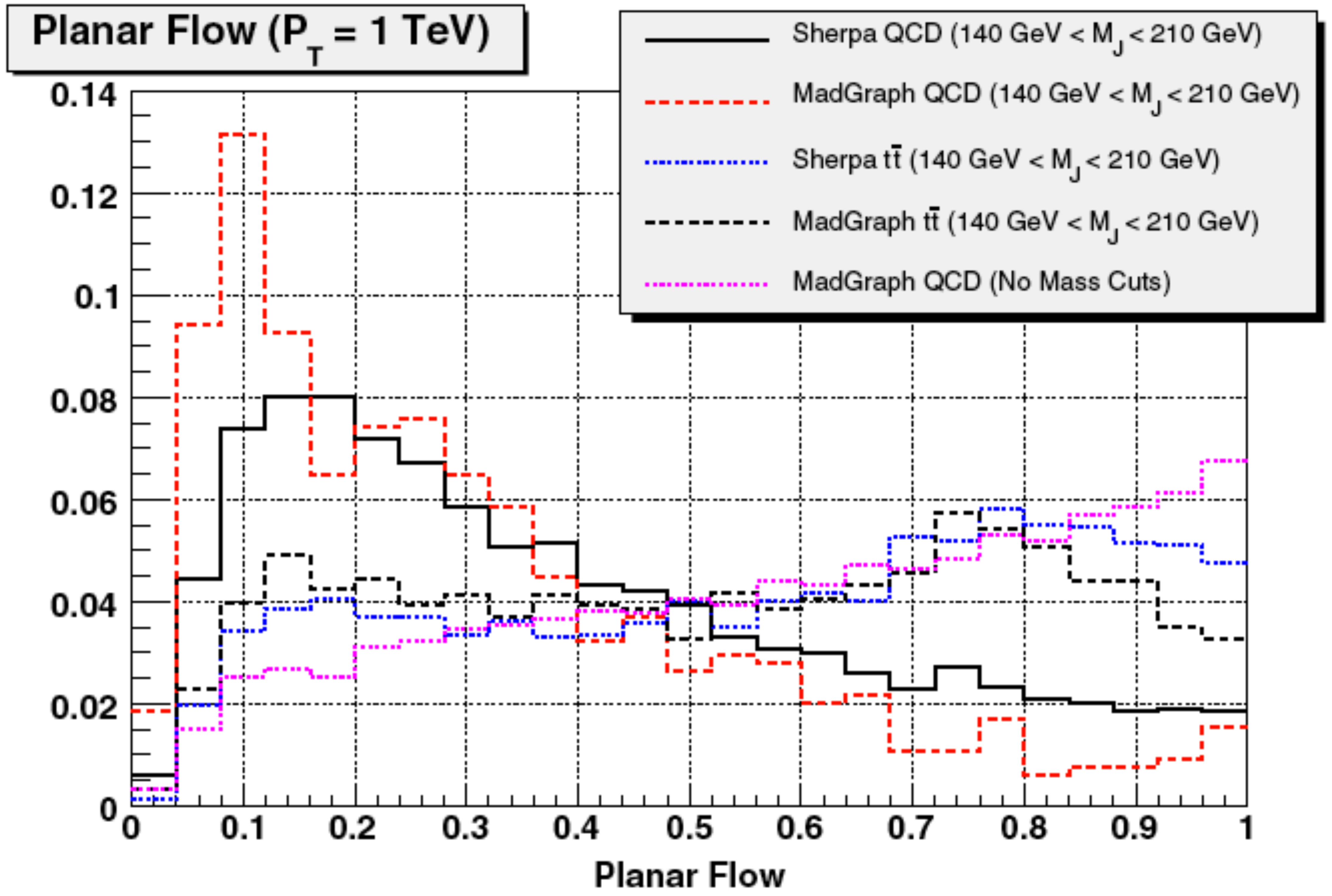

$$\frac{1}{J}\left(\frac{dJ}{dPf}\right)_{2\,\mathrm{body}} = \delta(Pf).$$

(hidden smearing effect)

Color Pull

J. Gallicchio, M.D. Schwartz, PRL105(2010) 022001

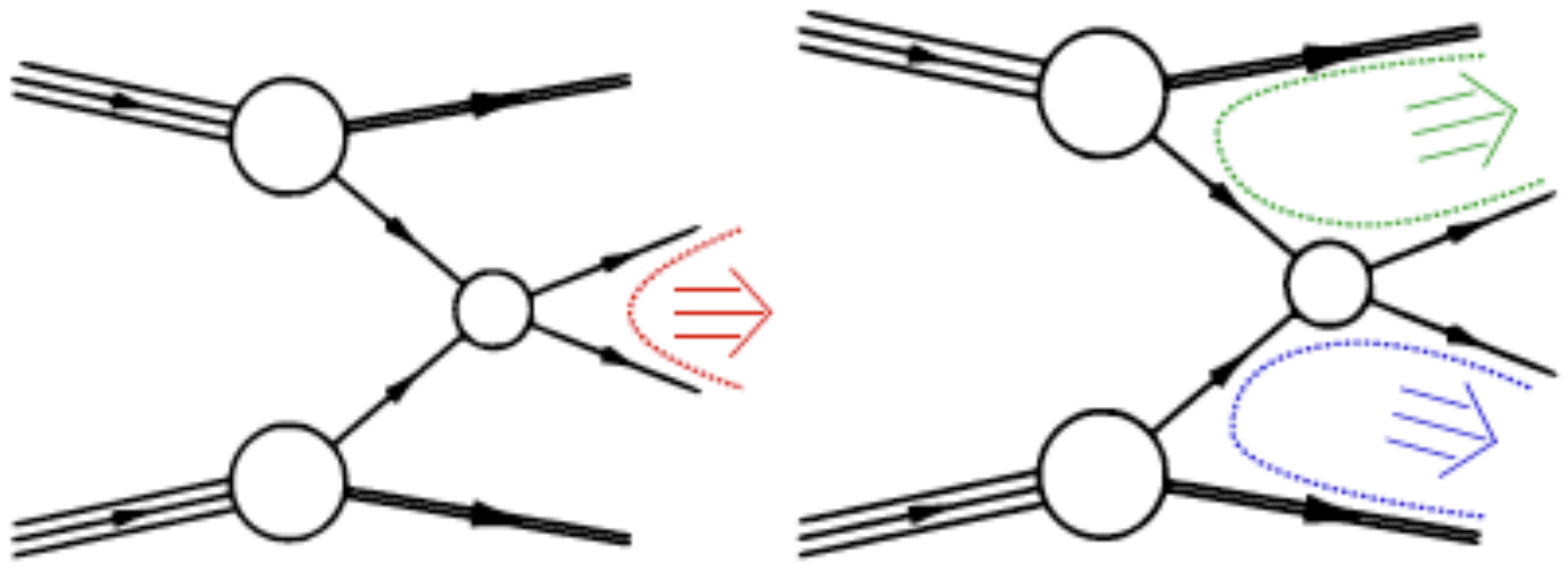

FIG. 1: Possible color connections for signal ($pp \to H \to b\bar{b}$) and for background ($pp \to g \to b\bar{b}$).

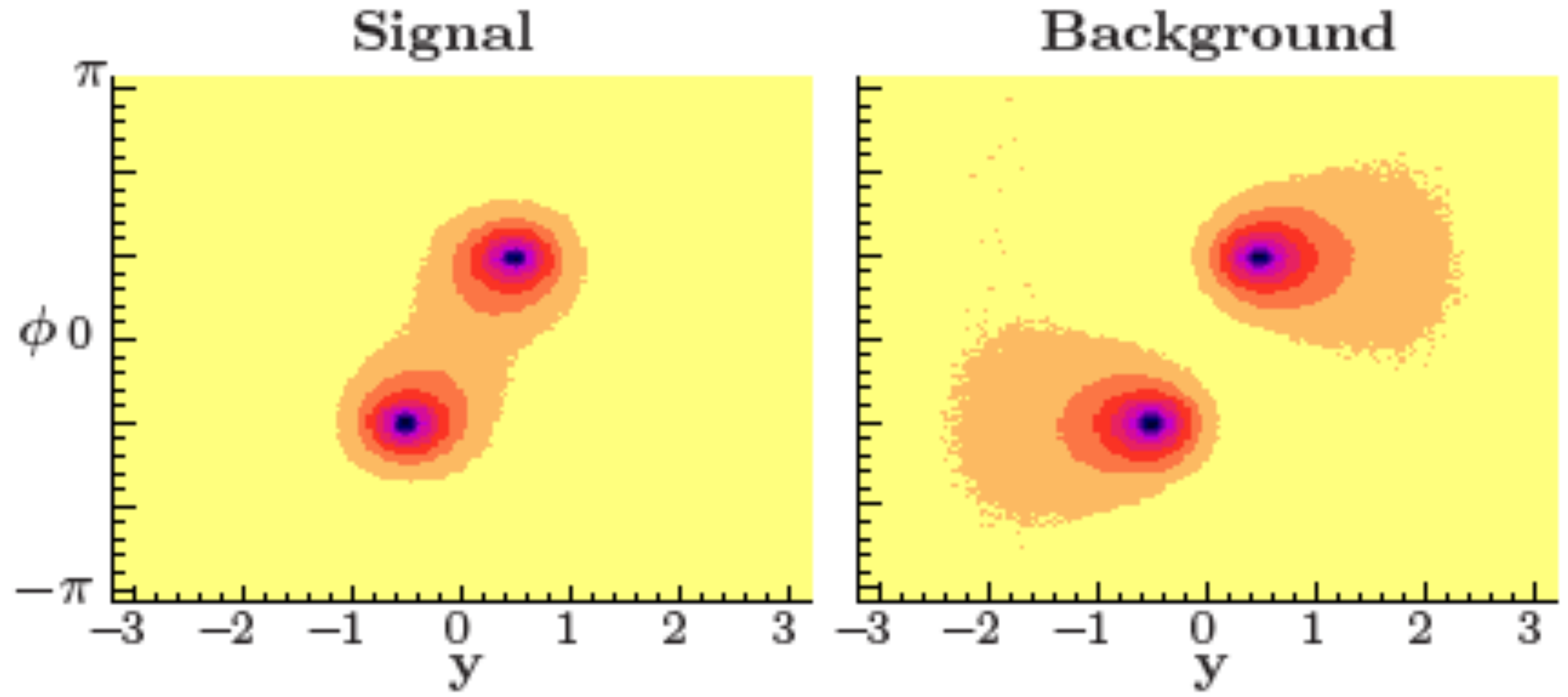

$$\vec{t} = \sum_{i \in \text{jet}} \frac{p_T^i \, |r_i|}{p_T^{\text{jet}}} \vec{r}_i \, .$$

$$\vec{t} = (|\vec{t}| \cos\theta_t, |\vec{t}| \sin\theta_t),$$

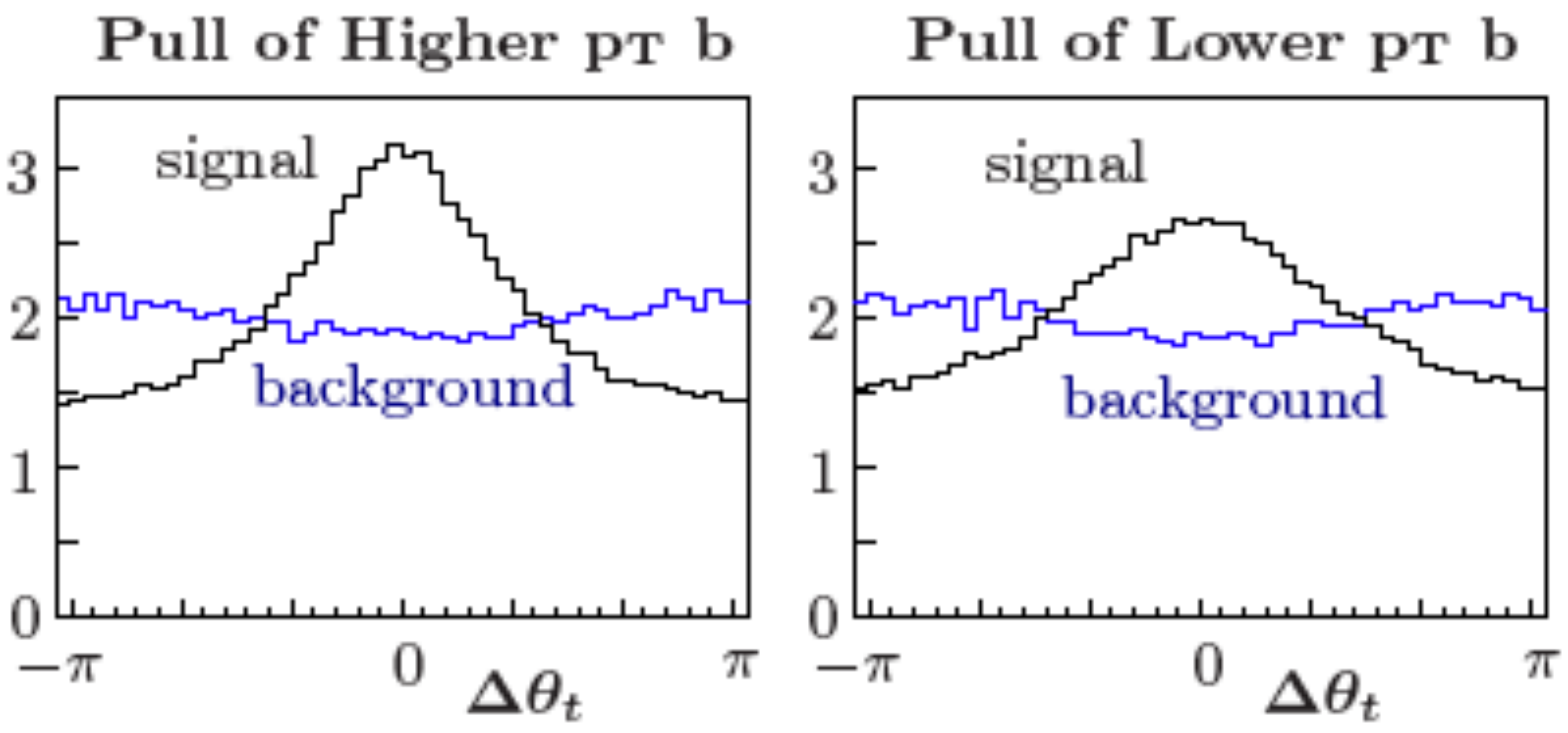

Template overlap

L. G. Almeida, S. J. Lee, G. Perez, G. Sterman, I. Sung, PRD82 (2010) 054034

$$Ov(j,f) = \max_{\tau_n^{(R)}} \exp\left[- \sum_{a=1}^{3} \frac{1}{2\sigma_a^2} \left(\sum_{k=i_a-1}^{i_a+1} \sum_{l=j_a-1}^{j_a+1} E(k,l) - E(i_a,j_a)^{(f)} \right)^2 \right],$$

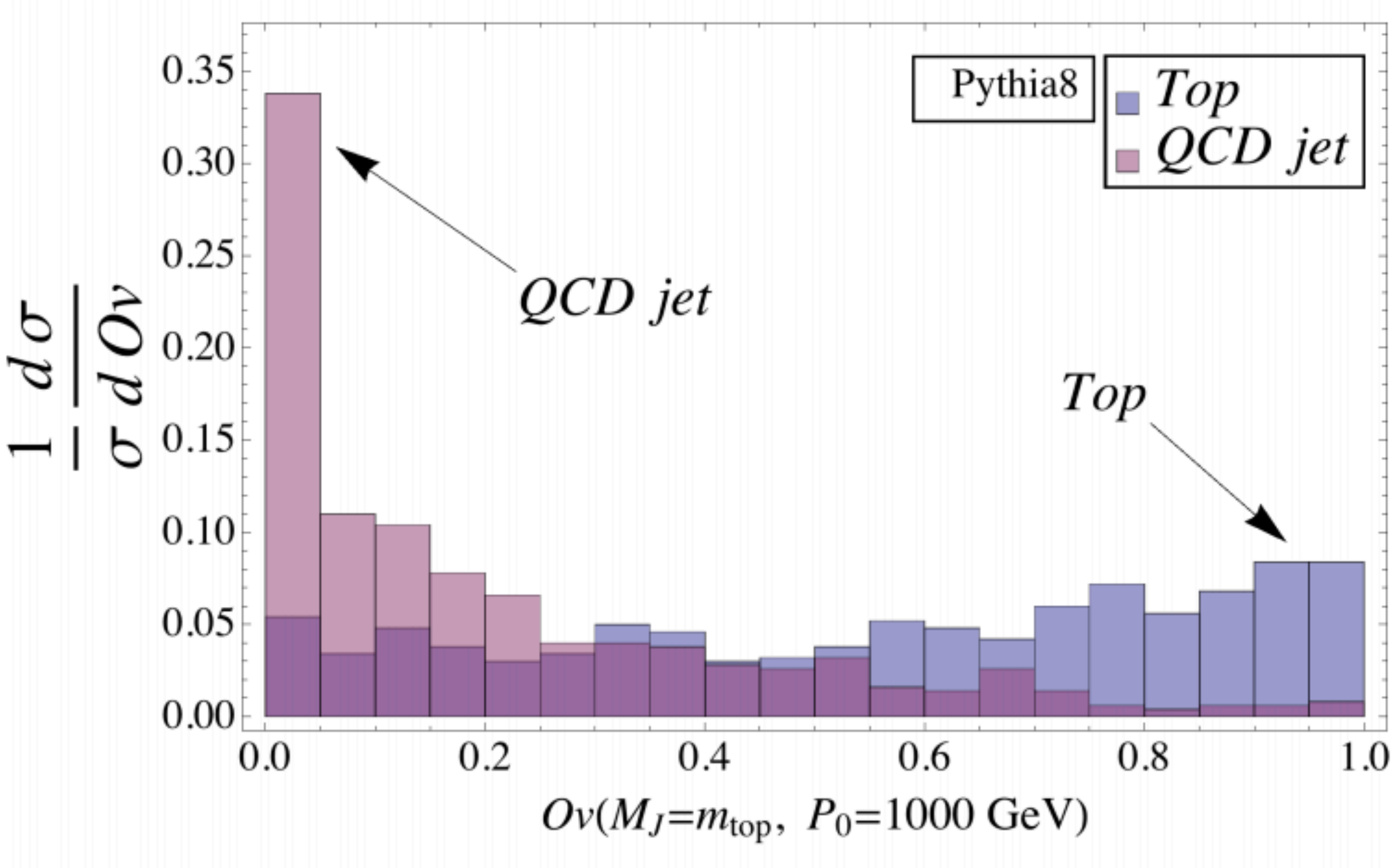

N-subjettiness

J. Thaler, K. V. Tilburg, JHEP 1103 (2011) 015

$$\tau_N = \frac{1}{d_0}\sum_k p_{T,k}\min\{\Delta R_{1,k}, \Delta R_{2,k}, \cdots, \Delta R_{N,k}\}. \qquad d_0 = \sum_k p_{T,k} R_0,$$

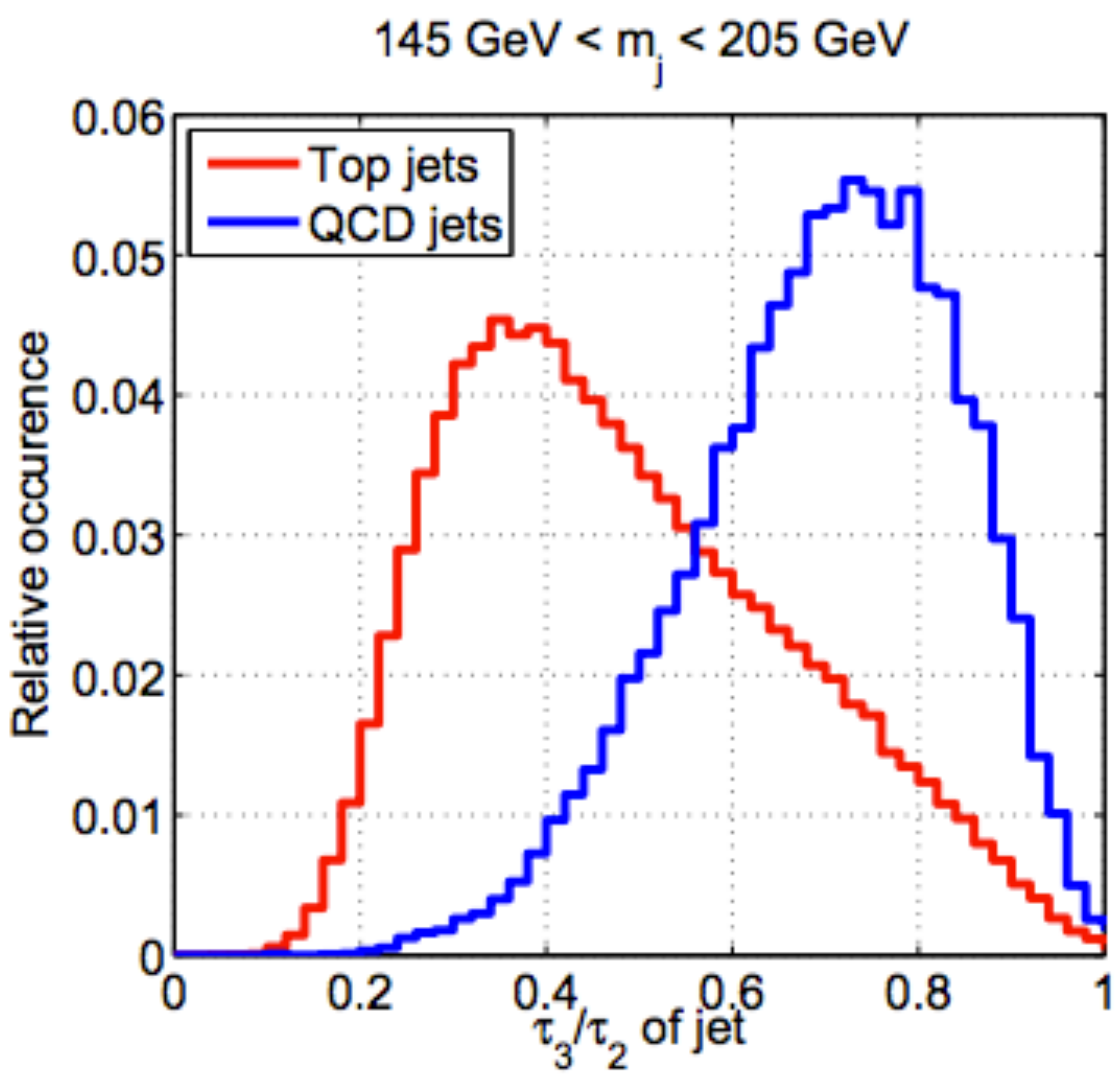

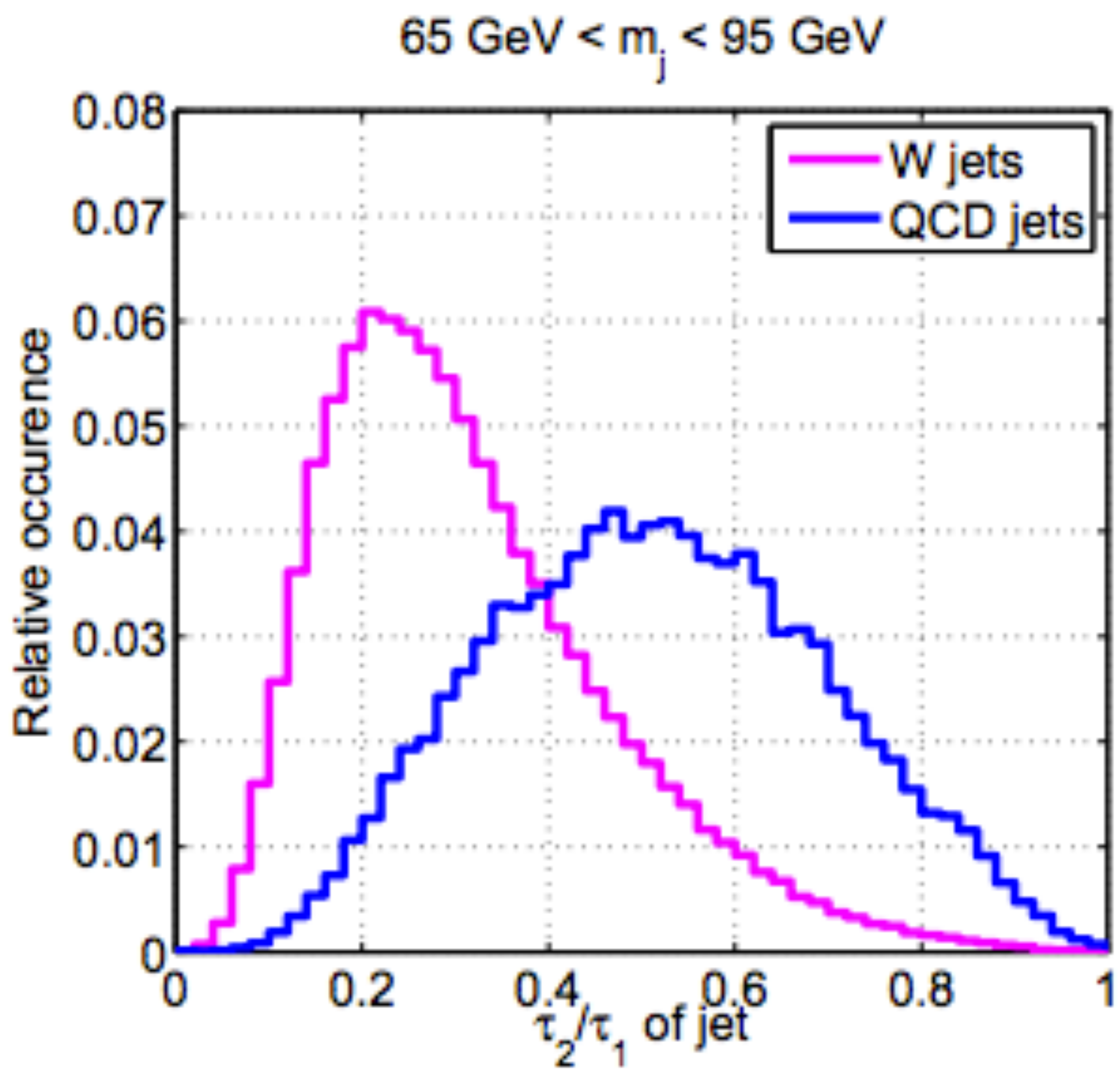

部分子硬散射截面

High Order QCD/EW Effect

Virtual Correction

Real Correction

$$\sigma_{pp\to\ell\bar{\ell}X} = \sum_{a,b=q,\bar{q},g} \int_0^1 d\xi_1 \int_0^1 d\xi_2 \widehat{\sigma}_{ab\to V\to\ell\bar{\ell}} \left(\frac{x_1}{\xi_1}, \frac{x_2}{\xi_2}; \frac{Q}{\mu}\right) f_{a/p}(\xi_1,\mu) f_{b/p}(\xi_2,\mu) + \mathcal{O}\left(\Lambda^2_{QCD}/Q^2\right)$$

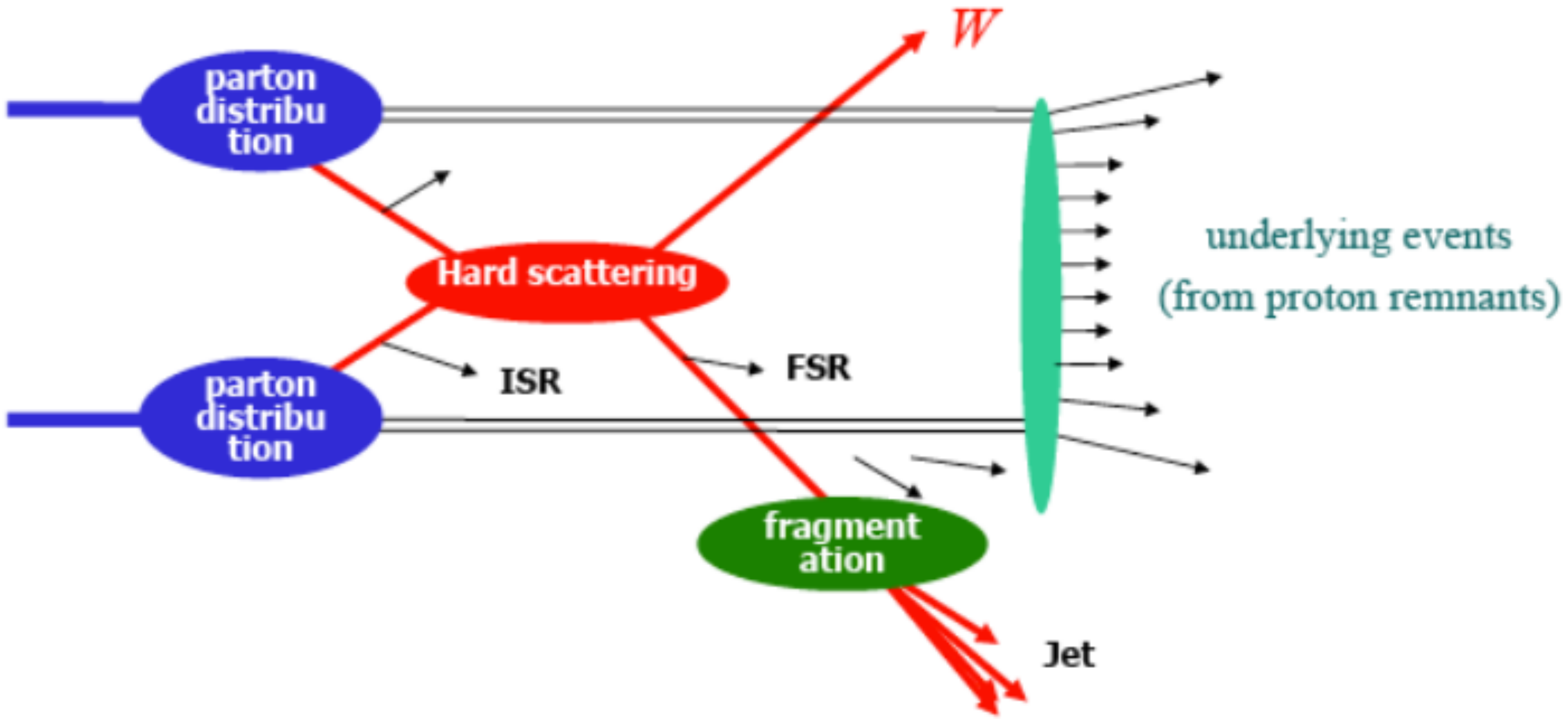

Virtual correction amplitudes

- Feynman振幅张量约化
- Feynman标量积分约化
- Feynman主积分计算

Difficulties in multi-loop amplitude

1. Reduce into scalar loop integrals (could be O(10^4) or more) i.e. tensor reduction

2. Reduce to master integrals (much less, maybe O(10^2)), mostly IBP reduction, newly series representation

3. Evaluation of master integrals (numerical or analytical) e.g. sector decomposition, Mellin-Barnes, series representation, etc.

振幅张量约化

Difficulties in tensor reduction

$$\mathcal{M} = \int \mathbb{D}^L q \frac{N(\{q_j\}_{j=1}^L, \{k_e\}_{e=1}^E)}{\prod_{i=1}^n \mathcal{D}_i^{\nu_i}},$$

Unlike SP between loop momentum and external momentum $q \cdot k$

(can be expressed as linear combination of denominators)

$$\boxed{q \cdot k = \frac{1}{2}\{[(q+k)^2] - [q^2 - m^2] - k^2 - m^2\}}$$

Numerator may contain ISP

$\bar{u} \not{k} \not{q} v$ **or** $q \cdot \varepsilon$

$$\boxed{\begin{aligned} N(q_1, q_2) = &\left(\frac{-\imath g_s^4 e^2 V_{tb} V_{ud}^\dagger}{8 s_W^2}\right)\left(\frac{\delta_{tb}\delta_{ud} + C_A(C_A^2 - 2)\delta_{tu}\delta_{bd}}{C_A^2}\right) \\ &\times \left[\bar{t}\gamma^\mu P_L(\not{k}_4 - \not{q}_1)\gamma^\beta(-\not{q}_1 + \not{q}_2 + \not{k}_2 - \not{k}_3)\gamma_\alpha b\right] \\ &\times \left[\bar{d}\gamma^\mu P_L(\not{q}_1 + \not{k}_3)\gamma^\alpha \not{q}_2 \gamma^\beta u\right], \end{aligned}}$$

Projection Method

Amplitude: $A = \sum_{i=1}^{n} C_i T_i$

Dependent of Mandelstam variables

Dirac structures

$$C_i = \sum_j (M_{ij})^{-1} (A T_j^\dagger),$$
$$M_{ij} = T_i T_j^\dagger$$

Phys.Rev.D90(2014)no.11,114024

General Tensor for H->ggg @ 2-loop

$$
\begin{aligned}
S_{\mu\nu\rho}(g_1;g_2;g_3)\epsilon_1^\mu\epsilon_2^\nu\epsilon_3^\rho = & \sum_{i,j,k=1}^{3} A_{i\,j\,k}\, p_i\!\cdot\!\epsilon_1\, p_j\!\cdot\!\epsilon_2\, p_k\!\cdot\!\epsilon_3 + \sum_{i=1}^{3} B_i\, p_i\!\cdot\!\epsilon_1\, \epsilon_2\!\cdot\!\epsilon_3 \\
& + \sum_{i=1}^{3} C_i\, p_i\!\cdot\!\epsilon_2\, \epsilon_1\!\cdot\!\epsilon_3 + \sum_{i=1}^{3} D_i\, p_i\!\cdot\!\epsilon_3\, \epsilon_1\!\cdot\!\epsilon_2 \\
= & \; A_{211}\, p_2\!\cdot\!\epsilon_1\, p_1\!\cdot\!\epsilon_2\, p_1\!\cdot\!\epsilon_3 + A_{212}\, p_2\!\cdot\!\epsilon_1\, p_1\!\cdot\!\epsilon_2\, p_2\!\cdot\!\epsilon_3 + A_{231}\, p_2\!\cdot\!\epsilon_1\, p_3\!\cdot\!\epsilon_2\, p_1\!\cdot\!\epsilon_3 \\
& + A_{232}\, p_2\!\cdot\!\epsilon_1\, p_3\!\cdot\!\epsilon_2\, p_2\!\cdot\!\epsilon_3 + A_{311}\, p_3\!\cdot\!\epsilon_1\, p_1\!\cdot\!\epsilon_2\, p_1\!\cdot\!\epsilon_3 + A_{312}\, p_3\!\cdot\!\epsilon_1\, p_1\!\cdot\!\epsilon_2\, p_2\!\cdot\!\epsilon_3 \\
& + A_{331}\, p_3\!\cdot\!\epsilon_1\, p_3\!\cdot\!\epsilon_2\, p_1\!\cdot\!\epsilon_3 + A_{332}\, p_3\!\cdot\!\epsilon_1\, p_3\!\cdot\!\epsilon_2\, p_2\!\cdot\!\epsilon_3 \\
& + B_2\, \epsilon_2\!\cdot\!\epsilon_3\, p_2\!\cdot\!\epsilon_1 + B_3\, \epsilon_2\!\cdot\!\epsilon_3\, p_3\!\cdot\!\epsilon_1 \\
& + C_1\, \epsilon_1\!\cdot\!\epsilon_3\, p_1\!\cdot\!\epsilon_2 + C_3\, \epsilon_1\!\cdot\!\epsilon_3\, p_3\!\cdot\!\epsilon_2 \\
& + D_1\, \epsilon_1\!\cdot\!\epsilon_2\, p_1\!\cdot\!\epsilon_3 + D_2\, \epsilon_1\!\cdot\!\epsilon_2\, p_2\!\cdot\!\epsilon_3\,, \qquad (3.4)
\end{aligned}
$$

Gehrmann et. al. JHEP 02 (2012) 056

Gauge invariant basis

$$S_{\mu\nu\rho}(g_1;g_2;g_3)\epsilon_1^\mu\epsilon_2^\nu\epsilon_3^\rho = A_{211}T_{211} + A_{311}T_{311} + A_{232}T_{232} + A_{312}T_{312}\,,$$

$$\begin{aligned}
T_{232} &= p_2\cdot\epsilon_1\, p_3\cdot\epsilon_2\, p_2\cdot\epsilon_3 - \frac{1}{2}\,\epsilon_2\cdot\epsilon_3\, p_2\cdot\epsilon_1\, s_{23} - \frac{p_3\cdot\epsilon_1\, p_3\cdot\epsilon_2\, p_2\cdot\epsilon_3\, s_{12}}{s_{13}} + \frac{1}{2}\,\frac{\epsilon_2\cdot\epsilon_3\, p_3\cdot\epsilon_1\, s_{23}\, s_{12}}{s_{13}}\,,\\
T_{211} &= p_2\cdot\epsilon_1\, p_1\cdot\epsilon_2\, p_1\cdot\epsilon_3 - \frac{1}{2}\,\epsilon_1\cdot\epsilon_2\, p_1\cdot\epsilon_3\, s_{12} - \frac{p_2\cdot\epsilon_1\, p_1\cdot\epsilon_2\, p_2\cdot\epsilon_3\, s_{13}}{s_{23}} + \frac{1}{2}\,\frac{\epsilon_1\cdot\epsilon_2\, p_2\cdot\epsilon_3\, s_{13}\, s_{12}}{s_{23}}\,,\\
T_{311} &= p_3\cdot\epsilon_1\, p_1\cdot\epsilon_2\, p_1\cdot\epsilon_3 - \frac{1}{2}\,\epsilon_1\cdot\epsilon_3\, p_1\cdot\epsilon_2\, s_{13} - \frac{p_3\cdot\epsilon_1\, p_3\cdot\epsilon_2\, p_1\cdot\epsilon_3\, s_{12}}{s_{23}} + \frac{1}{2}\,\frac{\epsilon_1\cdot\epsilon_3\, p_3\cdot\epsilon_2\, s_{13}\, s_{12}}{s_{23}}\,,\\
T_{312} &= p_3\cdot\epsilon_1\, p_1\cdot\epsilon_2\, p_2\cdot\epsilon_3 - p_2\cdot\epsilon_1\, p_3\cdot\epsilon_2\, p_1\cdot\epsilon_3 + \frac{1}{2}\,\epsilon_1\cdot\epsilon_3\, p_3\cdot\epsilon_2\, s_{12} + \frac{1}{2}\,\epsilon_1\cdot\epsilon_2\, p_1\cdot\epsilon_3\, s_{23}\\
&\quad - \frac{1}{2}\,\epsilon_1\cdot\epsilon_3\, p_1\cdot\epsilon_2\, s_{23} + \frac{1}{2}\,\epsilon_2\cdot\epsilon_3\, p_2\cdot\epsilon_1\, s_{13} - \frac{1}{2}\,\epsilon_1\cdot\epsilon_2\, p_2\cdot\epsilon_3\, s_{13} - \frac{1}{2}\,\epsilon_2\cdot\epsilon_3\, p_3\cdot\epsilon_1\, s_{12}\,.
\end{aligned} \tag{3.7}$$

Gehrmann et. al. JHEP 02 (2012) 056

$$A = \sum_{i=1}^{n} C_i \; T_i$$

$$C_i = \sum_j (M_{ij})^{-1} (A T_j^\dagger) ,$$
$$M_{ij} = T_i T_j^\dagger$$

- **Loop momenta have been decoupled from Dirac structures, polarization vectors etc.**

- **Numerator contains scalar products of loop momenta and external momenta at most.**

- **Loop integrals can be contracted into coefficients of form factors**

Tarasov's Method

$$\frac{1}{A_1^{\nu_1}\dots A_7^{\nu_7}} = \int \mathcal{D}x \;\exp\left(\sum_{i=1}^{7} x_i A_i\right),$$

$$\int \mathcal{D}x \;=\; \prod_{i=1}^{7} \frac{(-1)^{\nu_i}}{\Gamma(\nu_i)} \int_0^\infty dx_i\, x_i^{\nu_i-1},$$

$$\sum_{i=1}^{7} x_i A_i \;=\; a\,k^2 + b\,l^2 + 2\,c\,k\cdot l + 2\,d\cdot k + 2\,e\cdot l + f,$$

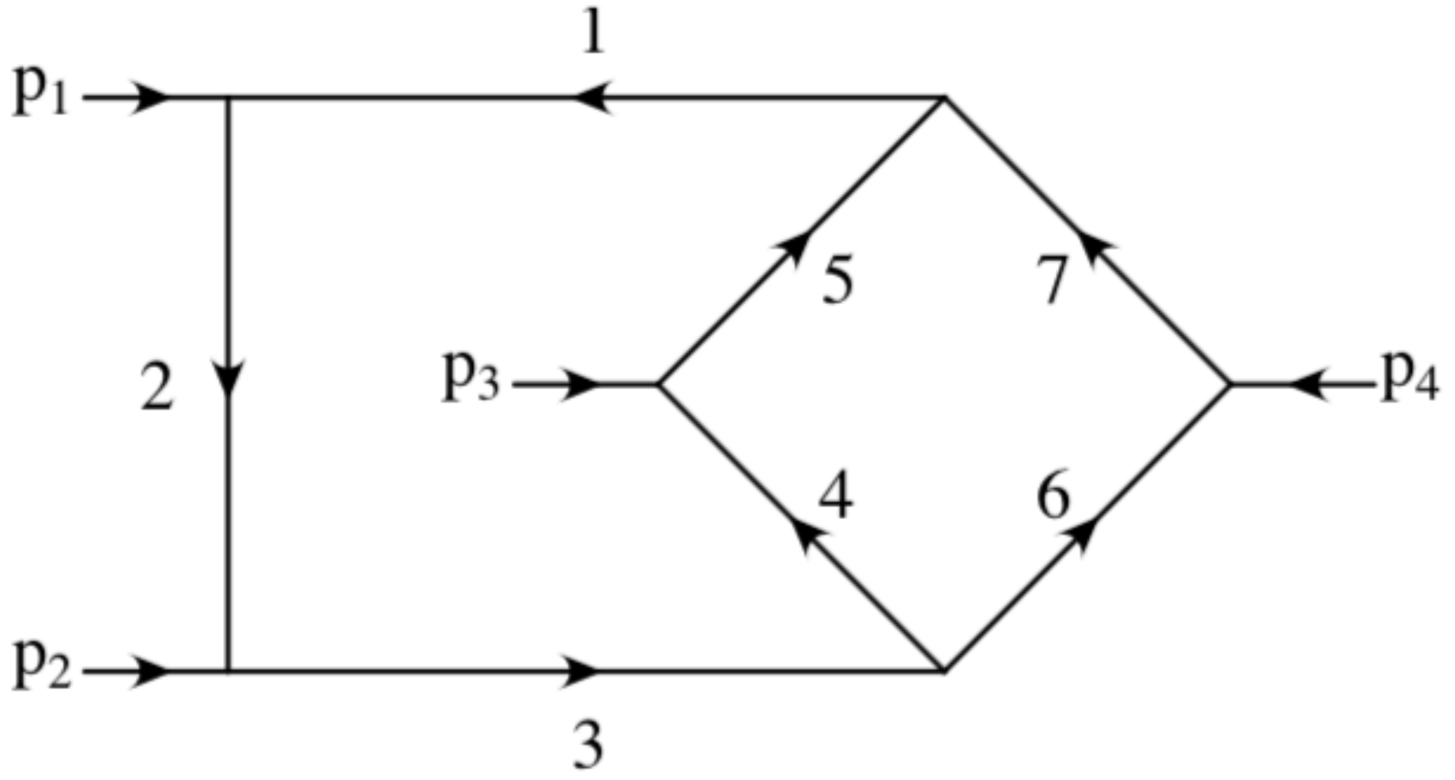

$$\begin{aligned}
a &= x_1 + x_2 + x_3 + x_6 + x_7\\
b &= x_1 + x_2 + x_3 + x_5 + x_4\\
c &= x_1 + x_2 + x_3\\
d^\mu &= x_1 p_{34}^\mu + x_2 p_{134}^\mu + x_7 p_4^\mu\\
e^\mu &= x_1 p_{34}^\mu + x_2 p_{134}^\mu + x_5 p_3^\mu\\
f &= x_1\, s.
\end{aligned}$$

Anastasiou et al, Nucl.Phys.B 580 (2000) 577-601

Tarasov's Method

$$k^\mu \;\rightarrow\; \left(K - \frac{cL}{a} + \mathcal{X}\right)^\mu ,$$

$$l^\mu \;\rightarrow\; (L + \mathcal{Y})^\mu ,$$

$$\mathcal{X}^\mu \;=\; \frac{1}{\mathcal{P}}\Big\{ - [(x_2 + x_1)(x_7 + x_5 + x_4) + (x_5 + x_4 + x_3)x_7]\, p_4^\mu + [x_3 x_5 - x_4(x_2 + x_1)]\, p_3^\mu$$
$$- x_2(x_5 + x_4) p_1^\mu \Big\}, \qquad (3.7)$$

$$\mathcal{Y}^\mu \;=\; \frac{1}{\mathcal{P}}\Big\{ [x_3 x_7 - x_6(x_2 + x_1)]\, p_4^\mu - [(x_2 + x_1)(x_7 + x_6 + x_5) + (x_7 + x_6 + x_3)x_5)]\, p_3^\mu$$
$$- x_2(x_7 + x_6) p_1^\mu \Big\}, \qquad (3.8)$$

$$\mathcal{P} = (x_7 + x_6 + x_5 + x_4)\,(x_3 + x_2 + x_1) + (x_5 + x_4)\,(x_7 + x_6)\,.$$

Anastasiou et al, Nucl.Phys.B 580 (2000) 577-601

Tarasov's Method

$$\mathrm{Xbox}^D[k^{\mu_1}\dots k^{\mu_m} l^{\nu_1}\dots l^{\nu_n}] = \int \mathcal{D}x \int \frac{d^D K}{i\pi^{D/2}} \int \frac{d^D L}{i\pi^{D/2}}$$
$$\times \left(K - \frac{cL}{a} + \mathcal{X}\right)^{\mu_1} \dots \left(K - \frac{cL}{a} + \mathcal{X}\right)^{\mu_m} (L+\mathcal{Y})^{\nu_1} \dots (L+\mathcal{Y})^{\nu_n}$$
$$\times \exp\left(aK^2 + \frac{\mathcal{P}}{a}L^2 + \frac{\mathcal{Q}}{\mathcal{P}}\right), \tag{3.10}$$

$$\begin{aligned}
\mathrm{Xbox}^D(\nu_1,\nu_2,\nu_3,\nu_4,\nu_5,\nu_6,\nu_7;s,t) &= \int \mathcal{D}x\ \mathcal{I}, \\
\mathrm{Xbox}^D(\nu_1,\nu_2,\nu_3,\nu_4,\nu_5,\nu_6,\nu_7;s,t)\,[k^\mu] &= \int \mathcal{D}x\ \mathcal{X}^\mu \mathcal{I}, \\
\mathrm{Xbox}^D(\nu_1,\nu_2,\nu_3,\nu_4,\nu_5,\nu_6,\nu_7;s,t)\,[l^\mu] &= \int \mathcal{D}x\ \mathcal{Y}^\mu \mathcal{I},
\end{aligned}$$

$$\mathcal{I} = \frac{1}{\mathcal{P}^{D/2}}\ \exp\left(\frac{\mathcal{Q}}{\mathcal{P}}\right).$$

Anastasiou et al, Nucl.Phys.B 580 (2000) 577-601

Tarasov's Method

$$\frac{(-1)^{\nu_i} x_i^{\nu_i - 1}}{\Gamma(\nu_i)}\, x_i \implies -\nu_i \frac{(-1)^{\nu_i+1} x_i^{\nu_i}}{\Gamma(\nu_i + 1)} \equiv -\nu_i \mathbf{i}^+,$$

$$\mathbf{i}^{\pm} \mathrm{Xbox}^D (\ldots, \nu_i, \ldots) = \mathrm{Xbox}^D (\ldots, \nu_i \pm 1, \ldots),$$

$$\frac{1}{\mathcal{P}^{D/2}} \frac{1}{\mathcal{P}} \implies \frac{1}{\mathcal{P}^{(D+2)/2}}, \qquad \frac{1}{\mathcal{P}} \implies \mathbf{d}^+, \qquad \mathcal{P} \implies \mathbf{d}^-,$$

$$\mathbf{d}^{\pm} \mathrm{Xbox}^D = \mathrm{Xbox}^{D \pm 2}.$$

Finally obtain the combination of scalar integrals with higher power of propagators and higher dimensions.

Anastasiou et al, Nucl.Phys.B 580 (2000) 577-601

Resolve dimension shift (in Tarasov's Method)

$$I^{(d-2)} \propto D\left(\frac{\partial}{\partial m_i^2}\right) I^{(d)}$$

$$\begin{bmatrix} I_1^{(d+2)} \\ \vdots \\ I_i^{(d+2)} \end{bmatrix}_{Master} = M_{ii} \begin{bmatrix} I_1^{(d)} \\ \vdots \\ I_i^{(d)} \end{bmatrix}_{Master}$$

$$\begin{bmatrix} I_1^{(d)} \\ \vdots \\ I_i^{(d)} \end{bmatrix}_{Master} = M_{ii}^{-1} \begin{bmatrix} I_1^{(d+2)} \\ \vdots \\ I_i^{(d+2)} \end{bmatrix}_{Master}$$

Complicated

Nucl.Phys.B502(1997)455-482

IBP (integration by parts)

Feynman 积分

S. Laporta, Int. J. Mod. Phys. A 15 (2000) 5087

$$F(a_1, \ldots, a_n) \;=\; \int \cdots \int \frac{\mathrm{d}^d k_1 \ldots \mathrm{d}^d k_h}{E_1^{a_1} \ldots E_n^{a_n}} \, .$$

$$\int \ldots \int \mathrm{d}^d k_1 \mathrm{d}^d k_2 \ldots \frac{\partial}{\partial k_i} \left(p_j \frac{1}{E_1^{a_1} \ldots E_n^{a_n}} \right) = 0 \, .$$

$$\sum \alpha_i F(a_1 + b_{i,1}, \ldots, a_n + b_{i,n}) = 0 \, ,$$

FIRE, Kira, ...

Numerical approaches for multi-scale multi-loop

- **Mellin-Barnes Representation**
  Many tools, faster, difficult on many scales.

- **Sector Decomposition**
  More general, slower, okay for many scales.

- **Auxiliary Mass Flow**
  Latest algorithm, most efficient for now

Mellin-Barnes Representation

$$\frac{1}{(A+B)^\lambda} = \frac{1}{\Gamma(\lambda)} \int_{\mathcal{C}} \frac{dz}{2\pi i} \frac{B^z}{A^{\lambda+z}} \Gamma(\lambda+z)\Gamma(-z)$$

$$\int_{\mathcal{C}_1} \cdots \int_{\mathcal{C}_n} \frac{d^n z}{(2\pi i)^n} \frac{\prod_i \Gamma\left(\alpha_i + \beta_i \epsilon + \sum_j \gamma_{ij} z_j\right)}{\prod_i \Gamma\left(\alpha'_i + \beta'_i \epsilon + \sum_j \gamma'_{ij} z_j\right)} \prod_k s_k^{d_k} \ .$$

AMBRE, MBcreate, ...

Sector Decomposition

$$I = \int_0^1 dx \int_0^1 dy\; x^{-1-\epsilon} y^{-\epsilon} (x + (1-x)y)^{-1}$$

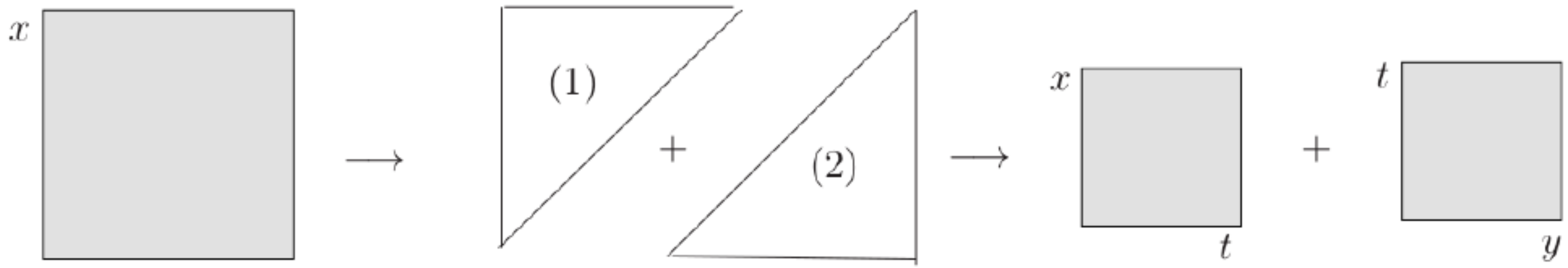

$$I = \int_0^1 dx\; x^{-1-\epsilon} \int_0^1 dt\; t^{-\epsilon}(1 + (1-x)t)^{-1}$$
$$+ \int_0^1 dy\; y^{-1-2\epsilon} \int_0^1 dt\; t^{-1-\epsilon}(1 + (1-y)t)^{-1}$$

G.Heinrich, Int.J.Mod.Phys.A23:1457-1486,2008

FIESTA, pySecDec, ...

$$G^{\mu_1\cdots\mu_R}_{l_1\cdots l_R} = \int \prod_{l=1}^{L} d^D\kappa_l \, \frac{k_{l_1}^{\mu_1}\cdots k_{l_R}^{\mu_R}}{\prod_{j=1}^{N} P_j^{\nu_j}\left(\{k\},\{p\},m_j^2\right)} ,$$

$$d^D\kappa_l = \frac{\mu^{4-D}}{i\pi^{\frac{D}{2}}} d^D k_l , \qquad P_j\left(\{k\},\{p\},m_j^2\right) = \left(q_j^2 - m_j^2 + i\delta\right) ,$$

Feynman parameterization

$$\frac{1}{\prod_{j=1}^{N} P_j^{\nu_j}} = \frac{\Gamma(N_\nu)}{\prod_{j=1}^{N}\Gamma(\nu_j)} \int_0^\infty \prod_{j=1}^{N} dx_j \, x_j^{\nu_j-1} \delta\left(1-\sum_{i=1}^{N} x_i\right) \frac{1}{\left[\sum_{j=1}^{N} x_j P_j\right]^{N_\nu}} ,$$

where $N_\nu = \sum_{j=1}^{N}\nu_j$, leads to

$$G^{\mu_1\cdots\mu_R}_{l_1\cdots l_R} = \frac{\Gamma(N_\nu)}{\prod_{j=1}^{N}\Gamma(\nu_j)} \int_0^\infty \prod_{j=1}^{N} dx_j \, x_j^{\nu_j-1} \delta\left(1-\sum_{i=1}^{N} x_i\right) \int d^D\kappa_1 \cdots d^D\kappa_L$$

$$\times \, k_{l_1}^{\mu_1}\cdots k_{l_R}^{\mu_R} \left[\sum_{i,j=1}^{L} k_i^{\mathrm{T}} M_{ij} k_j - 2\sum_{j=1}^{L} k_j^{\mathrm{T}}\cdot Q_j + J + i\delta\right]^{-N\nu} ,$$

Integrate out loop momenta

$$G^{\mu_1\cdots\mu_R}_{l_1\cdots l_R} = (-1)^{N_\nu} \frac{1}{\prod_{j=1}^{N}\Gamma(\nu_j)} \int_0^\infty \prod_{j=1}^{N} dx_j\, x_j^{\nu_j-1} \delta\left(1-\sum_{l=1}^{N} x_l\right)$$
$$\times \sum_{m=0}^{[R/2]} \left(-\frac{1}{2}\right)^m \Gamma(N_\nu - m - LD/2)[(\tilde{M}^{-1}\otimes g)^{(m)} \tilde{l}^{(R-2m)}]^{\Gamma_1,\ldots,\Gamma_R}$$
$$\times \frac{\mathcal{U}^{N_\nu-(L+1)D/2-R}}{\mathcal{F}^{N_\nu-LD/2-m}}, \tag{7}$$

where

$$\mathcal{F}(\mathbf{x}) = \det(M)\left[\sum_{j,l=1}^{L} Q_j M^{-1}_{jl} Q_l - J - i\delta\right], \tag{8}$$
$$\mathcal{U}(\mathbf{x}) = \det(M), \quad \tilde{M}^{-1} = \mathcal{U}M^{-1}, \quad \tilde{l} = \mathcal{U}v$$

U and F can be determined geometrically

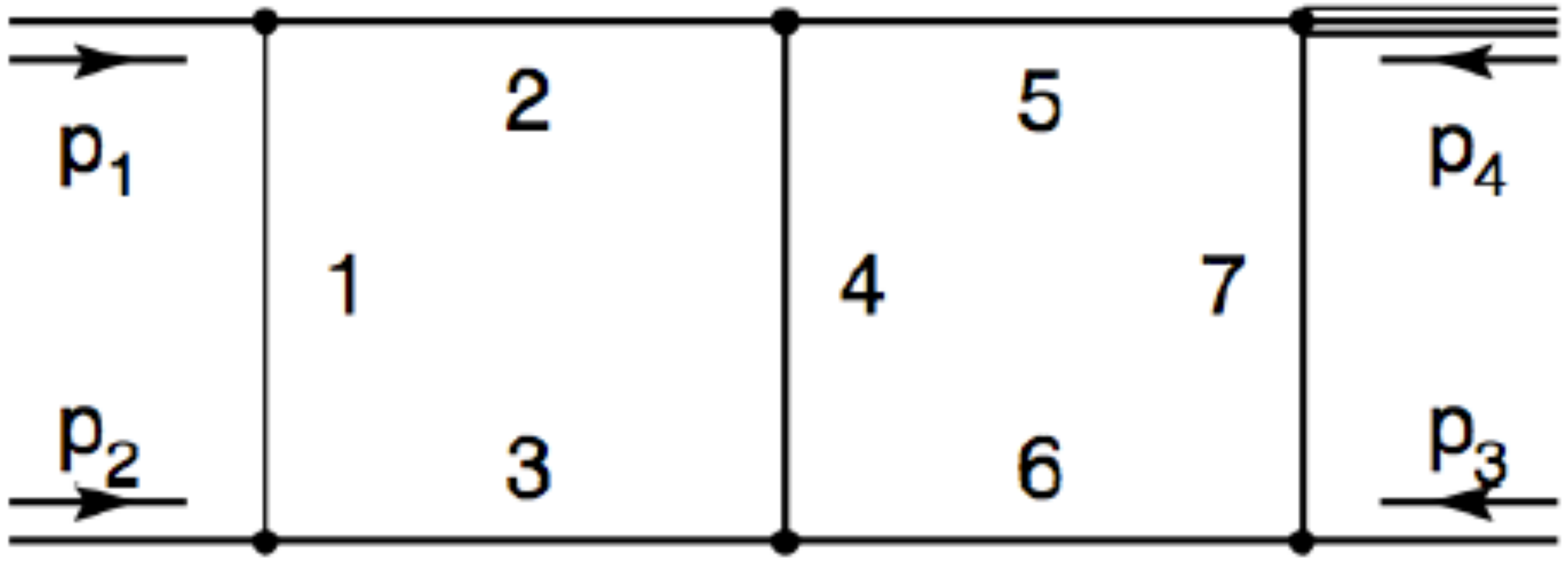

$$\mathcal{U}(\mathbf{x}) = \sum_{T \in \mathcal{T}_1} \Big[\prod_{j \in \mathcal{C}(T)} x_j \Big] ,$$

$$\mathcal{F}_0(\mathbf{x}) = \sum_{\hat{T} \in \mathcal{T}_2} \Big[\prod_{j \in \mathcal{C}(\hat{T})} x_j \Big] (-s_{\hat{T}}) ,$$

$$\mathcal{F}(\mathbf{x}) = \mathcal{F}_0(\mathbf{x}) + \mathcal{U}(\mathbf{x}) \sum_{j=1}^{N} x_j m_j^2 .$$

$$\mathcal{U} = x_{123} x_{567} + x_4 x_{123567} ,$$

$$\mathcal{F} = (-s_{12})(x_2 x_3 x_{4567} + x_5 x_6 x_{1234} + x_2 x_4 x_6 + x_3 x_4 x_5)$$
$$+ (-s_{23}) x_1 x_4 x_7 + (-p_4^2) x_7 (x_2 x_4 + x_5 x_{1234}) ,$$

where $x_{ijk\ldots} = x_i + x_j + x_k + \cdots$ and $s_{ij} = (p_i + p_j)^2$.

First generate primary sectors to eliminate Delta function

$$\int_0^\infty d^N x = \sum_{l=1}^{N} \int_0^\infty d^N x \prod_{\substack{j=1\\ j\neq l}}^{N} \theta(x_l \geq x_j) \,.$$

$$x_j = \begin{cases} x_l t_j & \text{for } j < l \,, \\ x_l & \text{for } j = l \,, \\ x_l t_{j-1} & \text{for } j > l \end{cases}$$

$$G_l = \int_0^1 \prod_{j=1}^{N-1} dt_j \, \frac{\mathcal{U}_l^{N_\nu-(L+1)D/2}(\mathbf{t})}{\mathcal{F}_l^{N_\nu-LD/2}(\mathbf{t})} \,, \quad l = 1, \ldots, N \,.$$

Determine a sub-set of parameters ti

$$\mathcal{S} = \{t_{\alpha_1}, \ldots, t_{\alpha_r}\}$$

Then divide into r sub-sectors

$$\prod_{j=1}^{r} \theta(1 \geq t_{\alpha_j} \geq 0) = \sum_{k=1}^{r} \prod_{\substack{j=1 \\ j \neq k}}^{r} \theta(t_{\alpha_k} \geq t_{\alpha_j} \geq 0) \, .$$

$$t_{\alpha_j} \to \begin{cases} t_{\alpha_k} t_{\alpha_j} & \text{for } j \neq k \, , \\ t_{\alpha_k} & \text{for } j = k \, . \end{cases}$$

$$G_{lk} = \int_0^1 \left(\prod_{j=1}^{N-1} dt_j \, t_j^{a_j - b_j \epsilon} \right) \frac{\mathcal{U}_{lk}^{N_\nu - (L+1)D/2}}{\mathcal{F}_{lk}^{N_\nu - LD/2}} , \quad k = 1, \ldots, r \, .$$

$$\mathcal{U}_{lk_1 k_2 \ldots} = 1 + u(\mathbf{t}) \, , \quad \mathcal{F}_{lk_1 k_2 \ldots} = -s_0 + \sum_\beta (-s_\beta) f_\beta(\mathbf{t}) \, ,$$

All the coefficients of divergences are finite (complicated).

Decomposition strategies

- **Hironaka's polyhedra game**
  Bogner and Weinzerl, Comput.Phys.Commun. 178 (2008) 596; A. V. Smirnov and V. A. Smirnov, JHEP 05 (2009) 004;

- **Geometric method**
  Kaneko and Ueda, Comput.Phys.Commun. 181 (2010) 1352

Iteration of certain strategy will show explicitly dimensional regulators, where poles can be extracted.

$$I_j = \int_0^1 dt_j \, t_j^{(a_j - b_j \epsilon)} \, \mathcal{I}(t_j, \{t_{i \neq j}\}, \epsilon) \,,$$

$$I_j = \sum_{p=0}^{|a_j|-1} \frac{1}{a_j + p + 1 - b_j \epsilon} \frac{\mathcal{I}_j^{(p)}(0, \{t_{i \neq j}\}, \epsilon)}{p!} + \int_0^1 dt_j \, t_j^{a_j - b_j \epsilon} R(\vec{t}, \epsilon) \,.$$

$$I_j = -\frac{1}{b_j \epsilon} \mathcal{I}_j(0, \{t_{i \neq j}\}, \epsilon) + \int_0^1 dt_j \, t_j^{-1 - b_j \epsilon} \Big(\mathcal{I}(t_j, \{t_{i \neq j}\}, \epsilon) - \mathcal{I}_j(0, \{t_{i \neq j}\}, \epsilon) \Big) \,,$$

Contour Deformation

$$I_s = C(\epsilon) \lim_{\delta \to 0} \int_0^1 \frac{\mathcal{D}(\vec{x}, \epsilon)\, \mathcal{H}_s(\vec{x}, \epsilon)}{[\mathcal{F}_s(\vec{x}, m_i^2, s_{jk}) - i\delta]^{a+b\epsilon}}$$

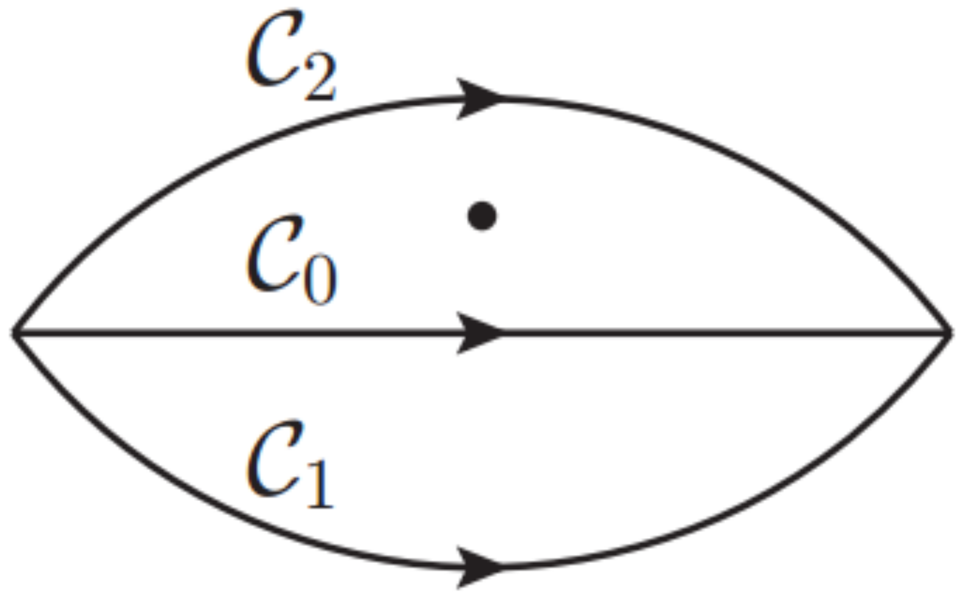

$$z_i = x_i - i\lambda x_i^{\alpha}(1 - x_i)^{\beta} \frac{\partial \mathcal{F}_s}{\partial x_i}$$

$$\lim_{\delta \to 0} \int_0^1 \frac{\mathcal{D}(\vec{x}, \epsilon)\, \mathcal{H}_s(\vec{x}, \epsilon)}{[\mathcal{F}_s(\vec{x}, m_i^2, s_{jk}) - i\delta]^{a+b\epsilon}} = \int_{\mathcal{C}} \frac{\mathcal{D}(\vec{z}, \epsilon)\, \mathcal{H}_s(\vec{z}, \epsilon)}{[\mathcal{F}_s(\vec{z}, m_i^2, s_{jk})]^{a+b\epsilon}}$$

Improve via quasi-Monte-Carlo

$$I(f) = \int_0^1 d^s x f(\vec{x}) \qquad I_{estimate}(f) = \sum_{i=0}^{n-1} f(\vec{x}_i)$$

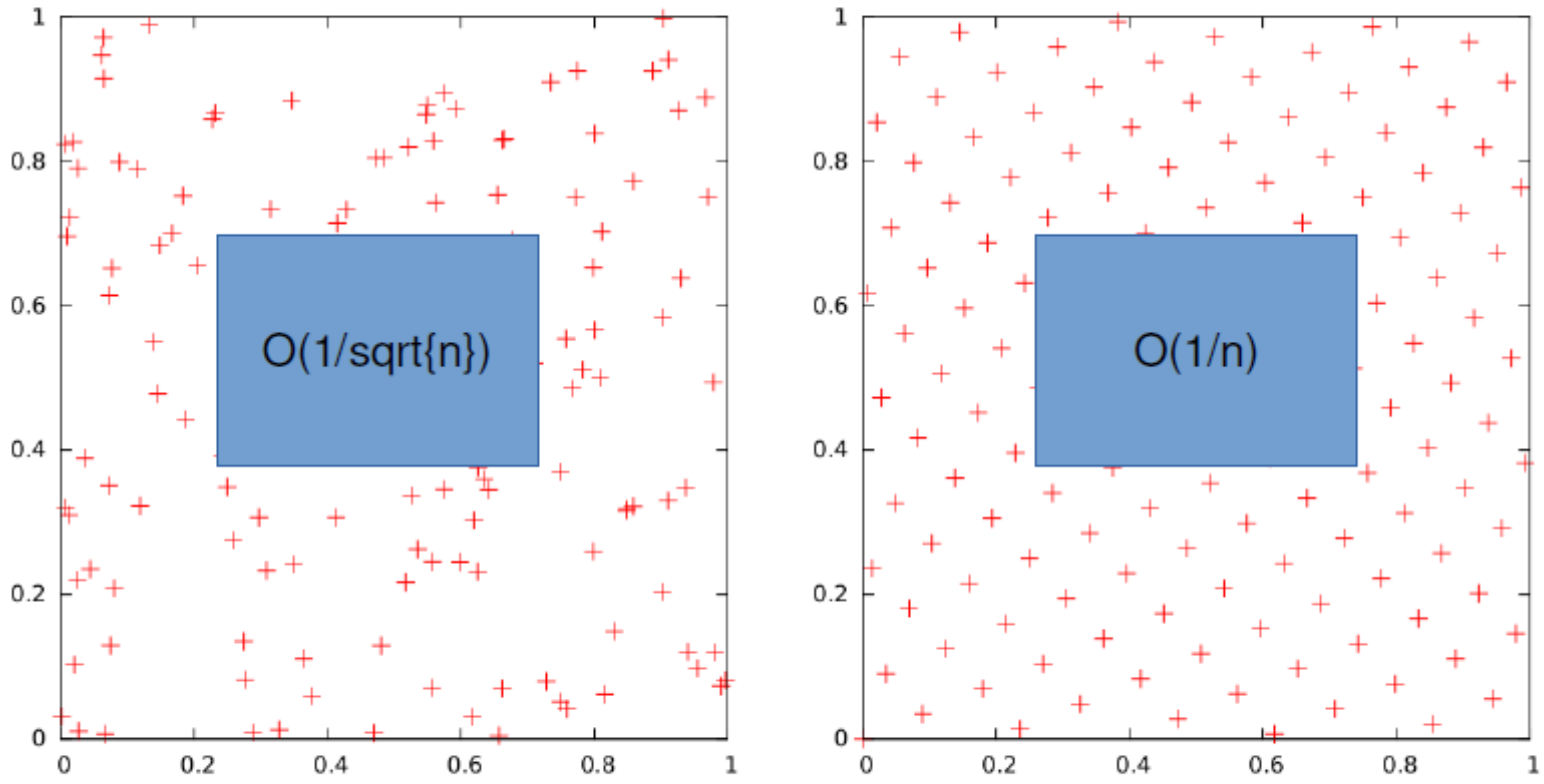

Z. Li et al., Chin.Phys. C40 (2016) no.3, 033103

Implementation on GPU

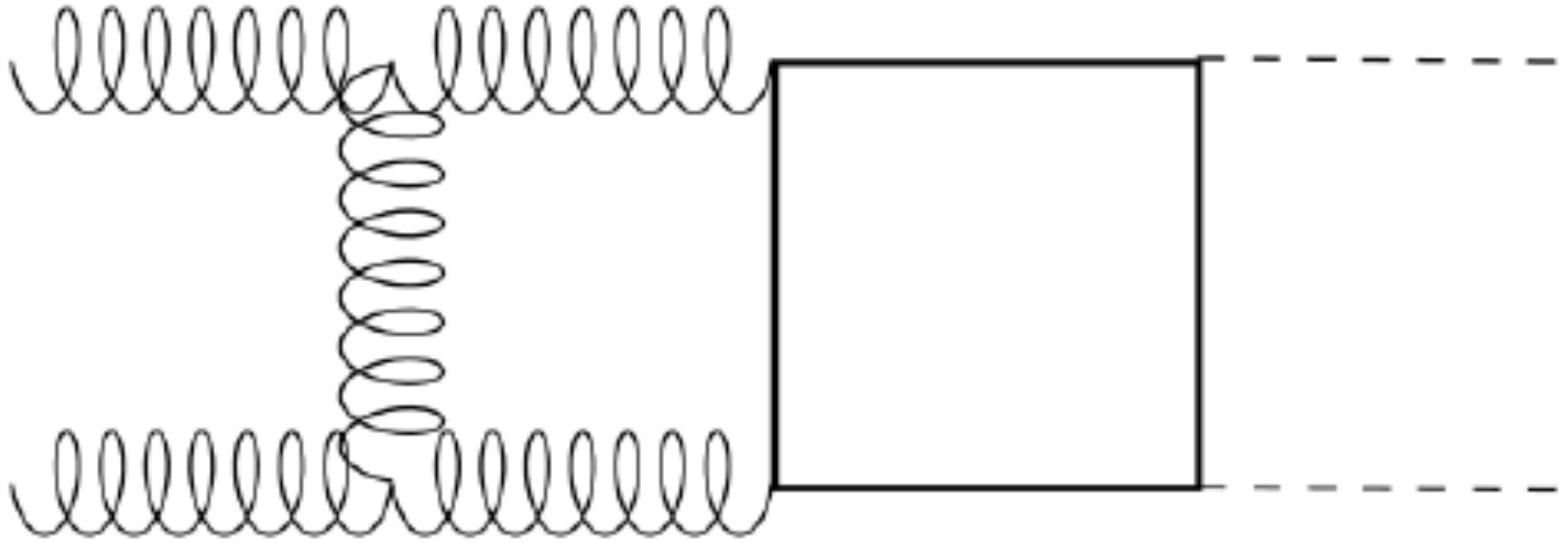

$$I_C = e^{-2\epsilon\gamma_E} s^{-3-2\epsilon} \sum_{i=0}^{i=2} \frac{P_i}{\epsilon^i}.$$

	Vegas/CPU	QMC/GPU
P_2	$-7.959 \pm 0.009 - 10.586i \pm 0.009i$	$-7.949 \pm 0.003 - 10.585i \pm 0.005i$
P_1	$3.9 \pm 0.1 - 28.1i \pm 0.1i$	$3.831 \pm 0.005 - 28.022i \pm 0.005i$
P_0	$-3.9 \pm 0.8 + 92.3i \pm 0.8i$	$-4.63 \pm 0.07 + 92.13i \pm 0.07i$
Integration Time	45540s	19s

Z. Li et al., Chin.Phys. C40 (2016) no.3, 033103

Auxiliary Mass Flow

Phys.Lett.B 779 (2018) 353-357

$$I(D;\{\nu_\alpha\};\eta) \equiv \int \prod_{i=1}^{L} \frac{\mathrm{d}^D \ell_i}{\mathrm{i}\pi^{D/2}} \prod_{\alpha=1}^{N} \frac{1}{(\mathcal{D}_\alpha + \mathrm{i}\eta)^{\nu_\alpha}},$$

$$I(D;\{\nu_\alpha\};0) \equiv \lim_{\eta \to 0^+} I(D;\{\nu_\alpha\};\eta),$$

$$\frac{\partial}{\partial \eta}\vec{I}(\eta) = A(\eta)\vec{I}(\eta),$$

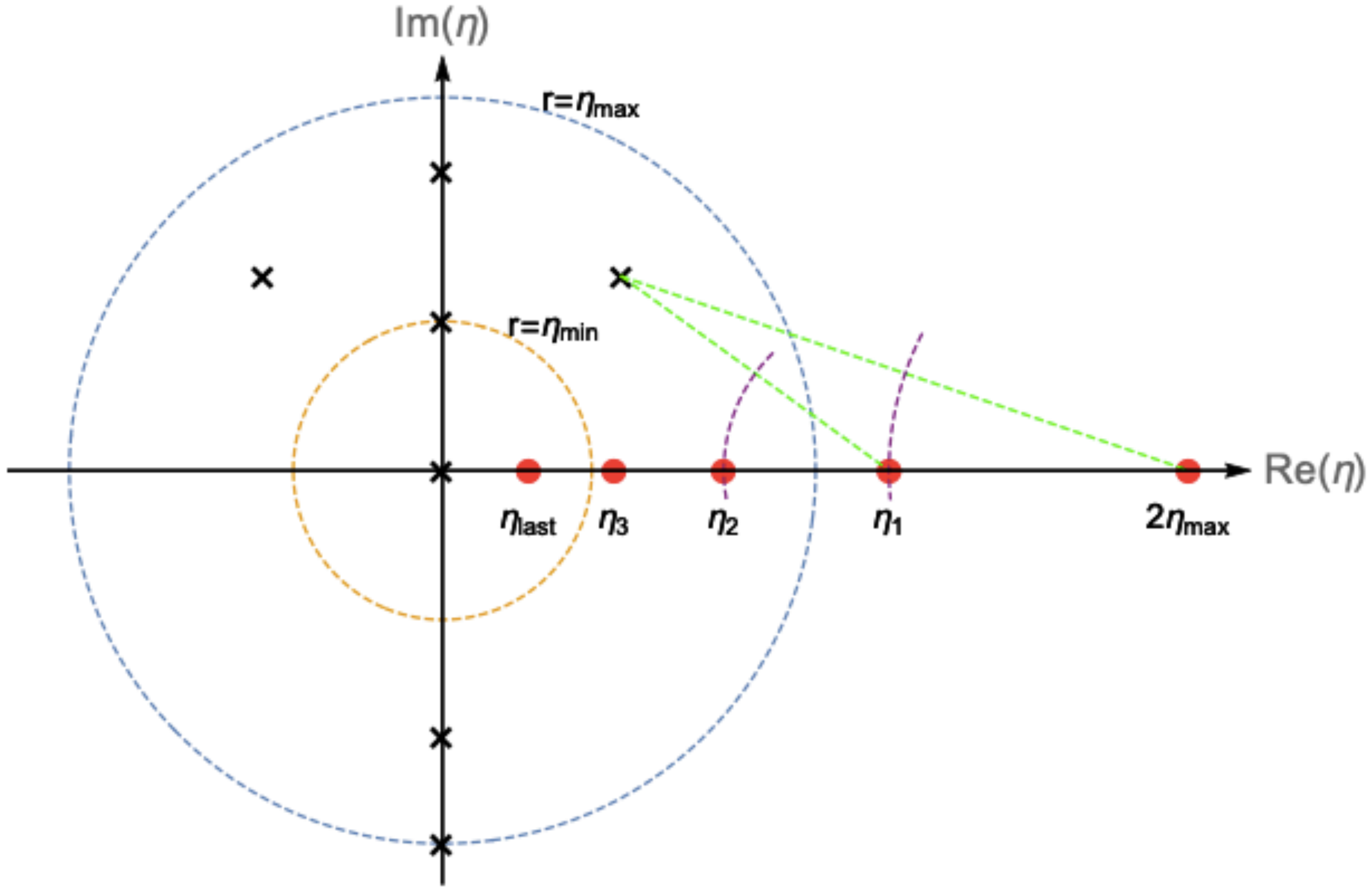

AMFlow

Real Corrections

NLO calculation

$$\hat{\sigma}^{(1)}_{ab} = \hat{\sigma}^{\mathrm{R}}_{ab} + \hat{\sigma}^{\mathrm{V}}_{ab} + \hat{\sigma}^{\mathrm{C}}_{ab} \,,$$

IR Divergence

$$\hat{\sigma}^{\mathrm{R}}_{ab} = \frac{1}{2\hat{s}}\frac{1}{N_{ab}}\int \mathrm{d}\mathbf{\Phi}_{n+1}\,\langle \mathcal{M}^{(0)}_{n+1}|\mathcal{M}^{(0)}_{n+1}\rangle\,\mathrm{F}_{n+1}\,, \quad \hat{\sigma}^{\mathrm{V}}_{ab} = \frac{1}{2\hat{s}}\frac{1}{N_{ab}}\int \mathrm{d}\mathbf{\Phi}_{n}\,2\mathrm{Re}\,\langle \mathcal{M}^{(0)}_{n}|\mathcal{M}^{(1)}_{n}\rangle\,\mathrm{F}_{n}\,,$$

$$\hat{\sigma}^{\mathrm{C}}_{ab}(p_1,p_2) = \frac{\alpha_s}{2\pi}\frac{1}{\epsilon}\left(\frac{\mu_R^2}{\mu_F^2}\right)^{\epsilon}\sum_c\int_0^1 \mathrm{d}z\left[P^{(0)}_{ca}(z)\,\hat{\sigma}^{\mathrm{B}}_{cb}(zp_1,p_2) + P^{(0)}_{cb}(z)\,\hat{\sigma}^{\mathrm{B}}_{ac}(p_1,zp_2)\right]\,,$$

Where is IR singularity?

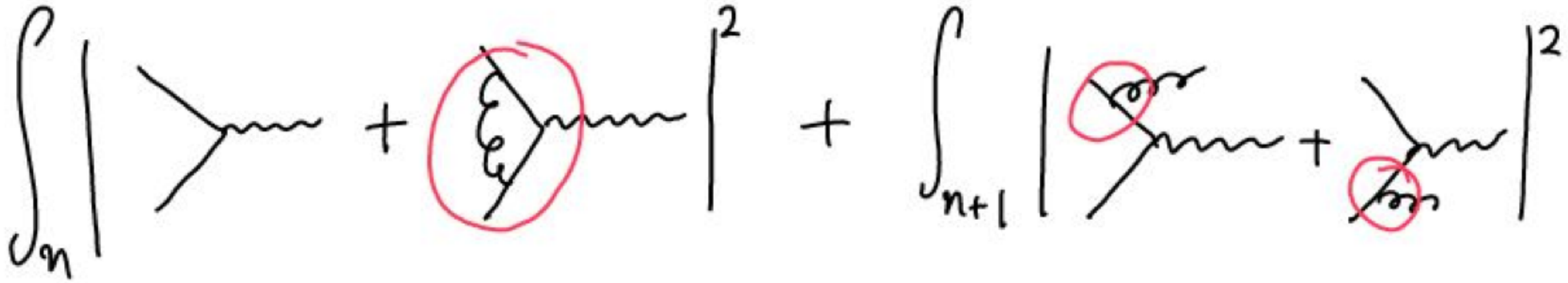

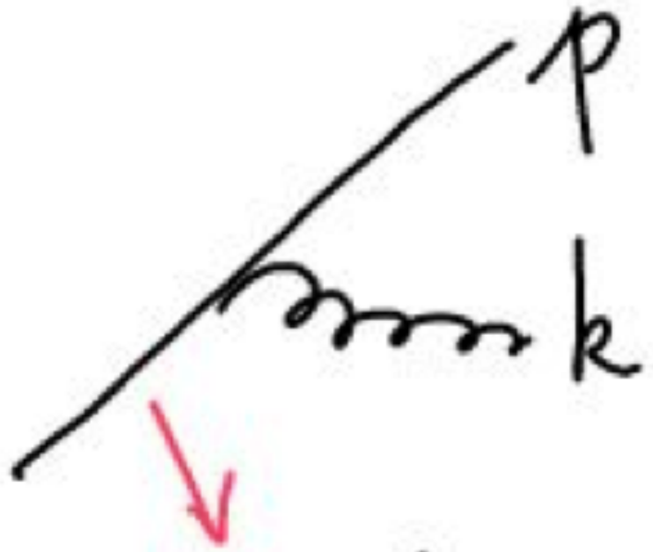

$$\frac{1}{(p+k)^2}=\frac{1}{2p\cdot k}=\frac{1}{2p^0\underbrace{k^0}_{\text{soft}}\underbrace{(1-\cos\theta)}_{\text{collinear}}}$$

NNLO effect

$$\hat{\sigma}_{ab}^{(2)} = \hat{\sigma}_{ab}^{\mathrm{RR}} + \hat{\sigma}_{ab}^{\mathrm{RV}} + \hat{\sigma}_{ab}^{\mathrm{VV}} + \hat{\sigma}_{ab}^{\mathrm{C1}} + \hat{\sigma}_{ab}^{\mathrm{C2}} ,$$

$$\hat{\sigma}_{ab}^{\mathrm{RR}} = \frac{1}{2\hat{s}}\frac{1}{N_{ab}}\int \mathrm{d}\mathbf{\Phi}_{n+2}\,\langle \mathcal{M}_{n+2}^{(0)}|\mathcal{M}_{n+2}^{(0)}\rangle\,\mathrm{F}_{n+2}\,, \quad \hat{\sigma}_{ab}^{\mathrm{RV}} = \frac{1}{2\hat{s}}\frac{1}{N_{ab}}\int \mathrm{d}\mathbf{\Phi}_{n+1}\,2\mathrm{Re}\,\langle \mathcal{M}_{n+1}^{(0)}|\mathcal{M}_{n+1}^{(1)}\rangle\,\mathrm{F}_{n+1}\,,$$

$$\hat{\sigma}_{ab}^{\mathrm{VV}} = \frac{1}{2\hat{s}}\frac{1}{N_{ab}}\int \mathrm{d}\mathbf{\Phi}_{n}\left(2\mathrm{Re}\,\langle \mathcal{M}_{n}^{(0)}|\mathcal{M}_{n}^{(2)}\rangle + \langle \mathcal{M}_{n}^{(1)}|\mathcal{M}_{n}^{(1)}\rangle\right)\mathrm{F}_{n}\,,$$

Phase space slicing

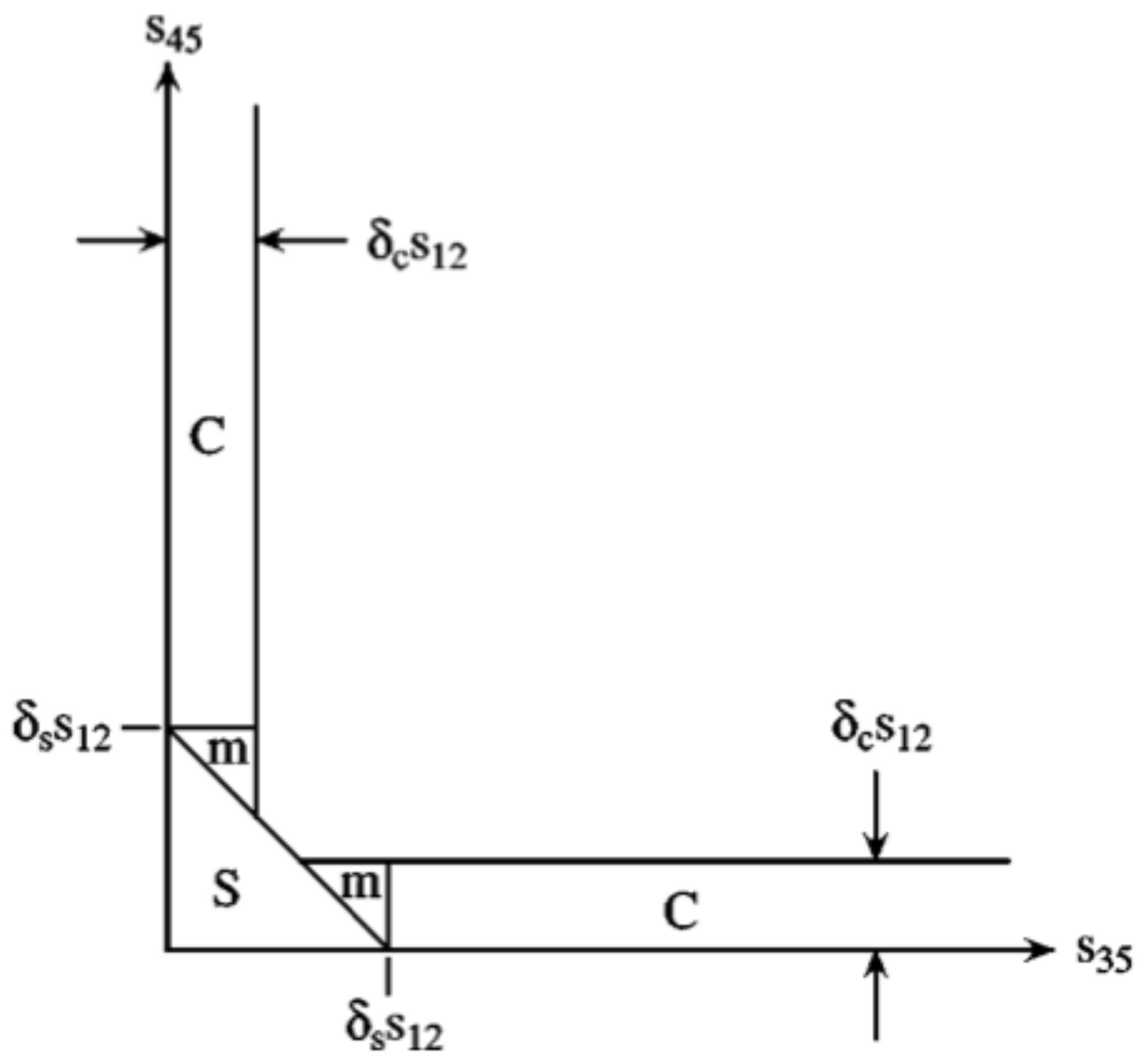

FIG. 7. The s_{35}-s_{45} plane for electron-positron annihilation to massless quarks showing the delineation into soft S and collinear C regions. The triangles marked "m" give vanishing contribution for $\delta_c \ll \delta_s$.

PHYSICAL REVIEW D, VOLUME 65, 094032

Two cutoff phase space slicing method

B. W. Harris*

High Energy Physics Division, Argonne National Laboratory, Argonne, Illinois 60439 and Robert Morris University, Coraopolis, Pennsylvania 15108

J. F. Owens†

Physics Department, Florida State University, Tallahassee, Florida 32306-4350

(Received 10 February 2001; published 13 May 2002)

PSS Efficiency Problem:

Eur. Phys. J. C 23, 259–266 (2002)
Digital Object Identifier (DOI) 10.1007/s100520100868

THE EUROPEAN PHYSICAL JOURNAL C

Comparison of phase space slicing and dipole subtraction methods for $\gamma^* \to Q\bar{Q}$

T.O. Eynck[1], E. Laenen[1], L. Phaf[1], S. Weinzierl[2]

[1] NIKHEF Theory Group, Kruislaan 409, 1098 SJ Amsterdam, The Netherlands
[2] Dipartimento di Fisica, Università di Parma, INFN Gruppo Collegato di Parma, 43100 Parma, Italy

Received: 15 October 2001 /
Published online: 25 January 2002 –

$s = 400$ GeV^2		
points	DIP	PSS
1000	0.04%	1%
10000	0.009%	0.3%
100000	0.003%	0.1%

Table 1: Accuracy $\delta r/r$ of the inclusive cross section attained for a given number of points per iteration in the two methods. The same phase space and random number generators are employed. The PSS results use the T_1 contribution only, with $s_{\text{min}} = 0.001\text{GeV}^2$.

Dipole subtraction

A General algorithm for calculating jet cross-sections in NLO QCD

S. Catani (Florence U. & INFN, Florence) , M.H. Seymour (CERN)

May 1996 - 116 pages

Nucl.Phys. B485 (1997) 291-419
Erratum-ibid. B510 (1998) 503-504
DOI: 10.1016/S0550-3213(96)00589-5
CERN-TH-96-029, CERN-TH-96-29
e-Print: hep-ph/9605323 | PDF

$$\sigma^{NLO} \equiv \int d\sigma^{NLO} = \int_{m+1} d\sigma^R + \int_m d\sigma^V \ .$$

$$\sigma^{NLO} = \int_{m+1} \left[d\sigma^R - d\sigma^A \right] + \int_{m+1} d\sigma^A + \int_m d\sigma^V \quad ,$$

$$\sigma^{NLO} = \int_{m+1} \left[\left(d\sigma^R \right)_{\epsilon=0} - \left(d\sigma^A \right)_{\epsilon=0} \right] + \int_m \left[d\sigma^V + \int_1 d\sigma^A \right]_{\epsilon=0} \quad ,$$

FKS subtraction

Three jet cross-sections to next-to-leading order

S. Frixione, Z. Kunszt (Zurich, ETH) , A. Signer (SLAC)

Dec 1995 - 48 pages

Nucl.Phys. B467 (1996) 399-442
DOI: 10.1016/0550-3213(96)00110-1
SLAC-PUB-7073, SLAC-PUB-95-7073, ETH-TH-95-42
e-Print: hep-ph/9512328 | PDF

A General approach to jet cross-sections in QCD

S. Frixione (Zurich, ETH)

Jun 1997 - 25 pages

Nucl.Phys. B507 (1997) 295-314
DOI: 10.1016/S0550-3213(97)00574-9
ETH-TH-97-14
e-Print: hep-ph/9706545 | PDF

Somogyi's subtraction

Subtraction with hadronic initial states at NLO: An NNLO-compatible scheme

Gabor Somogyi (Zurich U.)

Mar 2009 - 43 pages

JHEP 0905 (2009) 016
DOI: 10.1088/1126-6708/2009/05/016
ZU-TH-03-09
e-Print: arXiv:0903.1218 [hep-ph] | PDF

Matching of singly- and doubly-unresolved limits of tree-level QCD squared matrix elements

Gabor Somogyi, Zoltan Trocsanyi (Debrecen, Inst. Nucl. Res.) , Vittorio Del Duca (INFN, Turin)

Feb 2005 - 53 pages

JHEP 0506 (2005) 024
DOI: 10.1088/1126-6708/2005/06/024
DFTT-05-05
e-Print: hep-ph/0502226 | PDF

Antenna subtraction

Infrared Structure at NNLO Using Antenna Subtraction

James Currie (Zurich U.) , E.W.N. Glover, Steven Wells (Durham U., IPPP)

Jan 2013 - 65 pages

JHEP 1304 (2013) 066
DOI: 10.1007/JHEP04(2013)066
IPPP-12-82, ZU-TH-26-12
e-Print: arXiv:1301.4693 [hep-ph] | PDF

$$\mathrm{d}\hat{\sigma}_{ij,NLO} = \int_{n+1} \left[\mathrm{d}\hat{\sigma}^{R}_{ij,NLO} - \mathrm{d}\hat{\sigma}^{S}_{ij,NLO}\right] + \int_{n} \left[\mathrm{d}\hat{\sigma}^{V}_{ij,NLO} - \mathrm{d}\hat{\sigma}^{T}_{ij,NLO}\right],$$

$$\mathrm{d}\hat{\sigma}^{T}_{ij,NLO} = -\int_{1} \mathrm{d}\hat{\sigma}^{S}_{ij,NLO} - \mathrm{d}\hat{\sigma}^{MF}_{ij,NLO}.$$

Czakon's subtraction at NNLO

A novel subtraction scheme for double-real radiation at NNLO

M. Czakon (Aachen, Tech. Hochsch.)

May 2010 - 12 pages

Phys.Lett. B693 (2010) 259-268
DOI: 10.1016/j.physletb.2010.08.036
e-Print: arXiv:1005.0274 [hep-ph] | PDF

$$
\begin{aligned}
p_1^\mu &= \frac{\sqrt{s}}{2}(1,0,0,1)\,, \\
p_2^\mu &= \frac{\sqrt{s}}{2}(1,0,0,-1)\,, \\
n_1^\mu &= \frac{\sqrt{s}}{2}\beta^2(1,0,\sin\theta_1,\cos\theta_1)\,, \\
n_2^\mu &= \frac{\sqrt{s}}{2}\beta^2(1,\sin\phi\sin\theta_2,\cos\phi\sin\theta_2,\cos\theta_2)\,, \\
k_1^\mu &= \hat{\xi}_1\, n_1^\mu\,, \\
k_2^\mu &= \hat{\xi}_2\, n_2^\mu\,,
\end{aligned}
$$

$$
\begin{aligned}
d\Phi_3(p_1+p_2;k_1,k_2) &= \frac{\pi^{2\epsilon}}{8(2\pi)^5\Gamma(1-2\epsilon)} s^{2-2\epsilon}\beta^{8-8\epsilon}\left(\zeta(1-\zeta)\right)^{-\frac{1}{2}-\epsilon} \\
&\times \quad (\hat{\eta}_1(1-\hat{\eta}_1))^{-\epsilon}(\hat{\eta}_2(1-\hat{\eta}_2))^{-\epsilon}\frac{\eta_3^{1-2\epsilon}}{|\hat{\eta}_1-\hat{\eta}_2|^{1-2\epsilon}}\,\hat{\xi}_1^{1-2\epsilon}\hat{\xi}_2^{1-2\epsilon} \\
&\times \quad d\zeta\; d\hat{\eta}_1\; d\hat{\eta}_2\; d\hat{\xi}_1\; d\hat{\xi}_2\;.
\end{aligned}
$$

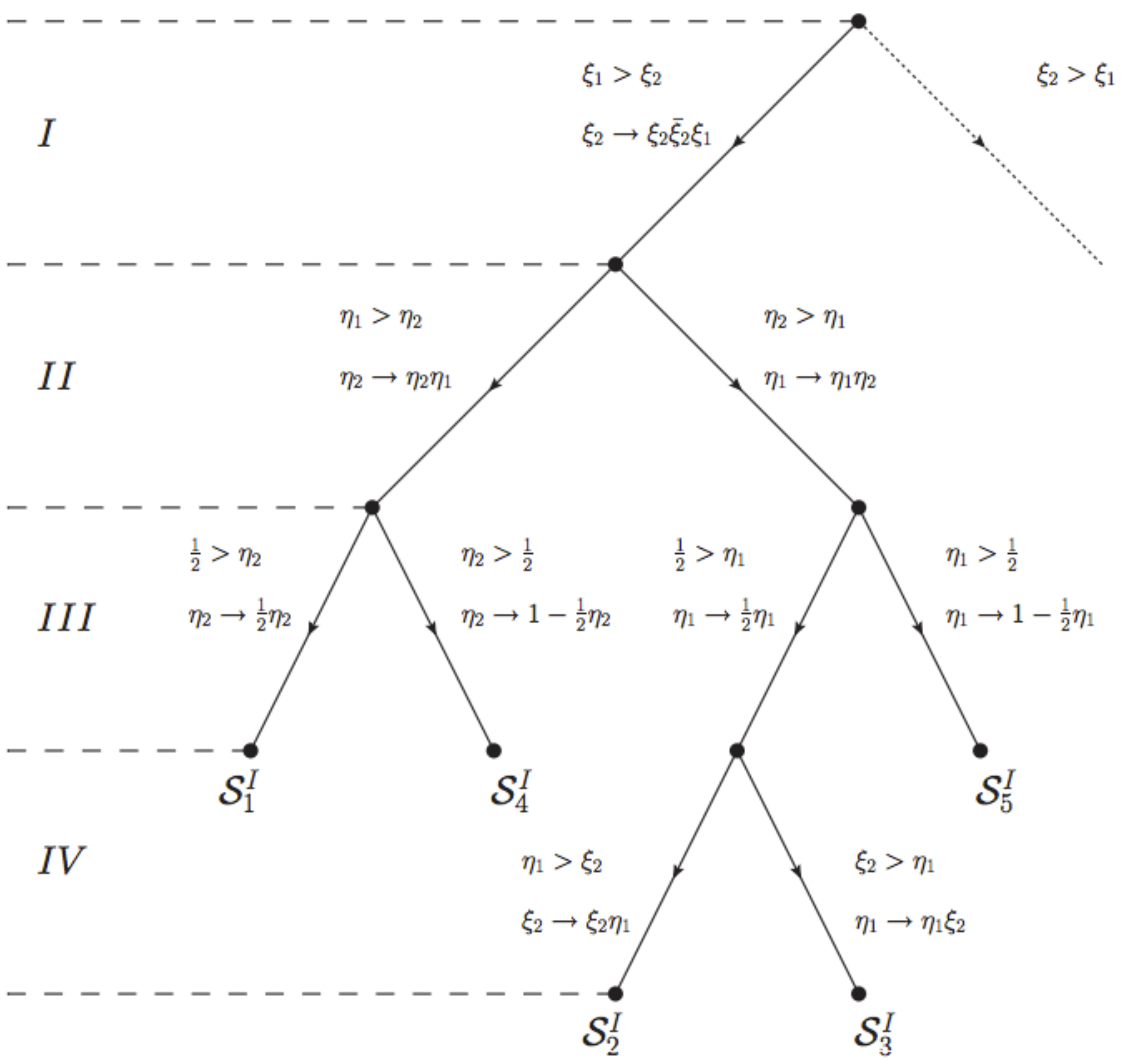

Feynman Diagram Generation

Generation via FeynArts

- Start from seed diagrams.
- Insert legs connecting to each propagators and vertices iteratively.
- Also obtain the symmetry factor.

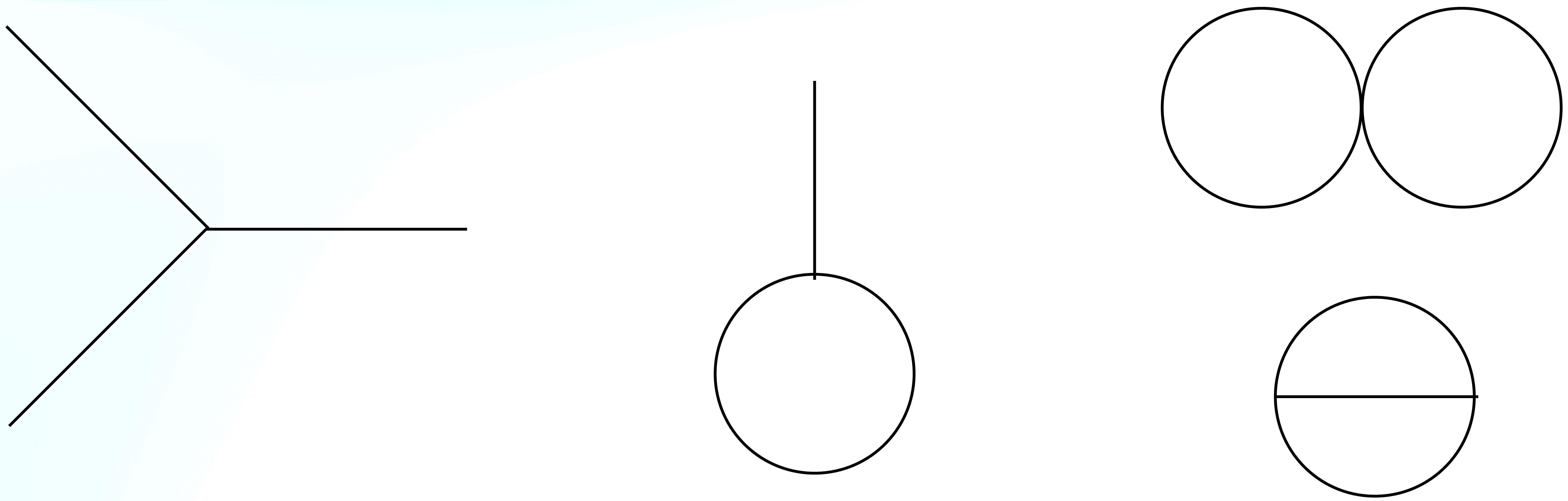

What's new (past 12 months)

Version 3.6.3 available

Version 3.5.2 available

A paper on diagram generation with mixed propagators

qgraf | *latest version:* ***3.6.3***

QGRAF is a computer program that generates Feynman diagrams for various types of QFT models — it is a research tool created with the obvious aim of contributing to extend the range of feasible, perturbative QFT calculations. It generates neither 0-point nor non-connected diagrams, though.
Diagrams are represented by symbolic expressions only; however, if some kind of graphical representation is required, have a look at some of the external links (in the first group).

- Latest version: `qgraf-3.6.3` (2022).
  Please report any error you may happen to find.

- Programming language: `Fortran 2008` for versions released since 2020, and `Fortran 77` for earlier versions.
  Executables/binaries are not distributed, the program has to be compiled and linked.
  Employing GNU Fortran for that task should be straightforward, eg there should be no need to specify a Fortran standard (see file `qgraf-3.6.3.pdf`).
  There are executable/binary versions of GFortran for several operating systems, as described in the GFortranBinaries webpage.

- The features added in the last three versions include (eg):

FeAmGen.jl

- Using QGRAF but interfaced with UFO format.
- Generate amplitude for each generated Feynman diagram.
- Prepare the visual diagram in the tikz-feynman style.
- Public @ github

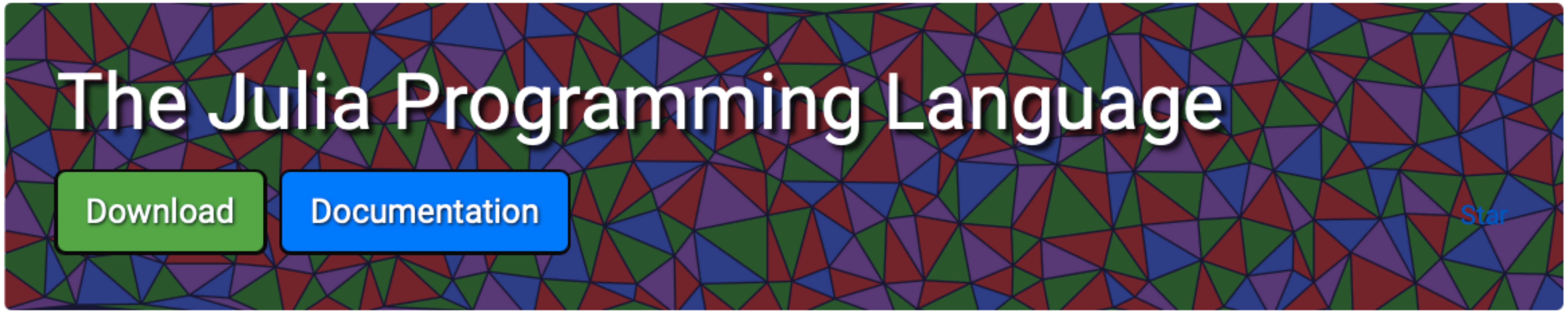

Resummation effect

PARTICLE PHYSICS

High-precision measurement of the *W* boson mass with the CDF II detector

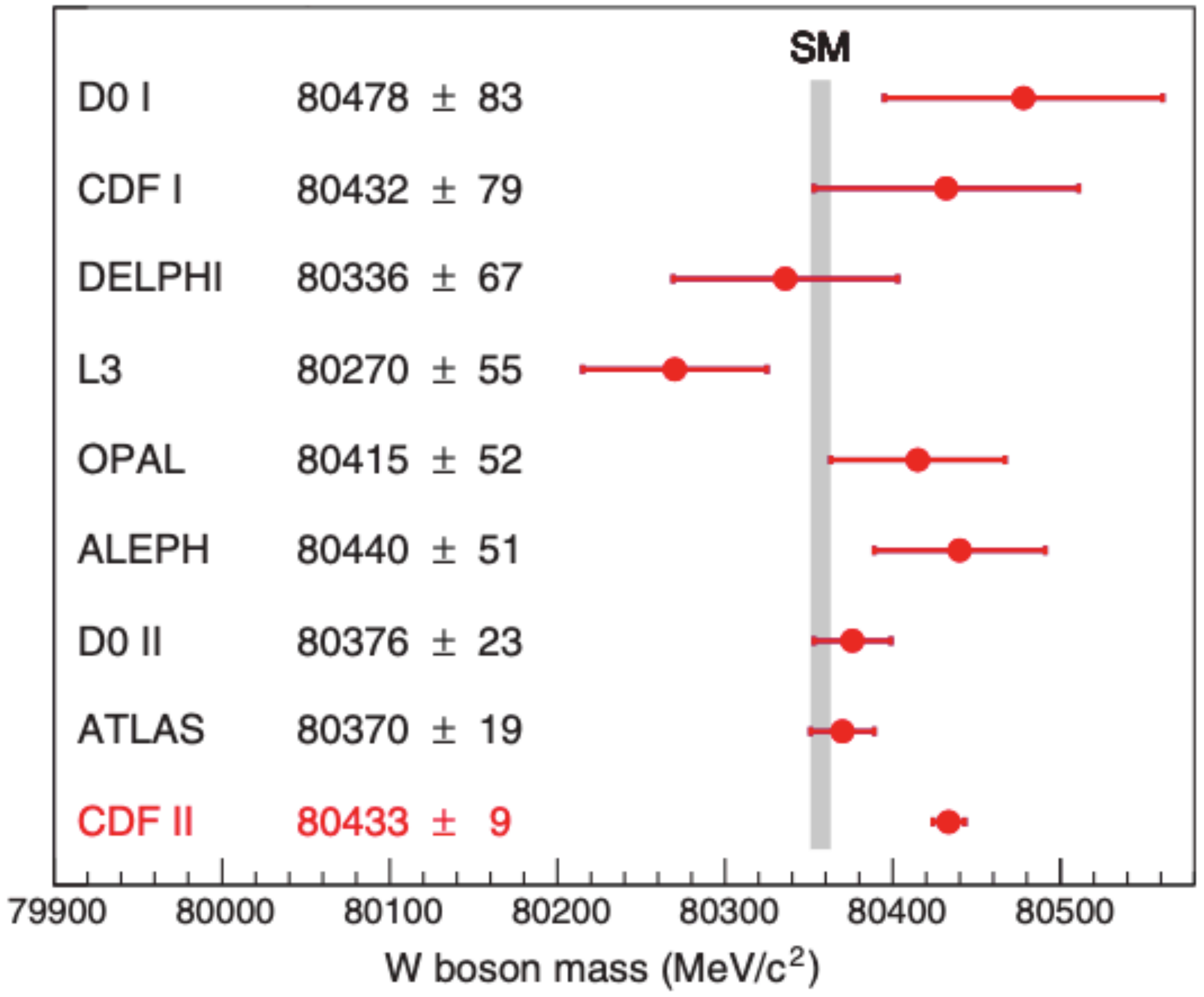

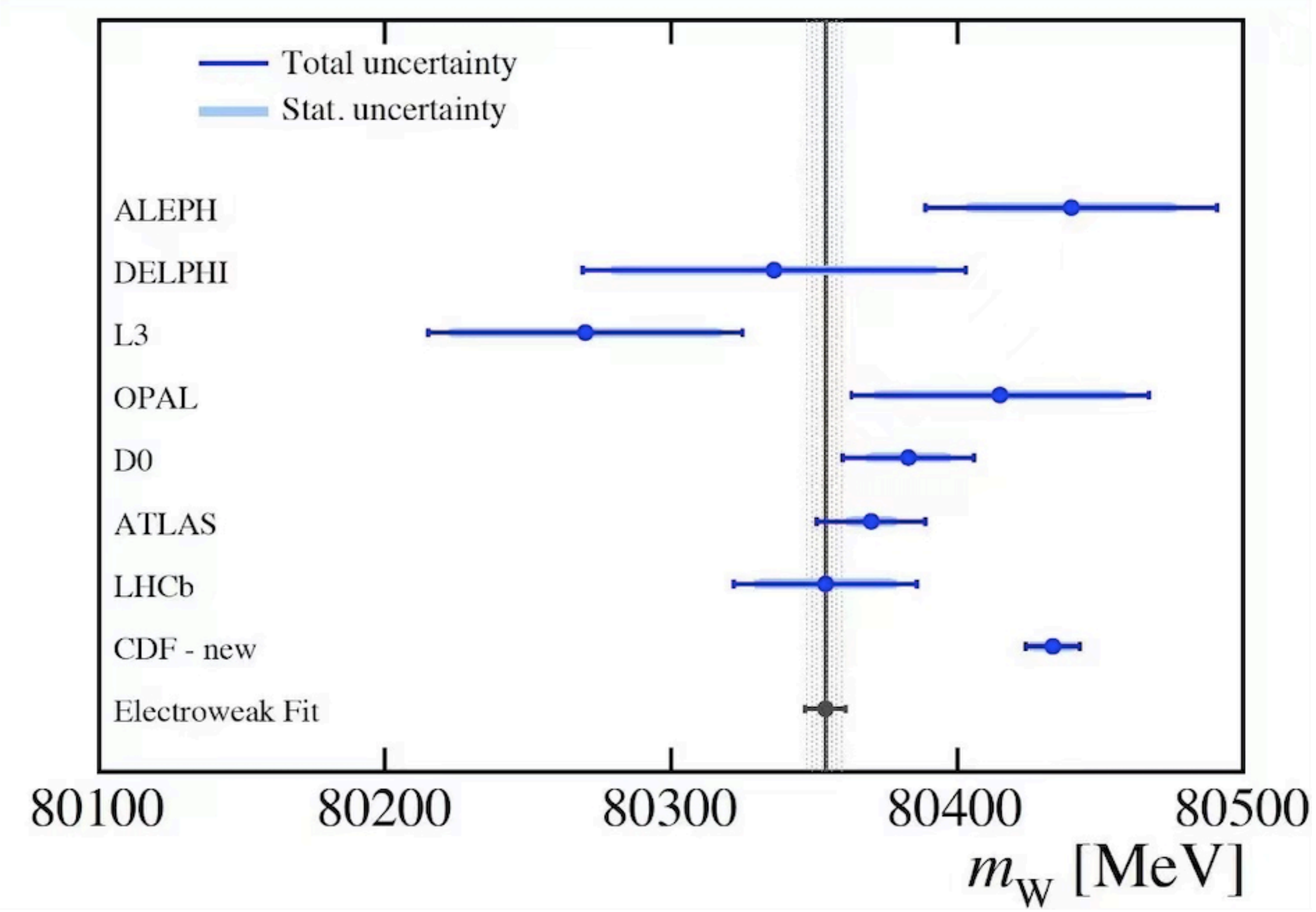

PARTICLE PHYSICS

High-precision measurement of the *W* boson mass with the CDF II detector

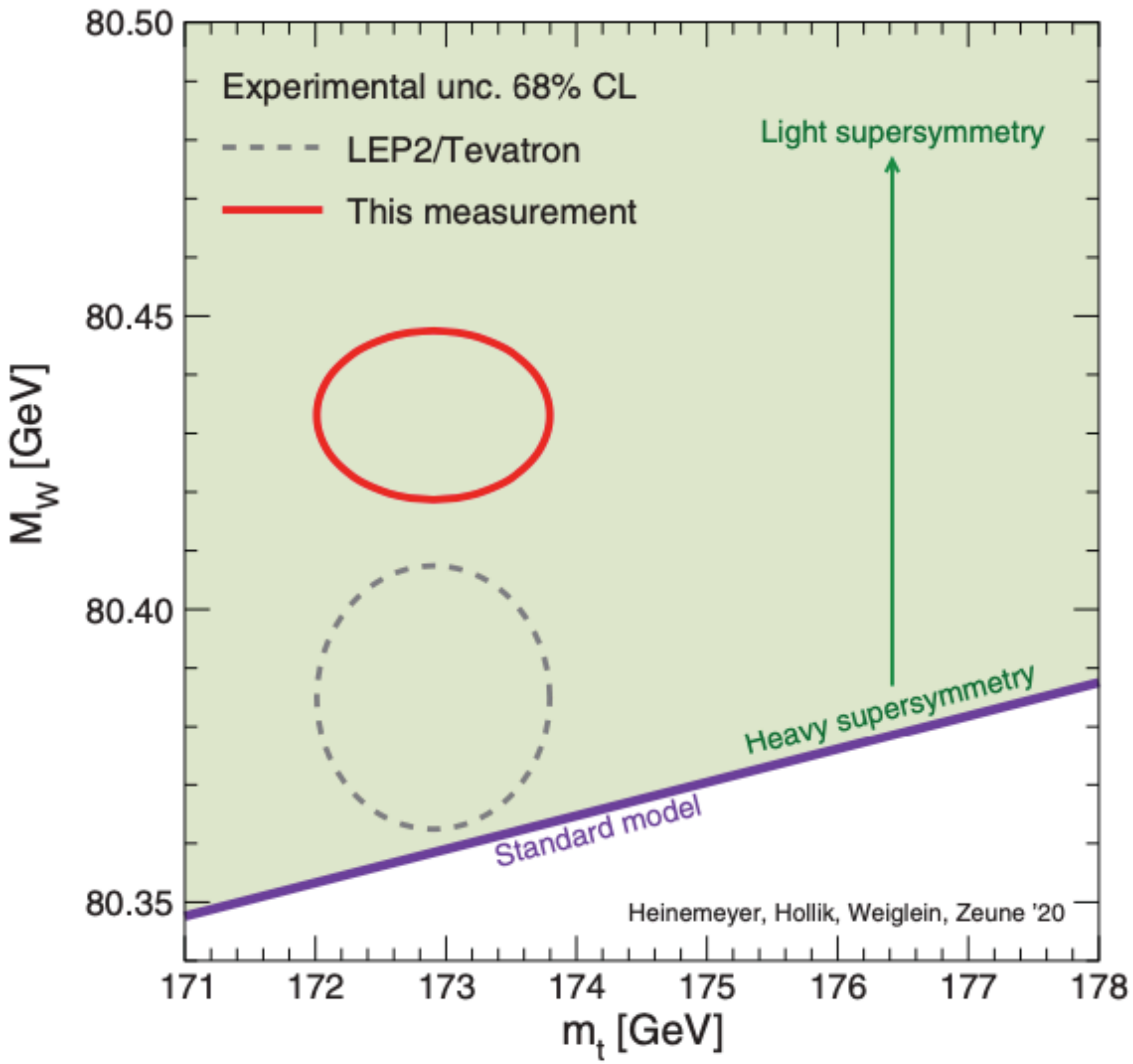

PARTICLE PHYSICS

High-precision measurement of the *W* boson mass with the CDF II detector

Table 2. Uncertainties on the combined M_W result.

Source	Uncertainty (MeV)
Lepton energy scale	3.0
Lepton energy resolution	1.2
Recoil energy scale	1.2
Recoil energy resolution	1.8
Lepton efficiency	0.4
Lepton removal	1.2
Backgrounds	3.3
p_T^Z model	1.8
p_T^W/p_T^Z model	1.3
Parton distributions	3.9
QED radiation	2.7
W boson statistics	6.4
Total	9.4

Table 1. Individual fit results and uncertainties for the M_W measurements. The fit ranges are 65 to 90 GeV for the m_T fit and 32 to 48 GeV for the p_T^ℓ and p_T^ν fits. The χ^2 of the fit is computed from the expected statistical uncertainties on the data points. The bottom row shows the combination of the six fit results by means of the best linear unbiased estimator (*66*).

Distribution	*W* boson mass (MeV)	χ^2/dof
$m_T(e,\nu)$	$80{,}429.1 \pm 10.3_{stat} \pm 8.5_{syst}$	39/48
$p_T^\ell(e)$	$80{,}411.4 \pm 10.7_{stat} \pm 11.8_{syst}$	83/62
$p_T^\nu(e)$	$80{,}426.3 \pm 14.5_{stat} \pm 11.7_{syst}$	69/62
$m_T(\mu,\nu)$	$80{,}446.1 \pm 9.2_{stat} \pm 7.3_{syst}$	50/48
$p_T^\ell(\mu)$	$80{,}428.2 \pm 9.6_{stat} \pm 10.3_{syst}$	82/62
$p_T^\nu(\mu)$	$80{,}428.9 \pm 13.1_{stat} \pm 10.9_{syst}$	63/62
Combination	$80{,}433.5 \pm 6.4_{stat} \pm 6.9_{syst}$	7.4/5

Parton Model
(in hadron collisions)

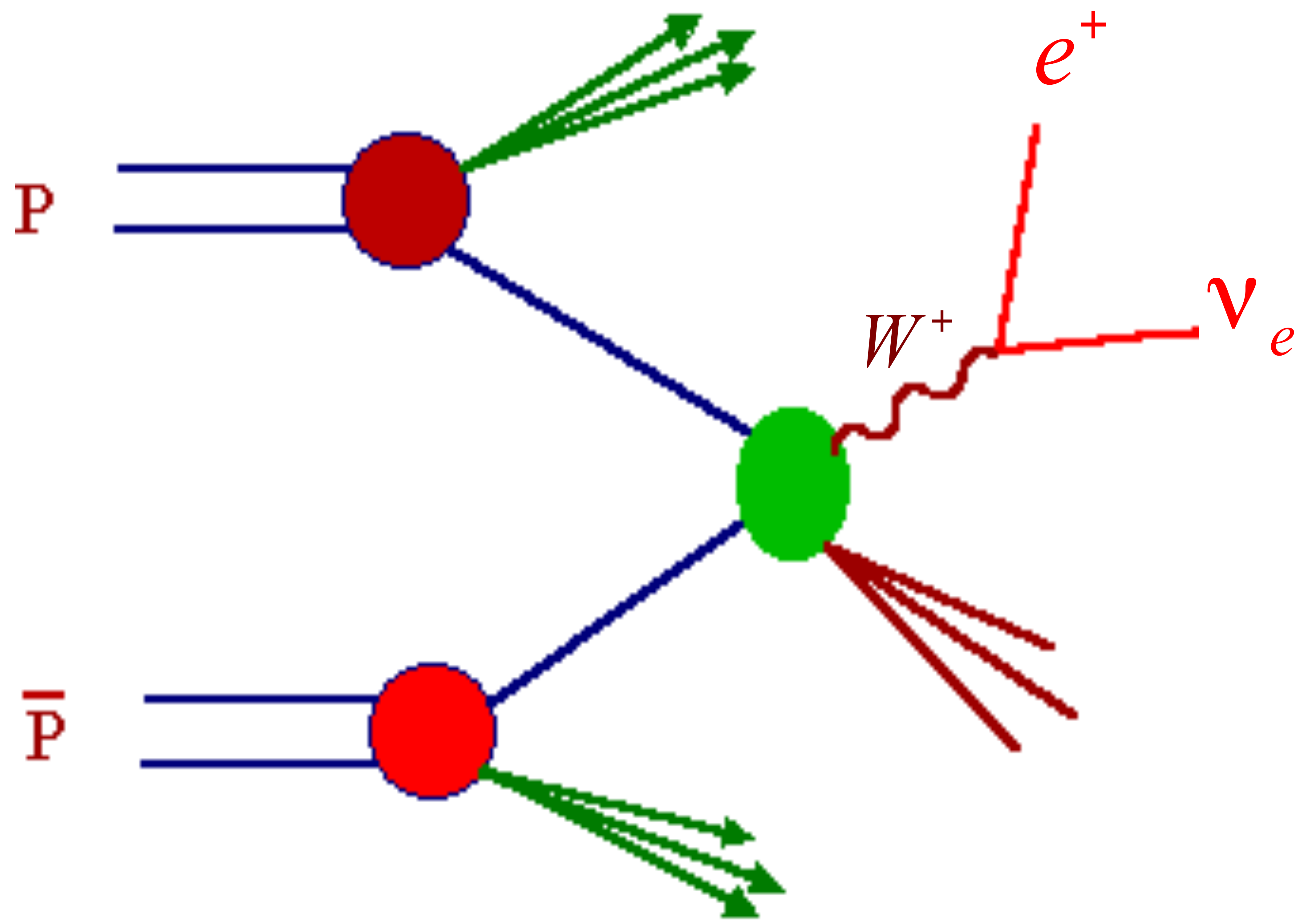

Up to next to Leading order corrections

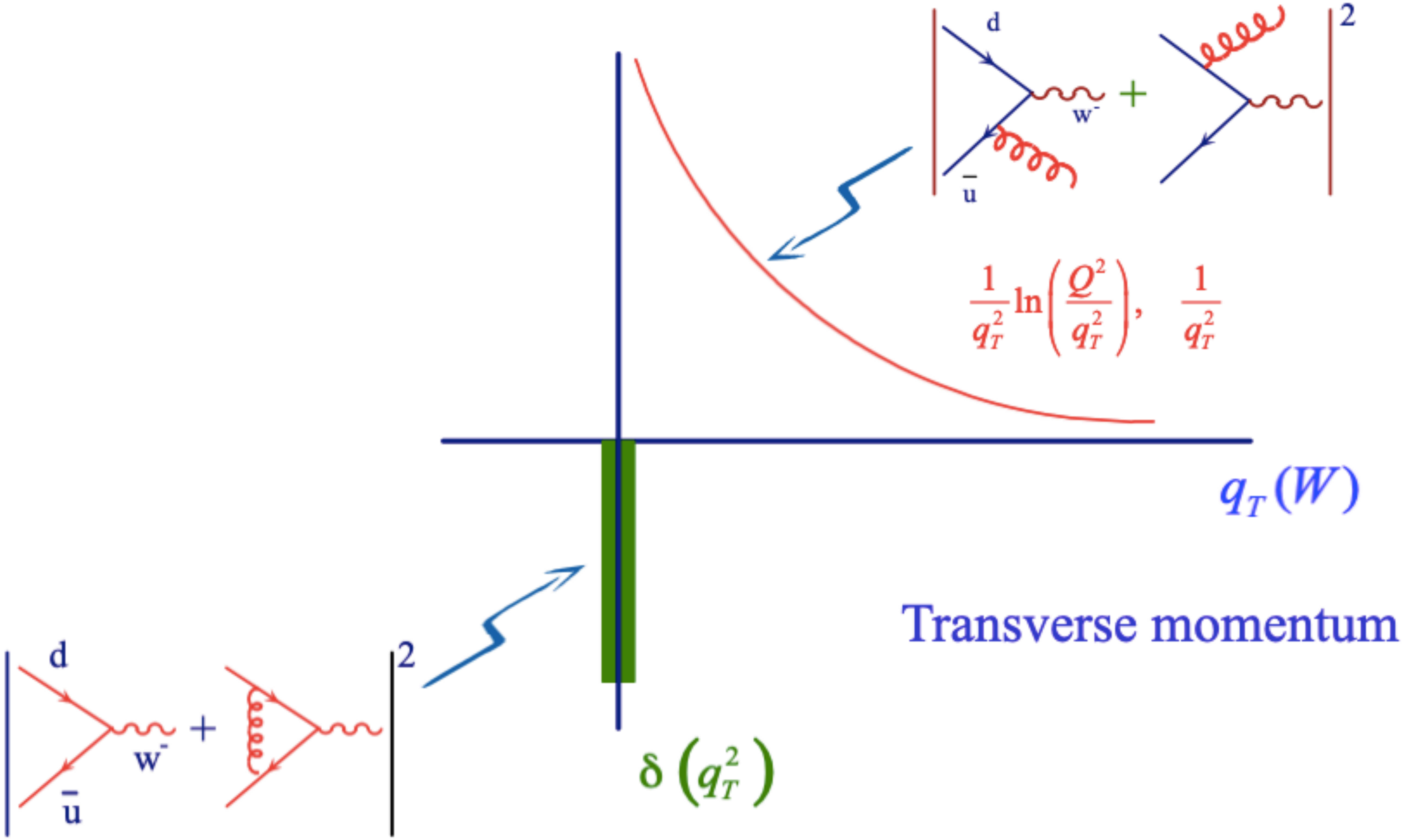

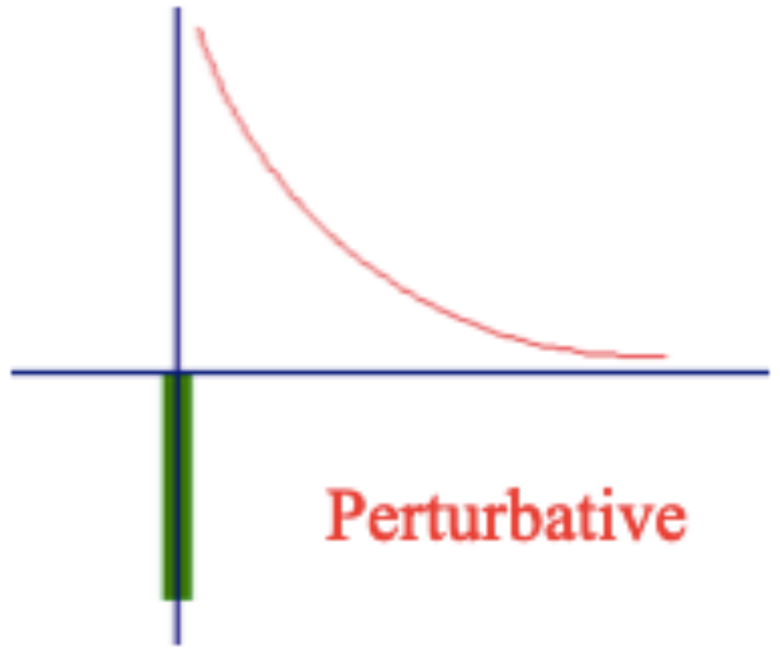

To describe data → Resummation is needed.

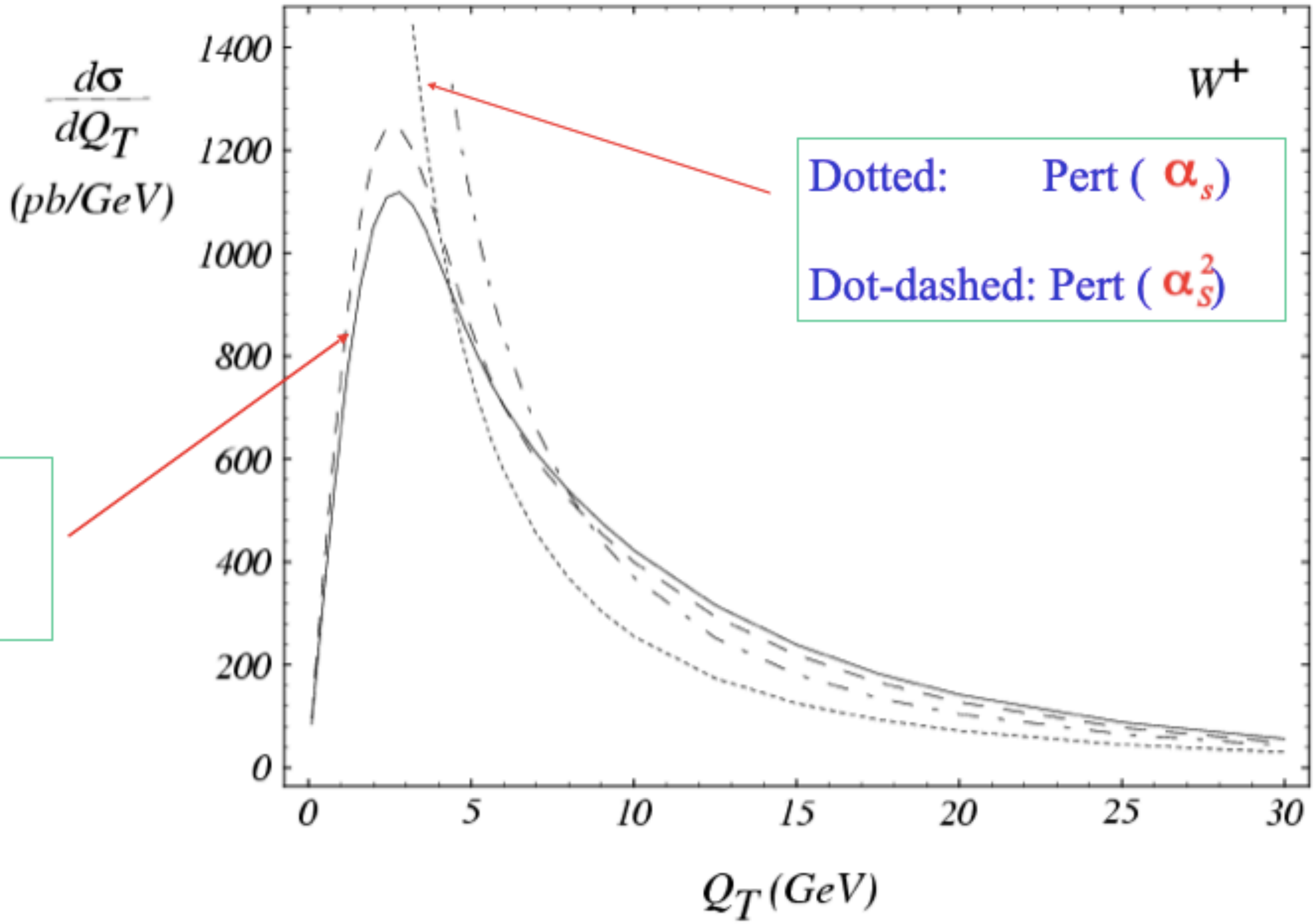

Dashed: CSS (1,1,1)

Solid: CSS (2,2,1)

Resummation

W-boson mass measurement from p_T^e

$$W^- \to e^- \overline{\nu}_e$$

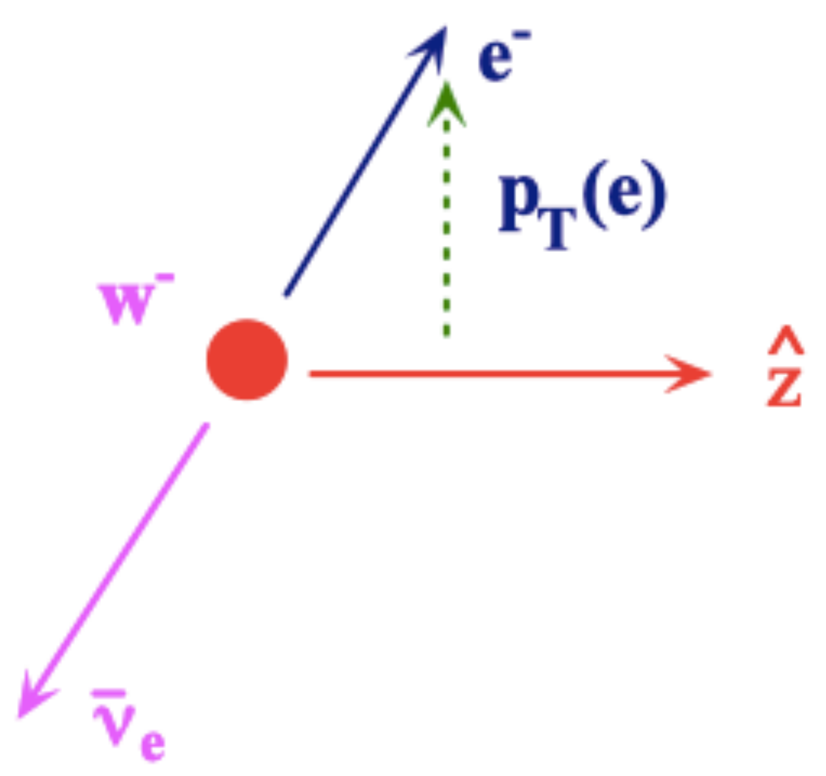

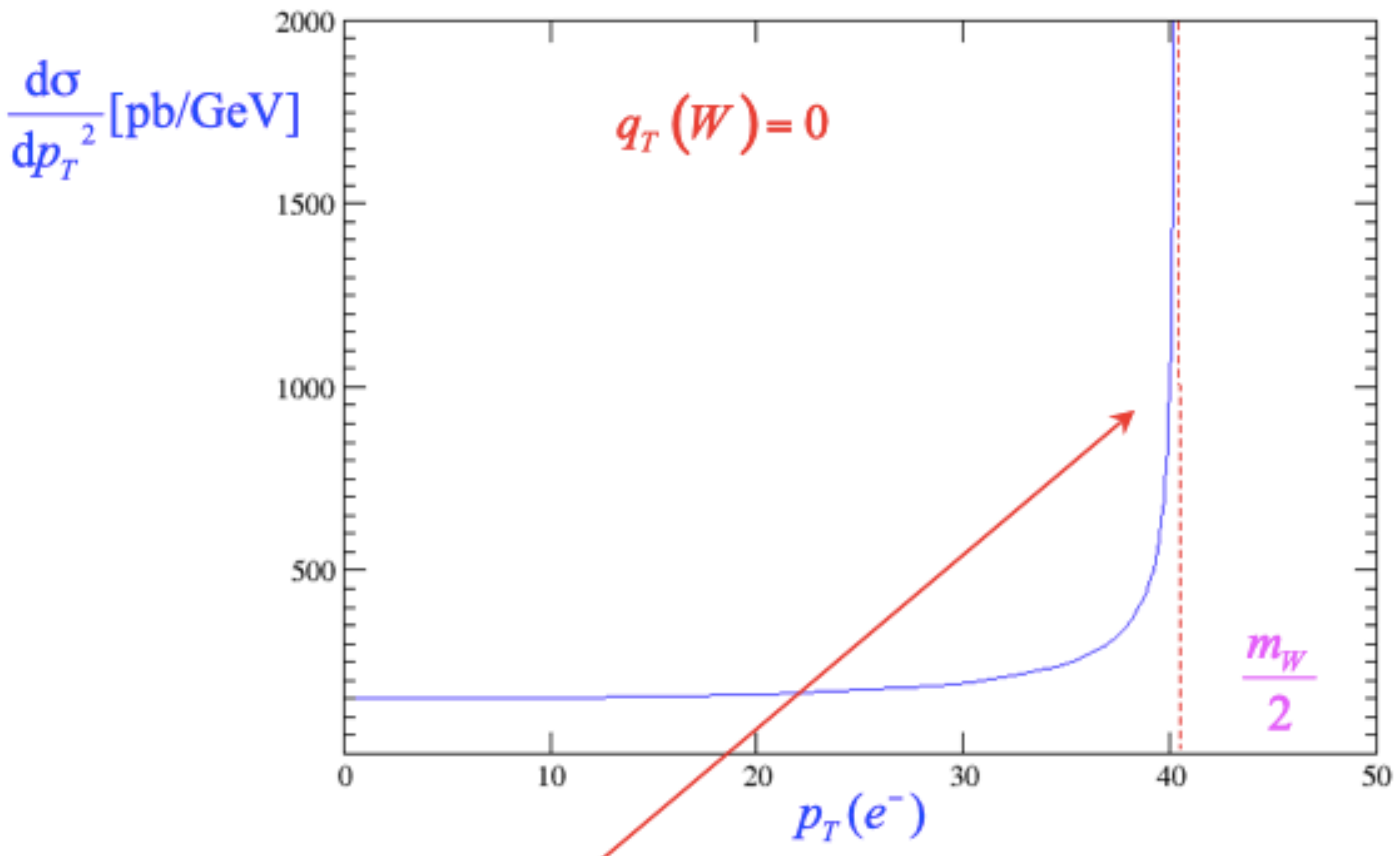

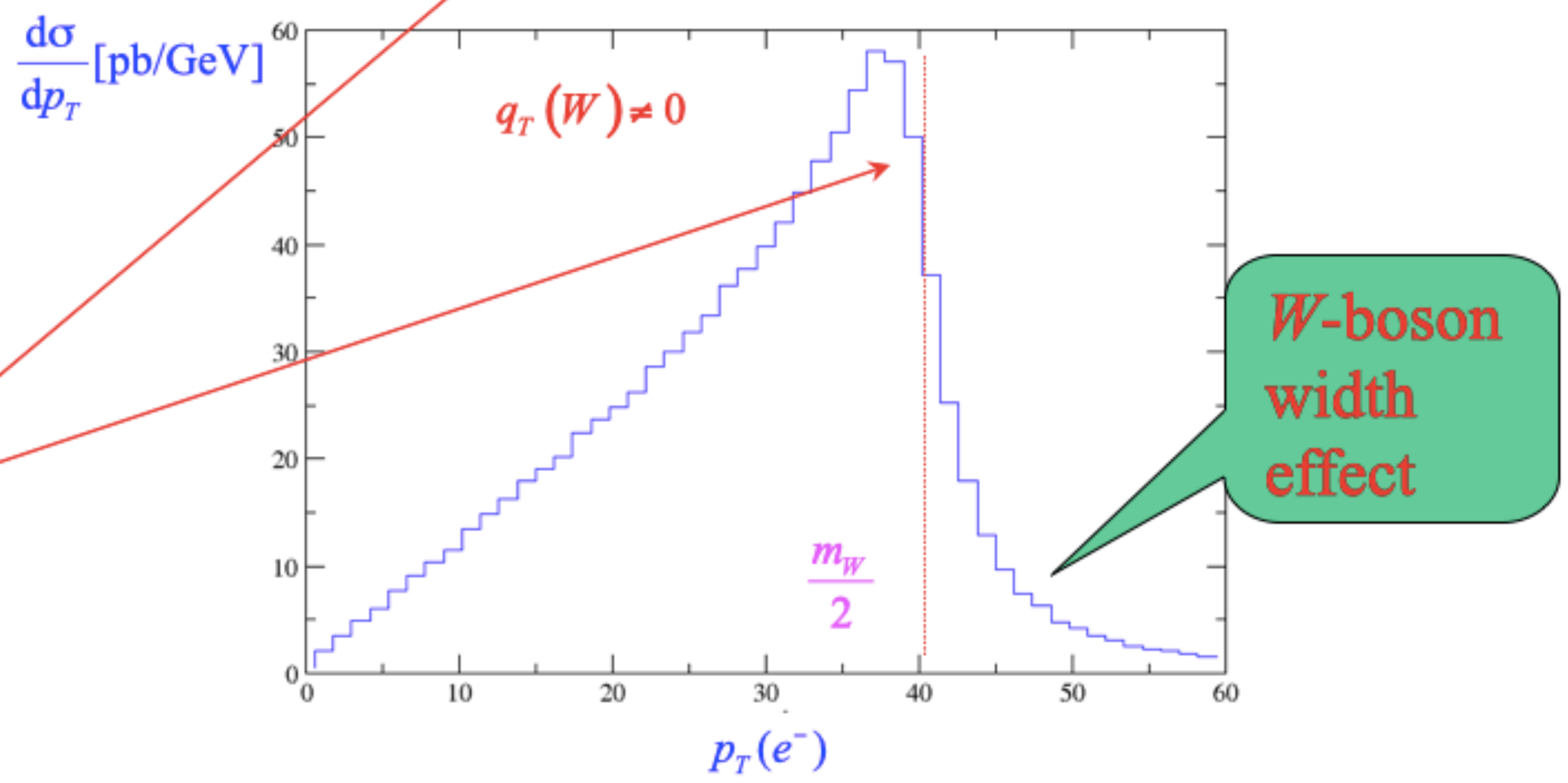

Kinematics Jacobian factor

$$\frac{d\sigma}{dp_T^2} \propto \frac{d\sigma}{d\,\mathrm{Cos}\theta}\,\frac{1}{\sqrt{1-4p_T^2/M_W^2}}$$

What's QCD Resummation?

All order quantum corrections

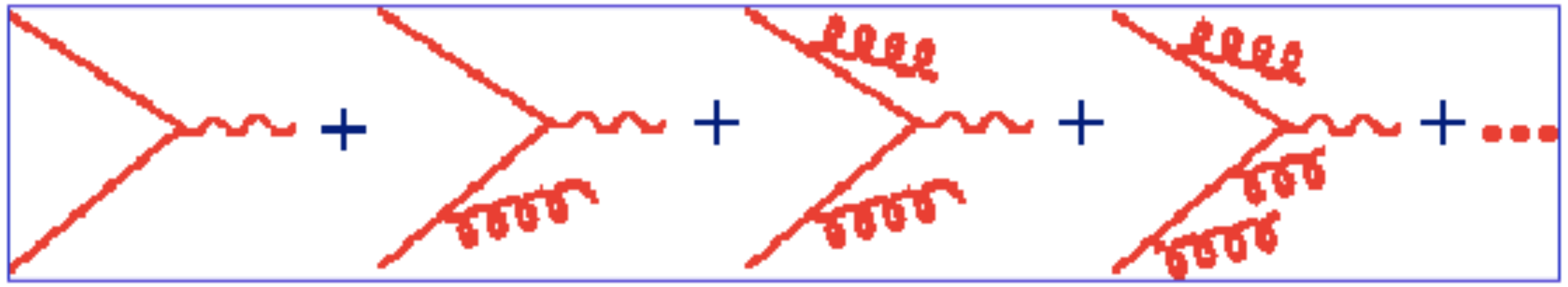

$$\frac{d\hat{\sigma}}{dq_T^2} \sim \frac{1}{q_T^2}\sum_{n=1}^{\infty}\sum_{m=0}^{2n-1}\alpha_S^{(n)}\ln^{(m)}\left(\frac{Q^2}{q_T^2}\right) \qquad L \equiv \ln\left(\frac{Q^2}{q_T^2}\right)$$

$$\sim \frac{1}{q_T^2}\Big\{\ \alpha_S\left(\underline{L+1}\right)$$

$$+\alpha_S^2\left(\underline{L^3+L^2}+\underline{L+1}\right)$$

$$+\alpha_S^3\left(\underline{L^5+L^4}+\underline{L^3+L^2}+\underline{L+1}\right)$$

$$+\cdots\ \Big\}$$

Resummation is to reorganize the results
in terms of the large Log's.

Resummation

$$
\begin{aligned}
\frac{d\sigma}{dq_T^2} \sim \frac{1}{q_T^2}\Big\{ & \left[\alpha_S(L+1) + \alpha_S^2\left(L^3+L^2\right) + \alpha_S^3\left(L^5+L^4\right) + \cdots\right] \\
& + \left[+ \alpha_S^2(L+1) + \alpha_S^3\left(L^3+L^2\right) + \cdots \right] \\
& + \left[+ \alpha_S^3(L+1) + \cdots \right] \\
& + \cdots \Big\}
\end{aligned}
$$

Renormalization Group Technique

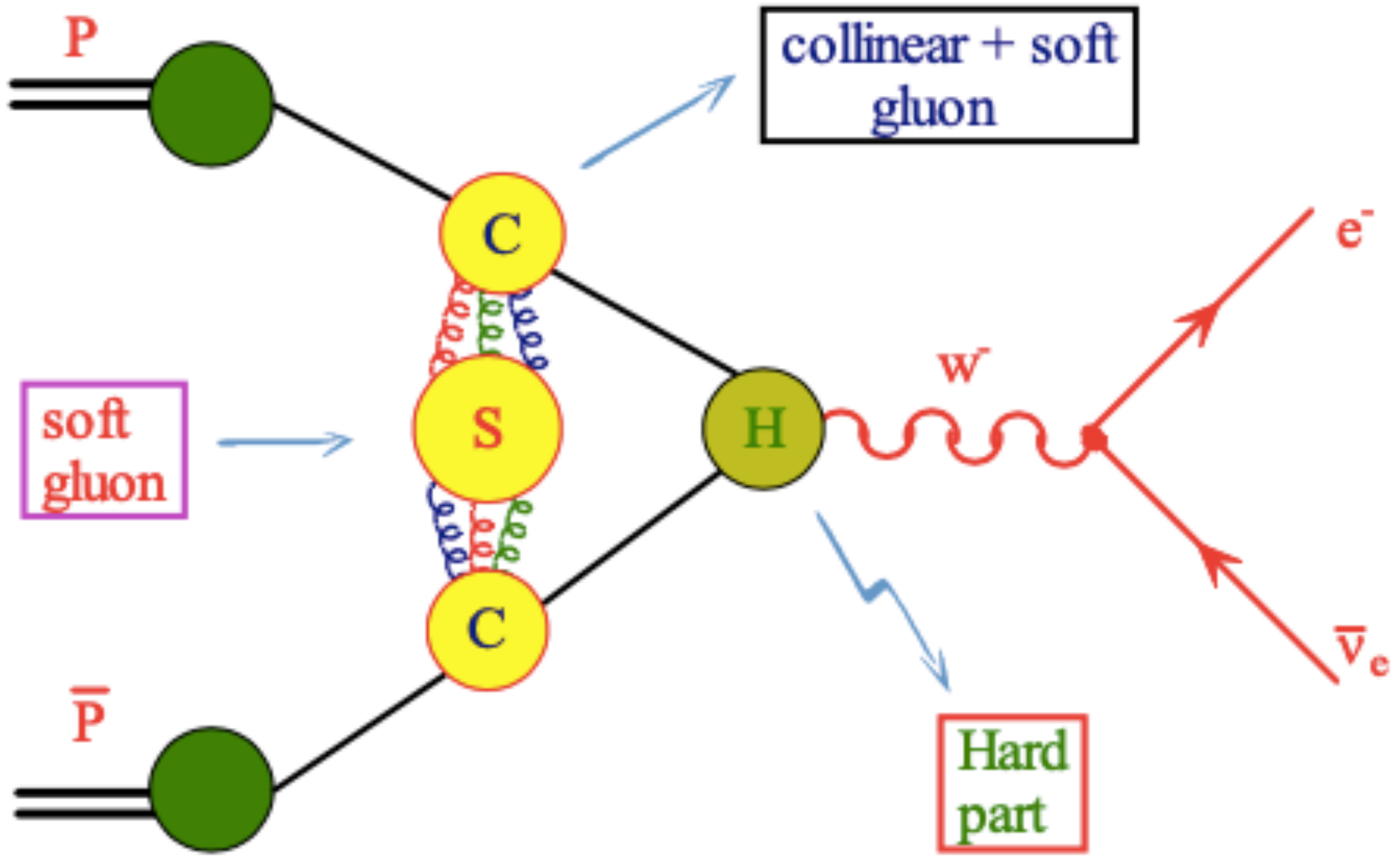

$P\bar{P} \rightarrow Z^0$ @ Fermilab Tevatron

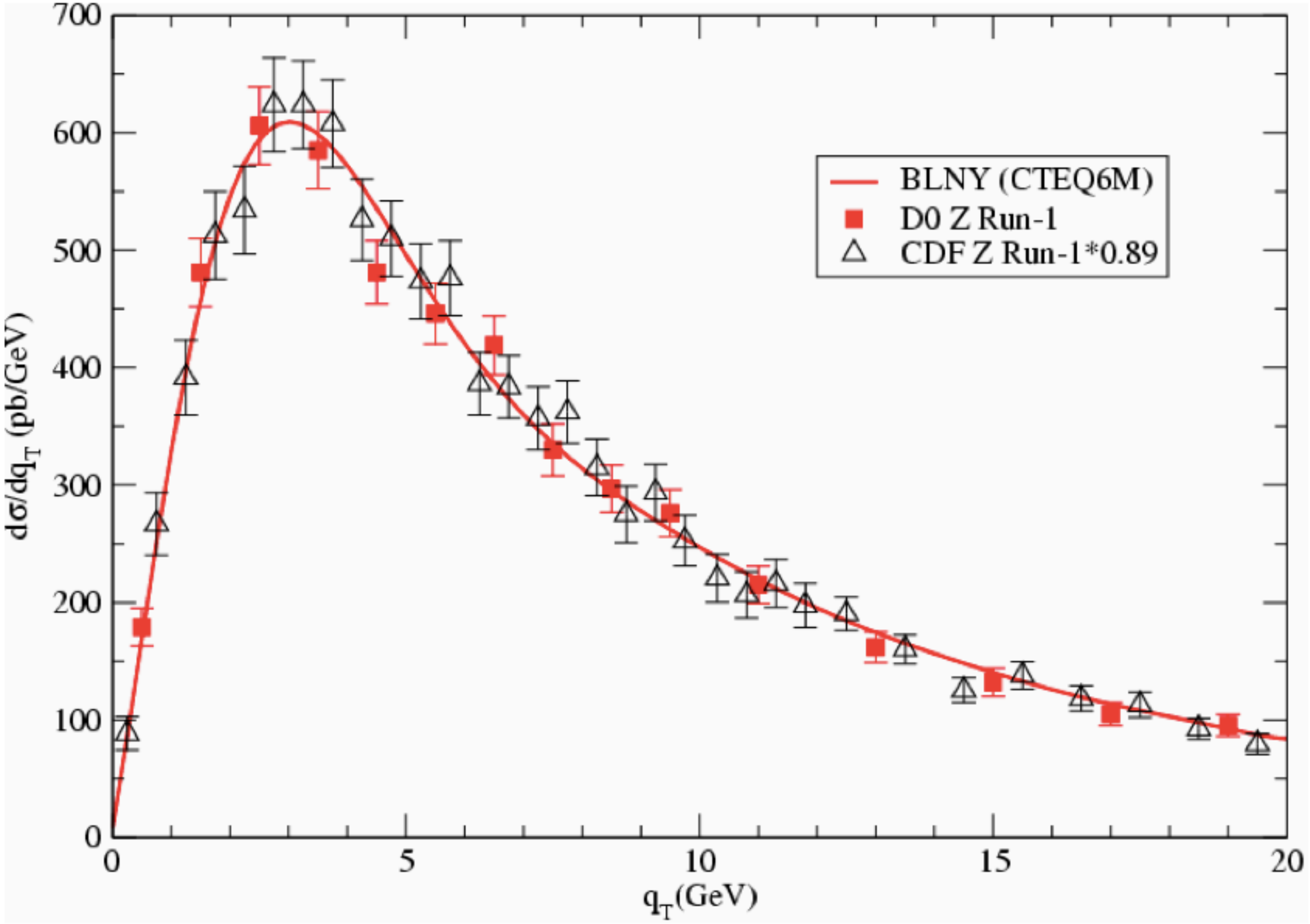

- To predict the transverse momentum of

Drell-Yan

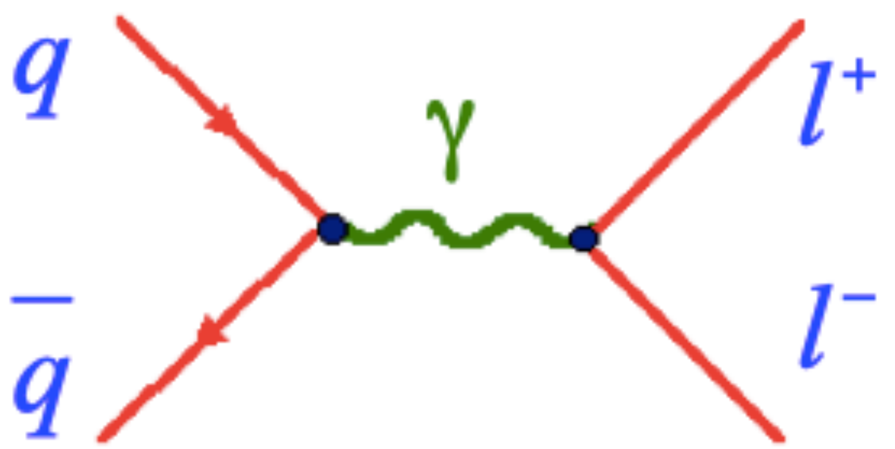

$W^\pm, Z$

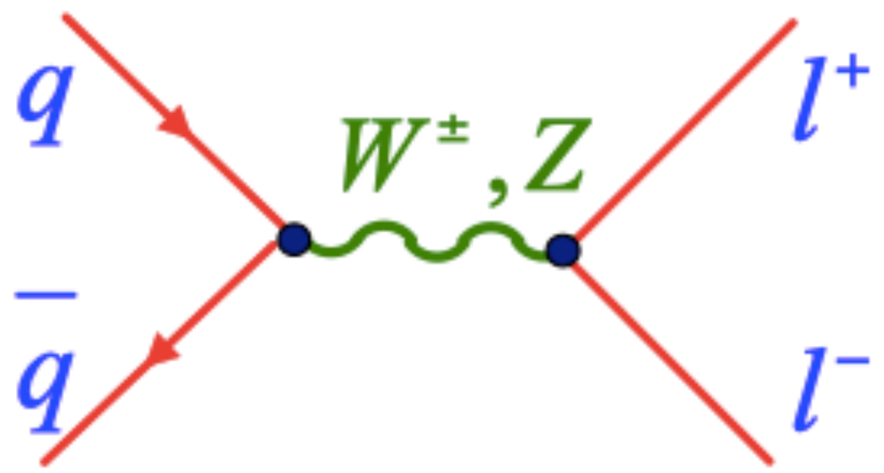

W H

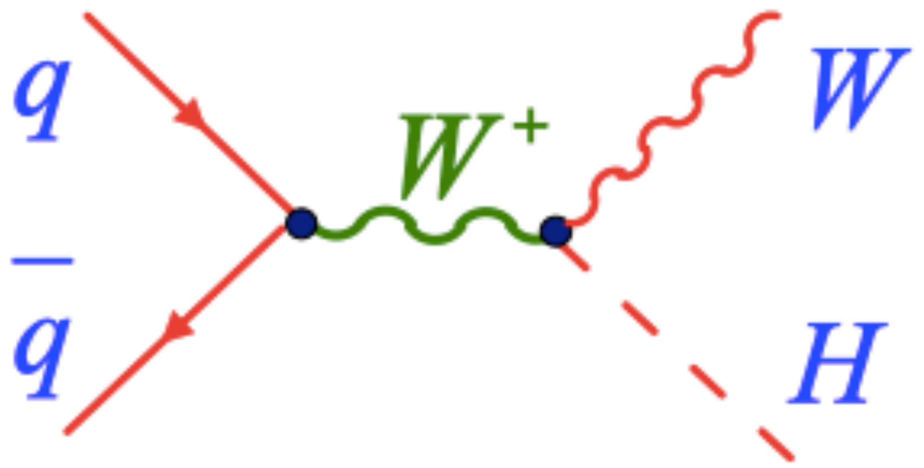

$g\,g \to H$

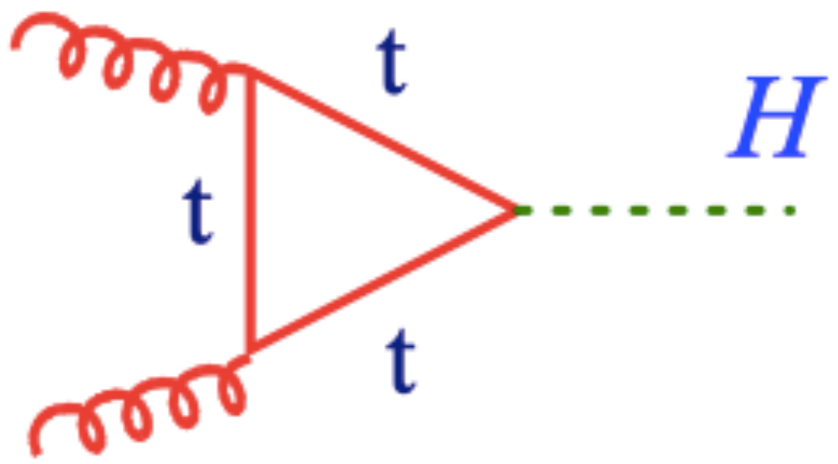

Must include QCD Resummation

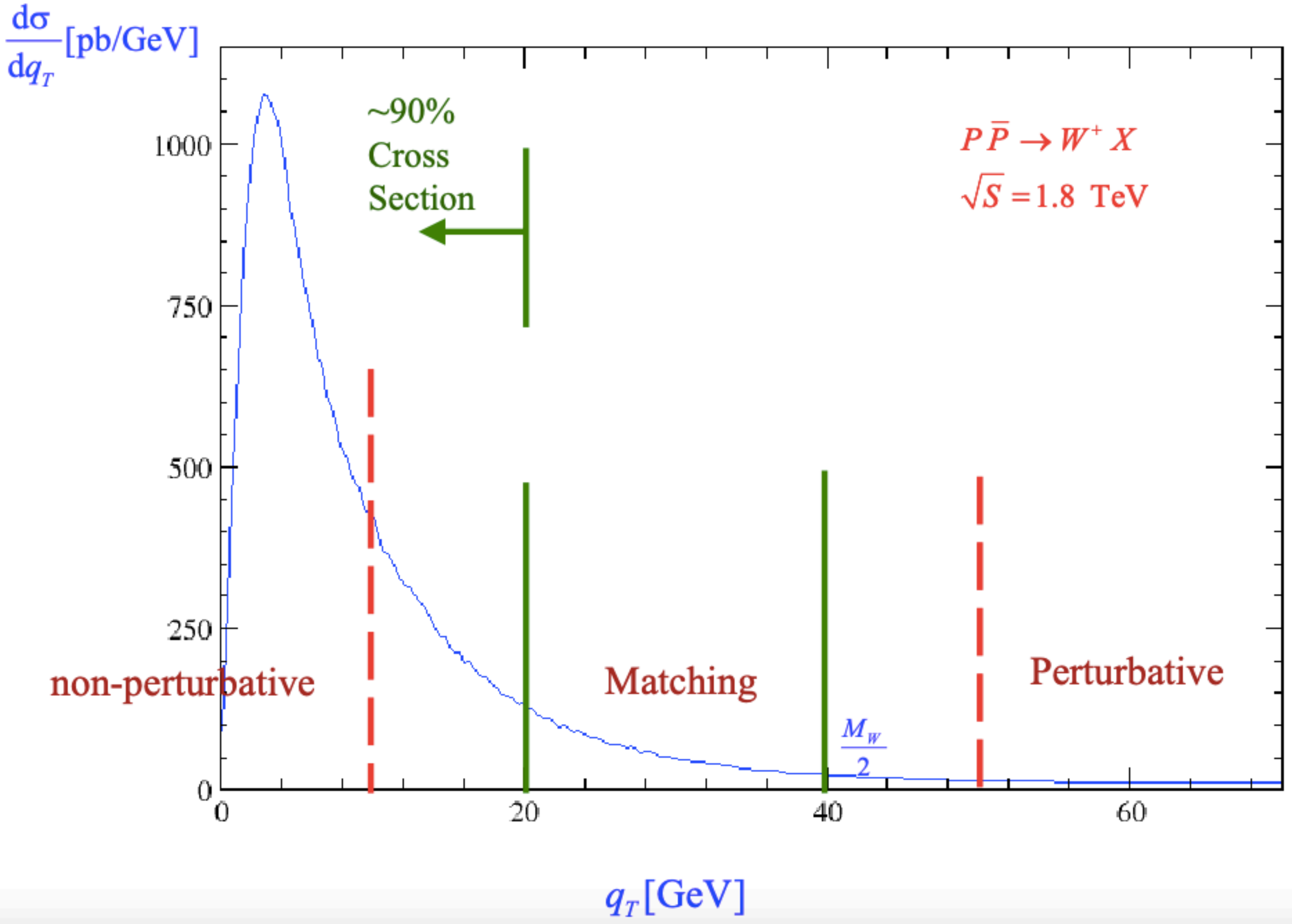

$\frac{d\sigma}{dq_T}$[pb/GeV]
1000
750
500
250
0
0
20
40
60
~90%
Cross
Section
$P\bar{P} \to W^+ X$
$\sqrt{S} = 1.8$ TeV
non-perturbative
Matching
Perturbative
$\frac{M_W}{2}$
q_T[GeV]

Resummed results:

Determined by $A^{(1)}$ and $B^{(1)}$

$$
\begin{aligned}
\frac{d\sigma}{dq_T^2} \sim \frac{1}{q_T^2}\Big\{ & [\alpha_s(L+1) \quad +\alpha_s^2(L^3+L^2)+\alpha_s^3(L^5+L^4) \quad +\cdots\ ] \\
& +[\qquad +\alpha_s^2(L+1) \quad +\alpha_s^3(L^3+L^2) \quad +\cdots\ ] \\
& +[\qquad\qquad +\alpha_s^3(L+1) \quad +\cdots\ ] \\
& +\cdots\ \Big\}
\end{aligned}
$$

Determined by
$A^{(2)}$ and $B^{(2)}$

Determined by
$A^{(3)}$ and $B^{(3)}$

QCD Resummation

In the formalism by Collins-Soper-Sterman, in addition to these perturbative results, the effects from physics beyond the leading twist is also implemented as

[non-perturbative functions].

CSS Resummation Formalism

$$\frac{d\sigma}{dq_T^2\,dy\,dQ^2} = \frac{\pi}{S}\sigma_0\delta\left(Q^2 - M_W^2\right)\cdot$$

$$\left\{\frac{1}{(2\pi)^2}\int d^2b \quad e^{i\vec{q}_T\cdot\vec{b}}\tilde{W}\left(b,Q,x_A,x_B\right)\cdot\text{[Non-perturbative functions]}\right.$$

$$\left.+Y\left(q_T,y,Q\right)\right\}$$

$$\sum_j\int_{x_A}^1\frac{d\xi_A}{\xi_A}C_{qj}\left(\frac{x_A}{\xi_A},b,\mu\right)\cdot f_{j/A}\left(\xi_A,\mu\right)$$

$$\tilde{W} = e^{-S(b)}\cdot C\otimes f\left(x_A\right)\cdot C\otimes f\left(x_B\right)$$

$$\sum_k\int_{x_B}^1\frac{d\xi_B}{\xi_B}C_{qk}\left(\frac{x_A}{\xi_A},b,\mu\right)\cdot f_{k/B}\left(\xi_B,\mu\right)$$

Sudakov form factor $S\left(b\right) = \int_{\left(\frac{b_0}{b}\right)^2}^{Q^2}\frac{d\bar{\mu}^2}{\bar{\mu}^2}\left[\ln\left(\frac{Q^2}{\bar{\mu}^2}\right)A\left(\bar{\mu}\right)+B\left(\bar{\mu}\right)\right]$

[Non-perturbative functions] are functions of (b,Q,x_A,x_B) which include QCD effects beyond Leading Twist.

[non-perturbative function] is a function of (b,Q,x_A,x_B), implemented to include effects beyond Leading Twist.

Until we know how to calculate QCD non-perturbatively, (Lattice Gauge Theory?), these functions can only be parameterized. However, the same functions should describe Drell-Yan, $W^{\pm}$, Z^0 data.

- Test QCD in problems involving multiple scales.
- Measuring these non-perturbative functions may help in understanding the non-perturbative part of QCD.

[non-perturbative functions] , dependent of Q, b, x_A, x_B, is necessary to describe q_T – distribution of Drell-Yan, $W^{\pm}$,Z^0 events.

Fits: • Brock-Landry-Nadolsky-Yuan

$$\exp\left[-g_1 b^2 - g_2 b^2 \ln\left(\frac{Q}{2Q_0}\right) - \underbrace{g_1 g_3 b^2 \ln(100 x_A x_B)}_{\text{New term with x-dependence}}\right]$$

$Q_0 = 1.6$ GeV

$g_1 = 0.21^{+0.01}_{-0.01}$ GeV^2

$g_2 = 0.68^{+0.02}_{-0.02}$ GeV^2

$g_3 = -0.60^{+0.05}_{-0.04}$

$(\ b_{max} = 0.5\ \text{GeV}^{-1}\ )$

CSS formalism

$$\frac{d\sigma(gg \to HX)}{dQ^2 dQ_T^2 dy} = \kappa\sigma_0 \frac{Q^2}{S} \frac{Q^2\Gamma_H/m_H}{(Q^2 - m_H^2)^2 + (Q^2\Gamma_H/m_H)^2}$$
$$\times \left\{ \frac{1}{(2\pi)^2} \int d^2b e^{iQ_T \cdot b} \widetilde{W}_{gg}(b_*, Q, x_1, x_2, C_{1,2,3}) \widetilde{W}_{gg}^{NP}(b, Q, x_1, x_2) + Y(Q_T, Q, x_1, x_2, C_4) \right\},$$

$$\widetilde{W}_{gg}(b, Q, x_1, x_2, C_{1,2,3}) = e^{-S(b,Q,C_1,C_2)} \sum_{a,b=q,\bar{q},g} \big(C_{ga} \otimes f_a\big)(x_1)\big(C_{gb} \otimes f_b\big)(x_2),$$

$$S(b, Q, C_1, C_2) = \int_{C_1^2/b^2}^{C_2^2 Q^2} \frac{d\bar{\mu}}{\bar{\mu}^2} \left[A(\alpha_s(\bar{\mu}), C_1) \ln\left(\frac{C_2^2 Q^2}{\bar{\mu}^2}\right) + B(\alpha_s(\bar{\mu}), C_1, C_2) \right] .$$

Theory Uncertainties

- μ_R uncert. (NLO, NNLO, ...)
- μ_F uncert. (NLL, NNLL, ... in DGLAP)
- PDF uncert.
- non-pert. uncert.
- resummation uncert. (soft scale & hard scale)
- scheme uncert., higher twist, hadronization effect, detector effect, etc.

Future colliders

Future colliders

- Higher energy / higher luminosity
- Z factory / Higgs factory: CEPC, ILC, FCC-ee, CLIC
- muon colliders?
- SPPC, FCC-hh
- Extremely accurate experiment data?
- QCD/EW NNLO/NNNLO/Resummation theory? Numerical approaches may be the only choice. What if theory cannot satisfy precision needs?

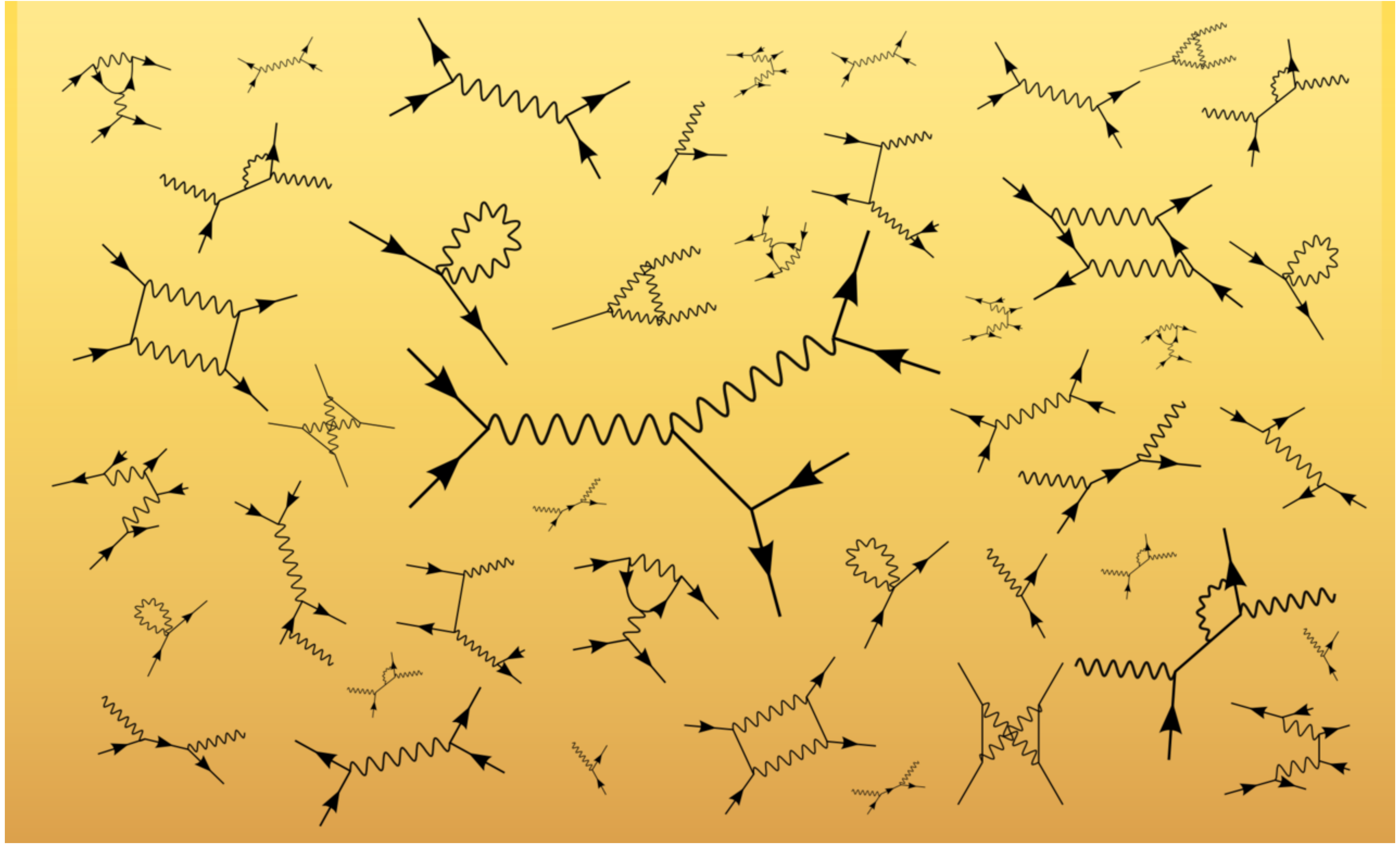

Thank you!